LI
LABORATORY INVESTIGATION
THE BASIC AND TRANSLATIONAL PATHOLOGY RESEARCH JOURNAL
VOLUME 99 | SUPPLEMENT 1 | MARCH 2019

USCAP 2019

ABSTRACTS

GENITOURINARY PATHOLOGY (INCLUDING RENAL TUMORS) (776-992)

USCAP 108TH ANNUAL MEETING

UNLOCKING YOUR INGENUITY

MARCH 16-21, 2019

National Harbor, Maryland
Gaylord National Resort & Convention Center

Published by
SPRINGER NATURE
www.ModernPathology.org

USCAP Creating a Better Pathologist
AN OFFICIAL JOURNAL OF THE UNITED STATES AND CANADIAN ACADEMY OF PATHOLOGY

EDUCATION COMMITTEE

Jason L. Hornick, Chair
Rhonda K. Yantiss, Chair, Abstract Review Board and Assignment Committee
Laura W. Lamps, Chair, CME Subcommittee
Steven D. Billings, Interactive Microscopy Subcommittee
Shree G. Sharma, Informatics Subcommittee
Raja R. Seethala, Short Course Coordinator
Ilan Weinreb, Subcommittee for Unique Live Course Offerings
David B. Kaminsky (Ex-Officio)
Aleodor (Doru) Andea
Zubair Baloch
Olca Basturk
Gregory R. Bean, Pathologist-in-Training
Daniel J. Brat
Ashley M. Cimino-Mathews
James R. Cook
Sarah M. Dry
William C. Faquin
Carol F. Farver
Yuri Fedoriw
Meera R. Hameed
Michelle S. Hirsch
Lakshmi Priya Kunju
Anna Marie Mulligan
Rish Pai
Vinita Parkash
Anil Parwani
Deepa Patil
Kwun Wah Wen, Pathologist-in-Training

ABSTRACT REVIEW BOARD

Benjamin Adam
Michelle Afkhami
Narasimhan (Narsi) Agaram
Rouba Ali-Fehmi
Ghassan Allo
Isabel Alvarado-Cabrero
Christina Arnold
Rohit Bhargava
Justin Bishop
Jennifer Boland
Elena Brachtel
Marilyn Bui
Shelley Caltharp
Joanna Chan
Jennifer Chapman
Hui Chen
Yingbei Chen
Benjamin Chen
Rebecca Chernock
Beth Clark
James Conner
Alejandro Contreras
Claudiu Cotta
Timothy D'Alfonso
Farbod Darvishian
Jessica Davis
Heather Dawson
Elizabeth Demicco
Suzanne Dintzis
Michelle Downes
Daniel Dye
Andrew Evans
Michael Feely
Dennis Firchau
Larissa Furtado
Anthony Gill
Ryan Gill
Paula Ginter
Tamara Giorgadze
Raul Gonzalez
Purva Gopal
Anuradha Gopalan
Jennifer Gordetsky
Rondell Graham
Alejandro Gru
Nilesh Gupta
Mamta Gupta
Krisztina Hanley
Douglas Hartman
Yael Heher
Walter Henricks
John Higgins
Mai Hoang
Mojgan Hosseini
Aaron Huber
Peter Illei
Doina Ivan
Wei Jiang
Vickie Jo
Kirk Jones
Neerja Kambham
Chiah Sui (Sunny) Kao
Dipti Karamchandani
Darcy Kerr
Ashraf Khan
Rebecca King
Michael Kluk
Kristine Konopka
Gregor Krings
Asangi Kumarapeli
Alvaro Laga
Cheng-Han Lee
Zaibo Li
Haiyan Liu
Xiuli Liu
Yan-Chun Liu
Tamara Lotan
Anthony Magliocco
Kruti Maniar
Jonathan Marotti
Emily Mason
Jerri McLemore
Bruce McManus
David Meredith
Anne Mills
Neda Moatamed
Sara Monaco
Atis Muehlenbachs
Bita Naini
Dianna Ng
Tony Ng
Ericka Olgaard
Jacqueline Parai
Yan Peng
David Pisapia
Alexandros Polydorides
Sonam Prakash
Manju Prasad
Peter Pytel
Joseph Rabban
Stanley Radio
Emad Rakha
Preetha Ramalingam
Priya Rao
Robyn Reed
Michelle Reid
Natasha Rekhtman
Michael Rivera
Michael Roh
Andres Roma
Avi Rosenberg
Esther (Diana) Rossi
Peter Sadow
Safia Salaria
Steven Salvatore
Souzan Sanati
Sandro Santagata
Anjali Saqi
Frank Schneider
Jeanne Shen
Jiaqi Shi
Wun-Ju Shieh
Gabriel Sica
Deepika Sirohi
Kalliopi Siziopikou
Lauren Smith
Sara Szabo
Julie Teruya-Feldstein
Gaetano Thiene
Khin Thway
Rashmi Tondon
Jose Torrealba
Evi Vakiani
Christopher VandenBussche
Sonal Varma
Endi Wang
Christopher Weber
Olga Weinberg
Sara Wobker
Mina Xu
Shaofeng Yan
Anjana Yeldandi
Akihiko Yoshida
Gloria Young
Minghao Zhong
Yaolin Zhou
Hongfa Zhu
Debra Zynger

776 Differential Lysophosphatidylcholine Acyltransferase 1 (LPCAT1) Expression Confers Aggressiveness and Independently Predicts Recurrence in Urothelial Bladder Carcinomas

Eman Abdelzaher[1], Amany Abdelbary[1], Ahmed Fahmy[1], Ebtesam Elzarrouk[1]
[1]*Alexandria Faculty of Medicine, Alexandria, Egypt*

Disclosures: Eman Abdelzaher: None; Amany Abdelbary: None; Ahmed Fahmy: None; Ebtesam Elzarrouk: None

Background: Urothelial carcinomas are highly heterogeneous in terms of biological behavior which certainly reflects different and complex metabolic and molecular pathways.

Novel biomarkers that will better assist the management of bladder carcinomas and help predict patients' outcome are eagerly needed. Ongoing researches in the relatively new field of lipid metabolism are promising in this respect.

Recently, overexpression of lysophosphatidylcholine acyltransferase 1 (LPCAT1), a key enzyme in lipid metabolism, has been implicated in the pathogenesis and progression of several tumors. However, the status and clinical significance of LPCAT1 expression in urinary bladder carcinomas has remained unexplored.

Design: We evaluated LPCAT1 immunohistochemical expression in 60 Egyptian patients with urothelial bladder carcinomas (UBCs) and statistically correlated its expression with other clinicopathological parameters including patients' outcome. Twenty non-neoplastic bladder tissues served as a control group.

Results: In UBCs, two distinct patterns of LPCAT1 expression were detected, in >50% of tumor cells, and were designated as strong and weak nuclear expression (Fig. 1&2 respectively).

Strong LPCAT1 nuclear expression was noted in all non-neoplastic tissues and it was associated with low grade and non-invasive tumors, however, this finding was not statistically significant. Interestingly, it was significantly associated with higher recurrence rate in both low and high grade tumors (p=0.004 & p=0.003) and it emerged as an independent predictor of tumor recurrence (p=0.019).

Conversely, weak LPCAT1 nuclear expression was exclusively noted in neoplastic tissues (p=0.002) and it was significantly associated with high grade ($p=0.035$) and invasive ($p=0.013$) tumors.

Figure 1 - 776

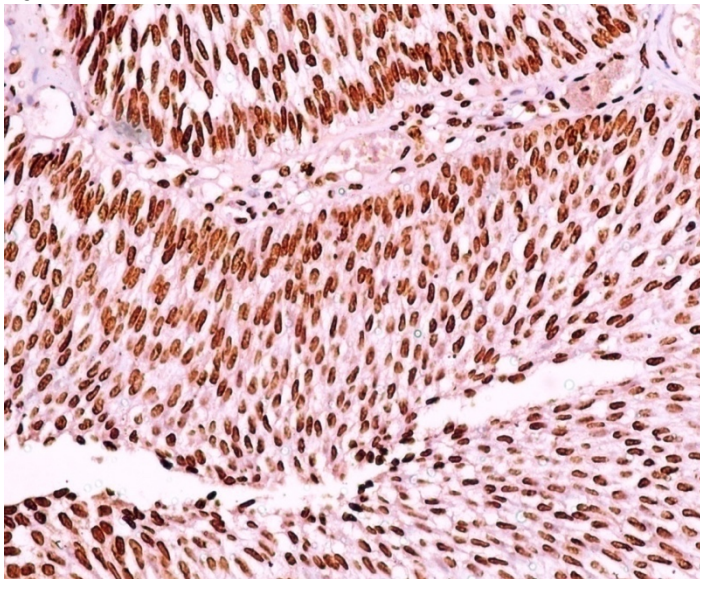

Figure 2 - 776

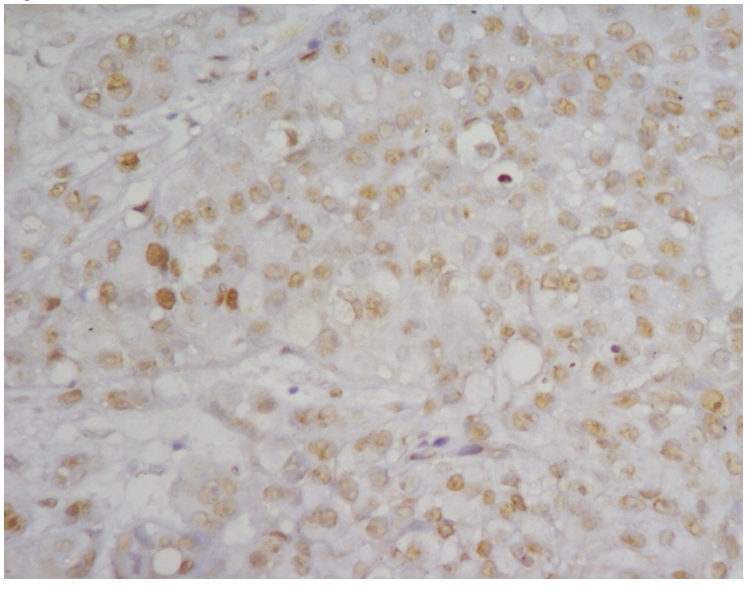

Conclusions: We conclude that LPCAT1 downregulation might be involved in urothelial carcinoma tumorigenesis and might contribute to tumor aggressive phenotype and behavior. Retained LPCAT1 expression in urothelial carcinomas is an independent predictor of tumor recurrence and thus it represents a promising novel prognostic marker which might help selection of candidates for stricter surveillance methods. Our study supports the postulation that alterations in lipid metabolism apparently play different roles during different stages of cancer evolvement.

777 Integrative molecular profiling of prostatic ductal adenocarcinoma reveals a distinct molecular spectrum, including frequent activating PI3K/AKT and WNT pathway alterations

Eman Abdulfatah[1], Komal Kunder[2], Simpa Salami[3], L. Priya Kunju[4], Angela Wu[5], Rohit Mehra[2], Scott Tomlins[2], Aaron Udager[3]
[1]Grosse Pointe Farms, MI, [2]University of Michigan, Ann Arbor, MI, [3]University of Michigan Medical School, Ann Arbor, MI, [4]University of Michigan Hospital, Ann Arbor, MI, [5]Ann Arbor, MI

Disclosures: Eman Abdulfatah: None; Komal Kunder: None; Simpa Salami: None; L. Priya Kunju: None; Angela Wu: None; Rohit Mehra: None; Scott Tomlins: *Consultant*, Hologic/Gen-Probe; *Major Shareholder*, Strata Oncology; *Major Shareholder*, Strata Oncology; Aaron Udager: None

Background: Prostatic ductal adenocarcinoma (PDA) is an uncommon, aggressive variant of prostate cancer. PDA typically manifests as a mixed tumor in combination with conventional acinar adenocarcinoma and only rarely occurs in a pure form. Over the past two decades, tremendous advances have been made in our understanding of the molecular pathology of prostate cancer, although PDA remains relatively understudied. Thus, in this study, we utilized targeted next-generation DNA and RNA sequencing to explore the molecular spectrum of PDA.

Design: PDA (pure or mixed with an acinar component) and available associated multifocal acinar tumors were retrospectively identified from a single large academic institution. H&E slides from all cases were reviewed by at least two genitourinary pathologists, and representative formalin-fixed paraffin-embedded (FFPE) tissue was selected for targeted next-generation DNA and RNA sequencing on an Ion Torrent Proton sequencer using the Oncomine Comprehensive Assay and a custom prostate cancer-focused panel, respectively. Prioritized somatic variants and copy number alterations (CNA) and ETS gene fusion status were manually curated using established in-house bioinformatics pipelines.

Results: Overall, 17 ductal and 26 acinar tumor samples were available for this study. Molecular features are summarized in the Table. Ductal tumors showed significantly higher mutational burden and genomic complexity than acinar tumors; in particular, activating molecular alterations in the PI3K/AKT pathway (i.e., *PTEN*, *AKT*, *PIK3CA*, and *PIK3R1*) and WNT pathway (i.e., *CTNNB1* and *APC*) were significantly enriched in ductal tumors. No prioritized somatic variants in mismatch repair genes were identified. ETS gene fusions were present in a subset of ductal tumors, but the frequency of ETS genes fusions was not significant different than acinar tumors in this cohort. Of the 9 PDA with a mixed acinar component, integration of next-generation DNA and RNA sequencing data demonstrated multiclonality in 1 case and clonality in 3 cases; clonality could not be definitively determined in the other 5 cases.

Molecular Features	Ductal (*n* = 17)	Acinar (*n* = 26)	*P*-value
Somatic Variants	Median = 1 (range = 0-3)	Median = 0 (range = 0-2)	**<0.001**
Copy Number Alterations	Median = 1 (range = 0-14)	Median = 0 (range = 0-2)	**<0.001**
PI3K/AKT Pathway Alterations	9 (52.9%) 8 (47.1%)	2 (7.7%) 24 (92.3%)	**0.001**
WNT Pathway Alterations	9 (52.9%) 8 (47.1%)	1 (3.8%) 25 (96.2%)	**<0.001**
ETS Gene Fusion Status • Positive • Negative	3 (20.0%) 12 (80.0%)	9 (34.6%) 17 (65.4%)	0.480

Conclusions: Integrative molecular profiling of PDA reveals a distinct molecular spectrum, including higher mutational burden and genomic complexity and frequent activating PI3K/AKT and WNT pathway alterations. Our data also demonstrate that a subset of tumors with mixed ductal and acinar components represents coalesced clonally-distinct tumor foci. Additional transcriptomic analyses are ongoing.

778 Small Foci of Gleason Pattern 4 in Core Biopsies Can Be Misleading: A Comparison with Final Gleason Grade/Grade Groups in Corresponding Radical Prostatectomy Specimens

Andres Acosta[1], Justine Barletta[1], Michelle Hirsch[2]
[1]Brigham and Women's Hospital, Harvard Medical School, Boston, MA, [2]Brigham and Women's Hospital, Boston, MA

Disclosures: Andres Acosta: None; Justine Barletta: None; Michelle Hirsch: None

Background: Active surveillance (AS) versus definitive management (ie, surgery, radiation therapy, clinical trial (CT)) for patients with prostate adenocarcinoma (PCa) is based on Gleason scoring (GS)/grade grouping (GrGr) in needle biopsies (NBX). For GS7/GrGr 2 or 3 PCas, it has become common to give the percent of Gleason pattern (GP) 4; however, in some NBX, the area of PCa is small (5-10% volume) making accurate grading difficult, which can lead to an erroneously high GrGr, most commonly GrGr 3 or 4. In our institution, such lesions are diagnosed as "small focus of PCa, not amenable to precise Gleason grading; however, GP4 is present" (referred to as 'small GP4'). The goal of this study was to evaluate outcome (radical prostatectomy, RP) data in consult diagnoses with a high GrGr that were 'downgraded' to "small GP4.

Design: 13 cases were identified based on the following: referral (consult) NBX diagnosis of GrGr 3-5 which was downgraded to 'small GP4', exclusion of cases with GrGr 4 or 5 in any other core upon re-review, subsequent corresponding RP available for review, and absence of neoadjuvant therapy. Pathologic parameters were compared between original and re-reviewed NBX diagnoses and the RP.

Results: Original NBX diagnoses included 6 intermediate grade PCas (GrGr3) and 7 high grade (GrGr4/5) PCas. All 13 cases were downgraded to 'small GP4" in at least one NBX; remaining NBX contained GrGr1-3 PCa only (low to intermediate grade). The original NBX diagnoses contained a higher GrGr than the corresponding RP in 10 cases (77% discordant), and remained the same in 3 cases (23% concordant). In contrast, re-reviewed 'small GP4' cases were concordant with the RP in 9 cases (69%); the 4 remaining cases were GrGr3 in the NBX and GrGr2 in the RP. None of the 13 RPs were diagnosed as GrGr4 or 5, although 4 did contain a minor component of GP5. Prior to re-review, all patients would have been eligible for a neoadjuvant CT ($\geq$GrGr3), and based on the RP results, 7 (54%) of these patients should not have been offered a CT (GrGr2 final diagnosis); the same was true for only 1 (8%) case based on re-review as 'small GP4'.

Conclusions: These results demonstrate that it is not uncommon for small foci of PCa in NBX to be erroneously misinterpreted as a high grade PCa. Such results can have an impact on patient management options and should be interpreted with caution. Our recommendation is to diagnose small foci of PCa that contain GP4 as 'small GP4' so that they are taken out of AS, but not overtreated.

779 PBRM1 but not BAP1 deficiency is a frequent feature of multifocal non-cystic low-grade clear cell renal cell carcinoma

Abbas Agaimy[1], Kiril Trpkov[2], Yuan Gao[3], Arndt Hartmann[4], Ondrej Hes[5]
[1]Erlangen, Germany, [2]University of Calgary, Calgary, AB, [3]University of Calgary, Calgary Laboratory Services, Calgary, AB, [4]Friedrich-Alexander-Universität Erlangen-Nürnberg, Erlangen, Germany, [5]Biopticka laborator s.r.o., Plzen, Czech Republic

Disclosures: Abbas Agaimy: None; Kiril Trpkov: None; Yuan Gao: None; Arndt Hartmann: None; Ondrej Hes: None

Background: vHL, *PBRM1* and *BAP1* inactivations, in decreasing order of frequency, represent the main molecular alterations in clear cell renal cell carcinoma (ccRCC). These three genes are located at the closely overlapping regions on chromosome 3p (3p25.3, 3p21.1 & 3p21.1, respectively). To our knowledge, the expression status of PBRM1 and BAP1, possibly reflecting the mechanisms underlying multifocal ccRCC, has not been previously investigated.

Design: We examined 45 ccRCC from 21 patients with 2≥RCC for PBRM1 and BAP1 expression using immunohistochemistry.

Results: 18 had multifocal ccRCC and 3 had clear cell tubulopapillary RCC in addition to at least one ccRCC. There were 12 males and 9 females, with an age range of 36-78 years (mean, 63). 18 patients had 2 tumors, and 3, 4 and 8 tumors were found in one patient each. PBRM1 loss was detected in 20/45 (44%) tumors from 11 patients (58% of purely solid tumors). Among 10 patients with 2 or more tumors, PBRM1 loss was concordant (found in all tumors) in 6, and discordant in 4 patients. Unequivocal BAP1 loss was detected in only 1/41 (2%) tumors and was mutually exclusive with the loss of PBRM1. Of 8 tumors from 3 patients with vHL syndrome, 6 had retained PBRM1 expression. One tumor had a PBRM1 loss indicating vHL is not mutually exclusive with PBRM1. The majority of PBRM1-deficient ccRCC had solid pattern (90%) lacking any cystic component while only 44% of PBRM1-intact tumors were purely solid.

Conclusions: The results of this study highlight the high frequency of PBRM1 loss in multifocal ccRCC, and suggest that PBRM1 represents a possible molecular driver in these cases. Exploring the *vHL* status is required to assess the frequency of co-inactivation of both genes, owing to large 3p deletions spanning both gene loci. The question of hereditary versus sporadic PBRM1 loss in multifocal ccRCC remains to be explored further.

780 Expression of HER2 and EGFR oncogenes in Adenocarcinomas of The Prostate: A Perspective from North Central Nigeria

Olanrewaju Ajetunmobi[1], Uta Drebber[2], Reinhard Buettner[3], Donatus Dzuachii[1], Raymond Vhriterire[4], Solomon Raphael[5], Olubanji Oguntunde[6], Oluwole Odujoko[7]
[1]Federal Medical Centre, Makurdi, Nigeria, [2]University Hospital Cologne Institute of Pathology, Cologne, Germany, [3]University Hospital Cologne, Cologne, Germany, [4]Benue State University Teaching Hospital, Makurdi, Nigeria, [5]University of Abuja, Abuja, Nigeria, [6]Lagos, Nigeria, [7]Obafemi Awolowo University Teaching Hospital, Ile Ife, Nigeria

Disclosures: Olanrewaju Ajetunmobi: None; Uta Drebber: None; Reinhard Buettner: None; Donatus Dzuachii: None; Solomon Raphael: None; Olubanji Oguntunde: None; Oluwole Odujoko: None

Background: The Human Epidermal Receptor[HER] family of receptor tyrosine kinases have been linked to downstream genetic pathways that result in uncontrolled proliferation. Members of this family, such as HER2 and EGFR proteins are overexpressed in several epithelial malignancies and serve as effective therapeutic targets in cancer management. However their role in prostate cancer development have been sparingly explored and with contrasting findings. Notably their relationship with prostate cancers cases seen in Sub-Saharan Africa are yet to be explored.

Design: A retrospective study involving histologically diagnosed cases of aednocarcinomas of the prostate, seen at a tertiary health facility in Makurdi, North-central Nigeria. Cases were classed according to the WHO/ISUP Gleason Prognostic groups[G1-G5]. Immunohistocehmical analysis was performed using monolconal antibodies for HER2 and EGFR, while in situ hybridization was carried out utilizing gene probes for the corresponding genes. Scores of +2 and +3 were regarded as positive for both antibodies, while a target gene:centromere ratio of >2 was set as the threshold for amplification. Patients characteristics, Gleason scores, expression profiles of HER2 and EGFR proteins as well as of their corresponding genes, were represented using frequency tables, graphs and charts

Results: A total of 44 cases were included in the study. The acinar type was the commonest morphologically, with Gleason group 5[Gleason scores 8-10] accounting for close to half o the cases [47-7%]. The median age of incidence was 63yrs while the peak age was between 51 and 60yrs. The HER2 antibody stained negative in the majority of cases [93.2%], being positive in only 3[6.8%] of cases seen. High level expression of EGFR [+2/+3]was observed in 25% of cases , low level expression was identified in 6 [13.6%] cases. All cases with HER2 positive malignancies displayed overexpression of EGFR. In situ-hybridization revealed the absence of high level amplification for both HER2 and EGFR, while polysomy was not detected in any of the cases.

Variable	Frequency	Percentage
Age Range	0	0
<40	3	6.8
41-50	15	34.1
51-60	12	27.3
61-70	9	20.4
71-80	4	9.1
>80	1	2.3
Not stated	**44**	**100**
Total		
Histologic type	38	86.4
Acinar	2	4.5
Ductal	4	9.1
Mixed	**44**	**100**
Total		
Gleason Group	11	25.0
G1 (≤6)	8	18.2
G2 (3+4)	4	9.1
G3 (4+3)	4	9.1
G4 (8)	17	38.6
G5 (>8)	**44**	**100**
Total		
Specimen type	3	6.8
Prostatectomies	41	93.2
Needle biopsies	**44**	**100**
Total		

Table 1: Summary of patient characteristics

Figure 1 - 780

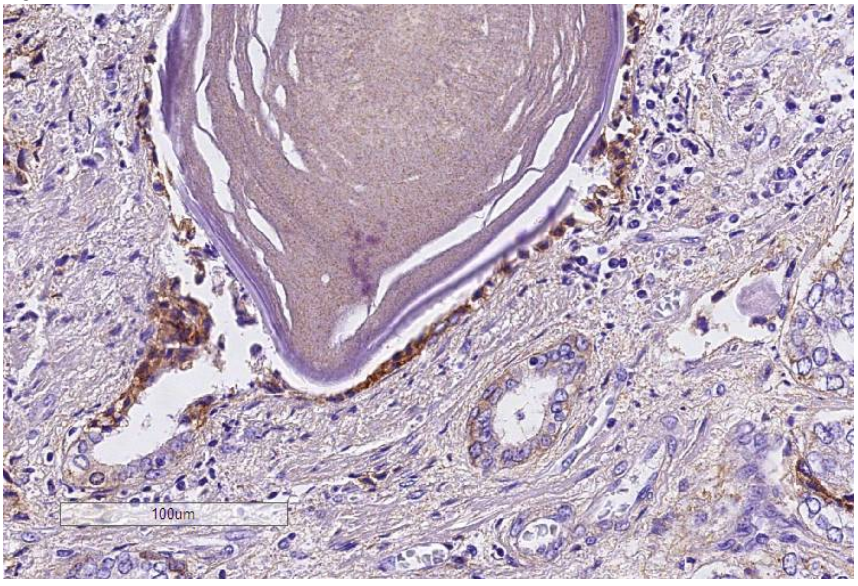

Figure 2 - 780

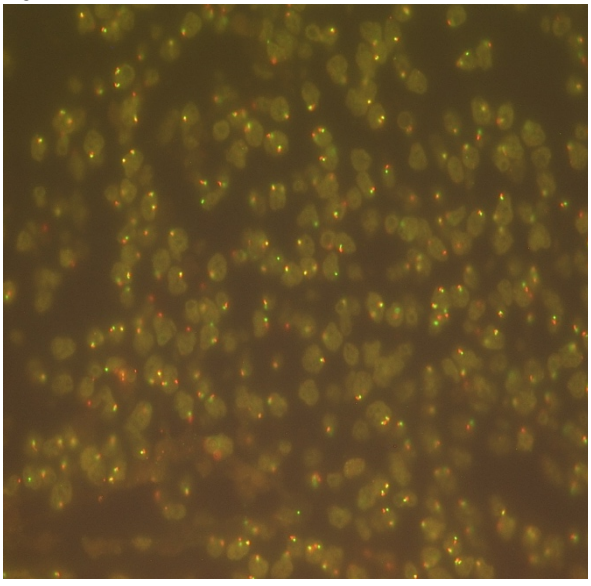

Conclusions: The overexpression of EGFR in prostate cancers has been demonstrated in a native African population, affirming its suitability for targeted therapy. Overexpression of HER2 in prostate cancer is inconstant, and amplifcation of the HER2 gene is less frequent than as compared to malignacies of the Breast and Ovary. There's a need for a standardized protocol for assessing HER2 in prostate cancer.

NB: This study was funded by the UICC.

781 TP53 and PTEN Mutational Status and Outcome Prediction in Chromophobe Renal Cell Carcinoma

Mahmut Akgul[1], Taebeom Kim[2], Yuan Qi[1], Nail Alouch[3], Paari Murugan[4], Steven Shen[5], Fadi Brimo[6], Priya Rao[1], Pheroze Tamboli[1], Ken Chen[1], Kanishka Sircar[1]
[1]The University of Texas MD Anderson Cancer Center, Houston, TX, [2]Pearland, TX, [3]Creighton University, Omaha, NE, [4]University of Minnesota, Minneapolis, MN, [5]Houston Methodist Hospital, Houston, TX, [6]McGill University, Montreal, QC

Disclosures: Mahmut Akgul: None; Taebeom Kim: None; Yuan Qi: None; Nail Alouch: None; Paari Murugan: None; Steven Shen: None; Fadi Brimo: None; Priya Rao: None; Pheroze Tamboli: None; Ken Chen: None; Kanishka Sircar: None

Background: Chromophobe renal cell carcinomas (ChRCC) are usually indolent with approximately 5% of cases exhibiting aggressive clinical behavior. Histologic assessment is of limited utility in predicting behavior due to the lack of a validated grading system in ChRCC. Though large scale genomic studies of ChRCC have been conducted, molecular markers are not used clinically for risk prediction. The aim of this study was to assess whether molecular assays could help to differentiate indolent from aggressive ChRCC in a clinical setting.

Design: We defined aggressive ChRCC as showing recurrence, metastasis or sarcomatoid features and indolent ChRCC as lacking these attributes. We extracted DNA from formalin fixed paraffin embedded tissues of a multi-institutional cohort of 16 aggressive ChRCC cases. Paired tumor and normal samples were subject to targeted sequencing of coding regions from 261 cancer related genes (HiSeq3000, Illumina, San Diego, CA). Public sequencing data from 49 aggressive and 95 indolent ChRCC were examined *in silico* and were added to our analysis.

Results: The most commonly mutated genes in ChRCC were *TP53* (60/160, 37%) and *PTEN* (27/160, 17%), respectively. Aggressive ChRCC showed enrichment for mutations in *TP53* (p=0.00022) and *PTEN* (p=0.0002) compared to indolent ChRCC, and mutations in either gene were associated with decreased survival (p=0.00058). Assuming a pre-test probability of aggressive ChRCC of 5%, patients with isolated *TP53* or *PTEN* mutations had a higher risk of developing aggressive disease: *TP53*, OR=3.67; LR=2.19; post-test probability 10%; *PTEN*, OR=5.59; LR=4.18; post-test probability 18%. Seventeen patients harbored both *TP53* and *PTEN* mutations; and having double *TP53/PTEN* mutations significantly increased the post-test probability of aggressive disease to 33%. By contrast, ChRCC that lacked either *TP53* or *PTEN* mutations (n=91) only showed a 3% post-test probability of aggressive disease.

Conclusions: Despite the rarity of aggressive ChRCC, targeted sequencing of ChRCC samples in a clinical setting provides information that may help to risk stratify patients and inform decisions made by physicians and patients.

782 Leptin Expression is Significantly Associated with Poor Prognosis in Urinary Bladder Carcinoma Patients

Jaudah Al-Maghrabi[1], Mohamad Nidal Khabaz[2], Imtiaz Qureshi[1], Nadeem Butt[2], Basim Al-Maghrabi[3]
[1]King Abdulaziz University, Jeddah, Saudi Arabia, [2]Rabigh Faculty of Medicine, King Abdulaziz University, Jeddah, Saudi Arabia, [3]University of Jeddah, Jeddah, Saudi Arabia

Disclosures: Jaudah Al-Maghrabi: None; Mohamad Nidal Khabaz: None; Imtiaz Qureshi: None; Nadeem Butt: None; Basim Al-Maghrabi: None

Background: This study investigated a mutual relationship between leptin immunophenotype and the clinical parameters in urinary bladder cancer.

Design: A set of 128 urinary bladder cancer cases and 24 samples of normal bladder tissue were utilized for an immunohistochemical detection of leptin expression using tissue microarrays.

Results: Leptin was identified as brown cytoplasmic granules in 60 (46.87%) urinary bladder tumors, while 12 (50%) control cases showed leptin expression. Strong immunohistochemical leptin staining in transformed epithelial cells has been found to be considerably correlated with high stages (P=0.001), muscularis propria infiltration (P=0.000), vascular invasion (P=0.024), lymph node involvement (P=0.015), metastases (P=0.043), and the alive/deceased status (P=0.024). On the other hand, leptin immunoexpression in stromal cells has been found to be significantly associated with high grades (P=0.033) and muscularis propria infiltration (P=0.003). Furthermore, Significant different survival distributions have been observed with leptin staining of transformed epithelium (P-Value=0.026), but they have not been observed with leptin staining of stromal cells. High leptin staining of transformed epithelial cells is positively associated with poor survival.

Conclusions: Our findings suggest a great value for using leptin immunostaining in predicting the prognosis of bladder carcinoma. These pilot results propose that leptin might be a valued biomarker for predicting grade, stage, and bad prognosis in urinary bladder cancer.

783 Atrophic Kidney-Like Tumor: Clinical and Pathological Analysis of a Distinct Provisional Entity

Khaleel Al-Obaidy[1], Liang Cheng[1], John Eble[1], Carlos Ribeiro[2], Ghazi Zaatari[3], Muhammad Idrees[1], David Grignon[1]
[1]Indiana University School of Medicine, Indianapolis, IN, [2]IRA - Instituto Roberto Alvarenga, Belo Horizonte, MG, Brazil, [3]American University of Beirut, New York, NY

Disclosures: Khaleel Al-Obaidy: None; Liang Cheng: None; John Eble: None; Carlos Ribeiro: None; Ghazi Zaatari: None; Muhammad Idrees: None; David Grignon: None

Background: Atrophic kidney-like tumor (ALKT) is a rare renal neoplasm that was described in 2014 by Hes et al. In that report, 3 cases of a distinct primary renal tumor simulating atrophic kidney were described. Subsequently, 3 additional cases from 2 patients have been reported. We described the morphologic, immunohistochemical and selected molecular analysis of 3 additional cases

Design: We reviewed the clinicopathologic characteristics of 3 ALKTs diagnosed at Indiana University. Immunohistochemical studies (WT-1, TFE-3, CD10, cytokeratin AE1/AE3, CK7, PAX-8, CD34, ERG, BRAF, cathepsin K, and TTF-1), FISH analysis for X:1 translocation and BRAF V600E mutation were performed

Results: The cohort comprised of 2 male and 1 female patients, all had no significant medical history. The ages at time of diagnosis were 16, 21 and 42 years. The youngest patient had been followed up radiologically for 3 years before resection with no change in tumor size. All tumors were stage pT1a. Grossly, all tumors were well-circumscribed, tan-yellow in color. The maximum dimensions were 2.5, 2.6, and 3.5 cm. Microscopically, the tumors were surrounded by a smooth muscle capsule, and formed of variable-sized cysts filled by eosinophilic secretions. The cysts are lined by either by a single layer of flat or cuboidal cells with ovoid or rounded nuclei, respectively. Occasionally, the cells are detached and displaced into the cysts' lumens where they had a rounded nuclear morphology. Collapsed cysts and entrapped tubules of variable size are seen between the larger cysts. The stroma was collagenized with numerous calcifications and extensive vascular channels. Immunohistochemically, the most consistent finding was the diffuse WT-1, CD10, TFE3 and AE1/AE3 positivity. PAX-8 differentially stained entrapped tubules' and most of the flat cells' nuclei. CK7 stained entrapped tubules. CD34 and ERG highlighted the extensive vascularity. BRAF, cathepsin K, and TTF-1 were negative. Given the TFE3 and WT-1 positivity, FISH analysis for X:1 and BRAF mutation were performed on one case (youngest patient) and both were negative. Over a range follow up period of 1-16 years, no evidence of tumor recurrence or metastasis was present

Conclusions: ALKT is very rare tumor. In addition to its distinct morphology; the consistent diffuse WT-1 positivity is similar to tumors of metanephric origin; however, none expressed BRAF and one case tested lacked *BRAF* V600E mutation. All 9 reported cases thus far, including ours, behaved in a benign fashion

784 L-1 Cell Adhesion Molecule (L1CAM) is a Sensitive and Specific Marker for Paratesticular Adenomatoid Tumors

Khaleel Al-Obaidy[1], Thomas Ulbright[1], Muhammad Idrees[1]
[1]*Indiana University School of Medicine, Indianapolis, IN*

Disclosures: Khaleel Al-Obaidy: None; Thomas Ulbright: None; Muhammad Idrees: None

Background: Adenomatoid tumor (AT) is the most common benign paratesticular appendageal lesion, accounting for 30% of cases. It usually presents as a painless mass or is found incidentally at autopsy or in orchiectomies. It is composed of cords and tubules of cuboidal cells with vacuolated cytoplasm in fibrous stroma. The shared immunohistochemical markers with mesothelial cells (calretinin and WT-1) indicate its mesothelial origin. Cases with atypical features, such as necrosis, high cellularity or invasive growth, may be challenging, especially in the distinction from malignant mesothelioma (MM). A recent study found activating mutations in the *TRAF7* gene that led to increased expression of L1CAM in a limited number of epididymal ATs but not in 7 peritoneal MMs. We therefore studied L1CAM expression in an expanded group of paratesticular ATs versus its primary differential consideration, paratesticular MM.

Design: A retrospective search of the pathology electronic medical record was performed for paratesticular AT and MM diagnosed between 1990 and 2018. Hematoxylin and eosin stained slides of each case were reviewed to confirm the diagnosis and additional unstained sections were obtained for immunohistochemical studies. Sections of 4 µm thickness were stained with antibodies directed against calretinin, WT-1, podoplanin (D2-40) and L1CAM in a Dako automated instrument. Positive and negative controls gave appropriate results for each stain.

Results: The cohort comprised 15 cases of AT and 14 cases of MM. The median ages were 40 years (range, 21-74) and 57 years (range, 24-85), respectively and the median tumor sizes were 1.1 cm (range, 0.6-3) and 6.8 cm (range, 1-8.5), respectively. Atypical pathologic features in the AT cases included: tumor infarction (n=7), and increased cellularity (n=2). On immunohistochemical staining, only L1CAM expression in AT (at least focal positivity in 15/15 cases) showed a significant difference versus MM (1/7 cases; p=<0.0001). Calretinin, nuclear WT-1 and podoplanin (D2-40) were positive in 14/14, 7/7, and 5/5 cases of AT and 14/14, 8/8, and 7/7 cases of MM, respectively (Table 1). No staining for L1CAM of the mesothelial lining of the tunica vaginalis was observed in any case.

Table 1: Immunohistochemical properties of adenomatoid tumors and malignant mesothelioma.

Stain	Adenomatoid tumor		Malignant mesothelioma		P-value
	No. of cases	%	No. of cases	%	
L1CAM	15/15	100	1/7	14.3	<0.0001
Calretinin	14/14	100	14/14	100	1.0
WT-1	7/7	100	8/8	100	1.0
D2-40 (Podoplanin)	5/5	100	7/7	100	1.0

Conclusions: Our results indicate that L1CAM is a reliable marker of paratesticular AT and assists with its distinction from paratesticular MM.

785 Thyroid-Like Follicular Renal Cell Carcinoma: Clinical and Pathological Analysis of a Distinct Provisional Entity

Khaleel Al-Obaidy[1], John Eble[1], Liang Cheng[1], Muhammad Idrees[1], David Grignon[1]
[1]*Indiana University School of Medicine, Indianapolis, IN*

Disclosures: Khaleel Al-Obaidy: None; John Eble: None; Liang Cheng: None; Muhammad Idrees: None; David Grignon: None

Background: Thyroid-like follicular renal cell carcinoma (TLF-RCC) is a rare renal tumor that was first described by Amin et al in 2004. In that report, cases of a distinct primary renal tumor simulating thyroid follicles were described. To date, 34 cases have been reported. We describe the morphologic and immunohistochemical analysis of 3 additional cases.

Design: We reviewed the clinicopathologic characteristics of 3 TLFRCC diagnosed at Indiana University. A retrospective systematic review of morphologic features as well as immunohistochemical staining studies (PAX8, CK7, CK19, cyclin D1, L1CAM, AMACR, WT-1, TTF1, and thyroglobulin) was performed on all cases.

Results: The cohort comprised ~~of~~ 3 female patients. The ages at time of diagnosis were 25, 40 and 58 years. In the youngest patient, the renal mass had been followed for 7 years without a significant change in size; however~~,~~ after a biopsy was performed the mass was resected. The maximum dimensions were 3.8, 4, and 5.6 cm. Two were stage~~s~~ pT1a and 1 was pT3a (case 3, renal sinus invasion). Microscopically, the tumors were unencapsulated, with closely packed anastomosing follicles filled by eosinophilic secretions of variable density. The cysts were lined by cuboidal cells with oval to rounded nuclei with mild to moderate pleomorphism ~~and were~~ arranged perpendicular to the lumen, giving a rosette-like appearance. The intervening stroma was minimal; however, areas of loosely packed follicles with more abundant stroma and associated inflammation were also present. In one case, thick-hyalinized stroma with compressed

follicles was seen (case 2). This contained numerous cholesterol clefts and abundant lymphoid inflammation. No calcifications or necrosis were present. Immunohistochemically, tumors were positive for PAX8 (3/3), CK7 (3/3), CK19 (2/3), cyclin D1 (3/3), L1CAM (3/3), AMACR (1/2) and were negative for WT-1, TTF1, and thyroglobulin. Over a follow up period of 1-7 years, no evidence of tumor recurrence or metastasis was present.

Conclusions: Overall, our study highlights a consistent morphologic features of TLF-RCC as well a unique and relatively consistent immunophenotypic pattern. Our findings suggests that so-called Thyroid-like follicular renal cell carcinoma remains a distinct diagnostic entity from other types of renal cell carcinoma.

786 Molecular Characterization of Rare Aggressive Prostate Cancer Variants Adenosquamous Carcinoma, Pleomorphic Giant Cell Carcinoma, and Sarcomatoid Carcinoma: An Analysis of 10 Cases

Mohamed Alhamar[1], Ioan Vladislav[2], Steven Smith[3], Liang Cheng[4], Lisa Whiteley[5], Shannon Carskadon[5], Nilesh Gupta[5], Juan Gomez-Gelvez[6], Dhananjay Chitale[7], Nallasivam Palanisamy[5], Sean Williamson[5]
[1]Henry Ford Health System, Dearborn, MI, [2]Phoenix, AZ, [3]Virginia Commonwealth University School of Medicine, Richmond, VA, [4]Indiana University School of Medicine, Indianapolis, IN, [5]Henry Ford Health System, Detroit, MI, [6]Henry Ford Hospital, Detroit, MI, [7]Henry Ford Hospital, West Bloomfield, MI

Disclosures: Mohamed Alhamar: None; Ioan Vladislav: None; Steven Smith: *Consultant*, Elsevier/Amirsys Publishing; Liang Cheng: None; Lisa Whiteley: None; Shannon Carskadon: None; Nilesh Gupta: None; Juan Gomez-Gelvez: None; Dhananjay Chitale: None; Nallasivam Palanisamy: None; Sean Williamson: None

Background: Adenosquamous, pleomorphic giant cell, and sarcomatoid prostate cancers are extremely rare variants. Although their biologic behaviors are highly aggressive, little is known regarding their molecular features.

Design: We retrieved 10 cases of prostate cancer with one or more of these variants in either the primary tumor or metastases. Paraffin tissue blocks were tested with a solid tumor gene fusion detection assay via next-generation sequencing (NGS), targeting over 50 known genes involved in recurrent fusions. Fluorescence in-situ hybridization (FISH) analysis was performed using bacterial artificial chromosome (BAC) derived break-apart probes against *ERG* and *BRAF*.

Results: Divergent differentiation included: sarcomatoid (n=6), adenosquamous (n=5), and pleomorphic giant cell carcinoma (n=2). Four patients had more than one variant, all of which were adenosquamous and sarcomatoid. Divergent differentiation was present only in metastases for 3 patients. *ERG* rearrangement was detected in 4 tumors (3 via NGS, showing *TMPRSS2-ERG* fusion, and 1 via FISH, showing rearrangement via deletion). Two tumors (20%) were detected to harbor *BRAF* gene fusion by NGS and FISH, with fusions being *FAM131A-BRAF* and *SND1-BRAF*. Three patients had histologically disparate tumors at different sites (adenosquamous carcinoma only in lymph nodes, separate adenosquamous and sarcomatoid metastases, and conventional vs pleomorphic carcinoma in 2 different metastatic sites). Of these, 2 were confirmed to have the same fusion in both components, whereas 1 had insufficient material to study the 2nd site. The remaining 4 cases were uninformative, with inadequate NGS QC metrics and/or FISH signals. One of these had *ERG*+ FISH in a low-grade adenocarcinoma component but negative FISH in the sarcomatoid component, suggesting two different clones.

Conclusions: *ERG* gene fusions are present in these rare prostate cancer variants with a similar frequency to conventional prostate cancer (4/10), and adenosquamous and sarcomatoid variants sometimes occur together. The presence of 2 *BRAF* gene rearrangements, although limited due to the small number of cases, suggests that this rare gene fusion may be enriched in this setting, as RAF kinase fusions usually account for 1-2% of prostate cancers. Further study will be helpful to determine whether this frequency is reproduced in larger cohorts and whether therapy targeting BRAF may be of value in patients with rearranged tumors.

787 Prognostic Significance of Pathologic Features of Lymph Node Metastasis in Prostate Cancer (PCa): A Study of 280 Cases

Mohamed Alhamar[1], Absia Jabbar[2], Mustafa Deebajah[3], Mireya Diaz-Insua[4], Sean Williamson[3], Shaheen Alanee[3], Daniel Schultz[3], Nilesh Gupta[3]
[1]Henry Ford Health System, Dearborn, MI, [2]Henry Ford Health System, Aurora, CO, [3]Henry Ford Health System, Detroit, MI, [4]Henry Ford Health System, Portage, MI

Disclosures: Mohamed Alhamar: None; Absia Jabbar: None; Mustafa Deebajah: None; Mireya Diaz-Insua: None; Sean Williamson: None; Shaheen Alanee: None; Daniel Schultz: None; Nilesh Gupta: None

Background: To determine the prognostic value of the number of positive lymph nodes (LN), extranodal extension (ENE), size and Grade Group (GG) of metastatic focus (MET) in PCa.

Design: We evaluated biochemical recurrence (BCR) in 280 node positive cases who underwent radical prostatectomy (RP) between 2006-2018 at our institution. Cases with prior treatment and known metastasis at the time of surgery were excluded. Parameters recorded included number & size of positive LN. Size & GG of largest MET & ENE were also noted.

Results: Average follow up period was 13.4 months. The Average number of LN retrieved was 14.7 with an average of 2 positive LN per case. ENE was identified in 99/244 (41%). Size of the largest positive LN was 10 mm or less in 71% of the cases. The size of the largest MET was $\leq$ 2 mm (micrometastasis) in 107/261 cases (41%); was > 2 mm (macrometastasis) in 154/261 (59%) of the cases. A solitary LN positive was found in 166/280 (59%) of the cases, 95/280 (34%) had 2-4 LN positive, and 19/280 (7%) had 5 or more LN positive. GG of the MET was as follows GG1-2: 29/224(13%); GG3: 27/224 (12%); GG4-5: 168/224 (75%).

RP pathology showed GG3 and higher in 85% of the cases, high volume disease in (77%), non-organ confined cancer in 96% with 35% showing extraprostatic extension & 61% showing seminal vesicle invasion (Table 1).

1. Minute metastatic foci (0.1 - 2 mm) were associated with lower BCR rate (micrometastasis) compared to metastatic foci > 2 mm in size (macrometastasis). [Figure 1a]

2. The differentiation of PCa within LN was significantly associated with BCR. BCR rate increased as GG increased. [Figure 1b]

3. The number of positive LN (categorized as 1, 2-4 and > 5) & the presence of ENE were significantly associated with BCR.[Figure 2a-2b]

4. No significant differences were observed in unilateral vs bilateral involvement of the LN. [Figure 2c]

PATHOLOGIC VARIABLE	NUMBER OF CASES
GRADE GROUP	
• **2**	30 (11%)
• **2 WITH MINOR 5**	13 (5%)
• **3**	34 (12%)
• **3 WITH MINOR 5**	45 (16%)
• **4**	36 (13%)
• **5**	122 (44%)
TNM STAGE	
• **T2**	11 (4%)
• **T3a**	98 (35%)
• **T3b**	170 (61%)
• **T4**	1 (0.4%)
SURGICAL MARGINS	
• **NEGATIVE**	128 (46%)
• **POSITIVE**	152 (54%)
TUMOR VOLUME	
• **1-14%**	65 (23%)
• **15-49%**	155 (55%)
• **50-100%**	60 (21%)
NUMBER OF POSITIVE LYMPH NODE(S)	
• **1**	166 (59%)
• **2-4**	95 (34%)
• **>5**	19 (7%)
SIZE OF METASTASIS	
• **MICROMETASTASIS (0.1-2mm)**	107 (41%)
• **MACROMETASTASIS (>2mm):** **- 2-5 mm** 81 cases **- >5-10 mm** 40 cases **- >10 mm** 33 cases	154 (59%)

Figure 1 - 787

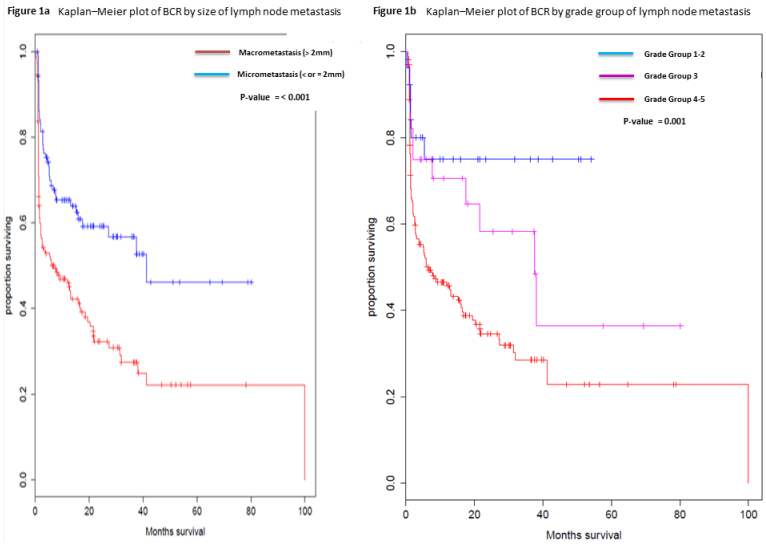

Figure 2 - 787

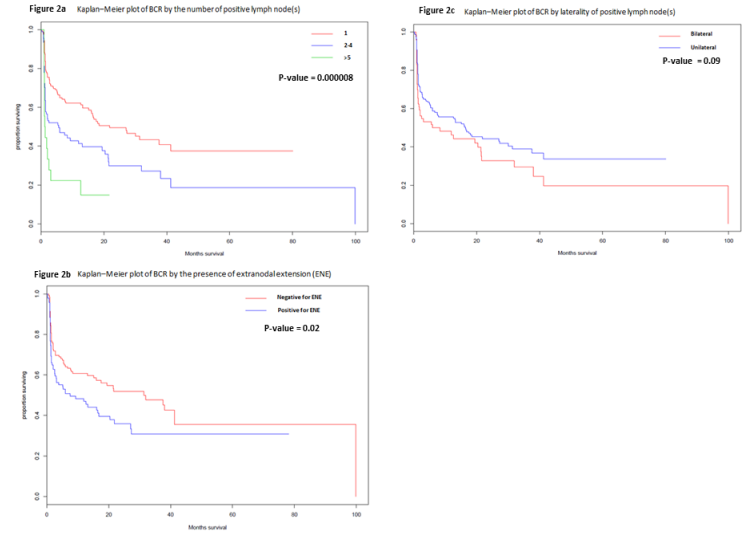

Conclusions: 1.The current TNM classification for PCa includes only N0 and N1 categories. It does not stratify based on number of positive LN or size of metastatic focus. In our study, we demonstrate that both of these factors are significant predictors of BCR. In addition, we found that GG of metastatic focus and ENE are clinically significant parameters. We recommend reporting these additional findings when assessing LN in cases of PCa.

2.The size of the largest positive LN was <= 10 mm in more than 2/3 of our cohort. These LN are difficult to detect as positive or suspicious on imaging evaluation in the pre-operative setting.

788 Aggressive Tubulocystic Carcinomas of the Kidney: A Clinical, Pathological and Immunohistochemical Study

Isabel Alvarado-Cabrero[1], Denisse Ramírez-González[2], Rafael Estevez-Castro[3], Ana Elena Martin-Aguilar[4], Raquel Valencia-Cedillo[5]
[1]Mexican Oncology Hospital IMSS, Mexico, MEX, Mexico, [2]Hospital de Especialidades, Centro Médico Nacional, IMSS, Mexico City, DF, Mexico, [3]Laboratorio de Patologia Dra. Rosario Castro, Santiago, Dominican Republic, [4]Hospital de Oncologia, CMN Siglo XXI IMSS, Mexico, MEX, Mexico, [5]Mexican Oncology Hospital IMSS, Cd Mexico, MEX, Mexico

Disclosures: Isabel Alvarado-Cabrero: None; Denisse Ramírez-González: None; Rafael Estevez-Castro: None; Ana Elena Martin-Aguilar: None; Raquel Valencia-Cedillo: None

Background: Tubulocystic renal cell carcinoma (TCRCC) is a rare renal tumor with distinct characteristics which was recognized as a new entity in 2012. The majority of cases reported to date have been stage T1 at presentation. Prognosis is usually excellent with only rare distant metastases or death from disease.

The aim of this study was to examine the clinicopathologic and immunohistochemical features of 25 patients with TCRCC with aggressive clinical course.

Design: Retrospective study of 5,000 renal cell carcinoma cases identified by an inpatient database during the period 2008-2017. Immunohistochemical labelling for AMACR, CK7, CK8, CK19, PAX 8, CD10 and carbonic anhydrase IX was assessed in all tumors.

Results: The patient´s age ranged from 26-72 years (mean 52 years), and the ratio of men to women was 2:1. The tumor sizes ranged from 6 cm to 20 cm (mean 8.5 cm) Histologically, all tumors were composed of closely packed tubules and cysts of varying sizes separated by fibrovascular septa. Tumor necrosis was seen in 14 cases and 8 cases had poorly differentiated areas. None of the cases coexisted with papillary renal cell carcinoma.

Immunohistochemistry revealed that all of the cases expressed AMACR, CK7, CK8, CK19, PAX 8, CD10 and carbonic anhydrase IX. Six tumors were stage pT2, 16 stage pT3 and 3 stage pT4.

Follow-up timeframe ranged from 12 months to 6 years. Disease progression ocurred in 23 patients, 11 with local recurrence and 12 with distant metastases to para-aortic lymph nodes, bone and liver. Two patients had wide spread intraabdominal metastases. Of the 25 patients, 15 are alive with disease and 10 died of disease.

Conclusions: Our data support that TCRCC is not always an indolent tumor with a good prognosis.

This is the first large series of TCRCC with an aggressive behavior.

789 Detailed Morphologic and Genetic Features of Urothelial Carcinoma in Patients with Lynch Syndrome

Bayan Alzumaili[1], Henning Reis[2], Jinru Shia[1], Anuradha Gopalan[1], Ying-Bei Chen[1], Samson Fine[1], S. Joseph Sirintrapun[1], Maria Arcila[1], Satish Tickoo[3], Michael Berger[1], Jonathan Coleman[1], David Solit[1], Victor Reuter[1], Gopa Iyer[3], Hikmat Al-Ahmadie[1]
[1]Memorial Sloan Kettering Cancer Center, New York, NY, [2]West German Cancer Center, University of Duisburg-Essen, Essen, Germany, [3]New York, NY

Disclosures: Bayan Alzumaili: None; Henning Reis: None; Jinru Shia: None; Anuradha Gopalan: None; Ying-Bei Chen: None; Samson Fine: None; S. Joseph Sirintrapun: None; Maria Arcila: None; Satish Tickoo: None; Michael Berger: *Advisory Board Member*, Roche Jonathan Coleman: None; David Solit: *Consultant*, Pfizer Inc.; *Consultant*, Loxo Oncology; *Consultant*, Illumina; Victor Reuter: None; Gopa Iyer: None; Hikmat Al-Ahmadie: None

Background: Urothelial carcinoma (UC) is the 3rd most common cancer in Lynch syndrome (LS) patients, preferentially developing in upper urinary tract. Only few studies and limited number of cases provide detailed morphologic and genomic features of these tumors. We report the morphologic and genetic spectrum of UC from LS patients that were detected by prospective next generation sequencing (NGS).

Design: The study includes 21 tumors from LS patients that underwent targeted NGS for tumor-germline pairs by MSK-IMPACT. Detailed histopthologic evaluation and immunohistochemistry for four mismatch repair proteins was performed on all cases.

Results: Tumor locations were renal pelvis (n=13, 62%), distal ureter (n=6, 29%) and bladder (n=2, 9%). Male:female distribution was 14:7 and age ranged from 31 to 86 years (median = 61). Upper tract tumors were 10 from the right and 9 from the left. All tumors exhibited papillary or polypoid morphology, 19 were high grade (90%) and 2 low grade (10%). Eight tumors (38%) were non-invasive (pTa), 5 were pT1 (24%), 1 was pT2 (5%) and 7 were pT3 (33%). Common histologic features include infiltrating borders (11, 52%), pushing edges (10,

48%), syncytial/solid growth (16, 76%), cytoplasmic basophilia (17, 81%), high N:C ratio with absent or minimal nuclear pleomorphism (15, 71%) and focal cystic change (5, 24%). Intratumoral lymphocytes ranged from 3-123 cells/10hpf (median 53). By IHC, 14 tumors (67%) lacked both MSH2 and MSH6 expression, 9 of which were associated with MSH2 germline mutation. In 4 tumors (19%), MSH6 expression was absent, all associated with MSH6 germline mutation and in 2 tumors (10%), MLH1 and PMS2 were absent, both were associated with MLH1 germline mutation. In one tumor from a patient with MSH2 germline mutation all 4 markers were retained. In 5 patients whose tumors lacked MSH2 and MSH6 expression, no germline mutations were detected in the 4 genes. The number of mutations per tumor ranged from 17 to 417 (median = 63). Hotspot mutations in *FGFR3* were identified in 15 tumors (71%), 12 of which were R248C and 2 were Y373C.

Conclusions: In patients with LS, urothelial carcinoma can develop in both upper and lower tracts but is significantly more common in renal pelvis and distal ureter than in the bladder. MSH2 germline alterations are the most common, but mutations in MLH1 or MSH6 can also be detected in this setting. These tumors are generally associated with high mutation rate and frequent FGFR3 hotspot mutations, particularly R248C.

790 Cellular Senescence in End Stage Renal Disease-Associated Renal Cell Carcinoma: Too Much of a Good Thing?

Joanne Ang[1], Katarzyna Brzezinska[1], Suganthi Soundararajan[2], Rekha Bhat[3], Claudio Torres[3], Christian Sell[1], Rhonda Binnebose[3]
[1]Drexel University College of Medicine, Philadelphia, PA, [2]Drexel College of Medicine, Philadelphia, PA, [3]Drexel University, Philadelphia, PA

Disclosures: Joanne Ang: None; Katarzyna Brzezinska: None; Suganthi Soundararajan: None; Rekha Bhat: None; Claudio Torres: None; Christian Sell: None; Rhonda Binnebose: None

Background: Induction of senescence is a potent tumor-suppressive mechanism, since cells are placed in a state of cell cycle arrest. However, a subset of renal cell carcinoma (RCC) that develops in patients with end stage renal disease (ESRD) on hemodialysis present an interesting conundrum with respect to senescence, namely, a non-functioning organ becomes neoplastic. Oxidative stress may be the trigger that activates a senescence program and promotes neoplastic transformation. Our study examines the differences in senescence markers in RCC arising in the background of ESRD (RCC-ESRD) and compare it to RCC arising de novo (RCC-Non-ESRD) to define the role of senescence in these tumors.

Design: Archived paraffin embedded tissue blocks of kidneys from the Department of Pathology and Laboratory Medicine were retrieved and divided into the following groups: RCC-ESRD and RCC-Non-ESRD. Immunohistochemical expression of cellular senescence markers (p16 and p21) was assessed using a semi-quantitative scoring (0-20%, 20-50% and >50%); with positive p16 and p21 expression set at a cutoff value of ≥20%.

Results: Of the 44 cases of RCC included (23 RCC-ESRD, 21 RCC-Non-ESRD), papillary RCC accounted for 45% (20/44); and clear cell type accounted for 50% (22/44). (See Table)

RCC-ESRD expressed significantly more p16 as compared to RCC-Non-ESRD (34 ± 35 vs. 13 ± 26; Mean ± S.D, $p<0.05$). RCC-ESRD papillary type expressed significantly more p16 as compared to RCC-Non-ESRD papillary type (22 ± 32 vs. 1 ± 2; Mean ± S.D, $p<0.05$). Conversely, RCC-Non-ESRD papillary type expressed more p21 as compared to RCC-ESRD papillary type; although it did not reach statistical significance (28 ± 34 vs. 3 ± 6; Mean ± S.D, $p=0.059$). Statistical testing was performed using student t-test. There was one case of RCC-ESRD, unclassified type, which was both p16 and p21 positive; and one case of RCC-Non-ESRD, chromophobe type, that was p16 positive and p21 negative.

Percentage of cases with positive expression of p16 and p21				
Number of cases	**With ESRD**		**Without ESRD**	
	p16 %(positive/total)	p21 %(positive/total)	p16 %(positive/total)	p21 %(positive/total)
Clear cell RCC	50 (5/10)	40 (4/10)	42 (5/12)	50 (6/12)
Papillary RCC	33 (4/12)	8 (1/12)	0 (0/8)	50 (4/8)
Total RCC	41 (9/22)	23 (5/22)	25 (5/20)	50 (10/20)

Conclusions: Senescence is a potent tumor suppressive mechanism. However, our results show that there is a significant accumulation of p16 in RCC-ESRD as compared to RCC-Non-ESRD. This may indicate that senescence has a pro-oncogenic effect in the setting of ESRD, which may be due to the secretion of inflammatory cytokines, induction of cell proliferation and eventual tumor progression. Interestingly, this effect appears more pronounced in the subset of RCC-ESRD with papillary type morphology. Modulation of senescence may play a role in delaying progression to RCC-ESRD.

791 BCOR-Overexpressing Malignant Renal/Perirenal Solitary Fibrous Tumor: A Close Mimic of Clear Cell Sarcoma of the Kidney

Pedram Argani[1], Brendan Dickson[2], David Swanson[3], Rita Alaggio[4], Yun-Shao Sung[5], Cristina Antonescu[5]
[1]Johns Hopkins Hospital, Ellicott City, MD, [2]Mount Sinai Health System, Toronto, ON, [3]Mount Sinai Hospital, Toronto, ON, [4]University of Pittsburgh Medical Center, Pittsburgh, PA, [5]Memorial Sloan Kettering Cancer Center, New York, NY

Disclosures: Pedram Argani: None; Brendan Dickson: None; David Swanson: None; Rita Alaggio: None; Yun-Shao Sung: None; Cristina Antonescu: None

Background: Clear cell sarcoma of the kidney (CCSK) mimics- and is mimicked by- a wide variety of other renal neoplasms. Its diagnosis is typically confirmed by BCOR immunopositivity, which is a sensitive and specific marker of CCSK in the context of other pediatric renal neoplasms. However, a subset of adult BCOR-positive renal tumors is negative for *BCOR* genetic alterations, including *BCOR* fusions or *BCOR*-Internal Tandem Duplication (ITD), and thus remains unclassified. We report four such undifferentiated renal/perirenal sarcomas which raised the differential diagnosis of CCSK due to their morphologic appearance and strong BCOR expression, but which on RNA sequencing (RNA-Seq) proved to be malignant solitary fibrous tumors (SFTs).

Design: The four cases derive from the consultation files of the authors and were originally considered as unclassified/undifferentiated renal sarcomas, closely resembling CCSK. All four cases were studied by targeted RNA-seq using the TruSight RNA Fusion Panel (Illumina, San Diego, CA), for further characterization.

Results: All four cases demonstrated a *NAB2-STAT6* gene fusion. The cases occurred in 3 females and 1 male, age range 30-62 years. Three were primary renal neoplasms while one was perirenal. All four neoplasms were cellular, non-pleomorphic sarcomas which demonstrated branching capillary vasculature and ovoid cells with round nuclei with uniformly-dispersed chromatin, similar to the morphology of CCSK. Cellular areas overlapped with other small round blue cell tumors of childhood. None of the cases demonstrated the typical prominent hyperchromatic fusiform nuclei, prominent collagen deposition and hemangiopericytomatous vasculature of SFT. All four cases were strongly immunopositive for BCOR. Two cases were CD34 negative, while the other two were only focally CD34 positive. STAT6 was subsequently positive by IHC in all three cases tested.

Figure 1 - 791

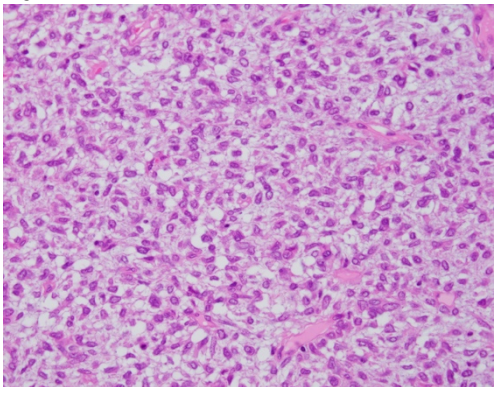

Figure 2 - 791

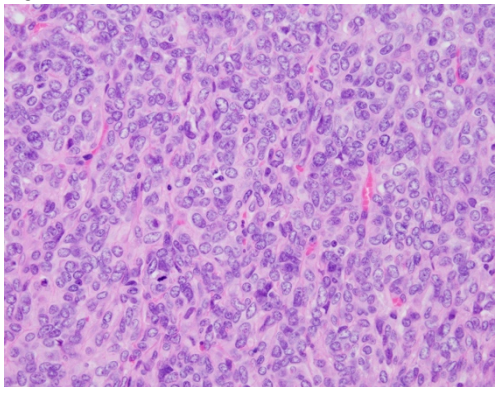

Conclusions: Malignant SFTs demonstrating undifferentiated/small round cell morphology along with branching capillary vasculature, strong immunoreactivity for BCOR, and minimal immunoreactivity for CD34 are a previously undescribed mimic of CCSK. As CCSK is treated with a specific effective chemotherapy regimen, this distinction has therapeutic implications.

792 Prostatic ductal adenocarcinoma (PDA) with cribriform architecture has worse prognostic features than non-cribriform-type

Sammy Au[1], Carlos Villamil[2], Reza Alaghehbandan[3], Gang Wang[4]
[1]University of British Columbia, Vancouver, BC, [2]BC Cancer Agency, Vancouver, BC, [3]Royal Columbian Hospital, University of British Columbia, New Westminster, BC, [4]BC Cancer Vancouver Centre, Vancouver, BC

Disclosures: Sammy Au: None; Carlos Villamil: None; Reza Alaghehbandan: None; Gang Wang: None

Background: PDA is an uncommon histologic subtype of prostate carcinoma characterized by large glands lined with tall columnar pseudostratified epithelium. PDA has several architectural patterns, with papillary and cribriform being the most common. PDA is typically graded as Gleason grade 4 and is often admixed with acinar carcinoma. The significance of cribriform architecture in PDA is uncertain. We

aimed to compare the adverse pathologic features between PDA with and without cribriform architecture. Additionally, we sought to compare the pathologic stage at radical prostatectomy (RP) between acinar carcinoma and PDA when matched for grade group (GG).

Design: We identified 49 cases of PDA, of which 32 underwent RP. Cases of PIN-like ductal adenocarcinoma were excluded from the study as they are known to behave similar to Gleason score 6 prostate cancer. Slides from all cases of PDA were reviewed. For the grade-matched comparison groups, we identified cases of acinar carcinoma of Gleason score 3+4 (GG2) (n=221), 4+3 (GG3) (n=231), 4+4 (GG4) (n=157) and 4+5 (GG5) (n=254).

Results: The majority (80%) of cases contained PDA admixed with acinar carcinoma. The median percentage of the ductal component in these cases was 40%. Of all PDA cases, 32.7% (16/49) were graded as GG4 and 40.8% (20/49) as GG5. At RP, 49% of cases presented as pathologic stage T3a and 24% as T3b. 73% of cases were positive for extraprostatic extension (EPE) and 24% for seminal vesical invasion. 53% of cases had positive margins and 20% had lymph node metastases. Cribiform architecture was present in 62% of PDA and was often admixed with papillary architecture. PDA with cribiform architecture demonstrated significantly higher likelihood of EPE and advanced pathologic stage compared to PDA without cribiform architecture (83% vs 50%, p=0.046). Compared to purely acinar carcinoma for GG2 to 5, there was no significant difference in pathologic stage at RP when matched for grade.

Figure 1 - 792

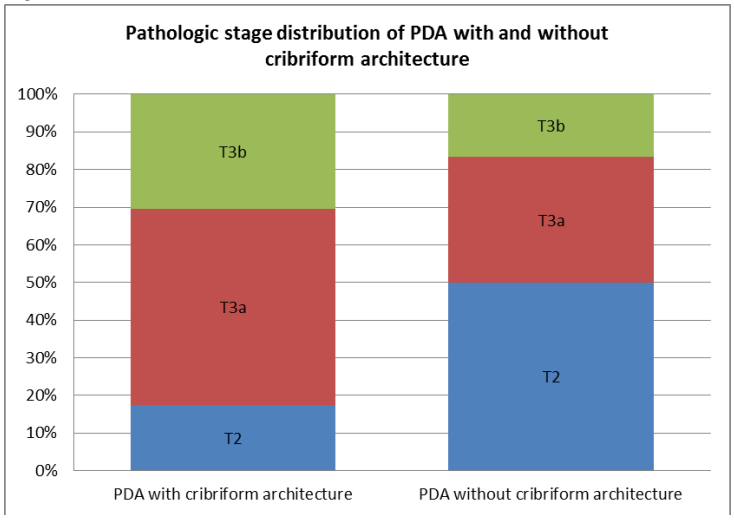

Figure 2 - 792

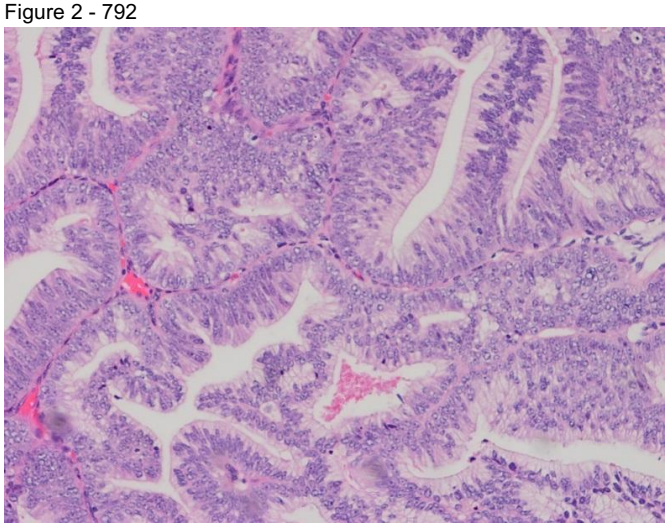

Conclusions: The vast majority of PDA presented as GG4 or GG5 and with advanced pathologic stage. The presence of cribiform architecture in PDA is associated with a significantly higher likelihood of EPE and advanced pathologic stage at RP.

793 Bladder cancers (BC) post-brachytherapy show variant morphologies and molecular subtypes

Sammy Au[1], Carlos Villamil[2], Mira Keyes[2], Isabel Serrano[2], Peyman Tavassoli[3]
[1]University of British Columbia, Vancouver, BC, [2]BC Cancer Agency, Vancouver, BC, [3]University of British Columbia, Richmond, BC

Disclosures: Sammy Au: None; Carlos Villamil: None; Mira Keyes: None; Isabel Serrano: None; Peyman Tavassoli: None

Background: The long term increased risk of secondary malignancy is a well-documented late effect of brachytherapy. However, the incidence, time interval, anatomic site and histopathology are not well studied. As our knowledge of molecular subtyping of urothelial carcinoma (UC) has advanced, we sought to characterize the secondary malignancies in a cohort of patients from 1998-2016.

Design: A cohort of 73 patients have been diagnosed with secondary malignancy following brachytherapy treatment. Slides were reviewed, and site and pathologic features were recorded. Individual slides were stained for GATA3, CK20 and CK5/6 and classified as luminal (LS) and basal (BS) subtypes.

Results: 70% (n=51) of cases in this cohort were high-grade, and 25% (n=18) were muscle-invasive. Non-invasive papillary UC comprised 51% of cases. 13 cases showed variant morphology, including small cell carcinoma (n=3), adenocarcinoma arising from prostatic urethra (n=3), sarcomatoid carcinoma (n=2), squamous cell carcinoma (n=2), UC with divergent differentiation (n=2), and nested variant of UC (n=1). LS was expressed in all papillary UC and all non-invasive cancers. All of the basal subtype cases were high-grade and invasive compared to 52% high-grade and 30% invasive in LS cases. Of the invasive conventional urothelial cancers, 57% were LS and 43% were BS. Among the variants, small cell carcinoma and sarcomatoid carcinoma were negative for all three markers, adenocarcinoma was positive for CK20 only, squamous cell carcinoma and UC with squamous differentiation both expressed basal subtype, and nested variant

of UC expressed LS. The most common sites of involvement were the trigone (30%), lateral wall (24%), bladder neck (18%) and prostatic urethra (14%). Compared to the tumors arising from other parts of the bladder, the tumors arising from bladder neck or prostatic urethra were more likely to be high grade (89% vs 63%, p=0.044), invasive (74% vs 40%, p=0.018), and non-papillary (63% vs 26%, p=0.008). The average time interval between brachytherapy and developing cancer was 6.3 years (range 1-17).

Histologic Subtype	N (%)	Muscularis propria invasion, N (%)	% LS	% BS	Immunohistochemistry
Low-grade papillary urothelial carcinoma, noninvasive	21 (29)	0 (0)	100	0	CK5/6-, GATA3+, CK20+
High-grade papillary urothelial carcinoma, noninvasive	16 (22)	0 (0)	100	0	CK5/6-, GATA3+, CK20+
Invasive urothelial carcinoma	23 (31)	11 (48)	57	43	
Small cell carcinoma	3 (4)	1 (33)			CK5/6-, GATA3-, CK20-
Adenocarcinoma	3 (4)	2 (67)			CK5/6-, GATA3-, CK20+
Sarcomatoid carcinoma	2 (3)	1 (50)			CK5/6-, GATA3-, CK20-
Squamous cell carcinoma	2 (3)	1 (50)	0	100	CK5/6+, GATA3-, CK20-
UC with divergent differentiation	2 (3)	1 (50)	0	100	CK5/6+, GATA3-, CK20-
Nested variant of urothelial carcinoma	1 (1)	1 (100)	100	0	CK5/6-, GATA3+, CK20+

Figure 1 - 793

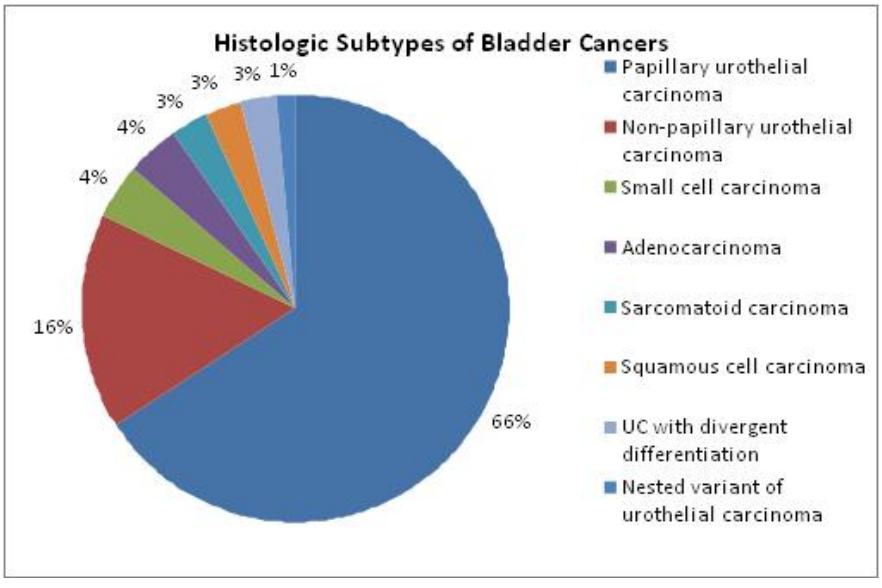

Conclusions: Bladder neck and prostatic urethra were among the common sites of involvement, and are more likely to be affected by brachytherapy. Compared to other sites, these tumors were more likely to be high-grade and invasive. A significant number of variant morphologies are seen, including small cell, sarcomatoid, nested variant, and adenocarcinoma arising from prostatic urethra, each demonstrating a specific immunophenotype.

794 PTEN and ERG Detection in Multiparametric MRI/US Fusion Targeted Prostate Biopsy Compared to Standard Biopsy

Erin Baumgartner[1], Maria Del Carmen Rodriguez Pena[2], Marie-Lisa Eich[1], Soroush Rais-Bahrami[2], Kristin Porter[2], Jeffrey Nix[2], Jennifer Gordetsky[2]
[1]The University of Alabama at Birmingham, Birmingham, AL, [2]University of Alabama at Birmingham, Birmingham, AL

Disclosures: Erin Baumgartner: None; Maria Del Carmen Rodriguez Pena: None; Marie-Lisa Eich: None; Soroush Rais-Bahrami: *Consultant*, Philips/InVivo Corp; *Advisory Board Member*, Genomic Health Inc; Kristin Porter: None; Jeffrey Nix: *Speaker*, Intuitive Surgical; *Consultant*, Phillips Invivo Corp; Jennifer Gordetsky: None

Background: Multiparametric magnetic resonance imaging (MR)/ultrasound (US) fusion targeted prostate biopsy has been shown in previous studies to outperform standard biopsy in the detection of clinically significant prostate cancer, as defined by higher grade tumors. Aside from tumor grade, tumor biomarkers such as phosphatase and tensin homolog (PTEN) and ETS-related gene (ERG) have been shown to have prognostic significance in prostate cancer and may help direct management of patients with low and intermediate risk tumors in terms of choosing active surveillance over definitive therapy. To date, there has been limited investigation of prognostic biomarkers in prostate cancer detected by MR/US targeted biopsy. Our objective was to compare the detection of PTEN and ERG expression in targeted versus standard prostate core biopsies.

Design: We performed immunohistochemical studies (IHC) for PTEN and ERG on prostate biopsy cores from patients with Grade Group (GG) 1 or GG 2 tumors who had undergone standard biopsy with concurrent MR/US targeted prostate biopsy. For each patient, all cores containing tumor were analyzed. PTEN and ERG expression in prostate cancer was compared between each patient's standard and targeted cores. PTEN loss was classified as homogeneous loss (Figure 1) or heterogeneous loss (Figure 2).

Results: A total of 33 cases had prostate biopsy tissue available for staining. ERG positivity was seen in 27/33 (81.8%) cases and PTEN loss was seen in 9/33 (27.3%) cases. The detection of ERG expression was not significantly different between targeted and standard biopsy (p=0.7). Targeted biopsy was superior to standard biopsy in the detection of PTEN loss (p=0.014). Targeted biopsy detected 9/9 (100%) cases of PTEN loss, compared to 3/9 (33.3%) cases detected by standard biopsy. The majority, 8/9 (88.9%), of cases with PTEN loss showed heterogenous expression. The GG was the same between targeted and standard biopsy in 8/9 (88.9%) cases with PTEN loss.

Figure 1 - 794

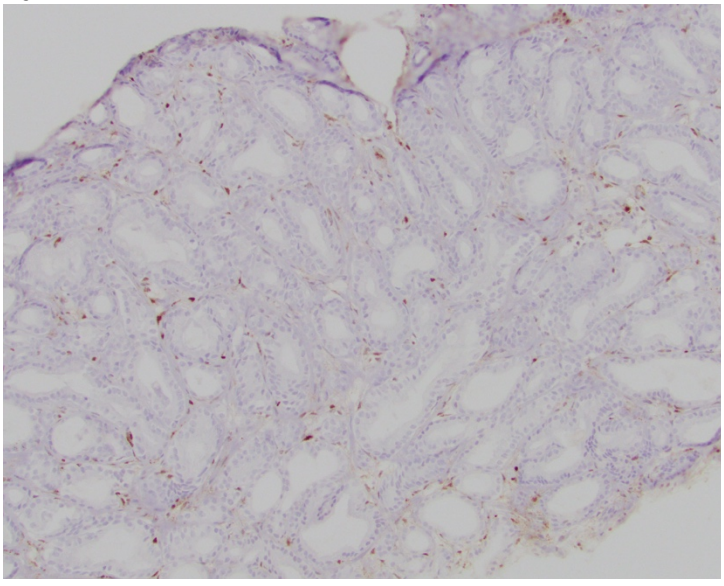

Figure 2 - 794

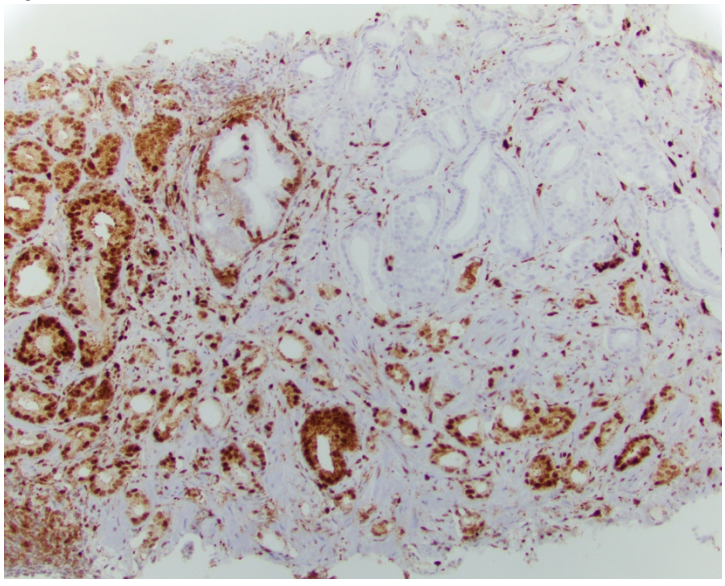

Conclusions: In our study, MR/US fusion targeted biopsy was superior to standard biopsy in the detection of PTEN loss in GG 1 and GG 2 prostate cancer. This finding suggests that, compared to tissue from standard cores, tissue from MR/US targeted cores may be more sensitive when utilizing prostate biopsy tissue for certain prognostic biomarkers.

795 Implementation of Current ISUP/WHO Guidance for Grading Prostatic Biopsy Reports by 378 Urological Pathologists

Daniel Berney[1], Lukas Bubendorf[2], Eva Compérat[3], Lars Egevad[4], Geert van Leenders[5], Ondrej Hes[6], Murali Varma[7], Glen Kristiansen[8]
[1]Queen Mary University of London, London, United Kingdom, [2]University Hospital Basel, Basel, Switzerland, [3]Tenon Hospital, Paris, France, [4]Karolinska University Hospital, Stockholm, Sweden, [5]Erasmus Medical Centre, Rotterdam, Netherlands,[6]Biopticka laborator s.r.o., Plzen, Czech Republic, [7]University Hospital of Wales, Cardiff, United Kingdom, [8]University of Bonn, Bonn, Germany

Disclosures: Daniel Berney: None; Lukas Bubendorf: None; Eva Compérat: None; Lars Egevad: None; Geert van Leenders: None; Ondrej Hes: None; Murali Varma: None; Glen Kristiansen: None

Background: There are many recent changes to recommendations on prostatic carcinoma grading, endorsed by both WHO and ISUP including the introduction of ISUP Grade Groups (GG). However it is unknown to what extent these recommendations are used in routine practice. We conducted a survey of urological pathologists to examine their current practice, and also by comparing replies with a previous survey conducted by our group, prior to these recommendation in 2012.

Design: A web-based survey was distributed among members of the European Network of Urological Pathology, the German Division of the IAP and the British Association of Urological Pathologists. The survey focused on contentious issues both in the recent ISUP/WHO guidance and also replicated a previous survey in 2012.

Results: Replies were received from 378 pathologists in 30 countries. 38% were in academic centres. Only 1 pathologist did not use Gleason grading. 96% claimed to used ISUP 2014/WHO 2016 consensus methodology. However only 66% gave a grade 4 to rounded regular cribriform glands, in contrast to 87% who gave grade 4 to poorly formed glands. 92% gave a grade of 4 to glomeruloid glands. 69% gave an estimation of the percentage of Gleason grade 4 in GG 2 and 3 and 47% of these give the % for each core, 19% give for each site and 28% give per case. 45% stated whether cribriform pattern was present. 70% incorporate tertiary scores of higher grade in the Gleason score. 29% assign a Gleason score to small cell carcinoma and 73% assign one to ductal adenocarcinoma. 15% grade pure intraductal carcinoma. 42% never graded hormonally treated cancers, while 21% always graded them. 65% give a concluding Gleason score for the case, and 60% of these give a 'global' Gleason score while 28% always report the highest Gleason score seen. While 95% assign an ISUP GG, there are over 13 different nomenclatures used. The most popular are ISUP GG (23%), GG (17%) and WHO GG (12%). 66% cite the GG in the conclusion while the remainder cite it for every site and/or core.

Conclusions: Many of the changes of the ISUP/WHO introduced in the past 5 years are now incorporated routinely in reports. However there is still large variation in how patterns are graded: surprisingly in the grading of rounded cribriform glands. Other areas where further education and standardisation is required include use of tertiary grades, grading of rarer subtypes and hormonal changes. ISUP GGs have been now very widely adopted, though confusion in terminology remains.

796 Benign Glands at the Inked Margin of Radical Prostatectomies in Organ-Confined (pT2), Gleason Score 6 and Negative Surgical Margins: Do They Influence Biochemical Recurrence?

Athanase Billis[1], Leandro Freitas[2], Larissa Costa[1], Icleia Barreto[1], Luís Magna[1], Ubirajara Ferreira[3], Wagner Matheus[1], Amanda Botega[1], Jezreel Costa[1], Nathalia Almeida[1], Tainah Rotta[1]
[1]State University of Campinas (Unicamp), Campinas, SP, Brazil, [2]UNICAMP - Brazil, Valinhos, SP, Brazil, [3]UNICAMP, Campinas, SP, Brazil

Disclosures: Athanase Billis: None; Leandro Freitas: None; Larissa Costa: None; Icleia Barreto: None; Luís Magna: None; Ubirajara Ferreira: None; Wagner Matheus: None; Amanda Botega: None; Jezreel Costa: None; Nathalia Almeida: None; Tainah Rotta: None

Background: In a consensus meeting of the International Society of Urological Pathology (ISUP) there was no consensus as to how pathologists should approach the presence of benign glands at the inked margin (BGIM) of radical prostatectomies (RP). Of those voting, 48% documented all instances of BGIM, regardless of extent; a further 41% recorded cases when there were numerous BGIM, and the remaining 11% of participants did not mention the presence of BGIM. We aimed to find any influence of BGIM in biochemical recurrence (BR) in patients with surgical specimens usually associated with very-low risk for BR following RP.

Design: We studied step-sectioned specimens of 88 consecutive patients with a mean, median, and range follow-up of 5.4, 4.0, and 0.3-15.6 years, respectively. BR was considered $\geq$ 0,2 ng/mL according to AUA. A mean of 35 quadrants were obtained from paraffin blocks. All cases were reviewed by a senior uropathologist. We evaluated: number and percentage of quadrants showing BGIM, age, prostate weight, presence of benign prostatic hyperplasia, preoperative PSA, PSA density, tumor extent evaluated by a semi-quantitative method (positive points), and clinical stage.

Results: Of the 88 patients, 71/88 (80.7%) had no BR, and 17/88 (19.3%) had BR; 36/71 (50.7%) without BR had BGIM (group 1) and 17/17 (100%) patients with BR had BGIM (group 2). Comparing the groups, group 2 had significantly higher number ($p < 0.001$) and

percentage (p < 0.001) of quadrants with BGIM, higher prostate weight (p=0.004), higher frequency of benign prostatic hyperplasia (p=0.035), higher level of preoperative PSA (p=0.044), and less extensive tumors (p=0.050). Considering percentile 95, specimens with >8 and/or >20% positive quadrants almost always belong to group 2. In multivariate logistic regression, there was a tendency for BGIM be present in patients with higher preoperative PSA (p=0.083), prostates with higher weight (p=0.063), and higher PSA density (p=0.050).

Conclusions: The frequency of 17/88 (19.3%) patients with BR, and the significant higher number and percentage of BGIM in group 2, favor that BGIM may possibly explain postoperative PSA elevation following RP. Pathologists should report BGIM in specimens with organ-confined cancer, Gleason score ≤ 6, and negative surgical margins. In cases of BGIM present in >8 and/or >20% positive quadrants, urologists should consider this possibility and avoid immediate definitive treatment unless presence of cancer is documented.

797 Prognostic Significance of Architectural Types of Gleason Pattern 4 Prostate Cancer in Radical Prostatectomy: A Semiquantitative Method of Evaluation

Athanase Billis[1], Leandro Freitas[2], Larissa Costa[1], Icleia Barreto[1], Ubirajara Ferreira[3], Wagner Matheus[1], Luís Magna[1], Ana Costa[1], Bruna Zaidan[1], Gabriel Tabosa[1]
[1]State University of Campinas (Unicamp), Campinas, SP, Brazil, [2]UNICAMP - Brazil, Valinhos, SP, Brazil, [3]UNICAMP, Campinas, SP, Brazil

Disclosures: Athanase Billis: None; Leandro Freitas: None; Larissa Costa: None; Icleia Barreto: None; Ubirajara Ferreira: None; Wagner Matheus: None; Luís Magna: None; Ana Costa: None; Bruna Zaidan: None; Gabriel Tabosa: None

Background: Studies have shown that Gleason pattern 4 architectural types may have different prognostic information. Using a semiquantitative point-count method, we aimed to evaluate a possible influence on biochemical recurrence (BCR) of each Gleason pattern 4 subtype extent in surgical specimens of patients with organ-confined tumor (pT2), Gleason score 7, and negative surgical margins.

Design: In this retrospective study, extent of each pattern 4 architectural subtype (fused glands, ill-defined glands, cribriform glands, and glomeruloid glands) was evaluated on step-sectioned specimens of 88 consecutive patients by a semiquantitative point-count method previously described. Briefly, drawn on a sheet of paper, each quadrant of the transverse sections contained 8 equidistant points each one corresponding to 10-15% of the quadrant area. During the microscopic examination of the slides, the tumor area of pattern 3 and pattern 4 subtypes were drawn on the correspondent quadrant seen on the paper using different colors. Gleason 4 subtypes were evaluated according to the 2014 consensus meeting of ISUP, and all cases reviewed by a senior uropathologist. BCR was considered as PSA ≥0.2 ng/mL according to AUA. Kaplan-Meier was used for time of BCR (TBCR), and Cox stepwise logistic regression model for predictors of shorter TBCR.

Results: 77/88 (87.5%) patients had Gleason score 3+4=7 and 11/88(12.5%) patients Gleason score 4+3=7; 66/88 (75%) patients had no BCR, and 22/88 (25%) patients had BCR following RP. Gleason score 4+3=7 was significantly associated with TBCR after RP (log-rank, p=0.001). Tumors with Gleason score 4+3=7 and patients with BCR were significantly associated with higher extent of cribriform glands and/or glomeruloid glands (p<0.001) and less extent of fused glands and/or ill-defined glands (p<0.001 Cribriform glands and/or glomeruloid glands were predictors of shorter TBCR in univariate analysis (p=0.024) but only Gleason score 4+3=7 (p=0.029) and preoperative PSA (p=0.022) were independent predictors in multivariate analysis.

Conclusions: Cribriform glands and/or glomeruloid glands are significantly more extensive than fused glands and/or ill-defined glands in specimens Gleason 4+3=7, and in patients with BCR following RP. The results favor that Gleason grade 4 subtypes have different prognostic significance. We propose that fused glands and/or ill-defined glands behave as low-grade Gleason 4 pattern, and cribriform and/or glomeruloid glands as high-grade Gleason 4 pattern.

798 Assessing Diagnostic Variation in 3,601 Transurethral Bladder Specimens Using Free Text, Synoptic Data, Control Charts, and an in silico Kappa

Michael Bonert[1], Alice Graham[1], Ihab El-Shinnawy[1], Anil Kapoor[1]
[1]McMaster University, Hamilton, ON

Disclosures: Michael Bonert: *Speaker*, Roche; *Major Shareholder*, Libre Pathology; Alice Graham: None; Ihab El-Shinnawy: None; Anil Kapoor: None

Background: The diagnostic rate (DR) and kappa are two ways to assess variation; however, they provide different information and are difficult to compare. A kappa-like value based on the DR may allow more insight into variation.

Design: All transurethral urinary bladder specimens (TUBS) accessioned 2011-2017 in a region were extracted and categorized with a structured/unstructured text algorithm (SUTA) that combined synoptic cancer reporting elements and hierarchical free text string matching. Pathologist diagnostic rates (PDRs) were calculated and normed by the highest volume pathologist. The normed PDRs were plotted on control charts centered on the group median diagnostic rate (GMDR). In silico kappas (kappas obtained via computer simulation of an inter-

rater variability study) were generated using the PDRs in the data set, and a maximal diagnostic overlap assumption (MDOA); this presumed all cases for a given diagnosis (e.g. "CIS present") by a pathologist will be diagnosed by all pathologists with a higher PDR.

Results: The study period contained 3,943 TUBS and 1,244 of those had a synoptic report. 25 pathologists interpreted >40 TUBS each (range: 47-313) and together read 3,601. The accuracy of the SUTA was 92% based on an audit of 200 TUBS. Staging info in the free text accounted for about half of the errors. The GMDR/normed PDR ranges (as % of all a pathologist's TUBS) were 1%/0-5% for dysplasia, 2%/0-6% for PUNLMP, 6%/0-18% for carcinoma in situ (CIS), 57%/41-65% for (all) urothelial carcinoma (UCC), 28%/15-36% for low-grade (LG) UCC, 30%/23-37% for high-grade UCC, 30%/21-40% no invasion in UCC, 12%/5-28% for lamina propria invasion (LPI), 8%/4-12% for muscularis propria invasion (MPI). The number of statistical outliers ($p<0.05$/$p<0.001$) to the GMDR of 25 pathologists were: 5/3 of 25 of dysplasia, 10/6 for PUNLMP, 7/3 for CIS, 10/3 for UCC, 14/7 for LGUCC, 3/0 for HGUCC, 10/4 for no invasion, 5/3 for LPI and 4/0 for MPI. The in silico kappas were: 0.44, 0.40, 0.62, 0.77, 0.68, 0.85, 0.76, 0.68, 0.73 for dysplasia, PUNLMP, CIS, all UCC, LGUCC, HGUCC, UCC without invasion, UCC with LPI and UCC with MPI.

Conclusions: The in silico kappas and control charts herein reproduce trends seen in prior studies; however, they are devoid of study associated confounders. The MDOA is the best case scenario for a given set of PDRs, and may approximate the disagreement pattern in clinical practice. Synoptic reporting is essential for accurate automated classifications and analysis work of this type.

799 Do Low Molecular Weight Keratin Immunostains Clarify the Architecture of High Grade Prostate Carcinoma in Needle Biopsies?

Dustin Bosch[1], Nicholas Reder[1], Funda Vakar-Lopez[1], Maria Tretiakova[1], Lawrence True[2]
[1]University of Washington, Seattle, WA, [2]University of Washington Medical Center, Seattle, WA

Disclosures: Dustin Bosch: None; Nicholas Reder: *Major Shareholder*, LightSpeed Microscopy, Inc; *Consultant*, NanoString; Funda Vakar-Lopez: None; Maria Tretiakova: None; Lawrence True: None

Background: Identifying high grade adenocarcinoma in prostate needle biopsies is important for appropriate treatment. Interobserver concordance for Gleason pattern 5 carcinoma has only been fair (kappa 0.38) in prior studies (PMID 25929349). We hypothesized that highlighting the architecture of cancer cells using low molecular weight cytokeratin 8 (LMWCK) immunostains would improve the accuracy of recognizing Gleason pattern 5 carcinoma.

Design: Forty-six prostate core needle biopsies (15 cases with highest Gleason pattern 5, 15 with highest Gleason pattern 4, and 16 equivocal for the presence of Gleason pattern 5 in the original pathology report) were studied. Concordance for Gleason grade and grade group (GG) among 4 specialized genitourinary pathologists was measured before and after LMWCK immunostains, using both Fleiss' kappa and the weighted concordance statistic for ordinal data, S* (PMID 24740999). Average grade among the 4 pathologists was correlated to subsequent prostatectomy (22 cases) GG and stage, as well as to biochemical recurrence-free survival.

Results: Average GG increased in 50%, remained unchanged in 28%, and decreased in 22% of cases when immunostained with LMWCK. Among 4 observers, the weighted concordance statistic (S*) for GG improved from 0.29 (95% C.I. 0.21-0.39) to 0.40 (95% C.I. 0.30-0.49) with the use of CK8 IHC. Fleiss' kappa was unchanged (0.20). Exclusion of one observer's systematically lower scores led to higher overall concordance (S* 0.59, kappa 0.41), but no statistically significant effect of LMWCK IHC on GG concordance. Concordance for GG among the 16 equivocal cases was lowest (kappa 0.13) and did not improve with LMWCK IHC (kappa 0.14). Similarly, correlation of needle biopsy and prostatectomy GGs, prediction of stage and biochemical recurrence-free survival were unaffected by the use of LMWCK IHC.

Figure 1 - 799

	Cases *n (%)*
Grade group change with IHC	
Increased	23 (50)
Unchanged	13 (28)
Decreased	10 (22)

4 pathologists

	without CK8		with CK 8	
	Fleiss kappa	**S* (95% CI)**	**Fleiss kappa**	**S* (95% CI)**
Gleason grade	0.19	0.34 (0.27-0.43)	0.20	0.38 (0.29-0.49)
Grade group	0.20	0.29 (0.21-0.39)	0.20	0.40 (0.30-0.49)
Gleason 5 present	0.32	N/A	0.24	N/A

3 pathologists

	without CK8		with CK 8	
	Fleiss kappa	**S* (95% CI)**	**Fleiss kappa**	**S* (95% CI)**
Gleason grade	0.39	0.65 (0.55-0.76)	0.37	0.65 (0.56-0.74)
Grade group	0.41	0.59 (0.47-0.69)	0.35	0.68 (0.59-0.76)
Gleason 5 present	0.51	N/A	0.40	N/A

Conclusions: LMWK immunohistochemistry increased overall detection of Gleason pattern 5 carcinoma in prostate needle biopsies and modestly improved statistical measures of interobserver concordance. However, LMWK IHC did not improve prediction of radical prostatectomy pathology or biochemical recurrence-free survival. We conclude that LMWK IHC is not useful for detecting Gleason pattern 5 in prostate biopsies with high grade adenocarcinoma.

800 Multiparametric Magnetic Resonance Imaging Biopsies - Critical Review of Experience with ~1,900 Prostate Biopsies from a Single Institution

Shaun Boyes[1], Alessa Aragao[1], Maria Picken[1]
[1]Loyola University Medical Center, Maywood, IL

Disclosures: Shaun Boyes: None; Alessa Aragao: None; Maria Picken: None

Background: Prostate cancer (PCa) is the most frequent malignancy among men in the United States. Systematic biopsies (SBx), which typically sample six different regions of the prostate, are performed to further investigate abnormally elevated prostate specific antigen (PSA) levels. Over the past two years, multiparametric magnetic resonance imaging (mpMRI) has been utilized in our institution for better identification and targeting of suspicious prostatic lesions. The mpMRI is interpreted utilizing the Prostate Imaging Reporting and Data System (PIRADS), which is a five point scale with a rating of increasing suspicion for maligancy from most probably benign (1) to most probably malignant (5). Utilizing mpMRI and PIRADS enables targeted biopsy (TBx) of radiologically suspicious prostatic lesions. The objective of our study was to evaluate experience with mpMRI targeted biopsies by comparing the year to year and overall rate of PCa detection per biopsy in SBx versus TBx in a greater than two year period.

Design: This single-institution retrospective study included 1861 biopsies from 244 patients who underwent SBx and TBx from 7/2015 through 10/2017. The percent of prostatic adenocarcinoma between SBx and TBx was analyzed on a year to year basis and over a greater than two year period.

Results: Over a two year period from 7/2015- 10/2017, there were 1861 region specific needle core biopsies consisting of 1395 SBx and 466 TBx. The percent of PCa diagnosed histologically for SBx was 13.5%, and the percent of PCa diagnosed histologically for Tbx was 23.4% (Z-score 5.050 ; $p<0.0001$). Over the first year period from 7/2015-7/2016, percent of SBx positive for PCa was 14.4% and percent TBx positive for PCa was 29.1% (Z-score 3.855 ; $p<0.0001$). Over the second year period from 7/2016-7/2017, percent of SBx positive for PCa was 12.3% and percent TBx positive for PCa was 21.7% (Z-score 3.448 ; $p=0.0003$). There was a statistically nonsignificant decrease of percent TBx positive of 29.1% from the first year to 21.7% in the second year (Z-score 1.572 ; $p= 0.1164$)

7/2015- 10/2017	Number of cores with Pca	Total Cores	Cores with Pca(%)
SBx	189	1395	13.5
TBx	109	466	23.4
7/2016-7/2017			
SBx	85	692	12.3
TBx	48	221	21.7
7/2015-7/2016			
SBx	60	417	14.4
TBx	39	134	29.1

Conclusions: The study shows that mpMRI-guided TBx has a statistically significant increased detection of cancer 23.4% over SBx 13.5% (p <0.001), and that this detection has remained statistically significant on a year by year analysis. Discordance between radiologic and pathologic correlation may be urologist (sampling error) and radiologist-dependent (over or under interpretation of suspicious lesions) factors.

801 The Prognostic Role of PD-L1 Expression in Patients Who Received Active Surveillance for Metastatic Clear Cell Renal Cell Carcinoma

Matteo Brunelli[1], Anna Calio'[2], Enrico Munari[3], Guido Martignoni[1]
[1]Verona, Italy, [2]University of Verona, Verona, Italy, [3]Sacro Cuore Hospital, Verona, Italy

Disclosures: Matteo Brunelli: None; Anna Calio': None; Enrico Munari: None; Guido Martignoni: None

Background: Active surveillance (AS) is one possible option to manage patients with a recent diagnosis of metastatic renal cell carcinoma. Unfortunately, there are not predictive factors to select patients to AS. We aimed to analyze the potential of PD-L1 expression in improving the selection of patients eligible to AS and we also studied the heterogeneity of PD-L1 expression between primary and metastatic tumors.

Design: Patients who started AS at our institution from January 2007 to April 2016 with available diagnostic tissue were included. Kaplan-Meier method was used to estimate survivals according to the expression of PD-L1 on neoplastic cells (clone SP263 Ventana).

Results: All carcinoma included were clear cell histotype, according to WHO 2016. 52 patients received AS and 43 were analyzed for PD-L1 expression, using two cut-off (1% and 5%) to define positivity. The cut-off of 5% was associated with a difference in the median AS: 9.8 months in PD-L1+ group compared to 26.4 months in PD-L1- group (p=0.025). This difference remained significant even when adjusted for IMDC prognostic class – good vs. intermediate/poor – (HR=2.53, 95%CI 1.18 – 5.44; p=0.018). No differences in OS were found. When the value ?5% for PD-L1 positivity was considered, among the 6 cases with positive expression on the primary tumor, only 1 (16.6%) had the same degree of expression on the metastatic sites; among the 22 cases with negative expression on the primary tumor, 7 (31.8%) had positive expression on the metastatic sites.

Conclusions: We reported for the first time that the expression of PD-L1 is a prognostic factor that can help in the selection of patients for AS. Moreover, we reported the magnitude of heterogeneity of PD-L1 expression between primary and metastatic tumor lesions, being the 22 tumour tissues negative on the primary renal tumor while 32% positive on the metastatic sites.

802 Nonlinear Microscopy (NLM): A New Method to Evaluate Prostate Tissue

Lucas Cahill[1], Tadayuki Yoshitake[2], Yubo Wu[3], Michael Giacomelli[4], Douglas Lin[5], Huihui Ye[3], Oscar Carrasco-Zevallos[2], Andrew A. Wagner[3], James G. Fujimoto[2], Seymour Rosen[3]
[1]MIT-Harvard, Cambridge, MA, [2]Massachusetts Institute of Technology, Cambridge, MA, [3]Beth Israel Deaconess Medical Center, Boston, MA, [4]Massachusetts Institute of Technology, Rochester, NY, [5]Beth Israel Deaconess Medical Center, Needham, MA

Disclosures: Lucas Cahill: None; Tadayuki Yoshitake: None; Yubo Wu: None; Michael Giacomelli: None; Douglas Lin: None; Huihui Ye: None; Oscar Carrasco-Zevallos: None; Andrew A. Wagner: None; James G. Fujimoto: None; Seymour Rosen: None

Background: It is currently uncommon to evaluate prostate tissue during a radical prostatectomy. Furthermore, as we have increased our comfort with active surveillance, there is a trend towards higher grade cancer in the men undergoing radical prostatectomy and thus less focus on nerve sparing surgery. However, studies that thoroughly evaluate prostate tissue during surgery, such as those described using the NeuroSAFE protocol (Schlomm, Eur. Urol., 2012), have successfully reduced positive margin rates and increased the amount of nerve sparing possible. Techniques that examine large areas of tissue during surgery may be essential in optimizing patient outcomes. Nonlinear

microscopy (NLM) is an optical imaging technique that enables nondestructive, rapid evaluation of multicentimeter-sized, freshly excised tissue.

Design: 106 (74 freshly excised, 32 fixed) prostate tissue specimens from 36 radical prostatectomies were stained for 1-2 minutes with nuclear and stromal/cytoplasmic fluorescent dyes without paraffin processing, freezing, or microtoming. The tissue specimens, which ranged in size from 1x1x0.5 cm to 7x7x1 cm, were placed on a glass specimen holder and evaluated on an NLM microscope.

First, a pathologist reviewed the specimens in real-time by moving the specimens to areas of interest at variable magnification (5-20x) like a typical histology microscope. Unlike a typical microscope, NLM enables real-time evaluation of specimens up to 100 µm into the tissue surface providing virtual analysis of up to ~25 serial sections. The images were displayed in an H&E color scale. After review, the specimens were scanned by the NLM microscope analogously to a histology slide scanner. Paraffin H&E slides were made for comparison to NLM.

Results: Prostatic adenocarcinoma could be readily identified in 32 specimens with NLM, Gleason-graded, and separated from benign conditions such as inflammation (Fig. 1). Extraprostatic extension/margin involvement could also be evaluated (Fig. 2). NLM images of fresh specimens exhibit some differences from H&E histology. For example, nucleoli tended to be larger than in paraffin sections, foamy gland carcinoma had intensely stained luminal secretions, and cytoplasmic color and stromal density differences were seen. Despite these differences, NLM similarities to H&E sections are sufficient that interpretation is possible with a minimal learning curve.

Figure 1 - 802

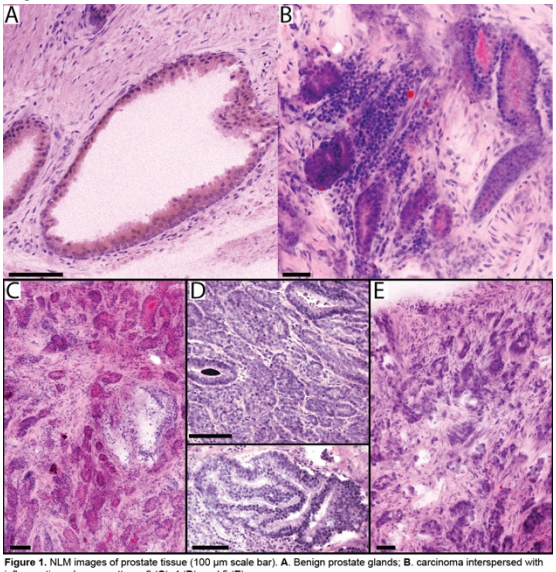

Figure 1. NLM images of prostate tissue (100 µm scale bar). **A.** Benign prostate glands; **B.** carcinoma interspersed with inflammation; gleason patterns 3 (**C**), 4 (**D**), and 5 (**E**).

Figure 2 - 802

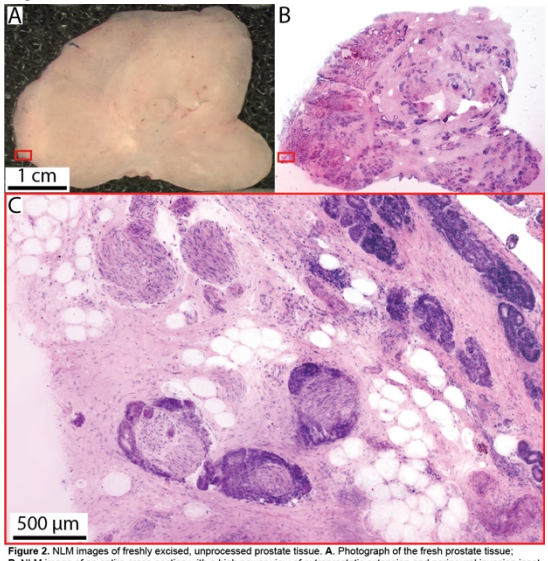

Figure 2. NLM images of freshly excised, unprocessed prostate tissue. **A.** Photograph of the fresh prostate tissue; **B.** NLM image of an entire cross-section with a high power view of extraprostatic extension and perineural invasion inset (**C**, red box).

Conclusions: In conclusion, NLM presents a new opportunity to assess intraoperative radical prostatectomies.

803 Morphologic Heterogeneity Correlates with Clinical Phenotypes in Clear Cell Renal Cell Carcinoma

Qi Cai[1], Alana Christie[2], Min Kim[3], Qinbo Zhou[2], Ellen Araj[2], Dinesh Rakheja[2], Renee McKay[2], James Brugarolas[4], Payal Kapur[4]
[1]University of Texas Southwestern Medical Center, Tucson, AZ, [2]University of Texas Southwestern Medical Center, Dallas, TX, [3]UT Southwestern Medical Center, Dallas, TX, [4]University of Texas Southwestern, Dallas, TX

Disclosures: Qi Cai: None; Alana Christie: None; Ellen Araj: None; Dinesh Rakheja: None; James Brugarolas: None

Background: Clear cell renal cell carcinoma (ccRCC) exhibits a broad spectrum of clinical scenarios and intratumoral heterogeneity in histopathology. Currently, pathologic grading for ccRCC is mainly based on nucleolar size. Although sarcomatoid and rhabdoid changes are known to be associated with aggressive behavior, the significance of the histopathologic intratumoral heterogeneity occurring in ccRCC remain largely unknown.

Design: We identified sequential cases with a diagnosis of ccRCC at our institution between 2006 and 2015 for which follow-up information was available beyond 1.5 years. The minimum follow-up period was waived for patients who died. Architectural patterns and cytologic features were predefined and quantitated in nephrectomy specimen slides, which were reviewed by an experienced GU pathologist. Twelve of architectural patterns and ten of cytologic features were correlated with disease-free survival (DFS) and overall

survival (OS). Kaplan-Meier curves were generated to visualize survival distributions. Statistical analyses were conducted using SPSS Statistics software. *P* values <0.05 were considered statistically significant.

Results: A total of 549 cases met selection criteria and were comprehensively reviewed including, 16 grade 1 (2.9%), 278 grade 2 (50.6%), 201 grade 3 (36.6%) and 54 grade 4 (9.8%). The distribution of pathologic tumor stage ranged from 63.9% of pT1 (n=351), 6.0% of pT2 (n=33), 27.5% of pT3 (n=151), to 2.6% of pT4 (n=14). The following patterns: microcystic, tubular, bleeding follicles, and small compact nest, were associated with better DFS and OS. Large nests, thick trabecular, solid sheet, alveolar or papillary/pseudopapillary were associated with worse DFS and OS (p<0.0001). In addition to multinucleated giant cells, sarcomatoid and rhabdoid changes, cytologic features including large intracytoplasmic eosinophilic inclusions, voluminous cytoplasm, cytoplasmic spindling, a giant nucleus with perinuclear halo, and a wrinkled nucleus with perinuclear halo were associated with worse DFS and OS (p<0.0004)

Conclusions: Architectural patterns and cytologic features observed in ccRCC predict tumor behavior and are associated with clinical prognosis. Evaluation of histopathologic heterogeneity will shed light on tumor biology, evolution, trajectories and their outcomes.

804 Looking for a Druggable Target in MiT Family Translocation Renal Cell Carcinoma. An Immunohistochemical and Molecular Study of 30 Cases

Anna Calio'[1], Matteo Brunelli[2], Giampaolo Cordioli[3], Diego Segala[4], Guido Martignoni[2]
[1]University of Verona, Verona, Italy, [2]Verona, Italy, [3]University of Verona, Villafranca di Verona, Italy, [4]Peschiera del Garda, Italy

Disclosures: Anna Calio': None; Matteo Brunelli: None; Giampaolo Cordioli: None; Diego Segala: None; Guido Martignoni: None

Background: A tyrosine kinase inhibitor with activity against VEGF, MET, and AXL has been recently proposed in the treatment of advanced renal cell carcinomas. It has been demonstrated *in vitro* the inhibition of the osteoclast differentiation, down-regulating several molecules such as cathepsin K, after non-cytotoxic doses of this treatment. We sought to investigate MET and AXL immunohistochemical expression in a series of renal cell carcinomas which more commonly expressed cathepsin K, like MiT family translocation renal cell carcinomas, looking for possible predictive markers in tumor tissue.

Design: Thirty cases of MiT family translocation renal cell carcinomas were retrieved. Fluorescence *in situ* hybridization using dual color break-apart TFE3, TFEB, and VEGFA probes was performed. All cases were immunohistochemically stained with the following antibodies: cathepsin K, HMB-45, Melan-A, PAX-8, MET, and AXL.

Results: *TFE3* gene rearrangement was demonstrated in twenty-two *Xp11* renal cell carcinomas whereas *TFEB* gene rearrangement was observed in eight t(6;11) renal cell carcinomas. One case of Xp11 renal cell carcinoma showed increased *TFE3* gene copy number (4-5 copies of fluorescent signals) with concurrent increased *TFEB* and *VEGFA* gene copy number and behaved aggressively. Three cases of t(6;11) renal cell carcinomas showed increased *TFEB* and *VEGFA* gene copy number and demonstrated an aggressive behavior. All but one cases tested were positive for PAX8. Cathepsin K was expressed in 14 of 21, HBM-45 in 5 of 19 and Melan-A in 3 of 17 Xp11 renal cell carcinomas. With regards of t(6;11) renal cell carcinomas, all cases were positive for cathepsin K and Melan-A, labeling for HMB-45 was observed in 6 of 8 tumors. Staining for MET was found in 12 of 18 Xp11 renal cell carcinomas and in 5 of 8 t(6;11) renal cell carcinomas with different percentage and intensity. None of MiT family translocation renal cell carcinomas expressed AXL.

Conclusions: VEGF, MET but not AXL may be potential predictive markers for targeted therapy in MiT family renal cell carcinomas.

805 Detection of HPV and P16 in Mixed Squamous Cell Carcinoma of the Penis: A Study of 101 Cases

Sofía Cañete-Portillo[1], Laia Alemany[2], Diego F Sanchez[1], María José Fernandez-Nestosa[3], Omar Clavero[4], Belen Lloveras[5], Ingrid Rodríguez[3], Nubia Munoz[6], Wim Quint[7], Silvia de Sanjosé[2], Francesc Xavier Bosch[8], Antonio Cubilla[9]
[1]Instituto de Patologia e Investigacion, Asuncion, Paraguay, [2]Institut Catala d'Oncologia, Barcelona, Spain, [3]Universidad Nacional de Asunción, Asunción, Paraguay, [4]1. Centro de Investigación Biomédica en Red de Cáncer 2.Institut Català d'Oncologia, L'Hospitalet de Llobregat, Madrid, Spain, [5]Hospital del Mar, Barcelona, Spain, [6]National Cancer Institute of Colombia, Bogota, Colombia, [7]DDL Diagnostic Laboratory, Rijswijk, Netherlands, [8]Catalan Institute of Oncology (ICO), L'Hospitalet de Llobregat, Spain, [9]Instituto de Patologia e Investigacion, Asunción, Paraguay

Disclosures: Sofía Cañete-Portillo: None; Laia Alemany: None; Diego F Sanchez: None; María José Fernandez-Nestosa: None; Belen Lloveras: None; Ingrid Rodríguez: None; Antonio Cubilla: None

Background: In mixed squamous cell carcinomas of the penis, two -or more- clearly recognized histological variants coexist. They represent about 10% of all carcinomas. The aim of this study was to determine and evaluate the prevalence of HPV and p16 respectively in these unusual tumors.

Design: Cases were selected from a larger international series of 1095 cases of penile carcinomas centralized in Barcelona (Alemany et al, Eur Urol 2016). Mixed carcinomas were grouped in two as follows: carcinomas with Warty or Basaloid features mixed with other variants

of SCC (Usual and Verrucous) (71 cases) and carcinomas without Warty or Basaloid features (mixtures of keratinizing differentiated variants like Usual, Verrucous, Papillary NOS, Pseudohyperplastic, Cuniculatum and Adenosquamous) (30 cases). HPV detection and p16 immunostain was performed in all cases. En bloc full tumor staining was the utilized criteria for positivity. For HPV detection, whole tissue section (WTS)-PCR analyses was performed by SPF10-DEIA-LiPA25 (version 1). P-values were determined by Fisher's exact test using STATA SE version 11.2.

Results: Presence of HPV, p16 staining and HPV genotypes in mixed carcinomas are shown in Table 1.

Table 1. HPV prevalence and p16 staining in mixed carcinomas.

Mixed carcinoma	No of cases	HPV Positive *(%)**	P16 positive *(%)***	HPV genotypes (# of cases)
W/B + others	71	32 *(45)*	26 *(81)*	16(21), 18(1), 26(1), 33(1), 39(1), 52(1), 53(1), 58(1), 59 (1), 6/16(1), Undetermined(2)
Non-W/B	30	2 *(7)*	1 *(50)*	16(1), 66(1)

*,**Fisher's test P-value <0.0005.

Conclusions: Highest rate of HPV detection, mostly HPV 16, was observed in carcinomas with Warty or Basaloid features associated with other tumors (45%) and lowest rate in non-Warty/Basaloid mixed carcinomas usually represented by low grade keratinizing variants of squamous cell carcinomas. P16 was positive in 79% of HPV positive cases. High risk HPV 16 was the most frequently found genotype (65%). Rare low risk genotypes were present. HPV rates of positivity in mixed tumors of the penis are inversely related to the presence of lower grade keratinizing variants of squamous cell carcinoma.

806 The Relative Value of P16 for HPV Detection in Penile Carcinomas: A Study of 219 of the Most Common HPV-Related Neoplasms

Sofía Cañete-Portillo[1], Diego F Sanchez[1], Laia Alemany[2], María José Fernandez-Nestosa[3], Belen Lloveras[4], Omar Clavero[5], Natalia Elizeche-Santacruz[1], Ingrid Rodríguez[3], Wim Quint[6], Nubia Munoz[7], Silvia de Sanjosé[2], Francesc Xavier Bosch[8], Antonio Cubilla[9]

[1]Instituto de Patologia e Investigacion, Asuncion, Paraguay, [2]Institut Catala d'Oncologia, Barcelona, Spain, [3]Universidad Nacional de Asunción, Asunción, Paraguay, [4]Hospital del Mar, Barcelona, Spain, [5]1. Centro de Investigación Biomédica en Red de Cáncer 2.Institut Català d'Oncologia, L'Hospitalet de Llobregat, Madrid, Spain, [6]DDL Diagnostic Laboratory, Rijswijk, Netherlands, [7]National Cancer Institute of Colombia, Bogota, Colombia, [8]Catalan Institute of Oncology (ICO), L'Hospitalet de Llobregat, Spain, [9]Instituto de Patologia e Investigacion, Asunción, Paraguay

Disclosures: Sofía Cañete-Portillo: None; Diego F Sanchez: None; Laia Alemany: None; María José Fernandez-Nestosa: None; Belen Lloveras: None; Natalia Elizeche-Santacruz: None; Ingrid Rodríguez: None; Antonio Cubilla: None

Background: The importance of separating HPV from non-HPV carcinomas, like in the current 2016 WHO classification, is related to the better prognosis reported by some authors for the former tumors. The gold standard technique for HPV detection is whole tissue section (WTS)-PCR, although recently Laser Capture Microdissection (LCM)-PCR revealed more accurate information for precancerous lesions (MJ Fernandez et al, Am J Surg Path, 2017). Considering these techniques are not available in most routine practice p16 has been used as a surrogate for HPV detection. However, in a large study we found a lack of expected correspondence of P16 and PCR in a considerable number of tumors usually associated with HPV. The aim of this study was to evaluate this discordance.

Design: From an initial group of 1095 cases (Alemany et al, Eur Urol 2016), we selected 219 cases of the most common HPV-related carcinomas in which HPV was detected by WTS-PCR and P16 stain as follows: basaloid (123 cases), warty-basaloid (31 cases) and warty (condylomatous) carcinomas (65 cases). They were part of a retrospective cross-sectional international study of 1095 cases from 5 continents designed to estimate the HPV DNA prevalence of penile cancers (Alemany et al, Eur Urol 2016). HPV DNA detection was performed using SPF-10/DEIA/LiPA$_{25}$ system (version 1).

Results: There was a considerable number of false positives and negatives. The breakdown according to histological types of the false positive and negative diagnosis of P16, as well as the value and accuracy of this technique, are shown in Table 1.

Table 1. P16 false positive and negative cases, sensitivity, specificity and accuracy according to most common HPV-related subtypes.

Type of tumor	HPV-PCR Positive cases	P16 Negative/HPV-PCR Positive cases *(%)*	HPV-PCR Negative cases	P16 Positive/HPV-PCR Negative cases *(%)*	Sensitivity	Specificity	Accuracy
Basaloid	104	7 *(7)*	19	14 ***(74)***	93%	26.30%	82.50%
Warty-basaloid	27	5 *(19)*	4	2 *(50)*	80.70%	50%	76.60%
Warty	33	8 ***(24)***	32	8 *(25)*	75.70%	75%	75.30%
OVERALL	164	20 *(12)*	55	24 *(44)*	88%	56%	79.50%

Conclusions: False positive and negative diagnosis of p16 occurred in a fourth of the cases. The most common false negative diagnosis was in Warty (24%) and the less common in Basaloid carcinoma (7%). On the contrary, the most common false positive for p16 was in Basaloid (74%) and the less common was in Warty carcinoma (25%). P16 was very sensitive for the diagnosis of Basaloid carcinoma but not very specific (93 vs 26.3%). For the other subtypes, P16 had average to good sensitivity and specificity (80.7 vs 50% and 75.7 vs 75% for Warty-basaloid and Warty carcinomas, respectively). Although accuracy among the three carcinomas subtypes was good (75 to 82%), there was a rather low specificity of p16 to detect HPV in a considerable number of expected HPV-related penile tumors. To identify HPV in these cases another complementary technique such as in situ hybridization (ISH) may be evaluated and considered in routine practice.

807 Proposal of an Expansion of the WHO Classification and a Grading System of Penile Intraepithelial Neoplasia (PeIN)

Sofía Cañete-Portillo[1], Diego F Sanchez[1], María José Fernandez-Nestosa[2], Ingrid Rodríguez[2], Antonio Cubilla[3]
[1]Instituto de Patologia e Investigacion, Asuncion, Paraguay, [2]Universidad Nacional de Asunción, Asunción, Paraguay, [3]Instituto de Patologia e Investigacion, Asunción, Paraguay

Disclosures: Sofía Cañete-Portillo: None; Diego F Sanchez: None; María José Fernandez-Nestosa: None; Ingrid Rodríguez: None; Antonio Cubilla: None

Background: The WHO classification of PeIN separates precancerous lesions in non-HPV (Differentiated PeIN) and HPV-related groups (Basaloid, Warty-basaloid and Warty). Four subtypes of PeIN and no grading system were considered in the model. Emerging evidence is expanding the morphological spectrum of subtypes of precancerous lesions, especially those lesions that were thought not to represent a risk factor for developing carcinomas but recent studies have documented the importance of them in the natural history of carcinomas (Sudenga et al Eur Urol. 2016,; 69:166-73; da Silva et al Braz J Infect Dis. 2017, 21:376-385). For all the aforementioned, a need for an expansion of the classification system and grading is established.

Design: Besides the mentioned reports**,** this classification approach was based on our 3 recent studies. In a report of 73 cases of Differentiated PeIN, we found 3 distinctive patterns: Hyperplasia-like, 26 cases (36%); Classic, 38 cases (52%) and Pleomorphic, 9 cases (12%) (Cañete-Portillo S et al Mod Pathol 2018 A). In another study we identified minimally atypical or no atypical flat lesions which were associated with High Risk HPV (HR-HPV) (Fernández-Nestosa MJ et al, Mod Pathol 2018 A. Submitted for publication). In a Laser Capture Microdissection (LCM)-PCR evaluation of common condylomas, we found a significant number of them to be driven by High Risk HPV (Canete S et al Mod Pathol, 2016 A).

Results: Based on the atypia degree and the presence of HR-HPV, we suggest the following grading system shown in Table 1.

Table 1. Proposed new classification for penile intraepithelial neoplasia (PeIN)

PRECANCEROUS LESIONS	GRADING SCALE
Non-HPV-related (Differentiated PeIN)	
Hyperplasia-like	Grade 1
Classic	Grade 2
Pleomorphic	Grade 3
HPV-related	
HR-HPV positive Condyloma acuminatum	Grade 1
HR-HPV positive Flat lesion	Grade 1
Warty/Warty-basaloid PeIN	Grade 2 or 3
Basaloid PeIN	Grade 3

Conclusions: A more comprehensive approach for the classification of penile precancerous lesions is presented, which includes a grading system. Immunohistochemistry like Ki67 and p16 may be necessary to diagnose and classify some of the newly incorporated lesions.

808 PD-L1 and IDO Expression in Upper Tract Urothelial Carcinoma

Helen Cathro[1], Jennifer Ju[2], Jonathan Davick[3], Alejandro A. Gru[4], Stephen Culp[4]
[1]UVA School of Medicine-Pathology, Charlottesville, VA, [2]University of Virginia Health System, Charlottesville, VA, [3]Charlottesville, VA, [4]University of Virginia, Charlottesville, VA

Disclosures: Helen Cathro: None; Jennifer Ju: None; Jonathan Davick: None; Alejandro A. Gru: *Consultant*, Seattle Genetics; *Speaker*, Takeda; Stephen Culp: None

Background: Although immunotherapy using checkpoint inhibitors has had some success in metastatic urothelial carcinoma (UC), one recent Phase 3 trial showed no survival advantage over chemotherapy in platinum-resistant metastatic UC. Studies are underway examining combination immunotherapies including a novel indoleamine 2,3-dioxygenase (IDO) inhibitor that suppresses tryptophan metabolism. We examined programmed cell death-ligand 1 (PD-L1) and IDO immunohistochemical expression in upper tract urothelial carcinoma (UTUC), a particularly aggressive form of this disease.

Design: PD-L1 expression in 117 cases of UTUC was compared with that of 166 bladder urothelial (BUC) cases, using the Ventana SP142 antibody. IDO expression was examined in UTUC using the ABCAM SP260 antibody. Staining was graded as follows: <1% of tumor cells or tumor-infiltrating inflammatory cells stained = 0, 1 - <5% = 1, 5 - <25% = 2, and 25-100% = 3.

Results: A previous study had shown that 3.3% of the UTUC cohort were microsatellite instable (MSI high). 41.9% of UTUC were low-grade and 58.1% were high-grade. 41.8% of cases were Stage pTa, 15.3% were Stage pT1, 17.0% were Stage pT2, 21.3% were Stage pT3 and 4.2% were Stage pT4. Chemotherapy had been administered in 21% of patients and PD-L1 inhibitors in 5%, with 1.7% of patients receiving both.

PD-L1 staining of both tumor and tumor infiltrating cells was significantly higher in UTUC than in BUC (Grades1-3; p = 0.0188 and <0.00001 respectively). There was a positive association between PD-L1 and IDO expression in UTUC tumors using both univariate and multivariate analysis controlling for infiltrating cells (p<0.001 for both).

There was a positive association between PD-L1 UTUC tumor expression and tumor grade (p<0.001), tumor stage (p=0.001), and tumor specific survival (p=0.027), but there was no association with microsatellite instability. There was no association between IDO UTUC tumor expression and tumor grade, stage, microsatellite instability or tumor specific survival.

PD-L1 and IDO expression in Urothelial Carcinoma (UT=upper tract, B=bladder)						
Score	PD-L1 UT Tumor	PD-L1 B Tumor	PD-L1 UT Infiltrate	PD-L1 B Infiltrate	IDO UT Tumor	IDO UT Infiltrate
	n=117	n=166	n=106	n=166	n=117	n=106
0	90 (76.9)	144 (86.8)	19 (17.9)	115 (69.3)	98 (83.7)	22 (20.7)
1	14 (12.0)	4 (2.4)	59 (55.7)	22 (13.3)	14 (12.0)	68 (64.1)
2	4 (3.4)	2 (1.2)	14 (13.2)	19 (11.5)	1 (0.9)	14 (13.2)
3	8 (6.8)	5 (3.0)	13 (12.3)	10 (6.0)	4 (3.4)	2 (1.8)
4	1 (0.9)	7 (4.2)	1 (0.9)	0 (0)	0 (0)	0 (0)

Conclusions: - PD-L1 expression is higher in UTUC than in BUC, both within the tumor and in tumor infiltrating cells.

- PD-L1 and IDO expression are positively associated in UTUC tumors both alone and when controlling for tumor infiltrating cell expression.

- This study informs ongoing efforts to implement combination immunotherapy for metastatic UC with particular implications for tumors of the renal pelvis and ureter.

809 Molecular Characterization of Metanephric Adenomas Beyond BRAF: Are All Benign?

Emily Chan[1], Bradley Stohr[2], Nicole Croom[2], Soo-Jin Cho[2], Karuna Garg[2], Megan Troxell[3], John Higgins[4], Gregory Bean[5]
[1]UCSF School of Medicine, San Francisco, CA, [2]University of California, San Francisco, San Francisco, CA, [3]Stanford University Medical Center, Stanford, CA, [4]Stanford University Hospital, Stanford, CA, [5]Stanford University School of Medicine, Stanford, CA

Disclosures: Emily Chan: None; Bradley Stohr: None; Nicole Croom: None; Soo-Jin Cho: None; Karuna Garg: None; Megan Troxell: None; John Higgins: None; Gregory Bean: None

Background: Metanephric adenomas (MA) are generally regarded as rare renal tumors with indolent behavior. Histologically, they are characterized by uniform tightly-packed tubules and papillae lined by small cells with minimal cytoplasm; rare mitoses can be seen. MA are positive for WT1, CD57 and pan-cytokeratin but negative for CK7. Recently ~90% of MA have been shown to harbor hotspot *BRAF* p.V600E mutations, an alteration specific to MA among renal tumors. Together with BRAF V600E, p16 (*CDKN2A*) by immunohistochemistry (IHC) is consistently overexpressed; MA's benign nature has been attributed to senescence mediated by p16. However, limited case reports have described rare malignant MA with metastasis. Aside from *BRAF*, the molecular landscape of MA has not been fully characterized. Using capture-based next generation sequencing (NGS) we profiled a series of conventional MA and 1 tumor with malignant features.

Design: 9 cases were studied including 8 conventional MA. IHC for BRAF V600E, WT1, p16, CK7 and Ki-67 was performed. 1 renal tumor positive for WT1, CD57 and BRAF V600E with a biphasic appearance was included, with separate NGS of each component. One component was morphologically consistent with MA, and the second was composed of highly pleomorphic cells with vasoformative growth. Positive CD31 and ERG in the latter confirmed angiosarcoma. NGS targeted coding regions of 479 cancer genes. Single nucleotide variants, indels and copy number alterations (CNA) were evaluated.

Results: All tumors were positive for *BRAF* V600E. One MA (case 5) showed an additional *BRCA2* p.L2587fs pathogenic mutation. Differential profiling of the malignant tumor (case 1, Figure) revealed identical *BRAF*, *EIF1AX*p.K10E and *TERT* promoter c.-124C>T hotspot mutations in the epithelial and sarcomatous components. Deep deletion of *CDKN2A* was identified only in the angiosarcoma, consistent with p16 IHC. *MYC* amplification was also specific to the sarcomatous portion, while a *SETD2* p.N1396fs mutation was exclusive to the epithelial component. No other significant CNA were identified. All pathogenic alterations were confirmed to be somatic.

Case #	Age (y)	Gender	Tumor Size (cm)	Immunohistochemistry					Follow-up
				WT1	BRAF V600E	CK7	p16	Ki-67	
1	76	F	5.5	See Figure					DOD (4 m)
2	48	F	6	+++	+++	++	++	2%	LFU
3	64	F	1.7	+++	+++	-	++	3%	NED (5 m)
4	54	F	2	+++	+++	+	++	<1%	NED (9 y)
5	54	F	3.6	+++	- *	-	++	1%	NED (9 y)
6	44	F	3.5	+++	+++	+	++	<1%	NED (18 y)
7	52	F	1.4	+++	+++	-	++	<1%	NED (4 y)
8	38	F	2.4	+++	+++	+	++	3%	NED (1.5 y)
9	61	F	4	+++	++	+	++	<1%	NED (5 y)

**BRAF* V600E by NGS*

NED=no evidence of disease; DOD=died of disease; LFU=lost to follow-up

Figure 1 - 809

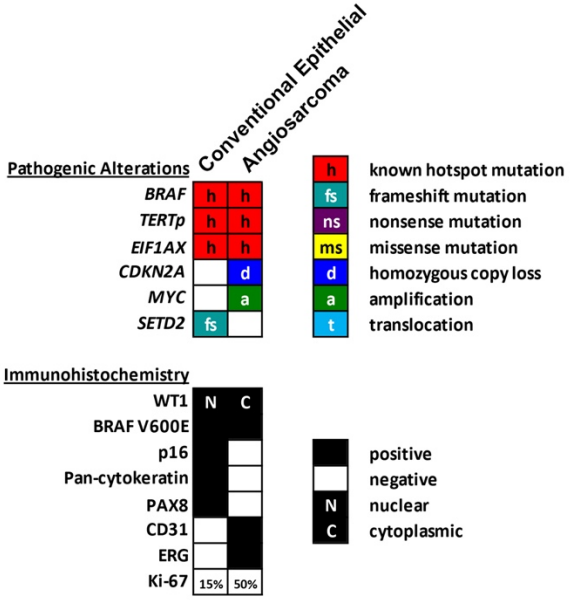

Conclusions: While the vast majority of cases show indolent behavior, rare molecular alterations can occur in MA in addition to *BRAF*. One conventional MA showed pathogenic *BRCA2* mutation. A BRAF-positive tumor with features of MA showed *TERT* promoter and *EIF1AX* mutations and genetic evidence of sarcomatous evolution with specific loss of *CDKN2A*/p16 and amplification of *MYC*.

810 Molecular Characterization of Histologically High Grade Tumors Involving the Urinary Bladder in Patients who Received Radiation Therapy for Prostatic Adenocarcinoma

Emily Chan[1], Karuna Garg[2], Jeffry Simko[2], Bradley Stohr[2]
[1]UCSF School of Medicine, San Francisco, CA, [2]University of California, San Francisco, San Francisco, CA

Disclosures: Emily Chan: None; Karuna Garg: None; Jeffry Simko: None; Bradley Stohr: None

Background: Distinction between high grade prostatic carcinoma (PC) and high grade urothelial carcinoma (UC) has important therapeutic and prognostic ramifications. In most cases, differentiation between these entities is straightforward with the use of morphologic criteria and immunohistochemical (IHC) stains. However, this distinction can become challenging in the setting of prior radiation and/or hormone therapy for PC, where PC can show ambiguous, and even misleading, histologic and IHC features. Recent studies have shown that PC

and UC can be molecularly distinguished by the presence of TMPRSS2-ERG fusion, seen in 40-50% of PCs, or TERT promoter mutation, seen in up to 70% of UCs.

Design: We performed capture-based next generation sequencing (NGS) on 25 cases of urinary bladder tumor resections (11 transurethral resections and 14 cystectomy/cystoprostatectomies) from patients who had received radiation therapy for PC. The NGS assay targets the coding region of 479 cancer-related genes and select introns from 47 genes, and the TERT promoter. The presence of either a previously described pathogenic TERT promoter mutation and/or a TMPRSS2-ERG fusion was assessed and correlated to the original diagnosis and IHC profile.

Results: A pathogenic TERT promoter mutation or TMPRSS2-ERG fusion was identified in 17/25 cases (68%) and correlated with the original diagnosis in most cases (see table). One discordant case consisted of a poorly differentiated carcinoma with papillary growth and squamous differentiation, positive for p63 and GATA3, and negative for PSA, supporting a diagnosis of UC. However, molecular analysis demonstrated a TMPRSS2-ERG fusion, which is consistent with a PC with squamous differentiation. Of the three cases that showed ambiguous morphologic and IHC features at initial diagnosis ("PD or HG carcinoma" in table), one case revealed a TERT promoter mutation and a second case revealed a TMPRSS2-ERG fusion. Further detailed IHC (GATA3, p63, PSA, PSAP, p501s, NKX3.1) and molecular characterization of these post-treatment tumors will be presented.

Original diagnosis*	TERT promoter mutation	TMPRSS2-ERG fusion	Neither
UC (n=16)	13	1	2
PC (n=6)	0	1	5
PD or HG carcinoma (n=3)	1	1	1

UC = urothelial carcinoma. PC = Prostatic adenocarcinoma.
PD = Poorly differentiated. HG = High grade.

Conclusions: Using molecular analysis, we identified a TERT promoter mutation or TMPRSS2-ERG fusion in the majority of our series of high grade carcinoma involving the bladder in the setting of radiation therapy for PC. Identification of these molecular abnormalities also resolved UC vs PC in the majority of ambiguous cases. While treated PCs may closely mimic UC by histology, this seems to be a rare occurrence and can be resolved with IHC.

811 Automated Gleason Scoring of Prostate Needle Biopsy Images Using Deep Neural Networks and Its Comparison with Diagnoses of Pathologists

Hyeyoon Chang[1], Sangjun Oh[1], Sanghun Lee[1], Hyoun Wook Lee[2], Seung Eun Lee[3], Su-Jin Shin[4], Kyungeun Kim[5], Tae-Yeong Kwak[6], Choi Yoon-La[7], Sun Woo Kim[1]
[1]Deep Bio Inc., Seoul, Korea, Republic of South Korea, [2]Samsung Changwon Hospital, Sungkyunkwan University School of Medicine, Changwon, Korea, Republic of South Korea, [3]Konkuk University Medical Center, Konkuk University School of Medicine, Seoul, Korea, Republic of South Korea, [4]College of Medicine, Hanyang University, Seoul, Korea, Republic of South Korea, [5]Kangbuk Samsung Hospital, Sungkyunkwan University School of Medicine, Seoul, Korea, Republic of South Korea, [6]Deep Bio Inc., Guro-gu, Korea, Republic of South Korea, [7]Samsung Medical Center, Sungkyunkwan University School of Medicine, Seoul, Korea, Republic of South Korea

Disclosures: Hyeyoon Chang: *Employee*, Deep Bio Inc.; Sangjun Oh: *Employee*, Deep Bio Inc.; Sanghun Lee: *Employee*, Deep Bio Inc. Hyoun Wook Lee: None; Seung Eun Lee: None; Su-Jin Shin: None; Kyungeun Kim: None; Tae-Yeong Kwak: *Employee*, Deep Bio Inc.; Choi Yoon-La: None; Sun Woo Kim: *Advisory Board Member*, Deep Bio Inc.

Background: In terms of diagnosing prostate cancer from tissue slides, the Gleason Grading system is widely used as the standard basis for prognostic prediction and treatment selection. However, as the system is qualitative, there are considerable inter- and intra-observer variabilities between pathologists. In this study, we propose automated Gleason scoring using deep neural networks to assist more precise and consistent diagnoses. We report its performance in comparison with certified pathologists.

Design: A total of 1461 prostate needle biopsy cores from 238 patients at three different institutions were prepared in the form of digitized whole slide images (WSIs), where 91.0% contained cancer. Among them, 1038 were annotated for Gleason patterns and used to train and tune the deep neural networks model. The remaining 423 were used to evaluate the trained model upon the Gleason scores independently and blindly diagnosed by three pathologists uninvolved in the training process. The model architecture was based on DeepLab v3+ and MnasNet.

We defined the reference standard as the majority vote of the three pathologists. We then compared the diagnoses from the original institutions and the model's diagnoses against the reference standard. The performance was measured in three levels: the Gleason scores distinguishing the primary and the secondary grades, the Gleason groups, and the existence of cancer. For the existence of cancer, diagnostic values were also evaluated. We further compared the diagnoses of individual pathologists in account of inter-observer variations.

Results: Kappa score was measured for 341, 376, and 423 cases for Gleason scores, Gleason groups, and existence of cancer, respectively, excluding cases where all three pathologists have different opinions. While our model showed better score in detecting the existence of cancer, it showed comparable performance in more complex tasks. For the existence of cancer, the accuracy, specificity, positive predictive value, and negative predictive value were 0.995, 0.895, 0.990, and 0.944, respectively. Comparison with pathologists showed that our model's diagnoses is similar to the inter-pathologist variability.

Table 1. Kappa score against the reference standard

	Our model	Original diagnoses
Gleason score	0.303	0.307
Gleason group	0.416	0.421
Existence of cancer	0.911	0.844

Figure 1 - 811

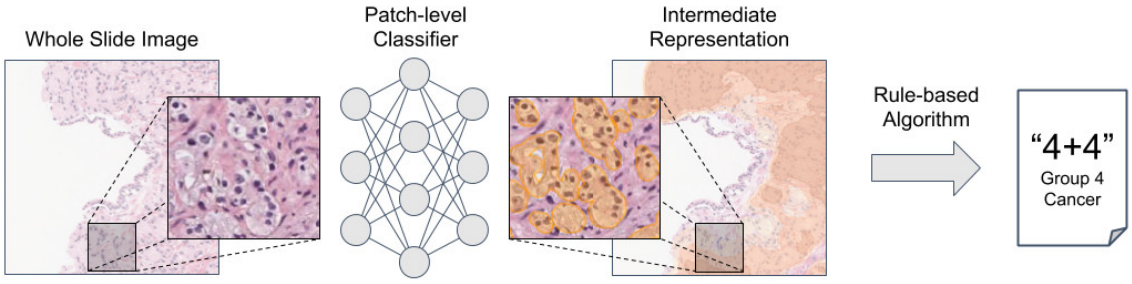

Figure 1. Automatic Gleason scoring process workflow

Figure 2 - 811

Figure 2. Inter-observer Kappa scores for Gleason scores (A), Gleason groups (B), and existence of cancer (C)

(A)

	Our model	Original diagnoses	Pathologist A	Pathologist B	Pathologist C
Our model	-	0.144	0.364	0.275	0.171
Original diagnoses	0.144	-	0.204	0.310	0.225
Pathologist A	0.364	0.204	-	0.348	0.293
Pathologist B	0.275	0.310	0.348	-	0.302
Pathologist C	0.171	0.225	0.293	0.302	-

(B)

	Our model	Original diagnoses	Pathologist A	Pathologist B	Pathologist C
Our model	-	0.236	0.462	0.321	0.321
Original diagnoses	0.236	-	0.306	0.428	0.335
Pathologist A	0.462	0.306	-	0.423	0.387
Pathologist B	0.321	0.428	0.423	-	0.371
Pathologist C	0.321	0.335	0.387	0.371	-

(C)

	Our model	Original diagnoses	Pathologist A	Pathologist B	Pathologist C
Our model	-	0.776	0.848	0.970	0.703
Original diagnoses	0.776	-	0.776	0.813	0.848
Pathologist A	0.848	0.776	-	0.852	0.703
Pathologist B	0.970	0.813	0.852	-	0.733
Pathologist C	0.703	0.848	0.703	0.733	-

Conclusions: To our knowledge, this is the first study to evaluate an automated Gleason scoring model of prostate needle biopsy images. As the results have shown that our model achieves a similar level of agreement as between pathologists, we expect that more training data will improve the model's performance further.

812 SMARCB1 Alterations and Protein Expression in Non-Medullary Renal Cell Carcinoma

Ying-Bei Chen[1], Liwei Jia[1], Gouri Nanjangud[1], Hikmat Al-Ahmadie[1], Samson Fine[1], Anuradha Gopalan[1], S. Joseph Sirintrapun[1], Satish Tickoo[2], Victor Reuter[1]
[1]Memorial Sloan Kettering Cancer Center, New York, NY, [2]New York, NY

Disclosures: Ying-Bei Chen: None; Liwei Jia: None; Gouri Nanjangud: None; Hikmat Al-Ahmadie: None; Samson Fine: None; Anuradha Gopalan: None; S. Joseph Sirintrapun: None; Satish Tickoo: None; Victor Reuter: None

Background: Loss of SMARCB1 expression, a core subunit of SWI/SNF complexes, has emerged as a crucial diagnostic marker for renal medullary carcinoma (RMC). Meanwhile, *SMARCB1* mutation or protein loss has been occasionally detected in other subtypes of renal cell carcinoma (RCC). The correlation between *SMARCB1* alterations and protein loss by immunohistochemistry (IHC) remains unclear in these non-medullary RCCs.

Design: We searched a targeted next-generation sequencing (NGS) database of our institution and public genomic databases to identify RCCs other than RMC that harbored *SMARCB1* alterations. We examined the clinicopathologic features and SMARCB1 protein expression by IHC in 16 non-RMC RCCs with *SMARCB1* alterations. FISH analysis (n=2) was also performed to confirm the status of *SMARCB1* locus.

Results: *SMARCB1* mutations were found in 16 of 1401 (1.1%) cases in nine published RCC genomic studies, including 9 (56%) truncating and 7 (44%) missense mutations; 6/7 missense mutations were variants with unknown significance. The frequencies of mutations were 5% in unclassified, 3% in chromophobe, 2% in papillary, and 1-2% in clear cell RCC. Additionally, *SMARCB1* mutations were identified in 17 (1.6%) and 15 (2.4%) of non-RMC cases in the AACR Project GENIE public RCC cohort (n=1036) and our internal database (n=614, overlapped with GENIE), respectively. The 16 patients in our study had a median age of 56 (30-75) and M:F ratio of 2.2:1. The histologic RCC subtypes were unclassified (8), clear cell (3), papillary (2), collecting duct (1), chromophobe (1), and TFE3 translocation (1). *SMARCB1* alterations detected were truncating (9/16, 56%), missense (5/16, 32%), rearrangement (1/16, 6%), and heterozygous deletion (1/16). Of 15 cases with material available for IHC, SMARCB1 expression was retained in 11 (73%) and lost in 4 (27%). SMARCB1 protein loss was seen in 3 unclassified and 1 papillary RCC, without clear correlation with alteration type. One of these 4 cases exhibited histologic features closely resembling RMC but occurred in a patient confirmed to lack sickle cell trait/disease; the other 3 had papillary (n=2) or solid (n=1) growth pattern. Cases with retained SMARCB1 protein despite mutations did not show clinicopathologic features of RMC.

Conclusions: SMARCB1 protein is retained in a large majority of non-RMC cases with *SMARCB1* somatic mutations. The role of *SMARCB1* mutation in these cases remains to be clarified. Combined with histomorphology, SMARCB1 loss is a highly specific marker for RMC.

813 Can Gleason Grade be Reliably Assigned Based on the Perineural Focus of Adenocarcinoma?

Fei Chen[1], Bogdan Isaila[2], Vamsi Parimi (Parini)[3], Qinghu Ren[4], Kyung Park[5], Hongying Huang[1], Fangming Deng[3], Jonathan Melamed[3]
[1]NYU Langone Health, New York, NY, [2]New York University Medical Center, New York City, NY, [3]New York University Medical Center, New York, NY, [4]New York University Langone Medical Center, New York, NY, [5]NYU Langone Health, New York City, NY

Disclosures: Fei Chen: None; Bogdan Isaila: None; Vamsi Parimi (Parini): None; Qinghu Ren: None; Kyung Park: None; Hongying Huang: None; Fangming Deng: None; Jonathan Melamed: None

Background: Adenocarcinoma of prostate (PCa) may infrequently be seen on needle biopsy as a microscopic focus limited to the perineural space (~0.6%). Efforts to grade limited cancer located in the perineural space (PNI) using the Gleason grading system are sometimes attempted, however this has not been validated. We therefore proposed to 1) assess the accuracy of assignment of a Gleason grade to the perineural focus, and 2) whether PNI grade patterns differentiate low from high grade (grade group 3 and higher) adenocarcinoma in the radical prostatectomy.

Design: To assess utility of pathologic assignment of a low versus high grade based on perineural pattern using an image-based simulation of "perineural cancer only" and correlate with grade assigned in the radical prostatectomy (RP). Digital photomicrographs were taken from the dominant lesion for 20 RP cases in each grade group with perineural invasion. For each case, 5 foci of perineural cancer (PNI) were digitally cropped (to include nerve and perineural cancer cuff) and provided as a panel of test image files. Images were then graded by two uropathologists who were blinded to all other details of the case, with instructions to attempt to assign a grade (GG) to each focus of perineural cancer (PNI) (400 foci in total), and an overall GG for each case based on images (PNI foci). The perineural grade (PNI GG) were correlated with the grade assigned previously to the radical prostatectomy (RP GG) to assess for concordance. The PNI and RP grade group were then assessed for concordance when combined as low (grade group 1 & 2) and high grades (3, 4 and 5). T-test was used to detect the difference.

Results: Perineural invasion is less frequently encountered in GG1 (29%) compared to higher grade groups (GG2-5, 62%). (table 1). While grade assignment based on PNI shows a high positive but not exact correlation with radical prostatectomy grade (correlation coefficient of

0.72) for an individual case, low and high grade PNI scores significantly differentiate between low and high grade groups in radical prostatectomy (p<0.001).

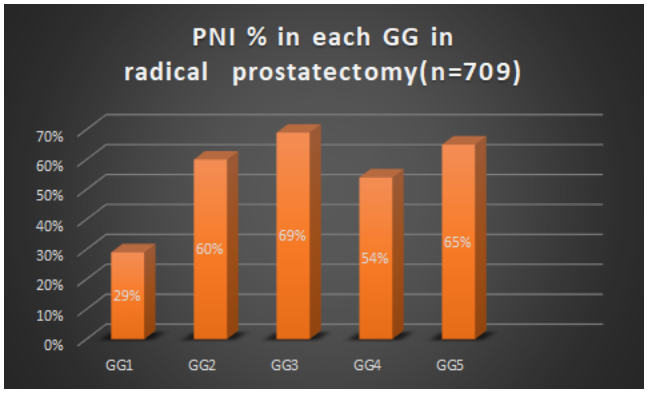

Conclusions: PNI score can significantly differentiate between low and high grade adenocarcinoma at radical prostatectomy (p<001) but is inexact for assignment as grade group. Further work is awaited to describe and validate the specific low and high grade perineural patterns.

814 Neuroendocrine Marker Insulinoma-Associated Protein 1 (INSM1) Showed Differential Expression in Prostatic High-Grade Neuroendocrine Carcinomas and Gleason Score 9-10 Acinar Adenocarcinomas with Neuroendocrine Differentiation

Jie-Fu Chen[1], Chen Yang[2], Dengfeng Cao[1]
[1]Barnes Jewish Hospital/Washington University, St. Louis, MO, [2]Yale University School of Medicine, New Haven, CT

Disclosures: Jie-Fu Chen: None; Chen Yang: None; Dengfeng Cao: None

Background: Insulinoma-associated protein 1 (INSM1) is a transcription factor involved in the development of neuroendocrine cells and is directly regulating expression of chromogranin and synaptophysin. INSM1 has been recently shown to be a sensitive marker for small cell carcinoma of the prostate. However, no study has investigated its expression in prostatic acinar adenocarcinoma with neuroendocrine differentiation (PCA-NED). Here we evaluate INSM1 expression in Gleason score (GS) 9-10 PCA-NEDs and compare its expression in prostatic high grade neuroendocrine carcinomas (HGNECs).

Design: Fifteen prostatic HGNECs (14 small cell, 1 large cell) and 15 GS9-10 PCA-NEDs were studied. One paraffin block containing tumor from each case was used to generate unstained slides for immunohistochemical stainings with antibodies to INSM1 (Santa Cruz Biotechnology, Clone A8, 1:200 dilution), chromogranin (Ventana, clone LK2H10, prediluted), synaptophysin (Cell Marque, Clone MRQ-40, prediluted), prostatic specific antigen (PSA, Cell Marque, clone ER-PR8, prediluted), prostein (Dako, clone 10E3, prediluted), and NKX 3.1 (Ventana, clone EP356, prediluted). The staining for INSM1 and NKX3.1 was nuclear; cytoplasmic for chromogranin, synaptophysin, PSA and prostein. The immunohistochemical stainings were semi-quantitatively scored as 0 (<1% cells staining), 1+ (1-25%), 2+ (26-50%), 3+ (51-75%), and 4+ (76-100%).

Results: Positive staining for INSM1 was seen in 13/15 (87%) prostatic HGNECs (1+ in 2, 2+ in 2, 3+ in 4, 4+ in 5; % cells stained: 0-95%, mean 50%, median 70%) and 3/15 (20%) GS9-10 PCA-NEDs (1+ in 2, 2+ in 1; % cells stained: 0-40%, mean 5%, median 0%), respectively (p = 0.003). There was no significant staining difference in synaptophysin or chromogranin between these two types of carcinomas (p = 0.24 and 0.22, respectively). HGNECs showed more CD56 staining than PCA-NEDs (p=0.053). Prostatic specific markers showed significant difference between these two types of carcinomas (p = 0.01 for PSA; p = 0.003 for prostein; p = 0.009 for NKX 3.1).

Marker	HGNEC					PCA-NED					P value
	0	1+	2+	3+	4+	0	1+	2+	3+	4+	
INSM1	2	2	2	4	5	12	2	1	0	0	0.003
CGA	1	4	2	3	5	5	3	0	1	5	0.2160
SYN	0	1	0	0	14	0	3	1	0	10	0.24020
CD56	3	1	2	3	4	11	1	0	1	1	0.053
PSA	14	1	0	0	0	3	1	0	1	4	0.01
Prostein	11	0	0	0	0	3	1	0	0	4	0.003
NKX 3.1	11	0	0	0	0	0	3	0	1	4	0.009

Conclusions: In prostatic HGNECs, INSM1 showed similar sensitivity as chromogranin and CD56 but was not as sensitive as synaptophysin. INSM1 showed significant difference between prostatic HGNECs and GS 9-10 PCA-NEDs, and is a useful marker to distinguish these two types of prostatic carcinomas.

815 STAT3 Phosphorylation at Ser727 is involved in prostate carcinogenesis and is associated with increased disease-associated mortality

Fei Chen[1], Qinghu Ren[2], David Levy[1], Peng Lee[3], Fangming Deng[4], Jonathan Melamed[4]
[1]NYU Langone Health, New York, NY, [2]New York University Langone Medical Center, New York, NY, [3]New York Harbor Healthcare System, NYU School of Medicine, New York, NY, [4]New York University Medical Center, New York, NY

Disclosures: Fei Chen: None; Qinghu Ren: None; David Levy: None; Peng Lee: None; Fangming Deng: None; Jonathan Melamed: None

Background: Stat3 as a transcription factor has been implicated in the promotion of growth and progression of prostate cancer. Phosphorylation of Stat3 at Tyr705 has been revealed to be required for Stat3 activation. However, the role of Ser727 phosphorylation on Stat3 in prostate cancer is not well established. The purpose of this study was to examine the status of Ser727 phosphorylation on Stat3 in human prostate cancer epithelial and stromal components and the correlation of Ser727 phosphorylation with prostate cancer progression.

Design: Immunohistochemistry was performed using specific antibodies against Ser727 phosphorylated Stat3 (Stat3-727pSer) in Formalin-Fixed and Paraffin-Embedded tissue microarray with a cohort of prostate cancers (n=207) with an average follow-up of 54 months and in benign prostate tissue (n=38). Intensity levels were scored with Allred scoring system [0 (negative) - 3 (strong)] of expression density and percentage score [0(0%) - 5 (100%)] were recorded, resulting in a combined score for statistical analysis with an unpaired t-test.

Results: Cytoplasmic and nuclear expression of Stat3-pS727 are both significantly increased in prostate cancer cells (epithelium) (1.7-fold and 2-fold, $p<0.005$), as well as in cancer stroma (1.7-fold and 2.1-fold, $p<0.005$), compared with its phosphorylation in benign prostate tissue. The cytoplasmic but not the nuclear abundance of Stat3-pS727 in cancer epithelium was significantly increased in patients who were expired during the follow-up (1.2-fold, $p<0.001$). A Kaplan-Meier survival curve showed cancer cell cytoplasmic expression of Stat3-pS727 correlated with disease-associated mortality ($p<0.01$). There was no significant difference in the abundance of Stat3-pS727 (epithelial and stromal; cytoplasmic and nuclear) among other clinicopathological factors studied, including patient race, age, Gleason score, stage, extraprostatic extension, and chemical recurrence.

Conclusions: This study demonstrates that the Ser727 phosphorylated forms of Stat3 is up-regulated in both epithelial and stromal components of prostate cancer, suggesting it plays roles in the carcinogenesis of prostate cancer. The up regulated phosphorylation of cytoplasmic Stat3-S727 is associated with patient disease-associated mortality in this cohort, indicating that it may serve as a useful biomarker for monitoring disease progression and suggesting a non-nuclear mechanism of action.

816 IDH1 Mutations Mark a High-Grade, Potentially Aggressive Variant of Prostate Cancer

Paolo Chetta[1], Giorgia Zadra[1], Maria Giulia Cangi[2], Ilaria Francaviglia[2], Roberta Lucianò[2], Sabina Davidsson[3], Svitlana Tyekucheva[4], Silvano Bosari[5], Ove Andren[6], Claudio Doglioni[7], Massimo Loda[1]
[1]Dana-Farber Cancer Institute, Boston, MA, [2]IRCCS San Raffaele Scientific Institute, Milan, Italy, [3]Örebro University, Faculty of Medicine and Health, Örebro, Sweden, [4]Dana-Farber Cancer Institute, Harvard T.H. Chan School of Public Health, Boston, MA, [5]Fondazione IRCCS Ca' Granda Ospedale Maggiore Policlinico, University of Milan, Milan, Italy, [6]Örebro University, Örebro, Sweden, [7]University Vita-Salute San Raffaele, Milano, Italy

Disclosures: Paolo Chetta: None; Giorgia Zadra: None; Maria Giulia Cangi: None; Roberta Lucianò: None; Sabina Davidsson: None; Svitlana Tyekucheva: None; Silvano Bosari: None; Ove Andren: None; Claudio Doglioni: None; Massimo Loda: None

Background: Oncogenic mutations in isocitrate dehydrogenase (IDH) 1 and 2 mark a radiosensitive, milder group of glioma and a targetable, relapse-prone form of acute myeloid leukemia. Recently, IDH1-mutant prostate cancer emerged as a rare molecular class, whose clinical and prognostic features are yet to be determined.

Design: We examined IDH1/2 mutational hotspots via Sanger/pyro-sequencing in 590 FFPE prostate adenocarcinomas, including 184 selected early-onset cases (age <50), 120 transurethral resections, and 143 samples with annotated metabolomics profiles. The mutant cases were analyzed for clinical and pathological features as well as metabolic profiles, when available (n=2). To corroborate metabolomics, we determined differentially expressed genes and enriched pathways in the IDH1-mutant group from the (The Cancer Genome Atlas) TCGA dataset.

Results: Twelve cases of 590 harbored heterozygous oncogenic IDH1 mutations (R132H, R132C, R132G, R132S and R132L). No IDH2 mutations were detected. The rate of events was 1.2% across all age groups and 3% in men diagnosed before the age of 50. There was a significant association with grade group 5 ($p<0.04$). Clinical information was available for five patients with mutated IDH1. All of these were administered androgen-deprivation therapy, which failed in two patients, one of whom died of metastatic disease. High levels of 2-hydroxyglutarate (2HG) were found in the two mutant cases that had annotated metabolic profiles. Several anaplerotic metabolites, e.g. ?-ketoglutarate and glutamate, were low, while glycolytic intermediates and glutathione were elevated. In line with the metabolomics data, upregulation of diverse Warburg-effect transcripts, including lactate dehydrogenase A and pyruvate kinase M2, was observed in the TCGA

dataset (p<0.01; FDR<0.1). Pathway analysis revealed enrichment for gene sets pertaining to glycolysis, oxidative phosphorylation, fatty acid metabolism, and oxidative stress.

ID	Gleason score	IDH1 status	Grade group	Age at diagnosis	T	N	M	Adjuvant targeted therapy	ADT resistance	Last follow-up
1	4+5	M	5	68	-	-	-	-	-	-
2	4+5	M	5	72	-	-	-	-	-	-
3	3+4	M	2	49	-	-	-	-	-	-
4	5+4	M	5	49	-	-	-	-	-	-
5	4+5	M	5	48	-	-	-	-	-	-
6	3+4	M	2	46	-	-	-	-	-	-
7	3+4	M	2	45	-	-	-	-	-	-
8	4+5	M	5	65	T3a	N0	M0	yes	no	living
9	4+5	M	5	49	T2b	Nx	Mx	yes	no	living
10	4+3	M	3	83	T1b	Nx	M0	yes	yes	living
11	4+3	M	3	68	T1b	Nx	M1	yes	yes	dead due to prostate cancer
12	5+4	M	5	80	T1a	Nx	M0	yes	no	living

Figure 1 - 816

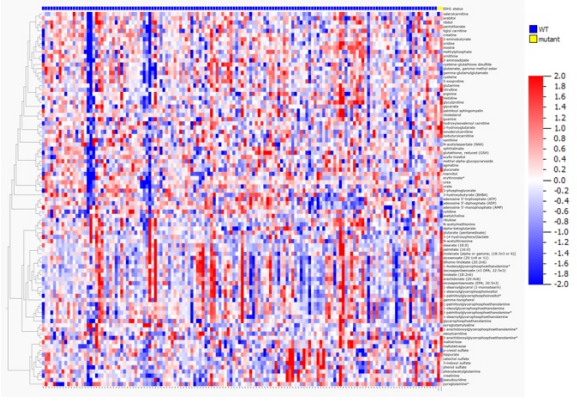

Figure 2 - 816

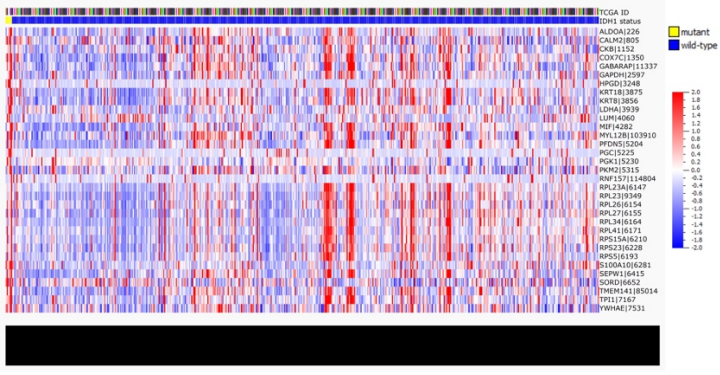

Conclusions: IDH1 mutations mark an early-onset, high-grade, potentially aggressive variant of prostate cancer with seemingly Warburg-like features. Our results suggest that serum 2HG screening and 18-FDG-PET might be useful adjuncts in the identification and follow-up of these patients. Radiotherapy or targeted inhibition of mutant IDH1 might be considered for advanced, castration-resistant cases.

817 Can In-bore MRI-guided Biopsy Accurately Predict Index Tumor Nodules in Radical Prostatectomy?

Suneetha Chintalapati[1], Qingnuan Kong[2], Franto Francis[3], Daniel Costa[4], Alberto Diaz de Leon[5], Naveen Subramanian[6], Julia Lotan[5], Ivan Pedrosa[5], Ming Zhou[7]

[1]University of Texas Southwestern Medical Center, Irving, TX, [2]1.University of Texas Southwestern Medical Center 2.Qingdao Municipal Hospital, Dallas, TX, [3]Irving, TX, [4]University of Texas Southwestern Medical Center, Dallas, TX, [5]UT Southwestern Medical Center, Dallas, TX, [6]University of Texas Southwestern Medical Center, Austin, TX, [7]Clements University Hospital, Dallas, TX

Disclosures: Suneetha Chintalapati: None; Daniel Costa: None; Naveen Subramanian: None; Ming Zhou: None

Background: Prostate cancer is frequently multifocal. The natural history of the disease is predominantly determined by the so-called index nodule (IN) which is usually the largest lesion with highest grade. Correct pretreatment identification of IN is critical for patient management, especially for focal therapy. In-bore MRI-guided prostate biopsy (MRGB) is associated with high detection rate of clinically significant prostate cancer (csPCa). We studied how often MRGB correctly identify Pca IN.

Design: MRI studies were performed in a 3 Tesla MRI using a multiparametric protocol. IN was defined as the largest with highest PI-RADS v.2 score. MRGB was performed with an 18-gauge needle mounted on an MRI-compatible interventional device for transrectal

prostate biopsies. 3 cores were obtained from each MRI-visible lesion. Systematic sampling was not performed. Radical prostatectomies with preoperative MRGB were reviewed for the IN characteristics including Gleason score (GS), location and size, which were then correlated with MRGB findings. GS>=3+4 PCa was considered csPCa

Results: In 34 patients, MRI identified a total of 70 significant tumor nodules (mean=2.1 [range 1-3]). PI-RADS v.2 score was 3, 4 and 5 in 8 (11.4%), 36 (51.4%) and 16 (22.9%). IN identified on MRGB matched those in RP for GS and location in 21/34 (61.8%). In 3/34 (8.8%) cases, the location did not match, including 2 cases with discrepant sides (right vs left) and 1 case with discrepant zones (transition zone vs peripheral zone). In 8/34 (23.5%) and 1/34 (2.9%), GS in RP was upgraded and downgraded, respectively, from MRGB GS, including upgrading from 3+3 to 3+4 in 2, from 3+3 to 4+3 in 2, from 3+4 to 4+3 in 3, and from 3+4 to 4+4 in 1 case. In 4/34 (12.5%), therefore, MRGB erroneously graded csPCa as low risk (GS 3+3) disease. In 1 case, GS was downgraded from 4+4 to 4+3. The mean size of IN measured on ib-GB and RP was 14.8 and 21.9 mm ($p<0.01$).

Conclusions: MRGB correctly identified and graded IN in 61.8% cases with regard to GS and location. Undergrading was seen in 23.5% of cases. The mean IN size measured on MRGB is significantly smaller than in RP. These findings may have significant impact on focal therapy and need to be confirmed in larger studies.

818 Pathological Features of Prostate Cancer Missed by Magnetic Resonance Imaging Using Imaging-derived, 3D-printed, Patient-specific whole-mount Analysis of Radical Prostatectomies

Suneetha Chintalapati[1], Qingnuan Kong[2], Franto Francis[3], Daniel Costa[4], Alberto Diaz de Leon[5], Claus Roehrborn[5], Kenneth Goldberg[6], Ivan Pedrosa[5], Ming Zhou[7]
[1]University of Texas Southwestern Medical Center, Irving, TX, [2]1.University of Texas Southwestern Medical Center 2.Qingdao Municipal Hospital, Dallas, TX, [3]Irving, TX, [4]University of Texas Southwestern Medical Center, Dallas, TX, [5]UT Southwestern Medical Center, Dallas, TX, [6]University of Texas Southwestern Medical Center, Lewisville, TX, [7]Clements University Hospital, Dallas, TX

Disclosures: Suneetha Chintalapati: None; Daniel Costa: None; Kenneth Goldberg: None; Ming Zhou: None

Background: Magnetic Resonance Imaging (MRI) of prostate cancer (PCa) has been shown to have high detection rate of clinically significant PCa. Most of PCa missed by MRI are small, Gleason score (GS) 3+3 PCa. We performed a detailed analysis of the pathological features of PCa missed by MRI using imaging-derived, 3D-printed, patient-specific whole-mount analysis of radical prostatectomies (RP) which provides excellent MRI-pathology correlation.

Design: MRI studies were performed in a 3 Tesla MRI scanner with a multiparametric protocol comprised of T2-weighted, diffusion-weighted and dynamic contrast-enhanced images. RP was processed using imaging-derived, 3D-printed, patient-specific whole-mount methods and all PCa foci were mapped with location, size, Gleason score (GS), % pattern 4, presence of cribriform cancer glands and intraductal carcinoma (IDC) and extraprostatic extension (EPE). These findings were correlated with preoperative MRI to identify tumor nodules that failed to be prospectively detected by MRI.

Results: 34 RP contained a total of 81 tumor nodules with a mean=2.4 (range 1-4) tumor nodules per RP. 32 (39.5%) nodules were not identified on MRI. Two were considered index nodules on MRI. Of these 32 nodules, 6 (18.9%) had adverse pathological features, including 3 with GS >=3+4 (pattern 4 >10%) (including 1 with EPE, 1 with cribriform cancer glands), 1 with GS 4+4 with cribriform glands, 1 with IDC and EPE. All these nodules were > 5mm. 26/32 (81.1%) cases were considered clinically insignificant with GS=<7 (pattern 4<=10%), no EPE, IDC nor cribriform cancer glands. 23 (88.5%) and 3 (11.5%) of them were in peripheral and transition zones. 12 (46.2%) and 14 (53.8%) were <5 mm and >=5 mm.

Conclusions: Using imaging-derived, 3D-printed, patient-specific whole-mount analysis of RP which yields excellent MRI-pathology correlation, we characterized the pathological features of PCa missed by MRI. Majority of PCa missed by MRI is potentially clinically insignificant. However, approximately 1 in 5 PCa missed by MRI harbor adverse pathological features.

819 Utility of Social Media and Whole Slide Imaging in Diagnostic Consultations on Urothelial Lesions

Suneetha Chintalapati[1], Qi Cai[2], Qingnuan Kong[3], Jyoti Balani[4], Fangming Deng[5], Franto Francis[4], Cheng Cheng Huang[6], Max Kong[7], Jianhong Li[8], Ming Zhou[9]
[1]University of Texas Southwestern Medical Center, Irving, TX, [2]University of Texas Southwestern Medical Center, Tucson, AZ, [3]1.University of Texas Southwestern Medical Center 2.Qingdao Municipal Hospital, Dallas, TX, [4]Irving, TX, [5]New York University Medical Center, New York, NY, [6]New York, NY, [7]Rego Park, NY, [8]Wynnewood, PA, [9]Clements University Hospital, Dallas, TX

Disclosures: Suneetha Chintalapati: None; Qi Cai: None; Jyoti Balani: None; Fangming Deng: None; Jianhong Li: None; Ming Zhou: None

Background: Social media has become increasingly popular in diagnostic consultation on problematic cases. Several representative images of a case are posted on social media available to a group of pathologists for their diagnoses and comments. However, little is known regarding the accuracy of, and factors that affect, diagnostic consultations using social media.

Design: 16 urothelial lesions encompassed 3 diagnostic categories: benign (5 cases: biopsy artifact, reactive atypia, atypia of uncertain significance and hyperplasia), urothelial dysplasia/CIS (D/CIS) (6 cases) and low grade papillary tumors (LGPT) (5 cases: papilloma, PUNLMP and low grade papillary carcinoma). 3 representative images from each case taken at 4, 10 and 20X magnifications were posted on WhatsApp and WeChat for review by 6 pathologists with subspecialty training in GU pathology. A diagnosis was deemed accurate if it fell in the same diagnostic category. After a wash-out period of 1 year, the same set of cases were digitalized on a scanner and reviewed by the 6 participants using the same diagnostic categories.

Results: Using social media, the overall diagnostic accuracy for 16 cases by 6 participants was 43.8% (42/96), and ranged from 31 to 69% among 6 pathologists. The accuracy was 36.7, 44.4 and 50% for benign, D/CIS and LGPT. Using whole slide scanned images, the overall diagnostic accuracy for 16 cases by 6 participants was 75% (72/96), significantly higher than that with social media (Chi-square test, p=0.0001), and ranged from 56.3 to 100% among 6 pathologists. The improvement ranged from 6.3 to 56.3%. The accuracy was 70 and 93% for benign and LGPT, significantly higher than those achieved with social media (Chi-square test, p=0.01, 0.0001). The accuracy for D/CIS was 63.7%, similar to that with social media (p=0.1).

Conclusions: Despite of the broad diagnostic categories used, the overall diagnostic accuracy by individual participants using social media is 43.8%. Using the whole slide scanned images, the overall accuracy significantly improved to 75%. The diagnostic accuracy for benign and LGPT significantly improved using whole slide scanning compared with social media. These findings suggest that diagnostic consultation using social media, often constrained by number and quality of images, is suboptimal in its accuracy. The whole slide scanning, with increased accessibility, should become the preferred mode of digital diagnostic consultation.

820 Different T cell exhaustion patterns in subtypes of muscle-invasive bladder cancer: Analysis of data from the cancer genome atlas (TCGA) bladder project

Vaibhav Chumbalkar[1], Tipu Nazeer[2], Yue Sun[2]
[1]Albany Medical Center, Albany, NY, [2]Albany Medical College, Albany, NY

Disclosures: Vaibhav Chumbalkar: None; Tipu Nazeer: None; Yue Sun: None

Background: In a previous large study of pembrolizumab in patients with bladder cancer, PD-L1 expression did not appear to impact responses in PD-L1-positive versus PD-L1 negative patients. However, a recent study demonstrated lower overall survival with pembrolizumab compared to chemotherapy in patients with PD-L1^{low} expressing urothelial carcinoma. Therefore, a better marker to predict treatment outcomes of checkpoint inhibitor therapy is still required. Checkpoint inhibitor therapy can provoke antitumor responses from functionally exhausted tumor-infiltrating lymphocytes (TILs). Recent studies demonstrate that memory-like exhausted T cells (PD-1^{mid}T-bet^{hi}TIM3^{low}) appear to be more responsive to checkpoint inhibitor therapy. While differentiated-exhausted T cells (PD-1^{hi}T-bet^{low}TIM3^{hi}EOMES^{hi}) are resistant to the treatment.

Design: Using publically available normalized mRNA expression data from muscle-invasive bladder cancer tumors with prominent TILs, 75 basal-squamous urothelial carcinoma (BS) and 84 other subtypes (OTHER) are identified based on mRNA expression. We analyzed effector T cell associated transcription factor (TBX21/T-bet, EOMES, and PRDM1) and functional effector gene (GZMA, GZMB, PRF1, and IFNG) expression, and their relationships with immunotherapy target genes (PD-1 and PD-L1).

Results: PD-L1 (PDCD1) and PD-1 (CD274) expression is significantly higher in the basal-squamous urothelial carcinoma ($p < 0.001$). In addition, effector T cell associated transcription factors (TBX21/T-bet, EOMES, and PRDM1) and functional effector gene (GZMA, GZMB, PRF1, and IFNG) showed significantly higher expression in the basal-squamous subtype ($p < 0.001$) (Figure 1). Importantly, strong correlations were found between PD-1 (CD274) expression and effector T cell associated transcription factors across all subtypes (Figure 2).

Figure 1 - 820

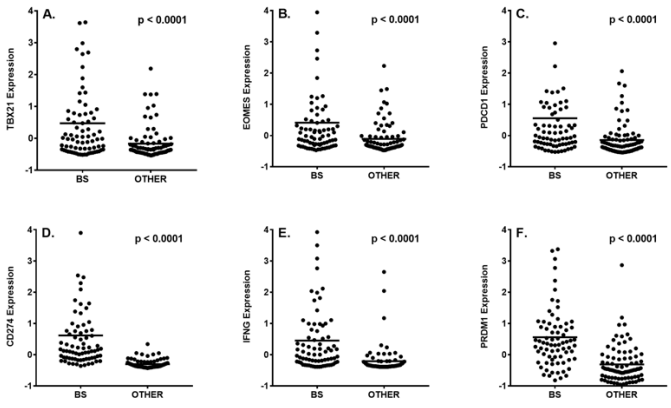

Figure 1. mRNA expression (Z scores) of TBX21/T-bet, EOMES, PD-1/PDCD1, PD-L1/CD274, IFNG, and PRDM1/Blimp1 in TCGA basal-sqamous urothelial carcinoma (BS) and other subtypes of urothelial carcinoma (OTHER).

Figure 2 - 820

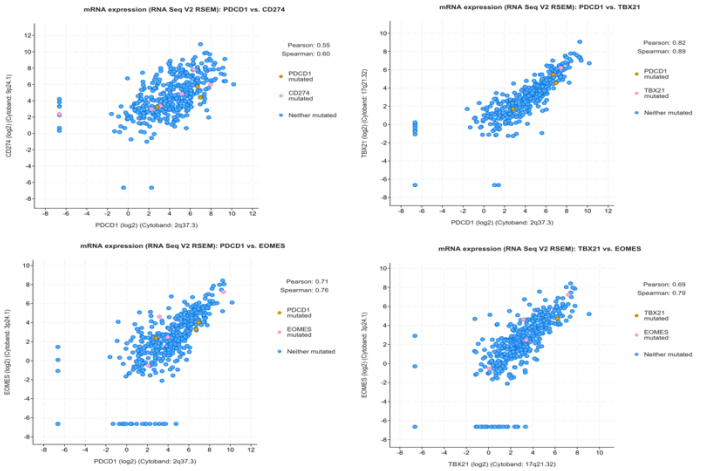

Figure 2. Correlations of mRNA expression between PD-1/PDCD1, PD-L1/CD274, TBX21, and EOMES.

Conclusions: TILs exhibit different exhaustion patterns in subtypes of muscle-invasive bladder cancer. Our analysis suggests that PD-1 expression along with TIL exhaustion/functional molecules may be evaluated as predictive markers of immune checkpoint therapy in urothelial cell carcinoma, especially in the basal-squamous subtype.

821 Significance of Paneth Cell-Like Differentiation in Prostatic Adenocarcinoma

Daniela Correia Salles[1], Douglas Mata[2], Jonathan Epstein[1]
[1]Johns Hopkins Medical Institutions, Baltimore, MD, [2]Brigham and Women's Hospital, Boston, MA

Disclosures: Daniela Correia Salles: None; Douglas Mata: None; Jonathan Epstein: None

Background: The grading and prognosis of prostatic adenocarcinomas with paneth cell-like neuroendocrine differentiation (PanEC) is controversial. There are limited data in the literature on their prognosis or associated findings.

Design: From 2006-2018, we identified 51 cases of conventional adenocarcinoma with paneth cell-like neuroendocrine differentiation or PanEC on biopsy(n=42), TURP(n=1), and RP(n=8).

Results: Of the 42 biopsy cases, 12 had only PanEC and a grade was not assigned as the tumor resembled higher grade cancer yet the morphology was distinctive for this entity. Of the remaining cases with associated usual prostatic adenocarcinoma, the Grade Groups(GG) were: GG1(n=16); GG2(n=4); GG3(n=7); GG4(n=0); and GG5(n=3). Of these, positive cores with PanEC were: 1(n=36); 2(n=2); 3(n=2); and 9(n=2) and total cores positive were: 1(n=21); 2(n=4); 3(n=4); and $\geq$5(n=13). To assess the prognostic significance of PanEC not confounded by co-existing higher grade cancer, we studied 25 biopsy specimens of PanEC with GG1-2 associated cancer or pure PanEC with available follow-up. The median follow up was 39 months (range,1-147 months). 10/25 cases underwent RP. RP GGs were: GG1(n=1); GG2(n=6) and GG3(n=1); 2 did not have assigned GGs, one due to treatment effect. RP stages were pT2(n=7) and pT3a(n=3), none had lymph node metastases. 1 patient underwent adjuvant radiation therapy and only 1 had post-RP biochemical recurrence (BCR). 5/25 patients were managed with active surveillance, none showed progression on follow-up. 10/25 patients were treated with radiation and/or hormone therapy, with 1 having biochemical progression. None of the 25 patients experienced death due to cancer or had metastatic disease. Of the 8 cases with PanEC first seen at RP, findings at RP were: GG2 (n=5); GG4 (n=1), GG1 (n=1), no grade due to treatment effect (n=1); pT2 (n=6), and pT3a (n=2), all with negative lymph nodes. One case with positive margins had biochemical recurrence at follow up with all 7 others free of disease at 3, 3, 14, 28, 46, 55, and 147 months.

Conclusions: Although PanEC may resemble Gleason patterns 4 and 5, only a minority are associated with biopsies with GG 2-5 usual prostate cancer. Also, PanEC on biopsy tends to involve only 1 core. Overall patients with PanEC as pure cancer or associated with usual GG1-2 cancer, tend to have a favorable prognosis with various treatments. Our study supports that PanEC should be considered as lower grade carcinoma and not be assessed using the Gleason grading system.

822 Less is More: Examination of Grossing Protocol for Cystectomy Specimens Following Neoadjuvant Chemotherapy

Cody Craig[1], Susan Maygarden[1], Sara Wobker[2]
[1]University of North Carolina, Chapel Hill, NC, [2]UNC Chapel Hill, Chapel Hill, NC

Disclosures: Cody Craig: None; Susan Maygarden: None; Sara Wobker: None

Background: In the past decade, neoadjuvant chemotherapy (NAC) has become the standard of care for muscle-invasive bladder cancer, leading to better clinical outcomes than cystectomy alone. Current cystectomy grossing protocols suggest "several" sections of grossly visible tumor, with deepest gross invasion, and "several" remote sections. However, protocols do not offer specific recommendations for NAC cases, where gross lesions are often not present. We undertook a retrospective review of our institution's grossing practices with regard to cystectomy specimens with and without NAC.

Design: Patients who underwent radical cystectomy for urothelial carcinoma between 2010 and 2018 were included. Patient age/sex, prior biopsy histology/grade/stage, final resection histology/grade/stage, neoadjuvant chemotherapy status, presence/absence of gross tumor/tumor bed, total blocks submitted, initial blocks of gross lesion, and subsequent blocks of gross lesion were abstracted from the medical record and pathology reports. For patients with additional sections submitted, slides were reviewed to determine if additional findings contributed to overall stage and diagnosis.

Results: 82 cystectomies were identified; 77 cases had prior biopsy or transurethral bladder resection (TURBT). 51/82 (62.2%) patients were treated with NAC. No gross tumor was identified in 32 cases, of which 24 (75%) were in patients who had received NAC. Of 16 cases with no residual microscopic carcinoma, 13 received NAC. Nine cases (8 NAC, 1 Non-NAC) had additional blocks submitted. Five cases had no histopathologic abnormality in additional blocks. In one case, UCIS was identified in the original and additional sections. In another case, a small focus of UCIS was found in the original sections and more convincing UCIS in the additional sections. In a third case, tumor was identified in initial random sections and additional random sections, but staging was not affected.

Total cystectomy cases (n=82)	**NAC**	**Non-NAC**
	51	31
Prior TURBT pathologic T stage (n=77)		
pTis	1	5
pT1	9	9
At least pT2	39	17
Final pathologic T stage		
pTis	11	8
pT0	13	3
pT1	3	0
pT2	8	2
pT3	12	10
pT4	4	5
No residual gross lesion (n=32)		
	24	8
No residual microscopic carcinoma (n=16)		
	13	3
Number of cases with additional blocks submitted (n=9)		
	8	1
Mean number of initial blocks submitted		
Mean = 17.6 (Range 8-77)	18.1	16.9
Mean number of of additional blocks submitted		
Mean number of lesion = 0.21	0.33 (0-9)	0 (0-0)
Mean number of random = 1.41	1.75 (0-50)	0.81 (0-25)

Conclusions: At our institution, NAC and Non-NAC cases are grossed with similar numbers of initial blocks (18.1 vs. 16.9). However, there is a tendency to submit additional blocks of both lesion and random bladder in NAC cases when compared to Non-NAC cases. Of 8 NAC cases with additional blocks, no changes to staging were made with the additional blocks. In our experience, accurate staging is possible for NAC cases with standard grossing protocol. Our data suggests that NAC cases should be grossed in a similar fashion to Non-NAC cases, without risk of incorrect staging.

823 Reproducibility of CD8 Positive T Cells Density Using Digitized Whole Slides in Tumor Areas

Igor Damasceno Vidal[1], Harsimar Kaur[1], Onur Ertunc[1], Tamara Lotan[2], Eugene Shenderov[2], Jessica Hicks[3], Christian Pavlovich[3], Trinity Bivalacqua[1], Karim Boudadi[2], Mohamad E Allaf[2], Carolyn Chapman[2], Paul Moore[2], Rehab Abdallah[2], Tanya O'Neal[2], Charles Drake[2], Drew Pardoll[2], Emmanuel Antonarakis[3], Hao Wang[2], Ashley Ross[2], Angelo De Marzo[1]
[1]Johns Hopkins University, Baltimore, MD, [2]Johns Hopkins School of Medicine, Baltimore, MD, [3]Johns Hopkins University School of Medicine, Baltimore, MD

Disclosures: Igor Damasceno Vidal: *Grant or Research Support*, MacroGenics, Inc., Rockville, MD, USA; Harsimar Kaur: None; Onur Ertunc: None; Tamara Lotan: None; Eugene Shenderov: None; Jessica Hicks: None; Christian Pavlovich: None; Karim Boudadi: None; Rehab Abdallah: None; Emmanuel Antonarakis: None; Hao Wang: None; Angelo De Marzo: *Grant or Research Support*, Macrogenics Inc

Background: Immune-checkpoint blockade has resulted in unprecedented treatment advances in multiple tumor types, although to date it has produced only modest results in prostate cancer (PCa). This study examines whether neoadjuvant enoblituzumab, a monoclonal antibody directed to block the activity of B7-H3, results in increased infiltrates of CD8 positive T cells in tumor areas in radical prostatectomy specimens from high-risk localized PCa patients. Also, we determined the reproducibility for CD8 counting between two observers independantly annotating the same standards slides.

Design: Thirteen cases of clinically localized prostate cancer (Gleason score from 7 to 10) were enrolled on a single arm, phase 2 study evaluating the safety, anti-tumor effect and immunogenicity of neoadjuvant enoblituzumab. Participants received enoblituzumab weekly for 6 doses prior to radical prostatectomy. Participants were matched to controls (n = 11) with similar final pathology, age and race. A representative FFPE tissue block from the index lesion was selected and stained for CD8 by a validated automated IHC assay. Since prostate cancer lesions often infiltrate between benign glands, which often show inflammation possibly unrelated to the tumor, whole slides were scanned and annotations were drawn carefully to encompass tumor areas and to exclude benign regions. For all cases, two separate observers with expertise in prostate pathology annotated these regions, blinded to patient treatment and blinded to the annotations of the other observer. We counted CD8 positive T cells per unit tumor area (CD8+ T cell density) using HALO software (Indica Labs) (Fig. 1).

Results: CD8+ T cell density was higher in tumor areas from enoblituzumab-treated patients as compared to matched controls when examined by either observer ($p = 0.0028$ for observer 1 and $p= 0.009$ for observer 2, Kruskal-Wallis). There was a correlation of T cell density between observers ($r^2 = 0.95$, $P < 0.0001$) (Fig. 2), indicating that blinded prostate cancer annotations are reproducible between observers.

Figure 1 - 823

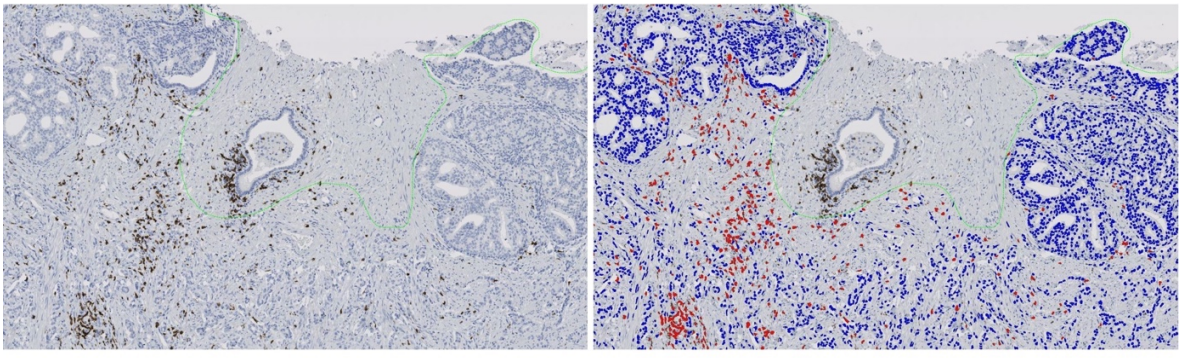

A) IHC for CD8 (brown)(left). Green highlights region excluded from tumor analysis area. Red (right) indicates T cells identified as positive.

Figure 2 - 823

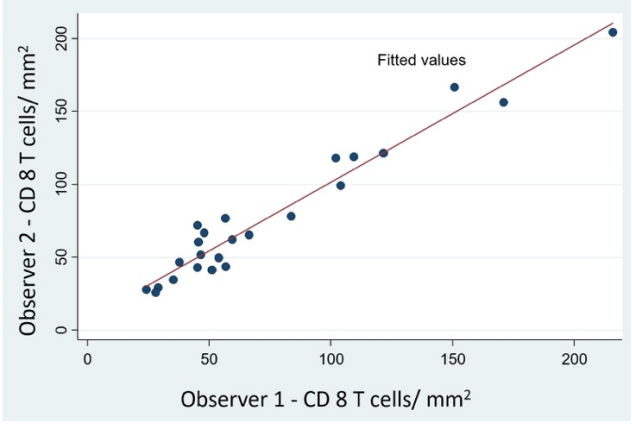

Conclusions: These results suggest that blocking of B7-H3 by enoblituzumab alters the tumor microenvironment that results in enhanced CD8 T cell infiltration – a hallmark of responsiveness to immunotherapy. Using digitized whole slides from radical prostatectomies, slide annotation to encompass tumor areas, while minimizing benign regions, is highly reproducible.

824 CD8+ Tumor Infiltrating Lymphocytes and Beta-2 Microglobulin Expression in Advanced Renal Cell Carcinoma: Correlation with Survival and Interleukin-2 Treatment Response

Dale Davis[1], Maria Tretiakova[2], Scott Tykodi[2], Brandon Hayes-Lattin[1], Christopher Kizzar[1], Christian Lanciault[1], Nicole Andeen[1]
[1]Oregon Health & Science University, Portland, OR, [2]University of Washington, Seattle, WA

Disclosures: Dale Davis: None; Maria Tretiakova: None; Brandon Hayes-Lattin: None; Christopher Kizzar: None; Christian Lanciault: None; Nicole Andeen: None

Background: Studies assessing correlations between tumor-infiltrating lymphocytes (TILs) in renal cell carcinoma (RCC) and clinical outcomes have mixed results. Given its interaction with CD8+ T-cells, we hypothesized that expression of MHC class I associated protein, beta-2 microglobulin (B2M), may be an important immunologic marker in RCC. We sought to understand potential implications of CD8+TILs and B2M expression on overall survival and response to interleukin-2 (IL-2) therapy, in a cohort of patients with advanced RCC.

Design: Four tumor regions from 46 patients' nephrectomies were assessed: highest grade, highest density of TILs (HD), infiltrative margin, and central tumor by tissue microarray (TMA) (n=25) or whole slide (n=21). RCC was considered CD8+TIL high if both 4-point case median exceeded the overall group median (40/400x) and CD8+TILs in HD area exceeded HD median (77/400x). RCC was considered B2M high if 4-point case median exceeded overall group median (5%). Findings were correlated with outcome data using Cox proportional hazard analyses and Fischers exact tests.

Results: 46 patients with metastatic RCC were identified; 43 had clear cell RCC and 37 had been treated with IL-2 therapy. At a median time to follow-up or death of 36 months, 13 (28%) patients had died and 22 (48%) were alive with disease. 14 (38%) patients had a response to IL-2 therapy, 12 of whom were still alive. 32% of RCCs were CD8+TIL-high, and 61% were B2M-high. Compared with patients with CD8+TIL-high RCCs, those with low CD8+TILs were associated with death (hazard ratio (HR) 6.19, p=0.02). Carcinoma expression of B2M corresponded with CD8+TIL rich areas. Compared with B2M-high cases, lower B2M expression had a non-significant trend toward lower survival (HR 5.84, p=0.10). 58% of patients with CD8+TIL-high RCCs had a response on IL-2 therapy and 77% of patients with no response to IL-2 therapy had low or medium CD8+TILs (p=0.15). B2M expression was not associated with response to IL2 therapy.

Figure 1 - 824

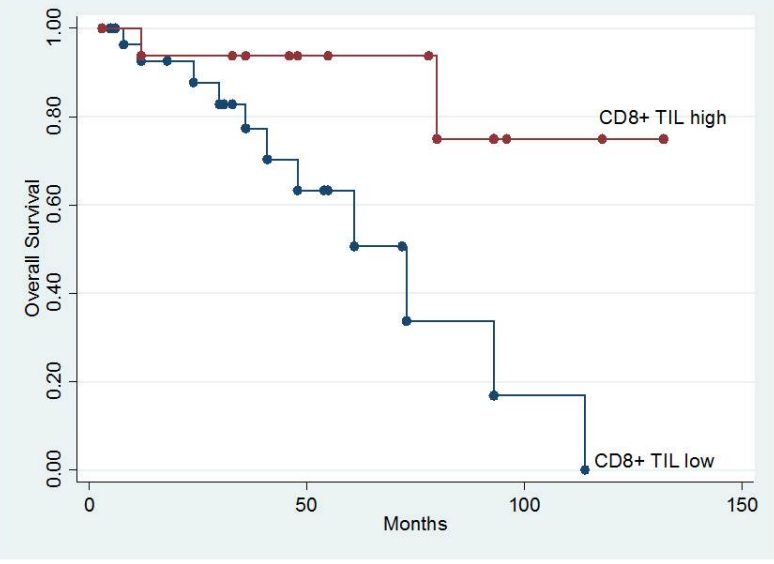

Conclusions: In contrast to some studies of RCC, in patients with metastatic RCC, abundant CD8+TILs were associated with longer overall survival. There were corresponding trends for higher IL-2 response rates in CD8+TIL-high RCCs and longer overall survival in cases with higher B2M expression, but these did not reach statistical significance. The findings warrant further study of CD8+TILs in selecting patients for IL-2 therapy, and for beta-2 microglobulin as an immunologic biomarker in RCC.

825 PTEN Expression is Independent of Morphologic Pattern 4 Subtypes in Prostatic Adenocarcinoma

Lauren Dehan[1], James Denney[2], Shanna Arnold Egloff[2], Lan Gellert[2], Kristen R Scarpato[2], Daniel Barocas[2], Giovanna A Giannico[2]
[1]Nashville, TN, [2]Vanderbilt University Medical Center, Nashville, TN

Disclosures: Lauren Dehan: None; James Denney: None; Shanna Arnold Egloff: None; Lan Gellert: None; Kristen R Scarpato: *Grant or Research Support*, Abbott Molecular; Daniel Barocas: None; Giovanna A Giannico: None

Background: Invasive cribriform (CRIB) and intraductal (IDC) prostatic adenocarcinoma is associated with unfavorable clinical outcome and biochemical recurrence (BCR). Loss of tumor suppressor protein phosphatase and tensin homologue (PTEN) has been is implicated with progression to androgen independence and adverse clinical outcome. We explored the association between PTEN expression by immunohistochemistry (IHC) and CRIB vs. non-CRIB Gleason pattern 4 morphology.

Design: One hundred sixty-two radical prostatectomies for adenocarcinoma (Gleason 3+4=7, N=30; 4+3 =7, N=26; 4+4=8, N=71; 4+5=9, N=20; 5+4=9, N=15) were evaluated by IHC for PTEN. We have previously established concordance of our PTEN IHC and FISH status. IDC was established by p63 IHC in selected cases with CRIB morphology. PTEN in ? 10% of cells was defined positive. Statistical analysis was performed with SPSS 25 for Windows.

Results: CRIB, poorly formed/fused (PF/F), glomeruloid (GLOM) and (IDC) patterns were present in 108/152 (71%), 138/161 (86%), 41/148 (28%) and 33/150 (22%) cases. Most cases presented multiple patterns [129/162 (79%)]. PTEN was positive in 65/108 (60%) CRIB, 77/138 (56%) PF/F, 32/41 (78%) GLOM, and 11/33 (71%) IDC cases. PTEN loss/expression was not significantly different between pattern 4 morphologies (P=0.725), but rather had a “field effect” distribution, unrelated to a specific morphology. PTEN was heterogenous in 26/108 (24%) CRIB, 27/138 (20%) PF/F, 5/41 (12%) GLOM, and 6/33 (18%) IDC cases. Heterogeneous PTEN was associated with CRIB compared to non-CRIB morphology when controlling for presence or absence of PTEN (P=0.028). CRIB was associated with an increased risk of BCR compared to non-CRIB morphology after adjusting for pathologic stage (OR=1.43, P<0.0001). Co-presence of GLOM morphology in patients with either CRIB (OR 0.80, P=0.008) or PF/F (OR 0.75, P=0.003) decreased risk of BCR after controlling for stage. Co-presence of PF/F did not affect BCR in patients with CRIB (P=0.838).

Conclusions: PTEN expression is not associated with any specific pattern 4 morphology, suggesting that the adverse effect of CRIB morphology is independent of PTEN loss. Heterogeneous PTEN expression is associated with CRIB morphology. Finally, although CRIB morphology is associated with increased risk of BCR, we show that GLOM morphology is protective against BCR.

826 Evaluation of MET Alterations in a Cohort of 11 Patients with Biphasic Papillary Renal Cell Carcinoma

Thomas Denize[1], Nelly Burnichon[2], Pierre-Alexandre Just[3], Hélène Blons[4], Aurélien Morini[5], Marie Auvray[2], Deborah Jakubowicz[6], Stéphane Oudard[2], Anne-Paule Gimenez-Roqueplo[2], Virginie Verkarre[2]
[1]APHP.5 Hôpital Européen Goerges Pompidou, Paris, France, [2]APHP.5 Hôpital Européen Georges Pompidou; INSERM UMR970, Paris Descartes University, Paris, France, [3]APHP, Hopital Cochin, Paris, France, [4]Hôpital Européen Georges Pompidou, Paris, France, [5]APHP.5 Hôpital Européen Georges Pompidou, Paris, France, [6]APHP.5 Hôpital Européen Georges Pompidou; INSERM UMR970, Paris, France

Disclosures: Thomas Denize: None; Nelly Burnichon: None; Pierre-Alexandre Just: None; Hélène Blons: None; Aurélien Morini: None; Marie Auvray: None; Deborah Jakubowicz: None; Stéphane Oudard: *Consultant*, Novartis, Pfizer, Ipsen, Bayer; Anne-Paule Gimenez-Roqueplo: None; Virginie Verkarre: None

Background: Biphasic papillary renal cell carcinoma (BPRCC), a recently described entity, seems to be a variant of papillary RCC (PRCC). Except two cases with germline *MET* mutation already reported, the relationship between BPRCC and MET alteration remain unknown. To further evaluate this association, we focused our study on MET alterations in BPRCC.

Design: We studied a monocentric series of 11 patients fulfilling diagnostic criteria of BPRCC based on the presence of large eosinophilic centro-alveolar cells stained by BCL1 surrounded by a papillary proliferation of small cuboidal cells CK7+ AMACR+ mostly BCL1 negative. Clinico-pathological data were analyzed. Using formalin fixed paraffin embebbed tissue tumor, we analyzed c-MET expression by immunohistochemistry (SP44, Ventana), *MET and* chromosome 7 copy number by fluorescence *in situ* hybridization and *MET* mutations by next generation sequencing (NGS) (Ion AmpliSeq Custom MET, exon 16-19). Germline *MET* mutation were searched by NGS (*TruSeq Custom Amplicon Low Input* (Illumina®)). c-MET expression was evaluated by a separated combined score CS (staining intensity x % of positive cell) on small and central large cells.

Results: Mean age at the diagnosis was 53.3 years (26-84 years) with sex ratio 1.75M:1F. Five total and 8 partial nephrectomies were performed. Three patients had multiple and bilateral tumors. Follow-up data were available for 8 patients (mean 34.8 months, 1-156 months). One patient developed lung and mediastinal metastasis (13 months after surgery).

On microscopic features, biphasic component was present from 5 to 100% of the tumor surface. Median ISUP grade was 2 on the small cells and 3 on the larger ones. Emperipolesis was found in all cases. 10 cases were pT1, 2 pT2, and 1 pT3a.

c-MET was expressed in all 11 cases (figure 1). Larger cells exhibit a higher CS score (mean ratio small/large = 0.54) with a more pronounced cytoplasmic staining. Trisomy 7 was found on 10/11 patients without any *MET* amplification (figure 2). Three patients had a *MET* mutation, two were previously known for carrying a *MET* mutation at germline level, 1 had a somatic mutation without germline mutation. *MET* mutation is going to be checked at germline level for 2 patients after genetic counseling and at somatic level for 8 patients.

Figure 1 - 826

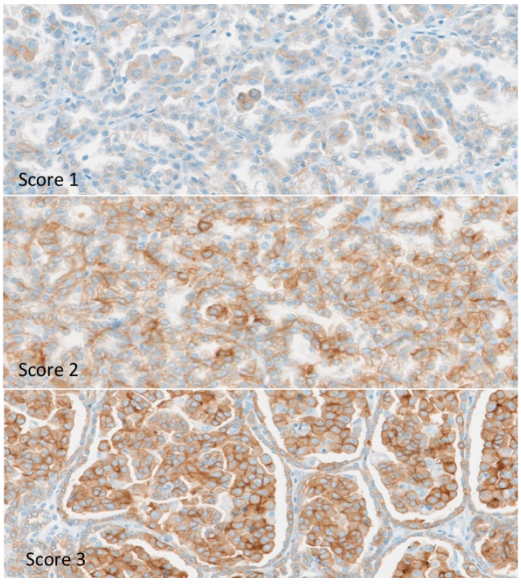

Figure 2 - 826

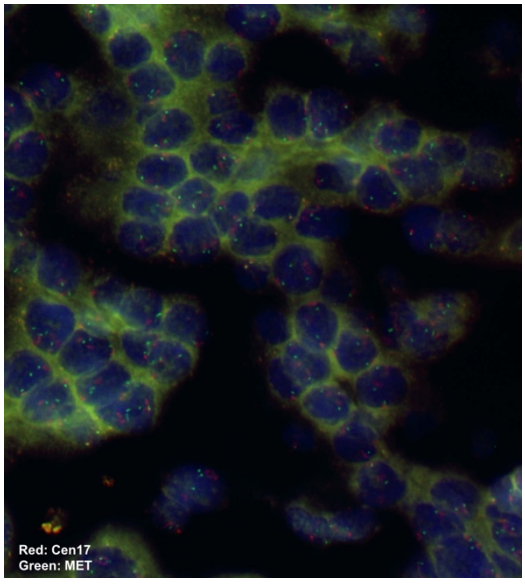

Conclusions: BPRCC display genomic alteration closely related to PRCC with trisomy 7, germline or somatic *MET* mutation and c-MET overexpression suggesting the use of anti-MET targeted therapy for metastasis BPRCC.

827 Clinicopathologic and Immunohistochemical Profile of a Cohort of Neuroendocrine Carcinomas of the Urinary Bladder - A Multi-institutional Review

Jasreman Dhillon[1], Ankit Tiwari[2], Manas Baisakh[3], Subhasini Naik[4], Spinderjeet Samra[5], Preeti Chawla[6], Subodh Das[7], Manas Pradhan[8], Kali Satapathy[9], Sambit Mohanty[10]
[1]Moffitt Cancer Center, Tampa, FL, [2]NISER, Jatni, India, [3]Apollo Hospitals, Bhubaneswar, India, [4]Prolife Diagnostics and Apollo Hospitals, Bhubaneswar, India, [5]Westmead Hospital, Westmead, NSW, Australia, [6]Prolife Diagnostics, Bhubaneshwar, India, [7]Advanced Medical and Research Institute, Bhubaneswar, India, [8]Kalinga Hospital, Bhubaneswar, India, [9]Apollo Hospital, Bhubaneshwar, India, [10]AMRI Hospital, Bhubaneswar, India

Disclosures: Jasreman Dhillon: None; Ankit Tiwari: None; Manas Baisakh: None; Subhasini Naik: None; Spinderjeet Samra: None; Preeti Chawla: None; Manas Pradhan: None; Kali Satapathy: None; Sambit Mohanty: None

Background: High-grade neuroendocrine carcinoma (HGNEC) of the urinary bladder, either in isolation or in association with high-grade urothelial carcinoma (HGUC) is relatively rare. We retrospectively analyzed a large cohort of HGNEC of the bladder from multiple institutions across three continents.

Design: Demographics, clinicopathologic features, immunohistochemical (IHC) profile, and survival parameters in a 126 cases of HGNEC of the bladder were analyzed.

Results: The median age of patients was 65 years (range 27-88 years). Figure 1 describes demographics and clinicopathologic features. The clinicopathologic stages of 88 tumors after neoadjuvant chemotherapy were: 23 T0 (18 small cell carcinoma (SmCC); 5 mixed, p=0.0001); 1Tis; 1Ta; 2 T1; 20 T2; 35 T4. Clinical follow-up was available for 96 patients with a mean of 27.5 months (range 1-153 months). 42 patients died in a mean of 26.8 months (range 2-153 months), and 54 patients were alive with mean follow up of 28 months (range 1-85 months). There was no significant difference observed between pure SmCC (median survival = 52 months) and mixed tumors (median survival = 42 months) as far as neoadjuvant setting is concerned (p=0.65), regardless of the proportion of neuroendocrine component (0.49) in a non-metastatic setting. However, when the disease developed metastasis, mixed tumors had a reduced median survival (19 months) than that of pure SmCC (24 months)(p<0.0001), irrespective the proportion of small cell component and neoadjuvant

status (Figure 2). No significant association was seen between the tumor type and metastatic status (p=0.39). 28% of the tumors with <50% of small cell component exhibited metastasis compared to 42% of tumors with >50% small cell component (p=0.04). The figure 2 illustatres the Kalpan-Meier curves to show the relationships of various clinicopathologic parameters with survival.

Figure 1 - 827

Characteristics	Number of Cases
Gender	
- Male	95
- Female	31
Tumor Histology (TURBT)	
- Pure Small Cell Carcinoma (SmCC)	47
Mixed Type	58
- HGUC with SmCC	4
- HGUC with large cell NEC component	6
- Adenocarcinoma with SmCC	2
- HGUC with Micropapillary and SmCC	5
- HGUC with Squamous differentiation and SmCC	2
- HGUC with plasmacytoid features and SmCC	2
- HGUC with sarcomatoid change and SmCC	
Tumor Staging (TURBT)	
- T1	13
- T2	113
P53 Expression (p=0.08)	
- Pure Small Cell Carcinoma	15
- Mixed Carcinoma	17
Molecular Subtype (p=0.79)	
- Basal	20 (6 SmCC; 14 Mixed)
- Luminal	0
- Non-basal and Non-luminal	71 (21 SmCC; 50 Mixed)
Clinicopathologic staging on follow up	
- T0	23 (18 SmCC; 5 Mixed)
- Ta	1 (Mixed)
- Tis	1 (Mixed)
- T1	2 (1 SmCC; 1 Mixed)
- T2	21 (Mixed)
- T3	6 (2 SmCC; 4 Mixed)
- T4	35 (16 SmCC; 19 Mixed)
Vital Status	
- Alive	54 (24 SmCC; 30 Mixed)
- Dead	42 (17 SmCC; 25 Mixed)

Figure 2 - 827

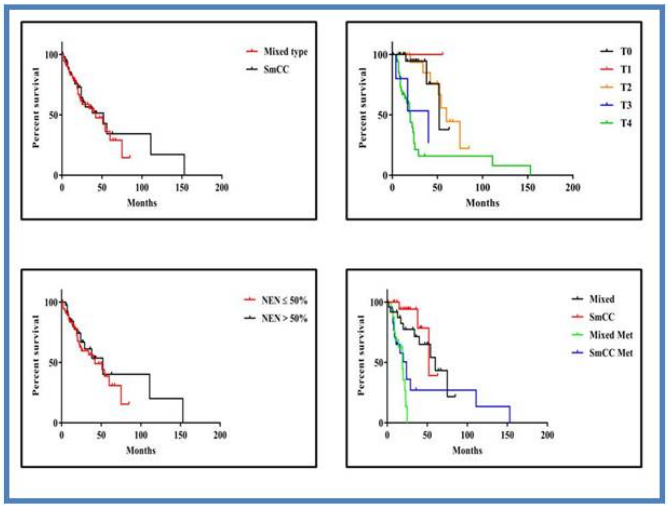

- SmC of the bladder is an aggressive neoplasm that usually presents at an advanced stage with metastases.
- Bladder confined pure SmCC does not have a significantly different clinical outcome than a mixed tumor
- In a metastatic setting, mixed tumors do significantly worse than SmCC and conventional UC (Figure 2).
- Presence of basal markers in a subset of SmCC in our cohort may underlie their response to chemotherapy.
- The tumors with > 50% small cell component, regardless of the neoadjuvant status, exhibited higher metastatic rate than those < 50% small cell component.

828 Urinary miRNA analysis to identify biomarkers of aggressive behaviour in early-stage renal cell carcinoma

Ashley Di Meo[1], Marshall Brown[2], Antonio Finelli[3], Michael Jewett[3], Eleftherios Diamandis[2], George Yousef[4]
[1]Toronto, ON, [2]The Advanced Centre for Detection of Cancer at the Lunenfeld-Tanenbaum Research Institute of Mount Sinai Hospital, Toronto, ON, [3]Princess Margaret Cancer Centre, Toronto, ON, [4]Hospital for Sick Children, Toronto, ON

Disclosures: Ashley Di Meo: None; Eleftherios Diamandis: None; George Yousef: None

Background: Background: To determine whether a limited miRNA signature could accurately distinguish between progressive and non-progressive clear cell renal cell carcinoma small renal masses (ccRCC-SRMs).

Design: Design: We performed an initial global screen of 754 urinary miRNAs by qRT-PCR in patients with progressive and non-progressive clear cell RCC-SRMs. Twenty-four miRNAs were validated by qRT-PCR. Survival analysis was performed using an independent set of samples from The Cancer Genome Atlas.

Results: Results: Univariate analysis identified miR-328 as the top performing miRNA. miR-328 was significantly down-regulated in progressive (2.97-fold change, p= 0.037), and showed significant discriminatory ability (AUC: 0.68, 95% CI: 0.52, 0.84, p= 0.037). We validated our results in an independent dataset of 195 early stage ccRCC patients (T1a and T1b) from The Cancer Genome Atlas (TCGA). Patients with elevated miR-328 expressing ccRCC tumors had significantly higher overall survival (p = 0.016) compared to patients with lower miR-328 expression. Furthermore, patients with elevated miR-328 expression had significantly higher disease-free survival (p= 0.028) compared to patients with lower miR-328 expression. Common cancer pathways predicted to be targeted by identified miRNAs, include the MAPK (p= 3.0×10^{-15}) and PI3K-Akt (p= 9.0×10^{-6}) signaling pathways. In addition, previously linked to RCC were identified, including the insulin signaling pathway (p= 3.5×10^{-7}) and VEGF signaling pathway (p<0.0001).

Conclusions: Conclusion: Taken together, dysregulated miRNAs represent potential prognostic biomarkers able to distinguish between progressive and non-progressive early-stage renal lesions. Moreover, using bioinformatics analysis, we identified many pathways targeted by candidate miRNAs.

829 Gleason Grade Patterns in Nodal Metastasis and Corresponding Prostatectomy Specimens: Impact on Patient Outcome

Michelle Downes[1], Bin Xu[2], Theodorus Van Der Kwast[3]
[1]Sunnybrook Health Sciences Centre, Toronto, ON, [2]Memorial Sloan Kettering Cancer Center, New York, NY, [3]University Health Network, Toronto, ON

Disclosures: Michelle Downes: None; Bin Xu: None; Theodorus Van Der Kwast: None

Background: Lymph node (LN) metastases at the time of radical prostatectomy are an infrequent finding but typically are seen in the context of high grade group (GG) carcinomas. The correlation of the pattern of LN metastases with patient outcome has yet to be explored.

Design: LN positive radical prostatectomy cases from two institutions were retrospectively identified and reviewed. The presence of cribriform carcinoma (CC), intraductal carcinoma (IDC) and GG were documented. The largest nodal metastasis was assessed for morphologic patterns present (solid, cribriform, fused, ill formed, pattern 3), size and extranodal extension (ENE). A GG was assigned to the nodal metastasis based on percentage morphologic patterns present. Patient outcome was recorded from the electronic patient record. Statistical analysis was performed using SPSS to assess disease specific survival (DSS), disease free survival (DFS) and distant metastasis free survival (DMFS).

Results: 102 cases were identified: GG5 (n=45), GG4 (n=7), GG 3 (n=35), n=10 GG 2 (n=10), no GG (n=5; treatment effect). IDC or CC was present in 92 (90%) prostatectomy specimens, with both in 44 cases (43%). The mean LN metastasis size was 6.4mm with 43 nodes showing ENE. >1 positive LN correlated with both worse DFS (p=0.016) and DMFS (p=0.010). No correlation was seen between the GG in the prostate and that assigned to the largest metastasis (kappa= 0.080). Both GG of prostatectomy and LN metastasis correlated significantly with DMFS (p= 0.008 and p=0.033, respectively). The presence of pattern 5 (solid pattern) in LN was seen in 31 cases (30%) and significantly correlated with DFS (p=0.030), DSS (p=0.029) and DMFS (p=0.014). Cribriform pattern showed no prognostic correlation and presence of pattern 3 in LN showed a non-significant trend towards better patient outcome (DMFS p=0.091).

Conclusions: IDC or CC is identified in 90% of LN positive radical prostatectomies. The morphologic pattern of the largest LN metastasis does not reflect the GG of the primary prostatic adenocarcinoma. The presence of solid pattern growth in the LN metastasis has prognostic significance.

830 Incidence and Distribution of UroSEEK Signature in a Multi-institutional Cohort of Invasive Bladder Cancer

Marie-Lisa Eich[1], Maria Del Carmen Rodriguez Pena[2], Simeon Springer[3], Diana Taheri[4], Aline Tregnago[5], Stephania Bezerra[6], Isabela da Cunha[7], Kazutoshi Fujita[8], Dilek Baydar[9], Trinity Bivalacqua[10], Nickolas Papadopoulos[3], Kenneth Kinzler[3], Bert Vogelstein[3], George Netto[2]
[1]The University of Alabama at Birmingham, Birmingham, AL, [2]University of Alabama at Birmingham, Birmingham, AL, [3]The Ludwig Center for Cancer Genetics and Therapeutics and Sidney Kimmel Comprehensive Cancer Center, Baltimore, MD,[4]San Francisco, CA, [5]Centro de Patologia Medica, Caxias Do Sul, RS, Brazil, [6]A.C. Camargo Cancer Center, São Paulo, SP, Brazil, [7]Rede D'OR - São Luiz, São Paulo, SP, Brazil, [8]Osaka University, Suita, Japan, [9]Hacettepe University, Ankara, Turkey, [10]Johns Hopkins University, Baltimore, MD

Disclosures: Marie-Lisa Eich: None; Maria Del Carmen Rodriguez Pena: None; Diana Taheri: None; Aline Tregnago: None; Isabela da Cunha: None; Bert Vogelstein: *Advisory Board Member*, PapGene, Inc; *Advisory Board Member*, Personel Genome Diagnostics, Inc.; *Advisory Board Member*, Morphotek, Inc.; *Advisory Board Member*, Syxmex Inostics, Inc.; *Advisory Board Member*, Exelixis GP; George Netto: None

Background: Non-invasive approaches for early detection of bladder cancer (BC) are actively being investigated. We recently developed a urine based molecular assay for the detection and surveillance of BC (UroSEEK;Springer et al.). UroSEEK is designed to detect alterations in 11 genes that includes most common genetic alterations in BC. This study describes the incidence and distribution of UroSEEK gene panel in a large multi-institutional cohort of invasive BC.

Design: One hundred and fourty one invasive urothelial carcinomas of bladder from trans-urethral resections (TURB) or cystectomies performed at 4 institutions (2009-2016) were analyzed. All histologic sections were reviewed by a genitourinary pathologist to confirm the diagnosis and select a representative tumor area. Corresponding FFPE blocks were cored for DNA purification. For TERT promoter mutation analysis (TERT-SeqS) a primer set amplifying a 73-bp segment containing the region of TERT promoter was applied. A multiplex PCR assay (Uro-SeqS) detecting mutations in hotspot regions of 10 additional genes (*FGFR3, PIK3CA, TP53, KRAS, HRAS, ERBB2,*

VHL, MLL, CDKN2A, and *MET*) was also performed. Follow-up data was obtained from medical records. Statistical analysis was performed using Pearson's Chi-Square test for categorical variables.

Results: Detailed findings are shown in table. One hundred cases with pathological stage pT1 and 41 cases with pT2 or higher stage were analyzed.

Overall, 90.8% of tumors showed at least one mutation in the 11 investigated genes. Seventy-three percent of pT1 and 63.4% of pT≥2 tumors harbored *TERT* promotor mutations (p-NS) with the g.1295228C>T alteration being the most common in both groups. Although relatively higher incidences of *FGFR3, PIK3CA, KRAS* and *HRAS* mutations were found in pT1 tumors compared to pT≥2, the difference was not statistically significant.

Significantly higher rates of TP53 and *CDKN2A* mutation (p=0.004 and 0.02, respectively) were encountered in pT≥2 tumors compared to those of pT1 stage.

	pT1		**pT≥2**		**p-value**	
TERT-SeqS	73/100	(73%)	26/41	(63.4%)	NS	
FGFR3	16/100	(16%)	4/41	(9.8%)	NS	
PIK3CA	8/100	(8%)	1/41	(2.4%)	NS	
KRAS	4/100	(4%)	0/41	(0%)	NS	
HRAS	3/100	(3%)	1/41	(2.4%)	NS	
TP53	28/100	(28%)	22/41	(53.7%)	**0.004**	
ERBB2	3/100	(3%)	1/41	(2.4%)	NS	
VHL	4/100	(4%)	0/41	(0%)	NS	
MLL	0/100	(0%)	0/41	(0%)	NS	
CDKN2A	5/100	(5%)	7/41	(17.1%)	**0.020**	
MET	0/100	(0%)	0/41	(0%)	NS	
Uro-SeqS	53/100	(53.0%)	32/41	(78.0%)	0.008	
UroSEEK	91/100	(91.0%)	37/41	(90.2%)	NS	

Conclusions: Over 90% of invasive BC tumors demonstrated at least one mutation in genes included in the UroSEEK assay. This confirms the comprehensive coverage of our recently developed non-invasive urine based assay. Prospective trials to validate the clinical utility of UroSEEK in improving management of urothelial carcinoma are needed.

831 Incidence of UroSEEK Gene Signature in Bladder Cancer Precursor Lesions

Marie-Lisa Eich[1], Maria Del Carmen Rodriguez Pena[2], Simeon Springer[3], Diana Taheri[4], Aline Tregnago[5], Stephania Bezerra[6], Isabela da Cunha[7], Kazutoshi Fujita[8], Dilek Baydar[9], Trinity Bivalacqua[10], Nickolas Papadopoulos[3], Kenneth Kinzler[3], Bert Vogelstein[3], George Netto[2]

[1]The University of Alabama at Birmingham, Birmingham, AL, [2]University of Alabama at Birmingham, Birmingham, AL, [3]The Ludwig Center for Cancer Genetics and Therapeutics and Sidney Kimmel Comprehensive Cancer Center, Baltimore, MD,[4]San Francisco, CA, [5]Centro de Patologia Medica, Caxias Do Sul, RS, Brazil, [6]A.C. Camargo Cancer Center, São Paulo, SP, Brazil, [7]Rede D'OR - São Luiz, São Paulo, SP, Brazil, [8]Osaka University, Suita, Japan, [9]Hacettepe University, Ankara, Turkey, [10]Johns Hopkins University, Baltimore, MD

Disclosures: Marie-Lisa Eich: None; Maria Del Carmen Rodriguez Pena: None; Diana Taheri: None; Aline Tregnago: None; Isabela da Cunha: None; Bert Vogelstein: *Advisory Board Member*, PapGene, Inc.; *Advisory Board Member*, Personal Genome Diagnostics; *Advisory Board Member*, Morphotek, Inc.; *Advisory Board Member*, Sysmex-Inostics, Inc.; *Advisory Board Member*, Exelixis GP; George Netto: None

Background: Non-invasive approaches for early detection of bladder cancer (BC) are actively being investigated. We recently developed a urine based molecular assay for the detection and surveillance of BC (UroSEEK; Springerl et al., 2018). UroSEEK is designed to detect alterations in 11 genes that includes the most common genetic alterations in bladder cancer and its precursors. This study describes the incidence and distribution of UroSEEK gene panel in a large multi-institutional cohort of BC precursor lesions.

Design: Three hundred and ninty-nine precursor lesions from trans-urethral resections (TURB) or cystectomies performed at 4 institutions (2009-2016) were analyzed. All histologic sections were reviewed by a genitourinary pathologist to confirm the diagnosis and select a representative tumor area. Corresponding FFPE blocks were cored for DNA purification. For TERT promoter mutation analysis (TERT-SeqS) a primer set amplifying a 73-bp segment containing the region of TERT promoter was applied. A multiplex PCR assay (Uro-SeqS) detecting mutations in hotspot regions of 10 additional genes (*FGFR3, PIK3CA, TP53, KRAS, HRAS, ERBB2, VHL, MLL, CDKN2A,* and *MET*) was also performed. Follow-up data was obtained from medical records. Statistical analysis was performed using Pearson's Chi-Square test for categorical variables.

Results: Detailed findings are shown in table. Overall, 93% of all lesions were positive for at least one genetic alteration. We found *TERT* promotor mutations in 76.6% of low-grade non-invasive papillary carcinoma (LGTCC) with relatively lower incidence of 65.5% in high-grade non-invasive papillary carcinoma (HGTCC) and 62.7% in "flat" carcinoma in situ (CIS); p=0.03. *FGFR3* and *PIK3CA* mutations were more frequent in LGTCC compared to HGTCC and CIS (p<0.0001 and p=0.0002; respectively), while the reverse was true for *TP53*; p<0.0001.

	LGTCC		**HGTCC**		**CIS**		**p-Value**
TERT-SeqS	147/192	(76.6%)	97/148	(65.5%)	37/59	(62.7%)	**0.033**
FGFR3	91/192	(47.4%)	43/148	(29.1%)	2/59	(3.4%)	**<0.0001**
PIK3CA	35/192	(18.2%)	9/148)	(6.1%)	2/59	(3.4%)	**0.0002**
KRAS	5/192	(2.6%)	4/148	(2.7%)	0/59	(0.0%)	NS
HRAS	7/192	(3.6%)	(3/148)	(2.0%)	0/59	(0.0%)	NS
TP53	15/192	(7.8%)	46/148	(31.1%)	15/59	(25.4%)	**<0.0001**
ERBB2	1/192	(0.5%)	(3/148)	(2.0%)	1/59	(1.7%)	NS
VHL	1/192	(0.5%)	(1/148)	(0.7%)	2/59	(3.4%)	NS
MLL	0/192	(0.0%)	1/148	(0.7%)	0/59	(0.0%)	NS
CDKN2A	10/192	(5.2%)	6/148	(4.1%)	1/59	(1.7%)	NS
MET	0/192	(0.0%)	0/148	(0.0%)	0/59	(0.0%)	NS
Uro-SeqS	135/192	(70.3%)	99/148	(66.7%)	22/59	(37.3%)	**<0.0001**
UroSEEK	189/192	(98.4%)	136/148	(91.9%)	46/59	(78.0%)	**<0.0001**

Conclusions: Overall 93% of BC precursor lesions demonstrated at least one mutation in genes included in the UroSEEK assay. This confirms the comprehensive coverage of our recently developped non-invasive urine based assay. Prospective trials to validate the clinical utility of the assay in early detection of BC are required. The differences in rate of genetic alterations between LGTCC and HGTCC/CIS are in line with their previously suggested divergent molecular pathogenesis.

832 Evaluation of The Reactive Stroma Grade as an Indicator for Recurrence in Prostate Cancer

Osama Elfituri[1], Shamira Sridharan Weaver[2], Haoliang Xu[3], Wasan Kumar[4], Andre Balla[5], Virgilia Macias[1]
[1]University of Illinois at Chicago, Chicago, IL, [2]University of California, Davis, Davis, CA, [3]University of Illinois Medical Center, Chicago, IL, [4]University of Illinois at Chicago, Skokie, IL, [5]University of Illinois, Chicago, IL

Disclosures: Osama Elfituri: None; Shamira Sridharan Weaver: None; Haoliang Xu: None; Wasan Kumar: None; Andre Balla: None; Virgilia Macias: None

Background: The role of stromal microenvironment in cancer has been established in scientific literature. In prostate cancer (PCa) the reactive tumor stroma influences tumorigenesis and progression. The desmoplastic response hallmark in other invasive tumors, is not easily recognized in prostate but special staining can characterize and measure it. The amount of reactive stroma has been used as a predictor of biochemical recurrence. The aim of our study is to perform a semi-quantitative analysis of reactive stroma in prostate cancer to examine effectiveness of a grading system in predicting recurrence.

Design: We used a tissue microarray from the Cooperative Prostate Cancer Tissue Resource composed of 0.6 mm quadruplicates of 200 prostate cancer cases with biochemical recurrence after prostatectomy paired with 200 cases without recurrence based on age, race, Gleason sum score and pathological stage. Slides from the array stained with Masson's Trichrome highlighted the reactive stroma in blue (collagen) and the host stroma in red (smooth muscle). The stained slides digitized with the Aperio AT2 scanner (Leica Biosystems, Vista, CA) were visualized with Aperio ImageScope software for the analysis of reactive tumor stroma. The reactive stroma grade (RSG) was assessed by the percentage of reactive stroma/epithelium ratio in every spot, and was scored by four independent raters as follows: grade 0, <5%; grade 1, 6-15%; grade 2, 16-50%, and grade 3, >50%. Scores were summed and averaged per subject among the recurrent and non-recurrent groups. The Wilcoxon Signed Rank test was used to assess differences in the RSG between case/control pairs.

Results: Data was available for analysis in 194 complete pairs. The Wilcoxon Signed Rank test for trichrome differences was not statistically significant between the recurrent vs. non-recurrent groups (*p*-value 0.0819). The area under the receiver-operating characteristic curve was 0.55.

Conclusions: Contemporary biomarkers for prostate cancer fail to prospectively differentiate recurring from non-recurring tumors. Grading the reactive stroma hopes to bridge that gap. This grading system validated by others, has demonstrated its predictive value for biochemical recurrence in both radical prostatectomies and biopsies. Our analysis showed that reactive stroma grade alone, was not able to distinguish between recurrence and non-recurrence when the cases are adjusted (paired) for stage, grade, race and age.

833 Clinical, pathologic, and oncologic findings of radical prostatectomy patients with extraprostatic extension diagnosed on pre-operative prostate biopsy

Farzana Faisal[1], Jeffrey Tosoian[2], Katarzyna Macura[1], Christian Pavlovich[1], Tamara Lotan[3]
[1]Johns Hopkins University School of Medicine, Baltimore, MD, [2]University of Michigan, Ann Arbor, MI, [3]Johns Hopkins School of Medicine, Baltimore, MD

Disclosures: Farzana Faisal: None; Jeffrey Tosoian: None; Katarzyna Macura: *Grant or Research Support*, GlaxoSmithKline; *Grant or Research Support*, Profound Medical Corp; Christian Pavlovich: None; Tamara Lotan: None

Background: Prostatic adenocarcinoma (PCa) with extraprostatic extension (EPE) noted on prostate needle biopsy (PNB) is uncommon and associated with other adverse features. As increasingly high risk patients undergo radical prostatectomy (RP), understanding the clinical and pathologic implications of findings such as EPE on PNB is important. The objective of this study was to describe the clinical, histopathologic, and oncologic findings in the largest cohort to date of PCa patients who had EPE identified on PNB and underwent subsequent RP.

Design: Using our institutional pathology database, we retrieved 83 cases of PCa patients with EPE on PNB between 2000 and 2018 who underwent subsequent treatment with RP and had clinical follow-up information. Clinical and pathologic outcomes were examined.

Results: Median PSA (IQR) at time of PNB was 6.0 ng/ml (3.9-10.8). Sixty-five percent of patients had clinical stage T2 or higher disease. The median number of biopsy cores positive for cancer was 8 (IQR 6-11), and the median percentage of cancer in each core was 90% (IQR 80-100). Sixty percent (50/83) of patients had biopsy grade group (GG) 4-5, and 81% (66/83) had perineural invasion on biopsy. EPE was confirmed in the RP specimen in 98% (81/83) of cases. Over 50% of patients had final GG 4-5, 45% (37/83) had seminal vesicle invasion, 37% (30/83) had lymph node involvement, and 59% (49/83) had positive surgical margins. Median length of follow-up after RP was 2 years (IQR 1-3). Overall, 45% (34/76) of patients received post-operative radiation at a median of 1 year after RP, and 11% (8/73) received chemotherapy at a median of 2 years after RP. To date, 48% (37/77) have developed biochemical recurrence (BCR); the 3-year BCR-free survival rate was 48.4% (95% CI 0.345-0.610), and the 3-year metastasis-free survival rate was 75.2% (95% CI 0.603-0.851).

Conclusions: Patients with EPE noted on PNB almost always have extraprostatic disease and other extremely adverse pathology at RP. Extensive high grade disease was the norm, and the majority had positive surgical margins. Half of these patients experienced early BCR, and most eventually required multi-modal therapy. These data can be useful in counseling such patients with regards to management approach and expected outcomes after surgery.

834 SPINK1 expression is not associated with pathologic or oncologic outcomes post-prostatectomy in race-specific cohorts

Farzana Faisal[1], Harsimar Kaur[2], Jeffrey Tosoian[3], Edward Schaeffer[4], Tamara Lotan[5]
[1]Johns Hopkins University School of Medicine, Baltimore, MD, [2]Johns Hopkins University, Baltimore, MD, [3]University of Michigan, Ann Arbor, MI, [4]Northwestern University Feinberg School of Medicine, Chicago, IL, [5]Johns Hopkins School of Medicine, Baltimore, MD

Disclosures: Farzana Faisal: None; Harsimar Kaur: None; Jeffrey Tosoian: None; Edward Schaeffer: None; Tamara Lotan: None

Background: The SPINK1 molecular subtype has been shown to be more common in African American (AA) men with prostatic adenocarcinoma (PCa) than European Americans (EA). Other studies have suggested that SPINK1 expression is associated with more aggressive disease. However, there have been limited studies examining clinical outcomes by SPINK1 status in racially diverse cohorts.

Design: The objective was to determine the associations between SPINK1 subtype, race, and clinical and pathologic outcomes after radical prostatectomy (RP). A total of 186 AA and 206 EA men who underwent RP at Johns Hopkins were matched according to pathologic Gleason grade. We examined SPINK1 status by immunohistochemistry on tissue microarrays using a genetically validated assay. ERG and PTEN were assessed previously using validated immunohistochemistry assays. SPINK1 prevalence was compared between races. Logistic regression and Cox proportional hazard analyses assessed the association of SPINK1 status with pathologic and oncologic outcomes in race-specific multivariate models.

Results: SPINK1-positive subtype was present in 25% (45/186) of AA and 15% (30/206) of EA men (p=0.013). SPINK1 expression was generally mutually exclusive with ERG expression and PTEN loss in both racial cohorts. There were no differences in pathologic grade group (GG), pathologic stage, biochemical recurrence (BCR)-free survival, or metastasis-free survival between SPINK1-positive and SPINK1-negative tumors in the overall cohort or by race. AA race was a predictor of SPINK1-positive subtype on multivariate analysis (OR 2.07, 95% CI 1.22-3.49, p=0.007). However, SPINK1 expression was not associated with pathologic GG≥3 (AA: OR 0.71, 95% CI 0.35-1.44, p=0.341; EA: OR 0.98, 95% CI 0.42-2.28, p=0.960), pathologic stage>T2 (AA: OR 0.77, 95% CI 0.39-1.51, p=0.450; EA: OR 1.04, 95% CI 0.48-2.27, p=0.920), BCR (AA: HR 0.99, 95% CI 0.56-1.75, p=0.976; EA: HR 0.88, 95% CI 0.43-1.77, p=0.720), or metastasis (AA: HR 0.79, 95% CI 0.25-2.49, p=0.691; EA: HR 1.55, 95% CI 0.58-4.11, p=0.381) in either the AA or the EA cohort.

Conclusions: SPINK1-positive subtype is more prevalent in AA than EA men with PCa. While previous studies showed that SPINK1 may be associated with more aggressive PCa, we found that SPINK1 expression was not associated with worse pathologic or oncologic outcomes including BCR and metastasis after RP in either AA men or EA men.

835 Tumor-Associated Macrophages is Associated with Poor Prognosis in Upper Tract Urothelial Carcinomas

Sahar Farahani[1], Priti Lal[2], Maria Elisa Smith[2], Aileen Grace Arriola[3], Anupma Nayak[4]
[1]Hospital of the University of Pennsylvania, Philadelphia, PA, [2]University of Pennsylvania, Philadelphia, PA, [3]Temple University Hospital, Jersey City, NJ, [4]Perelman School of Medicine at the University of Pennsylvania, Philadelphia, PA

Disclosures: Sahar Farahani: None; Priti Lal: None; Maria Elisa Smith: None; Aileen Grace Arriola: None; Anupma Nayak: None

Background: Upper tract urothelial carcinomas (UTUC) are aggressive tumors, treated by radical nephroureterectomy with long-term medical implications. Hence, developing immunotherapeutic approaches are of paramount significance. Tumor-associated macrophages (TAMs) an integral component of the tumor microenvironment, have been associated with poor outcome. TAMs are proposed to differentiate to pro-tumor M2 macrophages which promote angiogenesis, matrix remodeling and suppress T-cell proliferation. In this study, we aim to review the association of TAMs with histologic features, tumor grade, stage and clinical outcome of UTUC.

Design: Retrospective evaluation of 35 cases of UTUC was performed. IHC using anti-mouse monoclonal antibodies to TAM (CD68) and M2 macrophages (CD163) was done on paraffin-embedded whole tumor sections. Superficial non-invasive papillary areas and the invasive front of the tumor were scored separately for TAMs in the epithelium and stromal components. 5 to 10 HPFs with the highest density of macrophages were analyzed. Correlative analysis between TAM counts and tumor characteristics including outcomes was performed.

Results: The mean expression of CD68 and CD163 in the invasive epithelial component revealed a statistically significant association with outcomes on parametric as well as non-parametric statistical analysis. The patients who died of UC showed 4 to 5 times higher

macrophage count at the invasive front when compared to patients alive with disease or dead of other causes (CD68 44.7 ± 15.5 *vs* 9.0 ± 9.9, p=0.007; CD163 46.1 ± 21.1 *vs* 15.6 ± 17.3, p= 0.04). The ratio of CD68: CD163 was significantly higher in the epithelial component of the invasive front of UT with squamous differentiation (0.62 ± 0.11 vs 1.57 ± 1.68, p=0.04). The higher stage tumors were associated with higher average number of stromal CD68 macrophage in both invasive (44.4 ± 21.2 *vs* 20.4 ± 20.2, p=0.04) and non-invasive (22.2.1 ± 12.9 *vs* 12.1 ± 12.3, p= 0.02) fronts, and higher average number of stromal CD163 in non-invasive front (38.5 ± 18.8 *vs* 20.2 ± 17.2, p= 0.01).

	Non-invasive Front		Invasive Front		Non-invasive Front		Invasive Front	
	CD68 Epithelial	CD68 Stromal	CD68 Epithelial	CD68 Stromal	CD163 Epithelial	CD163 Stromal	CD163 Epithelial	CD163 Stromal
Stage								
Stage 0&1	5.4 ± 4.9	12.1 ± 12.3	8.5 ± 6.7	20.4 ± 20.2	8.0 ± 7.3	20.2 ± 17.2	20.8 ± 25.1	47.3 ± 27.3
Stage 2&3	6.8 ± 5.9	22.2 ± 12.9	14.7 ± 16.3	44.4 ± 21.2	9.5 ± 13.3	38.5 ± 18.8	21.3 ± 4.8	56.9 ± 27.5
P-value	0.46	**0.02***	0.38	**0.04***	0.72	**0.01***	0.96	0.46
Squamous Differentiation								
Absent	5.7 ± 4.7	15.9 ± 12.2	10.7 ± 13.9	32.4 ± 23.8	7.2 ± 6.5	27.3 ± 20.0	19.0 ± 19.1	48.4 ± 23.5
Present	7.5 ±7.6	21.9 ± 17.1	18.2 ± 15.7	44.6 ± 22.6	13.9 ± 19.2	37.1 ± 19.5	25.8 ± 26.6	67.8 ± 31.4
P-value	0.46	0.31	0.25	0.24	0.15	0.26	0.47	0.09
Disease-related Death								
No	9.3 ± 8.0	15.9 ± 16.8	44.7 ± 12.5	57.0 ± 20.0	13.9 ± 21.5	24.1 ± 24.6	46.1 ± 21.1	42.4 ± 31.6
Yes	4.5 ± 3.3	20.2 ± 14.8	9.0 ± 9.9	41.3 ± 24.5	5.7 ± 4.7	41.4 ± 25.3	15.6 ± 17.3	64.0 ± 25.0
P-value	0.17	0.65	**0.0007***	0.41	0.34	0.26	**0.04***	0.22

Conclusions: Tumor microenvironment with higher overall macrophage infiltrate is associated with higher tumor stage and poor outcome in UTUC suggesting the assessment of TAMS as a useful prognostic marker. Unlike studies in bladder cancer, we did not find polarization of TAMs towards M2 macrophages as a prognostic factor. Larger studies are needed to further corroborate our findings.

836 Rete Testis Invasion is Consistent with Pathologic Stage T1 in Germ Cell Tumors

Ayesha Farooq[1], Merce Jorda[2], Elizabeth Whittington[3], Oleksandr Kryvenko[2], Pavan Nicola[4], Kristyna Prochazkova[5], Lian Zhang[6], Tegan Miller[7], Kenneth Iczkowski[1]
[1]Medical College of Wisconsin, Milwaukee, WI, [2]University of Miami Miller School of Medicine, Miami, FL, [3]West Palm Beach, FL, [4]University of Miami Miller School of Medicine/Jackson Health System, Miami, FL, [5]Charles University, Plzen, Czech Republic, [6]University of Colorado, Aurora, CO, [7]Central Manchester University Hospitals NHS Foundation Trust, Manchester, United Kingdom

Disclosures: Ayesha Farooq: None; Merce Jorda: None; Elizabeth Whittington: None; Oleksandr Kryvenko: None; Pavan Nicola: None; Kristyna Prochazkova: None; Lian Zhang: None; Tegan Miller: None; Kenneth Iczkowski: None

Background: Testicular hilum is the main pathway for extratesticular extension of germ cell tumors. The independent effects with regard to staging of rete testis, hilar adipose tissue, epididymis, and tunica vaginalis invasion are uncertain, because these 4 structures are often invaded in conjunction with each other and with lymphovascular and spermatic cord invasion (LVI/SCI). We undertook the first comparison of these types of invasion with known stage ≥ pT2(LVI/SCI) cases vs. absence of invasions in nonseminomatous germ cell tumor (NSGCT) and seminoma, to determine their role in staging.

Design: 349 seminomas and NSGCT cases accessioned from 2000-2012 at 5 medical centers were reviewed by contributing pathologists. Tumor size, rete direct invasion (ReteD), rete pagetoid spread (ReteP) and invasion including: epididymis, hilar fat, spermatic cord, tunica vaginalis, LVI, and SCI were noted. Tumor histology was noted as seminoma or nonseminomatous including 46 with seminoma component. Pathologic staging was performed using the 8th ed. AJCC/TNM. Relapse at recent follow-up was queried; also, metastasis at presentation was used as a proxy for severity [PMID:23238629].

Results: ReteP was more frequent in seminoma than NSGCT (p<0.001). ReteD was also more frequent (p=0.064). Vital status showed no significant differences with respect to these invasions. *Seminoma:* Tumor size bifurcated at ≥ 3cm or <3cm predicted metastatic status (p=0.03) but not recurrence (p=0.09).When cases with LVI/SCI were excluded, size lost its correlation with metastatic status(p=0.08). Cases with ReteP were similar to tumor with no invasions (p=0.09) and different from tumor with LVI/SCI (p=0.047). The same trends were observed for ReteD (p=0.49 and p=0.001 respectively). *NSGCT:* Tumor size bifurcation did not predict metastatic status or recurrence. Size, in the presence of ReteD was similar to no invasion (p=0.2) and less than that with LVI/SCI (p=0.04). ReteP/ReteD did not differ from no invasion or LVI/SCI in metastatic status at presentation. Hilar fat, epididymis, and tunica vaginalis invasion seldom occurred alone, and thus significance was not attained.

Seminoma, n=171, median f/u 3.8 yr					
n=	No invasion, 76	Rete P only,28	Rete D only,15	LVI/SCI,36	*P*=
Size, cm	2.5	3.5	3.0	4.8	**.047**, ReteP vs LVI/SCI† **.001**, ReteD vs LVI/SCI†
Met at presentation	7%	7%	0	26%	NS, all comparisons‡
Recurrence	7%	4%	20%	33%	**.02**, ReteP vs LVI‡ 1.0, ReteD vs LVI
NSGCT, n=178, median f/u 4.8 yr					
n=	No invasion, 71	Rete P only,4	Rete D only,15	LVI/SCI,89	*P*=
Size, cm	2.8	4.3	2.0	3.5	.26, Rete P vs LVI/SCI† **.04**, ReteD vs LVI/SCI†
Met at presentation	12%	25%	7%	39%	NS, all comparisons‡
Recurrence	24%	0	7%	28%	NS, all comparisons‡

†Wilcoxon rank-sum test; ‡Fisher's exact test

Conclusions: No evidence was found to suggest that rete testis involvement, particularly the more-important ReteD, should justify a higher stage than pT1 [PMID: 28368923] for either seminoma or NSGCT. Our findings of seminoma size (≥ 3 cm or <3 cm) correlating with metastatic status at presentation supports current subdivision of pathologic T1a and T1b stages for seminoma.

837 Focused Submission of Tissue for Radical Prostatectomy Following Multiparametric MRI/US Fusion Targeted Biopsy

Danielle Fasciano[1], Marie-Lisa Eich[2], Maria Del Carmen Rodriguez Pena[3], Soroush Rais-Bahrami[3], Jennifer Gordetsky[3]
[1]Birmingham, AL, [2]The University of Alabama at Birmingham, Birmingham, AL, [3]University of Alabama at Birmingham, Birmingham, AL

Disclosures: Danielle Fasciano: None; Marie-Lisa Eich: None; Maria Del Carmen Rodriguez Pena: None; Soroush Rais-Bahrami: *Consultant*, Philips/InVivo Corp; *Advisory Board Member*, Genomic Health Inc; Jennifer Gordetsky: None

Background: Prostate cancer can be difficult to appreciate grossly and partial sampling of the gland can lead to incorrect grading, staging or margin status. Submitting the entire prostate is more time consuming and requires numerous blocks, which causes more processing and diagnostic time as well as increased cost. Magnetic resonance imaging (MR)/ultrasound (US) fusion targeted prostate biopsy has been shown to be superior to the standard of care sextant biopsy for the detection of clinically significant prostate cancer. We investigated the ability of targeted biopsy to be used for the selective submission of prostatectomy specimens.

Design: We performed a retrospective review of patients who had cancer on MR/US targeted prostate biopsy who underwent subsequent prostatectomy. Prostatectomy specimens were serially sectioned and submitted in their entirety and assessed for grade, extraprostatic extension (EPE), margins, and number of blocks submitted. For the Targeted-Grossing (TG) assessment, the apex margin, bladder neck margin, seminal vesicles and vas deferens sections were included. For the remainder of the prostate, only sections from areas shown to be positive for cancer on targeted biopsy were included.

Results: We identified 66 prostatectomy specimens that met inclusion criteria. The average age was 63.8±6.7 years. When submitting the entire prostate, EPE was found in 32/66 (48.5%) cases and positive margins were found in 14/66 (21.2%) cases, including apex (9), bladder neck (3) and peripheral (2). The TG method had an average of 16.2±6.3 blocks, compared to 44.2±11.7 blocks for the entire prostate (p<0.0001). Utilizing the TG method would have diagnosed the correct stage in 59/66 (89.4%) cases, the correct grade in 64/66

(97.0%) cases, and the correct margin status in 65/66 (98.5%) cases. There was no significant difference in the detection of stage, grade, or margin status between the two methods. When EPE was found on both methods, there would have been a change in focality in 6/26 (23.1%) cases. In 7 cases EPE was missed completely by the TG method, in which 5/7 (71.4%) cases had focal EPE. The TG method would have potentially impacted post op management in only 2/66 (3.0%) patients.

Conclusions: Prostatectomy grossing utilizing selective tissue submission from areas found to be positive for prostate cancer on MR/US targeted prostate biopsy allows for a high degree of accuracy in terms of grading, staging, and margins, while significantly decreasing the required number of blocks.

838 Variable HPV Genotypes in Basaloid, Warty-Basaloid and Warty (Condylomatous) Carcinomas of the Penis. A Study of 174 Cases

María José Fernandez-Nestosa[1], Diego F Sanchez[2], Laia Alemany[3], Sofía Cañete-Portillo[2], Belen Lloveras[4], Omar Clavero[5], Ingrid Rodríguez[1], Wim Quint[6], Nubia Munoz[7], Silvia de Sanjosé[3], Francesc Xavier Bosch[8], Antonio Cubilla[9]
[1]Universidad Nacional de Asunción, Asunción, Paraguay, [2]Instituto de Patologia e Investigacion, Asuncion, Paraguay, [3]Institut Catala d'Oncologia, Barcelona, Spain, [4]Hospital del Mar, Barcelona, Spain, [5]1. Centro de Investigación Biomédica en Red de Cáncer 2.Institut Català d'Oncologia, L'Hospitalet de Llobregat, Madrid, Spain, [6]DDL Diagnostic Laboratory, Rijswijk, Netherlands, [7]National Cancer Institute of Colombia, Bogota, Colombia, [8]Catalan Institute of Oncology (ICO), L'Hospitalet de Llobregat, Spain, [9]Instituto de Patologia e Investigacion, Asunción, Paraguay

Disclosures: María José Fernandez-Nestosa: None; Diego F Sanchez: None; Laia Alemany: None; Sofía Cañete-Portillo: None; Belen Lloveras: None; Ingrid Rodríguez: None; Wim Quint: *Major Shareholder*, DDL; Antonio Cubilla: None

Background: HPV is detected in 30 to 50% of all penile invasive carcinomas. Common subtypes of HPV-related invasive penile carcinomas are warty, warty-basaloid and basaloid carcinomas. Based on their distinct morphological features, we hypothesized a variation in the genotypic HPV composition of these neoplasms.

Design: We evaluated cases of HPV positive basaloid (115 cases), warty-basaloid (26 cases) and warty (condylomatous) (33 cases) invasive carcinomas. They were part of a retrospective cross-sectional international study of 1095 cases from 5 continents designed to estimate the HPV DNA prevalence of penile cancers (Alemany et al, Eur Urol 2016). HPV DNA detection and genotyping was performed using SPF-10/DEIA/LiPA$_{25}$ system (version 1). P-values were determined by Fisher's exact test using R version 3.4.3.

Results: There was a significant variation in the distribution of HPV 16 and non-HPV 16 genotypes according to histological subtype (Tables 1 and 2).

Table 1. HPV genotypes according to histological types.

Type of carcinoma	No of cases *(%)*	HPV genotypes	HPV 16 cases *(%)*	Non-HPV 16 cases *(%)*
Basaloid*	115 *(85)*	6(1)**, 16(99), 18(1), 31(1), 33(5), 35(4), 44(2)**, 45 (1), 51(1), 52(3), 53(1), 55(1)**, 56(2), 58(2), 66(1), 73(1)	99 *(86)*	16 *(14)*
Warty/basaloid	26 *(87)*	16(20), 18(1), 35(2), 53(1), 59(1), 70 (1), 73 (1)	20 *(77)*	6 *(23)*
Warty	33 *(51)*	6(3)**, 16(20), 31(2), 33(2), 35(1), 45(1), 52(1), 56 (2), 58(1), 59(1), 74(3)**	20 *(61)*	13 *(39)*

Fisher's test P-value = P=0.0068

*One case positive for an undetermined HPV genotype.

** Low risk HPV genotypes.

Conclusions: HPV 16 was the most common genotype found and it was especially prevalent in basaloid (86%) and warty basaloid carcinomas (77%). Non HPV16 genotypes were most commonly found in warty carcinomas (39%). Low risk genotypes were more frequent in warty carcinomas. This significant variation in HPV genotypes, also present in HPV-related penile intraepithelial neoplasia (Fernández-Nestosa et al., Am J Surg Path 2017), suggests that these tumors are distinct pathological and molecular entities, validating their classification as discrete types.

839 Low Risk HPV Genotypes (LR-HPV) in Subtypes of Penile Squamous Cell Carcinomas (SCC)

María José Fernandez-Nestosa[1], Laia Alemany[2], Sofía Cañete-Portillo[3], Diego F Sanchez[3], Belen Lloveras[4], Omar Clavero[5], Natalia Elizeche-Santacruz[3], Wim Quint[6], Nubia Munoz[7], Silvia de Sanjosé[2], Francesc Xavier Bosch[8], Antonio Cubilla[9]
[1]Universidad Nacional de Asunción, Asunción, Paraguay, [2]Institut Catala d'Oncologia, Barcelona, Spain, [3]Instituto de Patologia e Investigacion, Asuncion, Paraguay, [4]Hospital del Mar, Barcelona, Spain, [5]1. Centro de Investigación Biomédica en Red de Cáncer 2.Institut Català d'Oncologia, L'Hospitalet de Llobregat, Madrid, Spain, [6]DDL Diagnostic Laboratory, Rijswijk, Netherlands, [7]National Cancer Institute of Colombia, Bogota, Colombia, [8]Catalan Institute of Oncology (ICO), L'Hospitalet de Llobregat, Spain, [9]Instituto de Patologia e Investigacion, Asunción, Paraguay

Disclosures: María José Fernandez-Nestosa: None; Laia Alemany: None; Sofía Cañete-Portillo: None; Diego F Sanchez: None; Belen Lloveras: None; Natalia Elizeche-Santacruz: None; Antonio Cubilla: None

Background: SCCs of the anogenital region, including the penis, are etiologically related to High Risk HPV (HR-HPV). Recent studies detected occasional LR-HPV genotypes in carcinomas from these areas. The aim of this report is to explore the relation of LR-HPV according to subtypes of penile SCC.

Design: From a group of 301 HPV positive cases detected in an international study (Alemany et al, Eur Urol 2016) 266 were selected representing single HPV infections. Multiple HPV infections were excluded from this study. HPV DNA detection and genotyping were performed using SPF-10/DEIA/LiPA$_{25}$ system (version 1).

Results: The prevalence of high and low risk HPV according to histological subtypes is in Table 1. Low risk genotypes were identified in 22 of 266 HPV positive cases (8%). Subtypes associated with LR-HPV were usual, warty, verrucous and sarcomatoid carcinomas. Lowest or negative rates were for basaloid or mixed tumors containing basaloid cells. Genotypes among the LR cases are listed in Table 1.

Table 1. High and low risk HPV genotypes according to histological subtypes.

Subtypes of carcinoma	HPV positive	HR-HPV *(%)*	LR-HPV *(%)*	LR-HPV genotypes (# of cases)
Basaloid*	103	102 *(99)*	1 *(1)*	55(1)
Warty	29	24 *(83)*	5 *(17)*	6(3), 74(2)
Sarcomatoid	2	0 *(0)*	2 (100)	6(1), 43(1)
Verrucous	3	0 *(0)*	3 *(100)*	6(1), 32(1), 76(1)
Papillary NOS	9	7 *(78)*	2 *(22)*	6(1), 11(1)
Usual**	66	57 *(86)*	9 *(14)*	6(3),11(3), 27(1),32(1), 42(1)
Warty-basaloid	25	25 *(100)*	0 *(0)*	none
Mixed Warty/ Basaloid/ usual***	29	29 *(100)*	0 *(0)*	none

*One lesion with undetermined HPV type.

**Three lesions with undetermined HPV type.

*** W/B, usual.

Conclusions: Of 266 HPV positive carcinomas HR-HPV was detected in 92% and LR-HPV in 8% of the cases. Whereas HR-HPV genotypes, especially HPV 16, were preferentially associated with basaloid, warty-basaloid and mixed tumors composed of warty/basaloid and usual carcinomas, low risk genotypes, especially 6, 11, 32 and 74 were preferentially associated with verruciform tumors (warty, verrucous and papillary NOS). The epidemiologically based classification of HPV genotypes in low and high risk indicates a relationship with carcinomas in the majority but not in all the subtypes of invasive penile carcinomas.

840 Practice Patterns in Reporting Tertiary Grades at Radical Prostatectomy: Survey of a Large Group of Experienced Urologic Pathologists

Samson Fine[1], Devorah Meisels[1], Hikmat Al-Ahmadie[1], Ying-Bei Chen[1], Anuradha Gopalan[1], S. Joseph Sirintrapun[1], Satish Tickoo[2], Victor Reuter[1]
[1]Memorial Sloan Kettering Cancer Center, New York, NY, [2]New York, NY

Disclosures: Samson Fine: None; Devorah Meisels: None; Hikmat Al-Ahmadie: None; Ying-Bei Chen: None; Anuradha Gopalan: None; S. Joseph Sirintrapun: None; Satish Tickoo: None; Victor Reuter: None

Background: The finding of a “tertiary” higher grade pattern has been associated with biochemical recurrence after radical prostatectomy and when present, is a required element of routine pathology reporting. Variation among pathologists in terms of definition and application of “tertiary” higher grade patterns has not been well studied and may significantly impact risk category assignment and management in the post-RP setting.

Design: A 10 question survey combining queries regarding definition of “tertiary” patterns and their application in a range of clinical scenarios was circulated to 105 experienced urologic pathologists. Responses were collected and tabulated using SurveyMonkey©; descriptive statistics are reported.

Results: 95 responses were recorded. Regarding definition of “tertiary”: 40/95 (42%) chose “3rd most common pattern”, 51/95 (54%) chose “minor pattern / <5% of tumor” and 4/95 (4%) stated that “tertiary” was a third most common pattern that was also <5% of the tumor. In a tumor with predominant pattern 3 and <5% pattern 4, 35/95 (37%) would assign 3+3=6 with minor/tertiary pattern 4, while 56/95 (59%) would assign 3+4=7 (+/- comment regarding % pattern 4). In a tumor with predominant pattern 4 and <5% pattern 5, 51/95 (54%) would assign 4+4=8 with minor/tertiary pattern 5, while 43/95 (45%) would assign 4+5=9 (+/- comment regarding % pattern 4). Scenarios involving 3+4=7 and 4+3=7 cases with third most common pattern 5 are tabulated below; all pathologists would include pattern 5 in some fashion. 85/95 (89%) replied that a tertiary pattern would not impact assignment of Grade group.

Table 1.

Scenario	3+4=7 with minor/tertiary pattern 5	3+5=8 (+/- comment re: % pattern 5)
80% pattern 3, 17% pattern 4, 3% pattern 5	93/95 (98%)	2/95 (2%)
60% pattern 3, 25% pattern 4, 15% pattern 5	29/95 (31%)	66/95 (69%)
45% pattern 3, 30% pattern 4, 25% pattern 5	20/95 (21%)	75/95 (79%)

Table 2.

Scenario	4+3=7 with minor/tertiary pattern 5	4+5=9 (+/- comment re: % pattern 5)
80% pattern 4, 17% pattern 3, 3% pattern 5	88/95 (93%)	7/95 (7%)
60% pattern 4, 25% pattern 3, 15% pattern 5	28/95 (29%)	67/95 (71%)
45% pattern 4, 30% pattern 3, 25% pattern 5	19/95 (20%)	76/95 (80%)

Conclusions: The responses to this survey highlight variation in practice patterns regarding definition and application of “tertiary” grading in radical prostatectomy specimens. Greatest consistency was observed in 3+4=7 and 4+3=7 scenarios in which pattern 5 is truly minor (i.e. <5%). Likewise, a tertiary pattern would not influence Grade group assignment for nearly 90% of respondents. These findings may inform future studies assessing the predictive value of “tertiary” patterns. A follow-up survey regarding the impact of “tertiary” grading patterns on clinical management is underway.

841 In Organ-Confined Prostate Cancer at Radical Prostatectomy, neither Total Tumor Volume nor Maximum Tumor Diameter of the Index Lesion Aids in Prediction of Biochemical Recurrence

Samson Fine[1], Yujiro Ito[1], Emily Vertosick[1], Daniel Sjoberg[1], Andrew Vickers[1], Hikmat Al-Ahmadie[1], Ying-Bei Chen[1], Anuradha Gopalan[1], S. Joseph Sirintrapun[1], Satish Tickoo[2], Victor Reuter[1]
[1]Memorial Sloan Kettering Cancer Center, New York, NY, [2]New York, NY

Disclosures: Samson Fine: None; Yujiro Ito: None; Emily Vertosick: None; Daniel Sjoberg: None; Andrew Vickers: None; Hikmat Al-Ahmadie: None; Ying-Bei Chen: None; Anuradha Gopalan: None; S. Joseph Sirintrapun: None; Satish Tickoo: None; Victor Reuter: None

Background: In 8th edition AJCC staging, all organ-confined disease is assigned pathologic stage T2 (pT2), without sub-classification by laterality or extent. Whether total tumor volume (TTV) and/or maximum tumor diameter of the index lesion (MTD) are useful in improving prediction of biochemical recurrence (BCR) in pT2 patients has not been well studied.

Design: We identified 1657 patients with digital tumor maps and quantification of TTV/MTD who had pT2 disease on radical prostatectomy (RP). Multivariable Cox regression models were used to assess whether TTV and/or MTD are independent predictors of BCR when adjusted for a base model incorporating age, pre-operative PSA, RP Grade group, and surgical margin status. If either tumor quantification added significantly, we calculated and reported time-dependent area under the curve (AUC) at 5 years.

Results: Mean age and PSA for this cohort were 59 and 4.9 ng/ml, respectively. RP Grade group of 1-5 was seen in 39%, 51%, 8.2%, 1.2 % and 0.5% of cases. 11% of the cohort had positive surgical margins. 95 patients experienced BCR after RP; median follow-up for patients without BCR was 5.7 years. Time-dependent AUC at 5 years was 0.764 for the base model. Although there was some evidence of an association between TTV and BCR (p=0.088), this did not meet conventional levels of statistical significance and only provided a limited increase in AUC (0.770; c-index improvement: 0.006). MTD was not associated with BCR (p>0.9). In analyses excluding patients with Grade group 1 on biopsy (n=622; 59 with BCR), who would be less likely to undergo RP in contemporary practice, TTV/MTD showed no significance in enhancing BCR prediction (p=0.4 and 0.8, respectively).

Conclusions: In pT2 prostate cancer, tumor quantitation, in the form of either total tumor volume or maximum tumor diameter of the index lesion, does not add important predictive value for BCR. If corroborated with longer-term follow-up, these findings suggest that routine reporting of tumor quantitation in this scenario is unjustified.

842 Does PD-L1 Expression in Non-Muscle-Invasive Bladder Cancer Correlate with Recurrence and Progression?

David Gajzer[1], Maria Becerra[1], Maria Velasquez Escobar[1], Deukwoo Kwon[2], Chad Ritch[3], Oleksandr Kryvenko[3], Merce Jorda[3]
[1]University of Miami/Jackson Memorial Hospital, Miami, FL, [2]University of Miami, Miller School of Medicine, Miami, FL, [3]University of Miami Miller School of Medicine, Miami, FL

Disclosures: David Gajzer: None; Maria Becerra: None; Maria Velasquez Escobar: None; Deukwoo Kwon: None; Chad Ritch: None; Oleksandr Kryvenko: None; Merce Jorda: None

Background: Checkpoint blockade including Programmed Death Ligand 1 (PD-L1) mechanism has been reported in various cancers including urothelial carcinoma of the bladder where it may attenuate response to Bacillus Calmette-Guerin (BCG) immunotherapy by neutralizing T-cells. We evaluated PD-L1 expression pre- and post- BCG therapy as a predictor of recurrence and progression in non-muscle-invasive bladder cancer (NMIBC).

Design: We examined clinical data and biopsy specimens of 49 patients with stage pT1 NMIBC who underwent transurethral resection of the bladder (TURB) and BCG therapy. Of these, 30 patients (61.2%) were clinically high risk and 19 (38.8%) were part of the low or intermediate risk group. Histologic and immunohistochemical review was performed blindly to treatment outcome or patient risk status by two anatomic pathologists. PD-L1 protein expression was assessed with the FDA-approved PD-L1 pharm Dx assay (clone 22C3, Dako/Agilent, Carpinteria, CA) in the pre-BCG TURB specimens of all 49 patients and those post-BCG specimens with recurrent/residual carcinoma and positive PD-L1 in the pre-BCG specimen. Combined Positive Score was assigned. A positive reaction was characterized by a complete and/or partial circumferential membrane staining at any intensity that can be differentiated from background in ?10% of tumor cells. Descriptive summary statistics were reported to correlate clinicopathological variables with PD-L1 status. Hazard ratios using univariable Cox regression analysis and Fisher's exact binomial test were used. All tests were two-sided and p<0.05 was used as criteria for statistical significance.

Results: 7/49 (14.2%) patients had specimens which showed variable PD-L1 expression (25% - n=1 positive by CPS criteria; 1-10% - n=6) in pre-BCG specimens, and all of the corresponding post-BCG specimens from the same patients were negative for PD-L1. No significant differences in PD-L1 expression were found when considering age, gender, race, ethnicity, smoking status, stage, grade or AUA risk group. HRs of PD-L1 expression for progression (HR=1.9; 95%CI=0.52 to 6.9, p=0.328) and recurrence/persistence (HR=1.3; 95%CI=0.56 to 3.2, p=0.514) did not reach statistical significance. Median follow-up was 2.13 years (95%CI=1.73 to 3.38), without significant association with progression or recurrence.

Conclusions: PD-L1 protein expression was not significantly associated with therapy response and incidence of persistent/recurrent disease in patients with pT1 NMIBC receiving BCG therapy.

843 Clinicopathologic Features of Small Renal Masses Associated with Distant Metastatic Disease

Alexander Gallan[1], Tatjana Antic[2]
[1]Brookfield, IL, [2]University of Chicago, Chicago, IL

Disclosures: Alexander Gallan: None; Tatjana Antic: None

Background: Small renal masses measuring <4 cm in size are thought to have a low risk for distant metastatic disease, whether confined to the kidney (pT1a) or invading renal vein or the perinephric or renal sinus adipose tissue (pT3a). However, metastasis does occasionally occur in these patients. The purpose of our study was to assess the clinicopathologic features of these tumors, and the presence of previous or subsequent renal cancers which could potentially represent the source of metastatic disease.

Design: We identified radical or partial nephrectomies with renal cell carcinomas (RCCs) measuring <4 cm in size (pT1a or pT3a) from 2005-2015. Medical records were queried for the subsequent development of metastatic disease, and the presence of previous or subsequent renal cancers. Clinicopathologic features such as histologic tumor type and nuclear grade (if applicable) were compiled.

Results: A total of 590 RCCs <4 cm were identified, with a mean clinical follow-up time of 42 months (range: 0-153 months). Of these, 23 patients (3.9%) developed distant metastatic RCC by histologic confirmation or strong radiologic evidence, at a mean duration of 35 months after nephrectomy (range: 0-129 months). Metastatic disease was more common in stage pT3a tumors <4 cm than pT1a tumors (19% vs 3%, p<0.01). The histologic subtypes included clear cell RCC (16), papillary RCC type 2 (4), papillary RCC type 1 (1), TFE3 translocation RCC (1), and medullary carcinoma (1). The most common WHO/ISUP nuclear grades in the clear cell RCC cases were 2 (6), 3 (5), 4 (4) and 1 (1). Overall, 43% of patients had a previous RCC (30%) or subsequent RCC prior to development of metastasis (13%).

Conclusions: Distant metastatic disease was rarely encountered in patients with small renal masses. The finding was more common in stage pT3a tumors <4 cm than pT1a tumors. A large percentage of patients with distant metastases had either a previous or subsequent RCC - many of which were larger and higher grade – and could represent the source of metastatic disease in these patients.

844 Reporting Practices and Resource Utilization in the Era of Intraductal Carcinoma of the Prostate (IDCP): A Survey of Genitourinary (GU) Subspecialists

Jatin Gandhi[1], Steven Smith[2], Gladell Paner[3], Jesse McKenney[4], Radhika Sekhri[1], Theodorus Van Der Kwast[5], Adeboye O. Osunkoya[6], Alexander Baras[7], John Cheville[8], Kiril Trpkov[9], Naoto Kuroda[10], Maurizio Colecchia[11], Jae Ro[12], Rodolfo Montironi[13], Santosh Menon[14], Ondrej Hes[15], Sean Williamson[16], Michelle Hirsch[17], George Netto[18], Samson Fine[19], Deepika Sirohi[20], Rafael Jimenez[8], Luciana Schultz[21], Cristina Magi-Galluzzi[22], Ankur Sangoi[23], Brian Robinson[24], Charlotte Kweldam[25], Peter Humphrey[26], Donna Hansel[27], Rajal Shah[4], Rohit Mehra[28], Manju Aron[29], Seema Kaushal[30], L. Priya Kunju[31], Oleksandr Kryvenko[32], Angelo De Marzo[33], Fabio Tavora[34], Christopher Przybycin[4], James Kench[35], David Grignon[36], Jonathan Epstein[37], Victor Reuter[19], Mahul Amin[38]

[1]University of Tennessee Health Science Center, Memphis, TN, [2]Virginia Commonwealth University School of Medicine, Richmond, VA, [3]University of Chicago, Chicago, IL, [4]Cleveland Clinic, Cleveland, OH, [5]University Health Network, Toronto, ON, [6]Emory University School of Medicine, Atlanta, GA, [7]Baltimore, MD, [8]Mayo Clinic, Rochester, MN, [9]University of Calgary, Calgary, AB, [10]Kochi Red Cross Hospital, Kochi City, Japan, [11]Fondazione IRCCS Istituto Nazionale Tumori Milano, Milan, Italy, [12]Houston, TX, [13]University Politecnica delle Marche/Medicine, Ancona, Italy, [14]Tata Memorial Hospital, Mumbai, India, [15]Biopticka laborator s.r.o., Plzen, Czech Republic, [16]Henry Ford Health System, Detroit, MI, [17]Brigham and Women's Hospital, Boston, MA, [18]University of Alabama at Birmingham, Birmingham, AL, [19]Memorial Sloan Kettering Cancer Center, New York, NY, [20]University of Utah, Salt Lake City, UT, [21]Instituto de Anatomia Patológica, Anatomia Patologica Rede D'Or, Santa Barbara dOeste, SP, Brazil, [22]The University of Alabama at Birmingham, Birmingham, AL, [23]El Camino Hospital, Mountain View, CA, [24]Weill Cornell Medicine, New York, NY, [25]Erasmus Medical Centre, Rotterdam, Netherlands, [26]Yale University, New Haven, CT, [27]University of California, San Diego, La Jolla, CA, [28]University of Michigan, Ann Arbor, MI, [29]Keck School of Medicine of University of Southern California, Los Angeles, CA, [30]All India Institute of Medical Sciences, New Delhi, India, [31]University of Michigan Hospital, Ann Arbor, MI, [32]University of Miami Miller School of Medicine, Miami, FL, [33]Johns Hopkins University, Baltimore, MD, [34]Argos Laboratory / Messejana Heart and Lung Hospital, Fortaleza, Brazil, [35]Royal Prince Alfred Hospital, Sydney, NSW, Australia, [36]Indiana University School of Medicine, Indianapolis, IN, [37]Johns Hopkins Medical Institutions, Baltimore, MD, [38]Methodist University Hospital, Memphis, TN

Disclosures: Jatin Gandhi: None; Steven Smith: *Consultant*, Elsevier/Amirsys Publishing; Gladell Paner: None; Jesse McKenney: None; Radhika Sekhri: None; Theodorus Van Der Kwast: None; Adeboye O. Osunkoya: None; Alexander Baras: None; John Cheville: None; Kiril Trpkov: None; Naoto Kuroda: None; Maurizio Colecchia: None; Jae Ro: None; Rodolfo Montironi: None; Santosh Menon: None; Ondrej Hes: None; Sean Williamson: None; Michelle Hirsch: None; George Netto: None; Samson Fine: None; Deepika Sirohi: None; Rafael Jimenez: None; Luciana Schultz: None; Cristina Magi-Galluzzi: None; Ankur Sangoi: None; Brian Robinson: None; Charlotte Kweldam: None; Peter Humphrey: None; Donna Hansel: *Advisory Board Member*, Genentech; *Grant or Research Support*, Konica Minolta; *Consultant*, Taris; Rajal Shah: None; Rohit Mehra: None; Manju Aron: None; Seema Kaushal: None; L. Priya Kunju: None; Oleksandr Kryvenko: None; Angelo De Marzo: None; Fabio Tavora: None; Christopher Przybycin: None; James Kench: None; David Grignon: None; Jonathan Epstein: None; Victor Reuter: None

Background: IDCP is recently recognized in the WHO classification as a distinct entity, often occurring concurrently with invasive prostatic carcinoma (PCa) and rarely in a pure form; it is a marker for clinical aggressiveness. Despite increasing experience in this area, the specifics of its potential contribution to grade grouping (GG) and cancer quantitation in both needle biopsies (NBX) and radical prostatectomy (RP) specimens, and whether and under which circumstances basal cell or “PIN cocktail” or equivalent immunohistochemistry (IHC) should be used as adjunctive tests, remain unclear.

Design: An online survey containing 26 questions was undertaken by 41 GU subspecialists from nine countries. Measure of agreement or disagreement was graded as *significant majority* (>75%), *majority* (51-75 %), *minority* (26-50%) and *significant minority* (less than 25%).

Results: IDCP with or without invasive cancer is considered a contraindication for active surveillance by the *significant majority* (95%), although the *majority (66%)* also agreed that the clinical significance/behavior of IDCP on NBX or RP with PCa required further study. The *majority* do NOT upgrade PCa based on comedonecrosis seen only in the intraductal component in NBX (63%) or RP (70%) specimens; similarly, IDCP with GG1 was not a factor in upgrading in NBX (77%) or RP (71%) specimens. The *majority* (58.5%) of respondents include IDCP in % of linear assessment in NBX. The *significant majority* (78%) would use IHC to confirm or exclude intraductal carcinoma if other biopsies showed no PCa, while a *minority* (48%) would use it to confirm/quantitate intraductal component in NBX if it would change the overall GG or pattern 4 quantitation.The majority (58%) report IDCP in RP specimens. When obvious PCa is present in RP or NBX, IHC is almost never used to confirm the presence of IDCP by the *significant majority* (88% and 90% respectively); neither is it used for quantitation (88% and 83% respectively for NBX and RP)/GG assignment (~ 90% each for NBX and RP specimens).

Conclusions: Most GU pathologists consider IDCP to be a feature independent of the PCa grade. While opinion is split regarding its impact on PCa quantitation, the presence of IDCP (even with comedonecrosis) does not factor in GG. The use of PIN4 IHC varies widely and is performed for a multitude of indications. Further study and consensus on best practices recommendations are needed to provide guidance with regards to the most appropriate indications for IHC use in scenarios regarding IDCP.

845 Tertiary Gleason Pattern on Radical Prostatectomy in Grade Group 2 (Gleason Score 3+4) and Grade Group 3 (Gleason Score 4+3): Correlation with Adverse Prostatectomy Findings

Yuan Gao[1], Melissa Shea-Budgell[1], Asli Yilmaz[2], Kiril Trpkov[1]
[1]University of Calgary, Calgary, AB, [2]Calgary Laboratory Services, Calgary, AB

Disclosures: Yuan Gao: None; Melissa Shea-Budgell: None; Asli Yilmaz: None; Kiril Trpkov: None

Background: Previous studies have shown that tertiary pattern 5 (T5) in Grade Group 2 (GG2)/Gleason Score (GS) 3+4 and GG3/GS 4+3 is associated with worse prognosis. It remains unclear, however, how the T5 should be incorporated in the current prostate cancer Grade Group system.

Design: We evaluated the adverse pathologic findings (pT stage, tumor volume, lymphovascular invasion and node positivity) in 601 patients who had radical prostatectomy (RP) performed at our institution between 2005 and 2014. Specifically, we compared the adverse RP findings between GG2 T5 (n=58) with GG3 (n=282) and GG4 (n=54), and between GG3 T5 (n=97) and GG4 (n=54) and GG5 (n=110). We considered T5 to be any amount of pattern 5 cancer, less than the extent of the primary and the secondary cancer patterns.

Results: On RP, all analyzed adverse findings in GG2 T5 showed no significant differences compared with the adverse findings in GG4, but the tumor volume (p<0.01) and node positivity (p=0.03) in GG2 T5 were significantly different from GG3, as shown in the table. Similarly, all analyzed adverse findings in GG3 T5 were not significantly different compared to GG5; however, the ≥pT3 stage (p<0.01), tumor volume (p=0.04) and the lymphovascular invasion (p=0.04) in GG3 T5 were all significantly different from GG4.

	GG2 T5 vs GG3	p	GG2 T5 vs. GG4	p	GG3 T5 vs. GG4	p	GG3 T5 vs. GG5	p
≥pT3 (%)	53 vs.40	0.07	53 vs.44	0.34	74 vs.44	**<0.01**	74 vs.76	0.72
Tu Volume (%)	21 vs.15	**<0.01**	21 vs.17	0.16	23 vs.17	**0.04**	23 vs.24	0.49
LVI (%)	12 vs.9	0.5	12 vs.15	0.67	30 vs.15	**0.04**	30 vs.26	0.57
Node Positivity (%)	7 vs.2	**0.03**	7 vs.7	0.92	6 vs.7	0.77	6 vs.7	0.77

Conclusions: On RP, T5 is associated with similar adverse findings when compared with the corresponding GG+2 category (GG2 vs. GG4 and GG3 vs GG5, respectively). However, the adverse findings are significantly different when T5 is present in GG2 and GG3 in comparison to the next GG (GG+1) category (GG2 vs.GG3 and GG3 vs. GG4, respectively). A reproducible methodology to estimate the percent T5 may be essential to consider for future revision of the GG system, to clarify if such an upgrade is justified.

846 Partial Regression in Pure Seminomas: Clinicopathological study of 421 cases

Yuan Gao[1], Kiril Trpkov[1], Asli Yilmaz[2]
[1]University of Calgary, Calgary, AB, [2]Calgary Laboratory Services, Calgary, AB

Disclosures: Yuan Gao: None; Kiril Trpkov: None; Asli Yilmaz: None

Background: Spontaneous partial or complete regression in germ cell tumors is a well-recognized phenomenon. Previous studies have found that pure seminoma is the most common histologic sub-type associated with partial regression (PR). The incidence and prognostic significance of PR in seminomas has not been previously studied.

Design: We reviewed 421 consecutive pure seminomas, resected from 2000 to 2015 in our institution. We defined PR as a distinct area of fibrosis occupying at least 100X field. PR was further divided into two groups, based on the extent of the regressed area: focal PR, if found in less than or equal to 5% of tumor volume; and established PR, if found in more than 5% of tumor volume. We also documented the following variables: pathologic stage, tumor size, necrosis, vascular invasion and 'local tumor extent' (which included invasion into rete testis, hilar tissues, epididymis, and spermatic cord). We investigated the frequency of PR (focal and established). We also compared the frequency of the histopathologic findings and the presence of initial metastasis between seminomas with regression (focal and established), and seminomas without regression.

Results: PR was identified in 38% (161/421) of seminomas; 24% (103/421) were focal PR and 14% (58/421) were established PR. Comparison of the findings in the cohorts with and without PR are presented in the table.

Variables	Partial Regression		No regression	Focal vs. No regression (p)	Established vs. No regression (p)
	Focal	Established			
Size (cm)	3.9	3	4.1	0.49	**<0.01**
Local tumor extent (%)	66	47	61	0.39	**0.04**
Necrosis (%)	45	50	29	**<0.01**	**<0.01**
Vasc. inv. (%)	10	16	8	0.54	0.06
Initial met (%)	16	9	8	**0.03**	0.89
pT2+ (%)	18	16	11	0.11	0.35

Conclusions: PR is a common finding in pure seminomas and focal PR is more common than established PR. Tumor necrosis is strongly associated with PR, both focal and established. Seminomas with established PR tend to be smaller and are less likely to be associated with local tumor extension. Interestingly, seminomas showing only focal PR were significantly associated with initial metastatic disease. A routine documentation of PR and its extent in seminomas may provide further insights into its possible prognostic significance.

847 Challenges in Missmatch Repair Protein Expression Interpretation in Upper Tract Urothelial Carcinoma

Matthew Gayhart[1], Steven Smith[2]
[1]VCU School of Medicine, Richmond, VA, [2]Virginia Commonwealth University School of Medicine, Richmond, VA

Disclosures: Matthew Gayhart: None; Steven Smith: *Consultant*, Elsevier/Amirsys Publishing

Background: Contemporary series have documented variable prevalence of mismatch repair (MMR) deficient immunophenotype, microsatellite instability (MSI), and Lynch syndrome (LS) in in upper tract urothelial carcinoma (UTUC). Recommendations have differed, but the trend is toward recommendation of universal screening by immunohistochemistry (IHC). Moreover, beyond questions of differing overall prevalence, the patterns of single or "doublet" MMR protein loss documented in UTUC have differed widely across studies, limiting prospective interpretation *vis a vis* risk of LS and MMR deficiency indications for immunotherapy.

Design: We performed MMR IHC for MLH1, MSH2, MSH6, and PMS2 using routine CLIA-compliant protocols on a retrospective consecutive series of UTUCs using a tissue microarray constructed from 68 well characterized cases. Cases with lack of expression of at least one MMR protein were identified and tabulated, with confirmation using whole sections.

Results: In terms of patterns of MMR deficient phenotype associated previously with LS in UTUC, we observed a rate of 9% in our cohort (3 MSH2/MSH6, 2 MSH6 alone, 1 MLH1/PMS2). These cases arose in 4 males, 2 females, with a median age of 64 years. Three of these cases were associated with colorectal cancer; the MLH1/PMS2 case was genetically proven to be LS. However, we also observed additional patterns of unproven significance, including 2 cases with PMS2 loss only. Additional studies are pending to characterize these latter cases with respects to MSI.

Conclusions: The patterns of MMR loss observed in this series further expand the spectrum of MMR loss patterns observed in UTUC and highlight the limited experience in this area. Our overall rate of MMR deficiency in UTUC echos recent findings and supports universal screening in our population. However, we emphasize the limitations of present loss pattern interpretation in UTUC to our clinical colleagues, with regards to both likelihood of LS, and perhaps as saliently, predictive value for immunotherapy. Future meta-analyses and interinstitutional series should emphasize clarification of loss pattern implications to bring interpretation of MMR loss patterns in UTUC more in line with other Lynch-associated carcinomas.

848 Clear Cell Tubulo-Papillary and Clear Cell Renal Cell Carcinoma: A Comparative NGS Mutational Analysis

Francesca Giunchi[1], Michelangelo Fiorentino[2], Annalisa Altimari[3], Gruppioni Elisa[4]
[1]S.Orsola-Malpighi Hospital, Bologna, Italy, [2]Istituto Oncologico Addarii, Bologna, Italy, [3]S. Orsola Malpighi Hospital, Bologna, Italy, [4]S. Orsola-Malpighi Hospital, University of Bologna, Bologna, Italy

Disclosures: Francesca Giunchi: None; Michelangelo Fiorentino: None; Annalisa Altimari: None; Gruppioni Elisa: None

Background: Clear cell tubulo-papillary renal cell carcinoma (cctpRCC) is a rare entity recognized by the World Health Organization (WHO) classification since 2004. The indolent clinical behavior with no lymph-node metastasis, no local recurrence, and no distant

metastasis reported in the literature suggested that cctpRCC might be encountered as a benign lesion. The main challenge for pathologists resides in the differential diagnosis with clear cell renal cell carcinoma (ccRCC).

Design: In order to point out different genetic profiles between the two tumor types, we performed a wide spectrum mutational analysis in 8 cctpRCC and in 6 control cases of small ccRCC (stage pT1, nucleolar G1 (WHO 2016). Diagnostic immunohistochemistry (IHC) included cytokeratin 7(CK7), racemase (AMACR) and carbonic anhydrase IX (CAIX). Next generation sequencing (NGS) analysis was run on an Ion PGM™ System using the Ion AmpliSeq™Cancer Hotspot Panel v2 (ThermoFisher Scientific, Waltham, MA) covering 207 amplicons in 50 oncogenes or tumor suppressor genes (ThermoFisher Scientific, Walthem, MA).

Results: Among the 8 cctpRCC cases, 6 (75%) showed consistent IHC profile and were wild type for all the genes in the panel; 2 (25%) had consistent IHC but showed VHL gene mutations. Among the 6 ccRCC control cases, 3 (50%) showed expected VHL mutations and coherent IHC profile; 1 (16%) had consistent IHC profile but it was wild type for all the genes; 2 (33%) displayed inconsistent ICH profile and harbored mutations either in the p53 or the cKIT gene.

Conclusions: We found that the cases of cctpRCC with consistent morphology and IHC profile were also silent for mutations. This finding together with the indolent biological behavior lead to consider cctpRCC a benign lesion rather than a carcinoma. Renal cell tumors with morphological clear cell features belong to a wide range of lesions with different biological bases and behavior. In our study only 64% of the cases showed morphological and genetic concordance. The comprehensive differential diagnosis between ccRCC and ccptRCC requires the combination of histological features, IHC and mutational profiles.

849 Using Deep Convolutional Neural Networks to Classify Kidney Neoplasms

Dibson Gondim[1], Khaleel Al-Obaidy[2], Natasha Gibson[3], Yingnan Ju[3], David Crandall[4], Muhammad Idrees[2], John Eble[2], David Grignon[2], Liang Cheng[2]
[1]Saint Louis University, St. Louis, MO, [2]Indiana University School of Medicine, Indianapolis, IN, [3]Indiana University, Indianapolis, IN, [4]Indiana University, Bloomington, IN

Disclosures: Dibson Gondim: None; Khaleel Al-Obaidy: None; Natasha Gibson: None; Yingnan Ju: None; David Crandall: None; Muhammad Idrees: None; John Eble: None; David Grignon: None; Liang Cheng: None

Background: Deep convolutional neural networks have been successfully applied to a wide variety of image classification problems. The potential of this technique for the evaluation of histopathologic images has not been fully explored. There have been initial efforts to use deep learning in pathology for tasks such as mitosis detection, tumor grading, and classification. However, no studies have specifically addressed the development of a deep learning model to discriminate between several types of benign and malignant kidney neoplasms. Therefore, the aim of this project is to create a deep learning classifier for kidney neoplasms and to assess its performance.

Design: The four most common types of renal cell carcinoma (RCC) and two benign kidney neoplasms were chosen - clear cell RCC (n=56), papillary RCC type 1 and 2 (n=81), chromophobe RCC (n=51), clear cell papillary RCC (n=19), oncocytoma (n=39), and metanephric adenoma (n=6). The cases were randomly assigned to either the training/validation(n=197) or testing datasets (n=55). One to four slides from each case (total=385 slides) were scanned using Philips IntelliSite Pathology Solution (Philips, the Netherlands). Pre-processing of the digital slides included the selection of areas containing solid tumor from which numerous small image patches (350x350 pixels) were extracted. Between 28,541 and 40,000 randomly selected patches from each type of tumor were used to train the neural network, 8,293 to 10,000 patches were used for validation, and 750 to 3,750 were used for testing (total=298,071 patches). The deep learning model was created with AutoML Vision (Google, Mountain View, CA). The final classification of each testing dataset case was based on the most frequent classification result (voting) of a collection of 217 to 249 random patches of a given case.

Results: In terms of classification of individual patches, the best model achieved a precision of 88.2% and a recall of 86.3% with a threshold of 0.5. Regarding final classification of cases, 49/55 (89.0%) of testing dataset cases were correctly classified: clear cell RCC (12/13), papillary RCC (14/15), chromophobe RCC (10/11), clear cell papillary RCC (2/4), oncocytoma (9/9), and metanephric adenoma (2/3) - See Table.

	Model Prediction					
Pathology	Clear Cell RCC	Papillary RCC	Chromophobe RCC	Clear Cell Pap. RCC	Oncocytoma	Metanephric Adenoma
Clear Cell RCC	**12**	1	0	0	0	0
Papillary RCC	1	**14**	0	0	0	0
Chromophobe RCC	1	0	**10**	0	0	0
Clear Cell Pap. RCC	2	0	0	**2**	0	0
Oncocytoma	0	0	0	0	**9**	0
Metanephric Adenoma	0	1	0	0	0	**2**

Conclusions: This technique showed promising clinical utility in renal tumor classification. Models based on convolutional neural networks have the potential to accurately classify the majority of the three most common types of renal cell carcinoma and oncocytoma.

850 Expansile Cribriform Gleason Pattern 4 has Worse Outcomes at Prostatectomy than Glomerulation Gleason Pattern 4

Nancy Greenland[1], Li Zhang[1], Peter Carroll[1], Bradley Stohr[1], Jeffry Simko[1]
[1]University of California, San Francisco, San Francisco, CA

Disclosures: Nancy Greenland: None; Li Zhang: None; Peter Carroll: None; Bradley Stohr: None; Jeffry Simko: None

Background: The Gleason grading system informs prostate cancer prognosis based on the presence of one of several histopathologic features. Among types of Gleason pattern 4, the expansile cribriform subtype, which is defined by solid large acini with greater than 12 lumen spaces, has been associated with similar outcomes to Gleason pattern 5 carcinomas. By contrast, the glomerulation subtype, which is characterized by dilated glands that contain intraluminal cribriform structures with one or two points of attachment, has not been consistently associated with worse outcomes. The percentages of pattern 4, rates of seminal vesicle invasion (SVI), and presence and severity of extraprostatic extension (EPE) are markers of aggressiveness linked with poor outcomes in prostate cancer patients. We hypothesized that prostatectomy cases with expansile cribriform pattern 4, but not glomerulation pattern 4, would be associated with these features of aggressiveness.

Design: We evaluated prostatectomy cases within the past ten years from our institution with either expansile cribriform pattern 4, glomerulation pattern 4, or both patterns, using these groupings as predictors. Outcomes were the percentage of pattern 4, the presence or absence of SVI, and presence and extent (extensive or limited) of EPE. Associations were determined by chi-squared test and ordered logistic regression models.

Results: Cases with expansile cribriform had the worst outcomes at prostatectomy, with the highest rates of ≥50% pattern 4, SVI, and extensive EPE (Table 1). Cases with glomerulation pattern had the best outcomes at prostatectomy, with the lowest rates of ≥50% pattern 4, SVI, and extensive EPE. Comparing patients with expansile cribiform and glomerulation pattern, expansile cribiform pattern was associated with a 4.8-fold (95% CI 2.5-9.8) odds of having ≥50% pattern 4 versus ≤20% pattern 4, a 3.5-fold (95% CI 1.5-8.4) odds of SVI, and a 3.0-fold (95% CI 1.7-5.4) odds of EPE. The presence of both patterns was associated with an intermediate phenotype.

		Glomerulation but no Expansile Cribriform	Expansile Cribriform but no Glomerulation	Both Patterns Present	P value[1]	P value[2]
Variable	**# cases**	82	137	51		
% Gleason pattern 4	**≥50 %4**	28 (34.1%)	89 (65%)	30 (56.9%)	<0.001	<0.001
	>20-<50 %4	16 (19.5%)	23 (16.8%)	16 (33.3%)		
	≤20 %4	38 (46.3%)	25 (18.2%)	5 (9.8%)		
SVI Status	**SVI**	7 (8.5%)	34 (24.8%)	7 (13.7%)	0.007	0.005
	No SVI	75 (91.5%)	103 (75.2%)	44 (86.3%)		
EPE Status	**EPE**	41 (50%)	103 (75.2%)	31 (56.9%)	<0.001	<0.001
	No EPE	41 (50%)	34 (24.8%)	20 (39.2%)		
	Extensive EPE	20 (24.4%)	83 (61.3%)	24 (45.1%)	<0.001	<0.001
	Limited EPE	21 (25.6%)	20 (14.6%)	7 (13.7%)		

1. P value[1]: P value of the test of across all three groups.
2. P value[2]: P value of the test of between glomerulation pattern patients and expansile cribriform pattern patients.

Conclusions: The expansile cribriform pattern 4 at prostatectomy is associated with more histopathologic features of aggressiveness, while glomerulation pattern 4 is associated with less aggressive features.

851 Useful Immunohistochemical Markers in the Molecular Classification of Bladder Cancer

Charles Guo[1], Tadeusz Majewski[1], Colin Dinney[1], Bogdan Czerniak[1]
[1]The University of Texas MD Anderson Cancer Center, Houston, TX

Disclosures: Charles Guo: None; Tadeusz Majewski: None; Colin Dinney: *Consultant*, FKD Therapies Oy; *Grant or Research Support*, NCI; *Consultant*, Merck; Bogdan Czerniak: None

Background: Recent genomic profiling analyses have demonstrated that bladder urothelial carcinoma (UC) can be divided into two molecular subtypes, luminal and basal, each with distinct clinical behavior and sensitivity to chemotherapy. Our previous studies demonstrated that a number of immunohistochemical markers could help the molecular classification of bladder UC on tissue

microarray array (TMA) sections. Here we investigated whether immunohistochemistry could be used in the molecular classification of bladder UC on routine histologic sections.

Design: RNA was extracted from fresh frozen bladder UC samples (n=132) and genomic mRNA expressions were analyzed for the molecular classification. Immunohistochemical stains were performed on the matched formalin-fixed paraffin-embedded tumor samples that were processed routinely in our histologic laboratory. Clinical data were collected from medical records.

Results: The patients included men (n=100) and women (n=32) with a mean age of 67.2 years. The tumor samples consisted of invasive UC (n=98), low-grade (n=25), and high-grade (n=9) noninvasive papillary UC. Genomic mRNA expression analyses showed bladder UC were divided into luminal (n=94), basal (n=34), and double-negative (n=4) subtypes. The luminal subtype showed overexpression of GATA-3, CK18, CK20, and FOXA1 genes, while the basal subtype showed overexpression of CK5, CK6, CK14, and CD44. The double-negative subtype was characterized by low expression of claudin-related genes. Immunohistochemistry were performed on routine tissue sections using the luminal marker GATA3 and basal marker CK5/6, which identified the molecular subtype with over 90% accuracy. Survival analysis showed that the basal subtype invasive UC were more aggressive when compared to luminal cancers.

Conclusions: Basal and luminal subtypes of bladder UC exhibit distinct signatures of gene expressions as well as different clinicopathologic features. Immunohistochemistry is a cost-effective tool, which can be used to aid the molecular classification of bladder UC with a high accuracy in routine clinical practice.

852 Genome-Wide Characterization of Sarcomatoid Bladder Cancer

Charles Guo[1], Tadeusz Majewski[1], Bogdan Czerniak[1]
[1]The University of Texas MD Anderson Cancer Center, Houston, TX

Disclosures: Charles Guo: None; Tadeusz Majewski: None; Bogdan Czerniak: None

Background: Sarcomatoid carcinoma (SARC) is an aggressive variant of bladder cancer. We performed comprehensive genomic characterization of SARC, which identified unique molecular features associated with its aggressive nature that may be relevant for the early detection and treatment of this highly lethal disease.

Design: Genome-wide analyses, including micro-RNA expressions, genomic mRNA expressions, and whole-exome mutational profiles, were performed on 28 cases of SARC and 84 cases of conventional muscle-invasive urothelial carcinoma (UC). The Cancer Genome Atlas (TCGA) cohort of 408 muscle-invasive bladder cancers served as the control group.

Results: SARCs showed a distinct mutational landscape with enrichment of *TP53*, *RB1, and PIK3CA* mutations. They were related to the basal molecular subtype of conventional UC and could be further divided into “epithelial” and more clinically aggressive “mesenchymal” subsets. Expression analysis showed that SARC were driven by downregulation of TP63 and dysregulation of EMT regulatory networks. Nearly half of SARCs exhibited a heavily infiltrated immune phenotype with upregulation of PD-L1.

Conclusions: We conclude that SARCs are driven by profound dysregulation of the EMT network and that a large proportion of SARCs have an immune infiltration phenotype. Both of these features present new avenues of therapeutic potential in patients with this aggressive disease.

853 TFEB Expression Profiling in Renal Cell Carcinomas

Sounak Gupta[1], Pedram Argani[2], Ying-Bei Chen[1], Satish Tickoo[3], Samson Fine[1], Anuradha Gopalan[1], Hikmat Al-Ahmadie[1], S. Joseph Sirintrapun[1], Sean Williamson[4], Stephanie Skala[5], Rohit Mehra[5], Ondrej Hes[6], Cristina Antonescu[1], Marc Ladanyi[1], Maria Arcila[1], Victor Reuter[1]
[1]Memorial Sloan Kettering Cancer Center, New York, NY, [2]Johns Hopkins Hospital, Ellicott City, MD, [3]New York, NY, [4]Henry Ford Health System, Detroit, MI, [5]University of Michigan, Ann Arbor, MI, [6]Biopticka laborator s.r.o., Plzen, Czech Republic

Disclosures: Sounak Gupta: None; Pedram Argani: None; Ying-Bei Chen: None; Satish Tickoo: None; Samson Fine: None; Anuradha Gopalan: None; Hikmat Al-Ahmadie: None; S. Joseph Sirintrapun: None; Sean Williamson: None; Stephanie Skala: None; Rohit Mehra: None; Ondrej Hes: None; Cristina Antonescu: None; Marc Ladanyi: None; Maria Arcila: *Speaker*, Invivoscribe; *Speaker*, Raindance Technologies; *Speaker*, Archer; Victor Reuter: None

Background: *TFEB* is thought to act as a key oncogenic driver in renal cell carcinomas (RCC). Mechanisms of *TFEB* overexpression include t(6;11) and amplifications (Amp) at the *TFEB* locus on 6p21. As recent literature suggests that RCCs with 6p21 Amp behave more aggressively than t(6;11) RCCs, we compared relative *TFEB* gene expression in these tumors.

Design: Digital droplet PCR (ddPCR) was used to quantify *TFEB* mRNA expression from formalin fixed paraffin embedded (FFPE) tissue using *B2M* as a control. Experimental controls included low positives from cell-free RNA (n=3), paired non-neoplastic renal parenchyma

(n=13) and non-*TFEB*-altered tumors (n=5). These were compared to 6p21-Amp RCCs (n=9) and t(6;11) RCCs (n=16). *TFEB* status for these tumors was verified using a combination of FISH (n=22) or comprehensive molecular profiling, including 6p21 copy number status using a next generation sequencing (NGS) based platform.

Results: *TFEB*-altered tumors had higher *TFEB* mRNA expression (mean: 165%, n=25) compared to both non-neoplastic renal tissue (mean: 8.2%, n=13, *p*=0.02) and non-*TFEB*-altered renal tumors (mean: 3.9%, n=5, *p*=0.15). Interestingly, t(6;11) RCCs had higher *TFEB* expression (mean: 225%, n=16) compared to 6p21-Amp RCCs (mean: 51.2%, n=9; **Figure 1**). The latter analysis was not statistically significant, likely due to the limited number of cases profiled (*p*=0.08). Where paired non-neoplastic tissue was available, a mean 31-fold increase in expression was noted for cases with *TFEB* alterations (n=9) compared to non-*TFEB*-altered tumors (0.36-fold, n=4). ddPCR had a high specificity and positive predictive value (100%) when compared to FISH/NGS, while sensitivity (80%) and negative predictive value (78.3%) were lower (**Table 1**). Of the 5 cases that were negative by ddPCR and positive by FISH, 1 was a t(6;11) tumor with sarcomatoid transformation and 4 were 6p21-Amp RCCs.

Table 1

	FISH/NGS + (*TFEB* Alteration)	FISH/NGS - (*TFEB* Alteration)	
ddPCR + (*TFEB*/*B2M* =>20%)	20	0	**Positive Predictive Value = 100%**
ddPCR - (*TFEB*/*B2M* <20%)	5	18	**Negative Predictive Value = 78.3%**
	Sensitivity=80%	**Specificity=100%**	

Figure 1 - 853

Figure 1

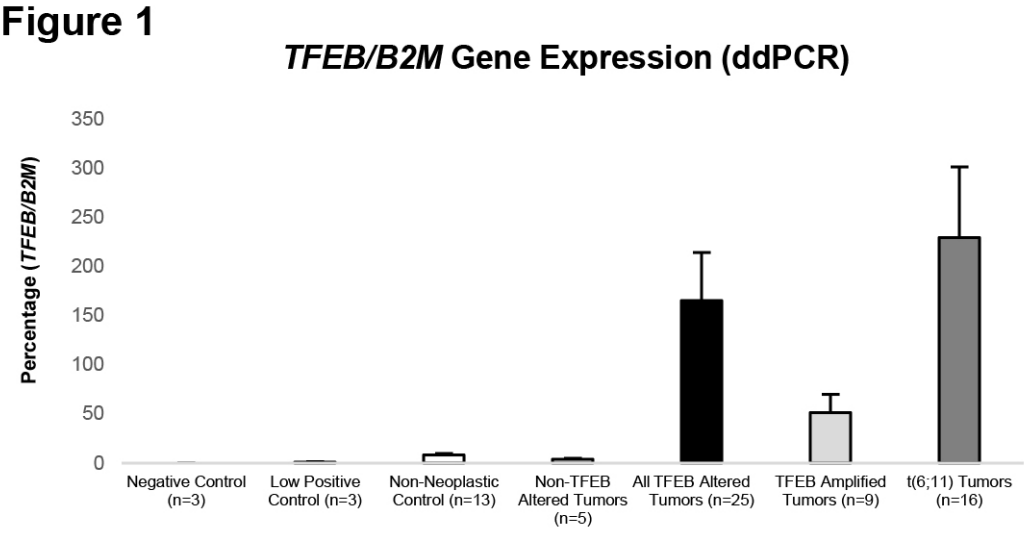

Conclusions: *TFEB* expression status, determined using ddPCR on FFPE material, can be correlated with *TFEB* copy number assesment by FISH to define a biologically significant threshold for 6p21-Amp. Our results suggest that 6p21-Amp RCCs do not show as much increased *TFEB* gene expression compared to t(6;11) RCCs, which correlates with the less consistent/diffuse expression of downstream markers of *TFEB* activation (Melan A, HMB45 and Cathepsin K) seen in these neoplasms. This implies that the aggressive biologic behavior of 6p21-Amp RCCs might be secondary to other genes at the 6p21 locus such as *VEGFA* or other genetic alterations.

854 Immunohistochemical Detection of Androgen Receptor in Metastatic Castrate Resistant Prostate Cancer

Sounak Gupta[1], Samson Fine[1], Satish Tickoo[2], Hikmat Al-Ahmadie[1], Ying-Bei Chen[1], S. Joseph Sirintrapun[1], Ann Bialik[3], Wassim Abida[1], Howard Scher[1], Marc Ladanyi[1], Victor Reuter[1], Anuradha Gopalan[1]
[1]Memorial Sloan Kettering Cancer Center, New York, NY, [2]New York, NY, [3]Brooklyn, NY

Disclosures: Sounak Gupta: None; Samson Fine: None; Satish Tickoo: None; Hikmat Al-Ahmadie: None; Ying-Bei Chen: None; S. Joseph Sirintrapun: None; Ann Bialik: None; Wassim Abida: None; Howard Scher: *Consultant*, Janssen Biotech, Inc; *Consultant*, Sanofi Aventis; *Consultant*, WCG Oncology; *Advisory Board Member*, Asterias Biotherapeutics (Board of Directors Member); *Grant or Research Support*, Janssen; Marc Ladanyi: None; Victor Reuter: None; Anuradha Gopalan: None

Background: Molecular profiling of prostatic adenocarcinoma by Stand Up to Cancer-PCF revealed frequent Androgen receptor (AR) alterations in metastatic disease. Our prior study focused on the metastatic disease spectrum confirmed that AR amplification (Amp) was seen in over half of all cases of metastatic castrate resistant prostate cancer (mCRPC). Studies have suggested that AR Amp prior to management with newer androgen deprivation therapy (ADT), in mCRPC, predicted worse outcomes. Separately, an AR-null non-neuroendocrine (NE) phenotype of mCRPC has also been reported, which may be less sensitive to ADT. We have conducted a pilot study to correlate AR status, as determined by next generation sequencing (NGS), with IHC.

Design: Histology was evaluated and IHC for full length AR (Clone: AR441, DAKO) was performed for 16 cases of mCRPC. AR copy number assessment (CNA) for all cases was determined using a hybridization exon-capture NGS-based assay. Controls included the PC3 cell line, which lacks AR expression and the androgen-sensitive LNCaP cell line. The institutional clinical sequencing cohort was accessed using cBioPortal to determine the relative frequency of AR Amp events across tumor types.

Results: Of 16 mCRPC cases, 13 had AR Amp as assessed by NGS-based CNA (mean fold change: 6.8, range: 2.8 to 15.1), while 3 cases lacked AR Amp. LNCaP cells and all 13 mCRPC with AR Amp showed diffuse, strong nuclear expression in >95% cells. PC3 cells and all 3 mCRPC without AR Amp showed complete absence of AR expression. AR non-Amp cases were adenocarcinoma (n=2) and adenocarcinoma with NE differentiation (n=1) and were characterized by *PTEN* loss, *TP53*alteration and *BRCA2* loss/*FGFR1* alteration in 1 case each. Querying the institutional clinical sequencing cohort (30,965 cases) revealed that among tumors where >100 cases had been profiled only prostatic adenocarcinomas showed a prevalence of AR Amp that was >1% (259 of 1885, 13.7%). None of the cases of urothelial carcinoma, which is often a differential diagnostic consideration, showed AR Amp (0 of 833 cases).

Conclusions: Our study, although limited, suggests that AR IHC reliably distinguishes AR null and over-expressing cases in the mCRPC setting. This might be particularly relevant when there is limited access to molecular testing, limited tumor material for molecular testing or when NGS copy number predictions fail due to low tumor content. Furthermore, AR IHC may be a useful diagnostic tool as AR Amp in tumors of non-prostatic origin is rare.

855 JAK2/PD-L1/PD-L2 (9p24.1) Amplified Renal Cell Carcinoma: Implications for Clinical Management

Sounak Gupta[1], John Cheville[2], Achim Jungbluth[1], Yanming Zhang[1], Lei Zhang[1], Ying-Bei Chen[1], Satish Tickoo[3], Samson Fine[1], Anuradha Gopalan[1], Hikmat Al-Ahmadie[1], S. Joseph Sirintrapun[1], Kyle Blum[1], Christine Lohse[2], A. Hakimi[1], R. Houston Thompson[2], Bradley Leibovich[2], Michael Berger[1], Maria Arcila[1], Dara Ross[1], Marc Ladanyi[1], Cristina Antonescu[1], Victor Reuter[1]
[1]Memorial Sloan Kettering Cancer Center, New York, NY, [2]Mayo Clinic, Rochester, MN, [3]New York, NY

Disclosures: Sounak Gupta: None; John Cheville: None; Achim Jungbluth: None; Yanming Zhang: None; Lei Zhang: None; Ying-Bei Chen: None; Satish Tickoo: None; Samson Fine: None; Anuradha Gopalan: None; Hikmat Al-Ahmadie: None; S. Joseph Sirintrapun: None; Kyle Blum: None; Christine Lohse: None; A. Hakimi: None; R. Houston Thompson: None; Bradley Leibovich: None; Michael Berger: *Advisory Board Member*, Roche; Maria Arcila: None; Dara Ross: None; Marc Ladanyi: *Advisory Board Member*, Bristol-Myers Squibb; *Advisory Board Member*, Merck; Cristina Antonescu: None; Victor Reuter: None

Background: Amplifications (Amp) of *JAK2*, *PD-L1* and *PD-L2* at 9p24.1 lead to constitutive expression of PD-L1. This, coupled with JAK2-activation leads to high tumor PD-L1 expression and consequent immune evasion.

Design: 9p24.1 Amp were evaluated in renal cell carcinomas (RCC) using a combination of next generation sequencing-based copy number analysis (Amp: tumor/normal fold change ≥1.5; **Figure A**) and FISH using probes for *JAK2/INSL6* and *PD-L1/PD-L2* (Amp: probe/centromere ratio ≥10:1 or copy number ≥10; **Figure B**). Expression of phospho-STAT3 (a downstream target of JAK2), PD-L1, PD-L2 and PD-1 was assessed using IHC (**Figure B**) and H-scores were calculated as the product of intensity of staining (0 to 3) and the percentage of positive cells (0 to 100%). Herein, we interrogated a “Discovery” cohort of 593 RCC, a “Validation” cohort of 398 high-grade RCC as well as The Cancer Genome Atlas (TCGA, 879 cases) and other public datasets using cBioPortal.

Results: These alterations are enriched in sarcomatoid RCC: of 13 identified cases, 10 had sarcomatoid features and 1, rhabdoid. The highest IHC concordance was for PD-L1 (mean H-score: 222, n=10). TCGA profiling of RCC cohorts with fewer high-grade tumors revealed a lower prevalence of 0.6% (3 of 533 cases) only amongst clear cell RCC. Amongst sarcomatoid RCC, the prevalence was 3.5%

in the "Discovery" cohort (29 cases), 6.5% in public datasets (92 cases) and 3.1% in the "Validation" cohort (127 cases). Analysis of cancer-specific survival and distant metastasis-free survival based on PD-L1 IHC expression status (282 cases) did not reveal a significant prognostic effect in the "Validation" cohort and may be reflective of the advanced disease status of these tumors. Likely constitutive PD-L1 expression in this cohort (H-score ≥250, of 300) amongst rhabdoid (6% of 83 cases) and sarcomatoid RCC (7.1% of 127 cases) suggest alternate mechanisms of constitutive PD-L1 expression. This is supported by TCGA gene expression datasets which show increased mRNA expression of *JAK2*, *PD-L1* and *PD-L2* in 9-11% of clear cell, papillary and chromophobe RCC. Of note, two patients with 9p24.1-Amp sarcomatoid RCC showed significant response to immunotherapy (alive with disease and dead of disease at 27.7 and 26 months of follow up, respectively).

Figure 1 - 855

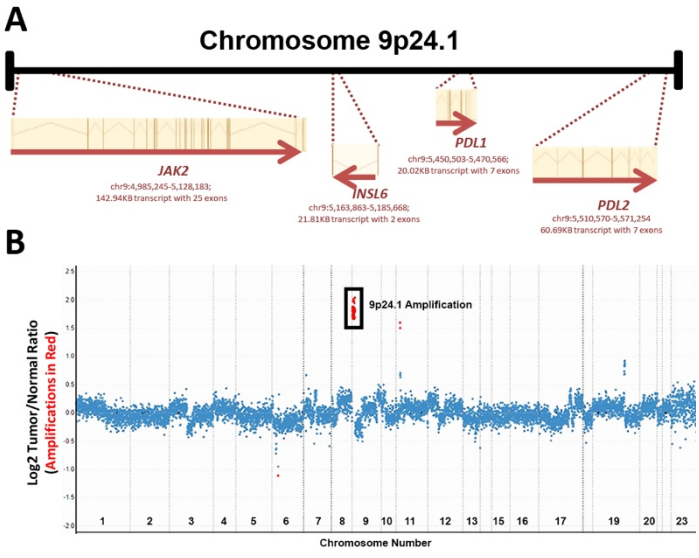

Figure 2 - 855

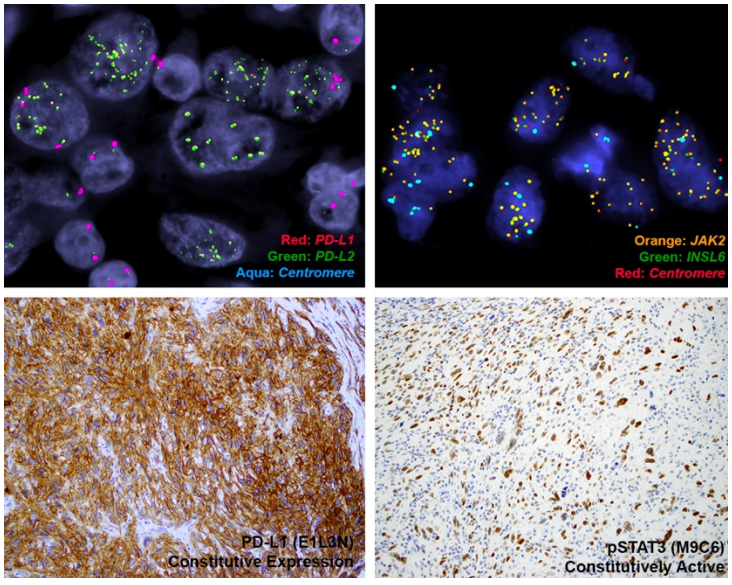

Conclusions: A subset of high-grade RCC with sarcomatoid and rhabdoid features show constitutive PD-L1 overexpression and these patients should be evaluated for enhanced response to immune checkpoint inhibitors in future studies.

856 Invasive High Grade Urothelial Carcinoma of the Bladder, Renal Pelvis, Ureter and Prostatic Urethra Arising in a Background of Urothelial Carcinoma With an Inverted Growth Pattern: A Contemporary Clinicopathologic Analysis of 91 Cases

Christina Gutierrez[1], Mehrdad Alemozaffar[1], Adeboye O. Osunkoya[2]
[1]Emory University, Atlanta, GA, [2]Emory University School of Medicine, Atlanta, GA

Disclosures: Christina Gutierrez: None; Mehrdad Alemozaffar: None; Adeboye O. Osunkoya: None

Background: Urothelial carcinoma (UCa) associated with an inverted/endophytic growth pattern can occasionally mimic inverted papilloma and may also pose diagnostic challenges when being evaluated for invasion. Making these distinctions are critical for appropriate treatment and improved patient outcomes. Few studies have analyzed the clinicopathologic features of invasive high grade UCa of the bladder, renal pelvis, ureter and prostatic urethra arising in a background of UCa with an inverted growth pattern.

Design: Bladder, renal pelvis, ureter and prostatic urethra cases with invasive high grade UCa arising in a background of UCa with an inverted growth pattern were obtained through our urologic pathology files and the senior author's consults. Clinicopathologic parameters including extent of invasion, variant histology, presence of UCa in situ, and clinical follow-up was obtained.

Results: Ninety-one cases from 82 patients were included in the study. The mean patient age was 69 years (range: 38-95 years) and 65 patients were male (80%). The distribution of the primary sites included bladder (77; 84%), ureter (7; 8%), renal pelvis (5; 6%), and prostatic urethra (2; 2%). Lamina propria invasion was present in 81% of bladder, 60% ureter, 20% renal pelvis, and 100% of prostatic urethra cases. Muscularis propria invasion was present in 19% of bladder, 14% ureter, and 20% of renal pelvis cases. UCa invaded periureteric fat in 29% of ureter cases and involved the renal parenchyma in 60% of renal pelvis cases. Adjacent UCa in situ was present in 43% of cases (39/91). In addition, micropapillary urothelial carcinoma was present in 5.5% of cases (5/91). Clinical follow-up was available for 77 patients (94%) with a mean duration of 18 months (range: 0.2-74 months). Recurrent UCa persisted in 77% of patients, 19% progressed with metastatic disease, and 22% of patients with bladder involvement died of disease.

Conclusions: This is the largest study to date of invasive high grade UCa arising in a background of UCa with an inverted growth pattern. This study further emphasizes the importance of distinguishing these tumors from benign mimickers of UCa. Recognition of invasive foci is also critical in view of the potentially high frequency of recurrence and the possibility of advanced disease in a subset of these patients.

857 The Clonal Relationship of Adjacent Gleason Pattern 3 and Gleason Pattern 5 Lesions in Gleason Scores 3+5=8 and 5+3=8

Michael Haffner[1], Jessica Hicks[2], Angelo De Marzo[3], Jonathan Epstein[4]
[1]Johns Hopkins Medicine, Baltimore, MD, [2]Johns Hopkins University School of Medicine, Baltimore, MD, [3]Johns Hopkins University, Baltimore, MD, [4]Johns Hopkins Medical Institutions, Baltimore, MD

Disclosures: Michael Haffner: None; Jessica Hicks: None; Angelo De Marzo: None; Jonathan Epstein: None

Background: Genomics studies have demonstrated a high level of intra-tumoral heterogeneity in prostate cancer. There is strong evidence suggesting that individual tumor foci can arise as genetically distinct, clonally independent lesions. However, recent studies have also demonstrated that adjacent Gleason pattern 3 and Gleason pattern 4 lesions can originate from the same clone, but follow divergent genetic and morphologic evolution. The clonal relationship of Gleason pattern 3 and Gleason pattern 5 lesions present in the same case has thus far not been investigated.

Design: We analyzed a cohort of 14 cases, 11 biopsy and 3 radical prostatectomy specimens with a Gleason score of 3+5=8 or 5+3=8 present in the same biopsy core or in a single dominant tumor nodule, respectively. Clonal and subclonal relationships between Gleason pattern 3 and pattern 5 lesions were assessed using immunohistochemical assays for ERG, PTEN and P53. These markers have been shown to tightly correlate with genomic alterations and have been extensively used to establish clonal relationships.

Results: 9/14 (64%) cases showed ERG reactivity in both pattern 3 and pattern 5 lesions. Only 1/14 (7%) cases showed a discordant pattern with ERG staining present only in the pattern 3 and not in the pattern 5 lesion. PTEN expression was lost concordantly in 2/14 (14%) cases. The remainder of the cases 12/14 (86%) showed intact PTEN. Nuclear p53 reactivity was present in 1/14 (7%) cases with concordance in Gleason pattern 3 and pattern 5.

Conclusions: This study provides first evidence that the majority of adjacent Gleason pattern 3 and 5 lesions are clonally related. The frequency of PTEN and p53 alterations observed in Gleason pattern 5 in this study is lower than reported previously for Gleason pattern 5 in the context of pattern 4. Collectively these analyses suggest that Gleason pattern 3 and 5 can likely arise from a common ancestral clone and although they show divergent morphologic features they share common driver alterations. These data further suggest that Gleason pattern 5 lesions arising in the context of pattern 3 might show molecular characteristics of less aggressive disease. These preliminary results need to be further corroborated with detailed sequencing studies.

858 Gleason pattern 4 with cribriform morphology on biopsy is associated with adverse clinicopathological findings on prostatectomy

Michael Haffner[1], Daniela Correia Salles[2], George Gao[3], Jonathan Epstein[2]
[1]Johns Hopkins Medicine, Baltimore, MD, [2]Johns Hopkins Medical Institutions, Baltimore, MD, [3]University of California, Davis, Sacramento, CA

Disclosures: Michael Haffner: None; Daniela Correia Salles: None; George Gao: None; Jonathan Epstein: None

Background: The prognostic significance of the Gleason grading system has been well established. However individual Gleason pattern comprise heterogeneous morphologies which might add additional prognostic information. Recent evidence suggests that Gleason pattern 4 with cribriform growth pattern is associated with adverse prognosis, however the association between cribriform pattern on biopsies and pathological findings on subsequent prostatectomies are not know.

Design: We determined the presence of cribriform architecture in 367 diagnostic biopsies from 2014 to 2018 with Gleason scores 3+4, 4+3 and 4+4 on a median number of 12 cores per case for which subsequent completely embedded radical prostatectomy specimens were available and correlated the presence cribriform morphology with histopathological features.

Results: Cribriform architecture was present in 63.5% of all biopsies and was correlated with the overall extend of Gleason pattern 4. In addition, cribriform morphology on biopsy showed a statistically significant association with higher Gleason grade, increased pathological stage and nodal metastasis on prostatectomies (**Table**). In subset analyses of cases with a biopsy Gleason score 3+4, these associations did not reach statistical significance, but the presence of cribriform growth in this subgroup showed a trend towards an association with increased upgrading to Gleason score 9/10 (1/104 (1%) vs. 5/104 (4.8%), P=0.06). Importantly, in cases with a biopsy Gleason score of 3+4 and either limited biopsy core involvement (<3 cores positive, n=32) or less than 10% pattern 4 (n=67) no differences in histopathological features on prostatectomy were observed when stratifying by presence of cribriform architecture.

Pathological stage					
CRIB			N	%	
No cribriform morphology	T2		82	61	
	T3A		46	34	
	T3B		6	4.5	
Cribriform morphology	T2		111	48	
	T3A		87	37	
	T3B		35	15	
Tumor grade			N	%	
No cribriform morphology	GS	GG	1	0.7	
	3+4	2	97	72	
	4+3	3	25	19	
	4+4	4	2	1.5	
	4+5, 5+4	5	9	6.7	
Cribriform morphology	GS	GG	1	0.4	
	3+4	2	109	47	
	4+3	3	66	28	
	4+4	4	25	11	
	4+5, 5+4	5	32	14	
Nodal status			N	%	
No cribriform morphology	negative		127	95	
	positive		4	3	
Cribriform morphology	negative		209	90	
	positive		15	6.4	
GS, Gleason Score; GG, Grade Group; N, number of cases.					

Conclusions: This largest study to date comparing biopsy and prostatectomy findings of cribriform architecture demonstrates that cribriform pattern 4 is associated with adverse prognostic features and highlights the need for recognizing specific morphologies that are associated with potentially more aggressive behavior.

859 Concordance analysis between Prostate Imaging - Reporting and Data System (PI-RADS v2) and prostatectomy histologic findings

Bing Han[1], Jhanvi Kanotra[1], Gloria Sura[1], Raman Danrad[2], Tracy Dewenter[3], Ritu Bhalla[4]
[1]Louisiana State University, New Orleans, LA, [2]Louisiana State University Health Science Center, New Orleans, LA, [3]LSU Health Sciences Center, New Orleans, LA, [4]Louisiana State University, Metairie, LA

Disclosures: Bing Han: None; Jhanvi Kanotra: None; Gloria Sura: None; Raman Danrad: None; Tracy Dewenter: None; Ritu Bhalla: None

Background: The purpose of prostate MRI is to identify and localize clinically significant disease, defined as prostate cancer with Gleason score ≥7, and/or volume ≥ 0.5 cc, and/or extraprostatic extension (EPE). PI-RADS v2 (version 2) assessment uses a 5-point scale, which correlates with the presence of a clinically significant cancer. This scale ranges from 1 to 5 (very low to very high probability of clinically significant disease). PI-RADS 4 – 5 are the indication for biopsy; while 2 - 3 are indeterminate; and 1-2 are not indications for biopsies. Although PI-RADS v2 is designed to improve detection, localization, characterization, and risk stratification in patients with suspected

cancer in treatment naïve prostates, there is limited literature correlating the parameters evaluated in PI-RADS scoring, with the final pathology on prostatectomies.

Design: A two-year retrospective review was performed to include cases utilizing PI-RADS v2 resulting in prostatectomies. A total of 23 prostatectomy cases were retrieved, which utilized prostatic MRI as part of the management.

Results: The PI-RADS score on these cases ranged from 3-5, with the majority in the 4-5 category (15/23). The following parameters, evaluated and reported in the prostate MRI, were compared (Table 1)

Only 18.6% and 30% correlation was observed for size and laterality of tumor respectively, as compared to other parameters including SVI, EPE, and LNI which had a higher correlation. More extensive disease was identified on prostatectomies relative to that reported in MRI.

PARAMETERS	% CORRELATION	COMMENT
SIZE	18.6%*	25% overestimated by MRI 56% underestimated by MRI
LATERALITY	30%	70% unilateral by MRI More extensive disease on resection
SEMINAL VESICLE INVASION (SVI)	78%	1 false negative, 4 false positive
EXTRAPROSTATIC EXTENSION (EPE)	78%	5 false positive
LYMPH NODES INVOLVEMENT (LNI)	95.7%	1 false negative

*MRI and prostatectomy lesional size were considered correlated if the reported MRI size was within ± 20% of the lesional size in prostatectomy.

Conclusions: Overall, this study corroborates the utility of PI-RADS v2 in detecting, characterizing and stratifying patients for appropriate management, in constellation with other factors. Correlation of size and laterality of tumor is poor within our center, which may be operator dependent. Since both these factors are critical, additional larger studies from other institutions would be helpful in studying these parameters.

860 Does Anterior Versus Posterior Location of Tumor Nodules Influence the Likelihood of Adverse Outcomes at Radical Prostatectomy?

Amin Hayee[1], Isabella Lugo[2], Oleksandr Kryvenko[3]
[1]University of Miami/Jackson Memorial Hospital, Miami, FL, [2]University of Miami, Davie, FL, [3]University of Miami Miller School of Medicine, Miami, FL

Disclosures: Amin Hayee: None; Isabella Lugo: None; Oleksandr Kryvenko: None

Background: There are controversial reports in the literature regarding the significance of the location of tumor nodules (TN) in radical prostatectomy (RP) in respect to the likelihood of extraprostatic extension (EPE), seminal vesicle invasion (SV), and positive margin status (M+). We analyzed a large number of RPs controlled for other recognized factors associated with adverse outcomes.

Design: We analyzed 679 RP entirely submitted for histological examination. Each TN was mapped on the histological slides and separately graded, staged, and its volume was assessed by mm^2 x 4 (average gross section thickness) x 1.12 (shrinkage factor). The plane crossing the prostatic urethra was considered to differentiate anterior and posterior tumors. Each TN was used as an independent event. We first conducted a univariate analysis (Chi-square and t-test) between anterior and posterior TN and then included all significant variables in multivariate analysis (logistic regression model). Significance was considered at two-tailed p? 0.05.

Results: 24 cases there was extensive bilateral disease leaving 642 patients for analysis. 1,798 separate TN were scored with median of 3 TN per RP (range, 1-7). 2 TN were at the apex where the exact location was difficult to determine and 104 TN extended from posterior to anterior prostate. 1,692 TN were included in the total analysis. There were 604 anterior and 1088 posterior TN. 26 tumor nodules had M+ in the areas of intraprostatic incision and were excluded in the assessment of EPE (pT2+). In univariate analysis posterior tumor nodules were more likely to invade SV (4.3 vs 0.3%), have EPE (13.7 vs 7.7%), and were higher grade (all p<0.001). There was no difference in incidence of M+ (6.3% vs 6.1%, p=0.86) and tumor volume (TV) (mean, 0.7 vs 0.7 ml, p=0.97) between posterior and anterior TN. In a multivariate analysis controlled for GG and TV, the factors with the established correlation with the adverse RP outcomes, posterior TN location remained as an independent risk factor for EPE (OR=2.1, CI 1.2-3.5, p=0.006) and SV invasion (OR=28.5, CI 4.8-167.9, p<0.001).

Conclusions: Our analysis of a large group of patients with RP demonstrates that the location of the TN is an independent variable influential on the adverse RP outcomes such as EPE and SV invasion. These conclusions hold true when effects of TV and GG are accounted for. These findings may be useful in planning surgical management of patients with prostate cancer.

861 Neuroendocrine Acquisition in Naïve and Post-Therapy Recurrent Prostate Cancer as well as Lymph Node Metastasis

Grant Ho[1], Catherine Suen[2], Guang-Qian Xiao[1]
[1]Keck School of Medicine of University of Southern California, Los Angeles, CA, [2]Fullerton, CA

Disclosures: Grant Ho: None; Catherine Suen: None; Guang-Qian Xiao: None

Background: Neuroendocrine (NE) lesions of prostate are uncommon, and include prostate cancer (PCa) with NE differentiation and small cell PCa. These entities are thought to develop from conventional PCa trans-differentiation. Reports on the incidence of NE-PCa in various clinical settings are rare. The aim of this study is to investigate the occurrence of NE-PCa in naïve PCa with lymph node metastasis (LNM), and in recurrent PCa after androgen depletion therapy (ADT) or radiation therapy.

Design: Four TMAs were used in the study: 2 from specimens received during the past 12 months containing naïve PCa and LNM, and 2 from salvage prostatectomies received during the last 2 years containing recurrent Pca following ADT or radiation treatment. All specimens were from different patients seen at our hospital. NE differentiation was confirmed by immunohistochemistry with synaptophysin and/or chromogranin. Cases with <5% and >=5% NE cells were considered negative and positive, respectively. The cases were divided into 5 groups (Table 1). Data was analyzed using Chi square test.

Results: NE cells were uniformly present in scattered fashion in benign prostatic glands and always accounted for <1% of the epithelial cells. The incidence of conventional NE differentiation in post-ADT recurrent PCa (18%) was significantly higher than in other groups ($p<0.05$). There were a total of 8 small cell PCa, 3 of which (38%) developed after ADT and none (0%) of which developed after radiation (Table 1).

Table 1: Neuroendocrine prostate cancer in various clinical settings

	Non-NE	PCa with NE
Naïve PCa, Gleason 3 (n=45)	42 (93%)	3 (7%)
Naïve PCa, Gleason 4/5 (n=90)	82 (91%)	8 (9%)
Post radiation (n=43)	39 (91%)	4 (9%)
Post ADT (n=60)	49 (82%)	11 (18%)
Lymph node metastasis (n=38)	36 (95%)	2 (5%)
Benign glands (n=92)	92 (100%)	0
Small cell PCa (n=8)	3 (38%) occur after ADT, 5 (62%) without treatment history	

PCa, prostate cancer; NE: neuroendocrine, ADT: androgen depletion therapy

Conclusions: Isolated NE cells are typical in benign prostatic glands. Approximately 7-9% of naïve PCa had NE, which does not appear to correlate with PCa Gleason scores. Post-radiation NE differentiation shared similar incidence with naïve PCa, whereas post-ADT presented with significantly higher NE (9% vs 18%). Small cell PCa exhibited much stronger association with ADT (38%). The underlying mechanisms for strong association of NE with ADT are unknown, but is likely driven by selective pressure from androgen blockade; radiation is a relatively acute and less selective process. The incidence of NE in LNM was slightly lower than in naïve PCa, which may imply NE-PCa confers lower LNM potential. In summary, ADT significantly increases NE trans-differentiation in PCa, while radiation has minimal effect. NE-PCa is known to correlate with resistance to treatment, disease progression and poor prognosis. Knowing NE-PCa in these clinical settings has significant implication in patient management as well as future research direction.

862 Expanded Characterization of the Immune Microenvironment in High Grade Urothelial Carcinoma of the Bladder

Anjelica Hodgson[1], Achim Jungbluth[2], Nora Katabi[2], Bin Xu[2], Michelle Downes[3]
[1]University of Toronto, Toronto, ON, [2]Memorial Sloan Kettering Cancer Center, New York, NY, [3]Sunnybrook Health Sciences Centre, Toronto, ON

Disclosures: Anjelica Hodgson: None; Achim Jungbluth: None; Nora Katabi: None; Bin Xu: None; Michelle Downes: None

Background: Exact knowledge of the immune microenvironment in high grade urothelial carcinoma (HGUC) of the bladder is pivotal for the understanding of tumor biology and immunotherapy. Increasingly, these tumours are treated with immunotherapy including inhibitors of the PD-1/PD-L1 axis and vaccine strategies to cancer antigens offer additional immunotherapeutic options. Due to their presence in various

types of cancers and their lack of expression in normal tissues except testicular germ cells, Cancer Testis Antigens (CTAs), are considered promising cancer vaccine targets. However, little is known about the presence of CTAs in HCUC of the bladder and its inflammatory tumor environment. We sought to evaluate the in-situ protein expression of two CTAs (PRAME, CT10) in HGUC of the bladder, and to correlate these findings with immunological parameters (MHC I, PD-L1, PD-1, FOXP3 and CD8) and oncologic outcome.

Design: Clinicopathologic and follow up data was available for 207 cases of HGUC of the bladder. Triplicate TMAs were immunohistochemciallly analyzed for the expression of: CD8 and FOXP3 in lymphocytes, PD-1 in immune cells (IC), PD-L1 in tumour cells (TC) and IC, PRAME in TC, CT10 in TC, and MHC I in TC. Statistical analysis was performed.

Results: PRAME and CT10 expression were detected in 15.4% (31/201) and 20.9% (42/201) of cases, respectively. MHC I expression was decreased in 87.6% (177/202) of cases. Pearson correlation coefficient analysis demonstrated multiple significant correlations between parameters including PRAME and CT10 (correlation coefficient r=0.170), PRAME and FOXP3 (r=0.271), CT10 and PD-L1 in TC (r=0.153), CT10 and FOXP3 (r=0.284), and MHC I and PD-1 (r=0.162), PD-L1 in TC (r=0.214), PD-L1 in IC (r=0.235), FOXP3 (r=0.171), and CD8 (r=0.449). Expression of CT10 was associated with significantly decreased disease-specific survival (p = 0.007).

Conclusions: PRAME and CT10 are expressed in a subset of HGUC of the bladder, and may represent a potential therapeutic option. CTAs and MHC1 strongly correlate with other important immunological parameters in HGUC. The association of the expression of CT10 and PD-L1 suggests a role of CTAs in the response to PD-L1 treatment in HGUC.

863 Morphologic Features in Urothelial Carcinoma Correlate with Intrinsic Molecular Subtypes

Anjelica Hodgson[1], Stanley Liu[2], Danny Vesprini[3], Bin Xu[4], Michelle Downes[2]
[1]University of Toronto, Toronto, ON, [2]Sunnybrook Health Sciences Centre, Toronto, ON, [3]Sunnybrook Health Sciences Centre - University of Toronto, Toronto, ON, [4]Memorial Sloan Kettering Cancer Center, New York, NY

Disclosures; Anjelica Hodgson: None; Stanley Liu: None; Danny Vesprini: None; Bin Xu: None; Michelle Downes: None

Background: Mulitple groups have delineated the molecular subtypes of urothelial carcinoma of the bladder (UC); some of these subtypes can be identified using routine immunohistochemical stains. Recent work has shown that certain morphological characteristics of UC of the bladder correlate with the molecular subtypes of bladder cancer as determined by gene expression signatures. We sought to correlate specific morphological features of UC with immunohistochemically determined molecular subtypes of this tumor.

Design: A cohort of 207 cases of invasive high grade UC comprised the study cohort. Tissue microarray sections were stained with GATA3 and CK5/6 in order to determine the molecular subgroup to which each case belonged. The following parameters were recorded or evaluated for each case: stage, percentage of divergent differentiation, presence of carcinoma in situ (and presence of pleomorphic change in carcinoma in situ, if applicable), and presence of marked nuclear atypia in invasive component. Tissue microarray sections were also stained with Ki67 and the percentage of cells staining was recorded. The online TCGA database was used to establish a validation cohort. Statistical analysis was used for correlation.

Results: A total of 205 cases from our cohort were evaluable. Cases were classified into luminal and basal subgroups using GATA3 and CK5/6 immunohistochemistry; 167 cases were luminal (GATA3+, CK5/6-) while 29 cases were basal (GATA3-, CK5/6+). Double negative cases were excluded. The presence of divergent differentiation (p<0.001), carcinoma in situ (p=0.002), and marked nuclear atypia in the invasive component (p<0.001) all significantly differed between luminal and basal subgroups. Evaluation of the TCGA data showed that divergent differentiation (p < 0.001), significant nuclear atypia (p < 0.001), and stage (p = 0.008) differed significantly between luminal and basal molecular subgroups. Basal tumors showed increased Ki67% >50% (p=0.077).

Conclusions: We show here that several morphological features are more commonly identified in basal subgroup cases compared to luminal subgroups cases of high grade invasive UC. These findings are important as they may help to easily identify basal subgroup cases of high grade UC which have been shown to have a worse prognosis and differential response to traditional chemotherapeutic regimens compared to their non-basal counterparts.

864 Prostate Cancer Diagnosis and Quantification using AI-enabled Software (SW)

Wei Huang[1], Samuel Hubbard[1], Parag Jain[2], Ramandeep Randhawa[3]
[1]University of Wisconsin, Madison, WI, [2]Dhristi, Inc, Sunnyvale, CA, [3]PathomIQ, Hermosa Beach, CA

Disclosures: Wei Huang: None; Parag Jain: *Major Shareholder*, Dhristi Inc.; Ramandeep Randhawa: *Employee*, Dhirsti Inc. (PathomIQ Inc.)

Background: Morphology is the gold standard for prostate cancer diagnosis. Evaluation of H&E stained biopsy slides is a time-consuming process. High inter- over variability in Gleason scoring has been reported: 40% discordance between general and sub-specialty pathologists. Digital pathology has gradually gained foothold in pathology practice. Yet the problems associated with manual scoring and

quantification remain. A universal and standardized platform for Gleason grading and Gleason pattern (GP) quantification trained by GU pathologists is needed to achieve accurate and reproducible diagnosis.

Design: One thousand prostate biopsy cases, including all Gleason Grade Group (GGG) cancers were selected from the pathology archive at the University of Wisconsin-Madison, and were scanned with Aperio CS2 (Leica) at 40x to create digital slides (WSI). The slides were split into a training set and a test set. The training slides were then annotated by the GU pathologist (WH) to assemble a balanced dataset of varied morphologies, including GP3, GP4, GP5 cancer, high-grade prostatic intraepithelial neoplasia (HGPIN), perineural invasion (PNI), vessels and lymphocytes. The team used this data to train their deep learning architecture, which comprises multiple Deep Convolutional Neural Networks that are a combination of classification and segmentation networks. This architecture was fine-tuned to be sensitive to very small amounts of high grade cancer. The trained software auto-annotates the entire WSI into the various cancer and benign pattern groups, and provides summary statistics of Gleason score, quantification of cancer area, and the percentage of each cancer pattern. The software was validated on a test set of 200 biopsy slides spread over the various cancer grade groups to establish concordance with the GU pathologist (WH).

Results: At this stage, the AI-enabled software showed high efficiency and precision in cancer scoring and quantification: It takes one click, less than 3 minute to score and quantify cancer in a WSI using the software, even with minor reassigning Gleason pattern for a few acini by the user (Figure 1). The overall accuracy in Gleason scoring cancer is 95% (Figure 2).

Figure 1 - 864

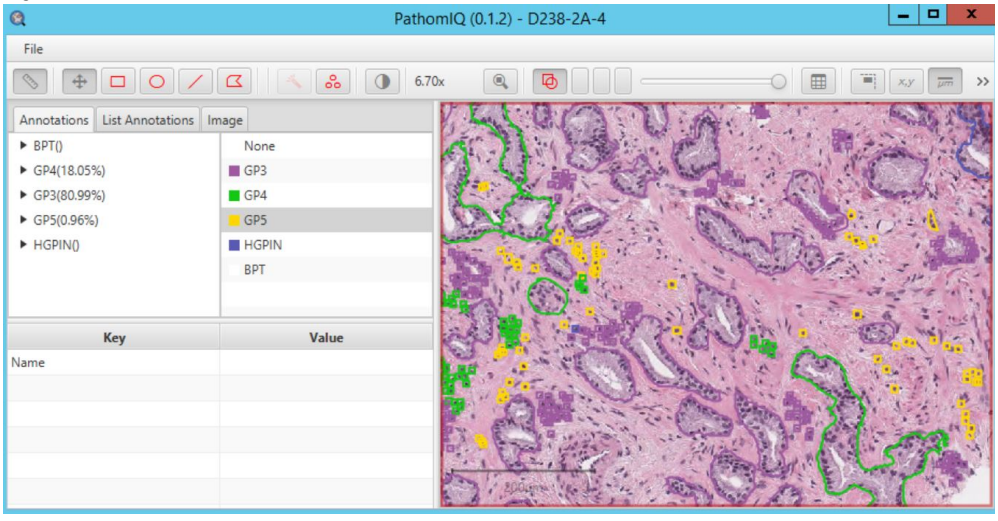

Figure 2 - 864

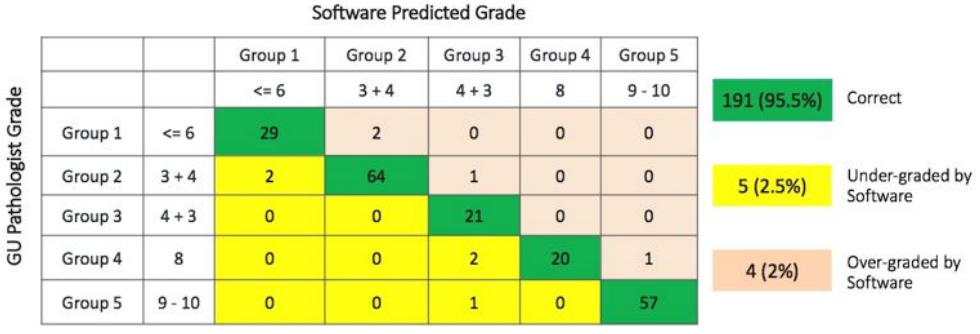

Conclusions: Deep learning enabled cancer-grading software offers objectivity, greater efficiency and precision in prostate cancer scoring and quantification. It has potential to help pathologists to minimize inter-observer variability and to increase efficiency in their practice.

865 Clinicopathologic Analysis of Bladder Cancer Involving Muscularis Mucosae or Smooth Muscle of an Indeterminate Type on Transurethral Resection Specimens

Michael Hwang[1], Bogdan Czerniak[1], Charles Guo[1]
[1]*The University of Texas MD Anderson Cancer Center, Houston, TX*

Disclosures: Michael Hwang: None; Bogdan Czerniak: None; Charles Guo: None

Background: Bladder urothelial carcinoma (UC) often invades smooth muscle tissue, including the muscularis mucosae (MM) and muscularis propria (MP). It is important to differentiate MM and MP involvement, as they are associated with different treatment and prognosis. However, in a small subset of cases, it may be difficult to determine whether the involved smooth muscle tissue in transurethral resection (TUR) specimens represents the MM or MP. We aimed to examine clinicopathologic features of bladder UC involving MM or smooth muscle of an indeterminate type (SMIT) in TUR specimens.

Design: We identified 103 consecutive cases of bladder TUR with UC that invaded either MM or SMIT. Patients with a prior history of MP invasion were excluded. The pathologic findings of all initial TURs and subsequent specimens were evaluated. Clinical outcomes were analyzed and compared with two control cohorts consisting of bladder UC invading the lamina propria (LP) (n=50) or MP (n=50).

Results: The patients included 85 men and 18 women with a mean age of 69 years (range 43-92). The initial TUR specimens showed MM (n=76) or SMIT (n=27) invasion. All patients received subsequent procedures, including TUR (n=82) and cystectomy (n=21), which revealed MP invasion in 36 patients. The interval between the initial and subsequent procedures had a median of 51 days. The lack of MP in the initial TUR specimens significantly increased the risk of MP invasion in the subsequent specimens (61% vs. 40%, p=0.049). SMIT invasion showed a significantly higher risk of MP invasion in the subsequent specimens than MM invasion (52% vs. 29%, p=0.038). The survival time of these patients was intermediate between those with MP invasion and LP invasion (Figure 1). Patients with MP invasion on the subsequent specimens showed comparable overall survival to the control cohort of MP invasion, whereas patients with no MP invasion showed similar survival to the control cohort of LP invasion (Figure 2).

Figure 1 - 865

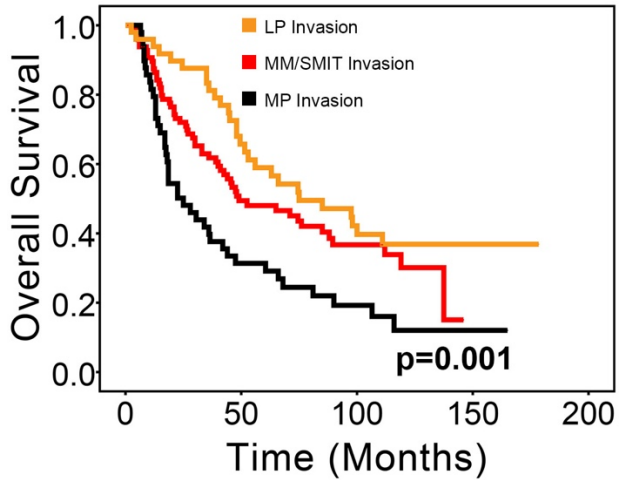

Figure 2 - 865

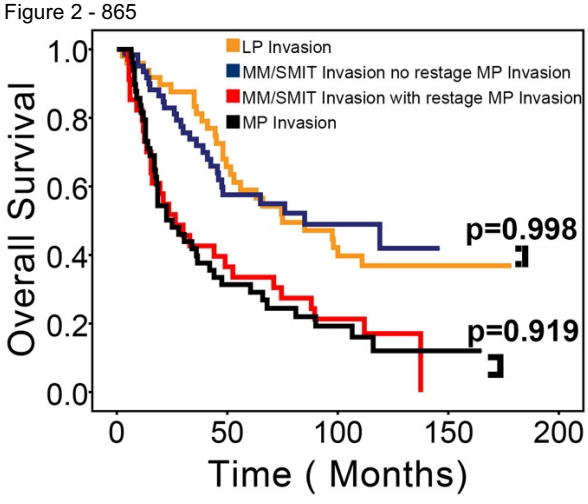

Conclusions: Bladder cancers invading the MM or SMIT on TUR specimens frequently demonstrate tumor upstaging in the subsequent specimens. The absence of MP in the initial TUR specimens is associated with a higher risk for tumor upstaging. Patients with SMIT invasion are more likely to develop MP invasion in the subsequent specimens than those with MM invasion. The patients show varied clinical outcomes, which highlights the importance of an immediate restaging procedure for accurate therapeutic and prognostic stratification.

866 Staging Post-Immunotherapy Renal Cell Carcinoma – Do conventional specimen Handling and AJCC Staging guidelines apply?

Michael Hwang[1], Kaleigh Lindholm[1], Rashmi Samdani[2], Pheroze Tamboli[1], Priya Rao[1]
[1]*The University of Texas MD Anderson Cancer Center, Houston, TX,* [2]*Georgetown University School of Medicine, California, MD*

Disclosures: Michael Hwang: None; Kaleigh Lindholm: None; Rashmi Samdani: None; Pheroze Tamboli: None; Priya Rao: None

Background: Newer immunotherapy agents, such as anti-PD1 (nivolumab) & anti-CTLA-4 (ipilimumab), have shown promising results in treating patients with advanced renal cell carcinoma (RCC). However, there are no standard guidelines for handling, reporting & staging of

post-nephrectomy specimens. Our study aims to highlight issues relating to conventional AJCC staging & specimen handling in a post-immunotherapy setting.

Design: 39 patients who received immunotherapy, followed by nephrectomy were included. Tumors were extensively sampled (2-3 sections/cm of T size), with extensive sampling of the sinus/perinephric fat. Percentage of viable residual tumor was estimated histologically by using a combination of gross & microscopic tumor burden. The change of tumor burden was determined radiographically by reviewing baseline & post-immunotherapy images. of the primaries & metastases.

Results: The pathologic findings & change of T burden are summarized in Figure1 & Table1. Identifiable therapy related changes included fibrosis, hyalinization, necrosis & inflammatory infiltrate associated with the tumor. 4 patients had gross pT3 disease, but showed only ypT0/ypT1 disease on microscopic examination. For this group, ypT stage was assigned based on the location & size of the residual viable tumor, and resulted in downstaging from the cT stage. 1 patient showed increase in the preop gross tumor size of 20% by imaging, without identifiable viable tumor microscopically (pseudoprogression). Patients staged as ypT3/ypT4 had wide range of viable tumor (5-95%) & change in tumor burden. There was correlation between percent viable tumor cells in the nephrectomy specimens & the change in the size of the metastatic foci (Figure 2).

pT stage post immunotherapy	No. of Cases	% Viable Tumor Cell in nephrectomy Mean (Range)	% Change of Tumor Burden in nephrectomy Mean (Range)
ypT0	2	0 (0)	-38 (-42 to -35)
ypT1	4	16 (5 to 30)	-36 (-64 to 0)
ypT3	30	61 (5 to 95)	-12 (-88 to 61)
ypT4	3	32 (5 to 70)	-24 (-29 to -20)

Figure 1 - 866

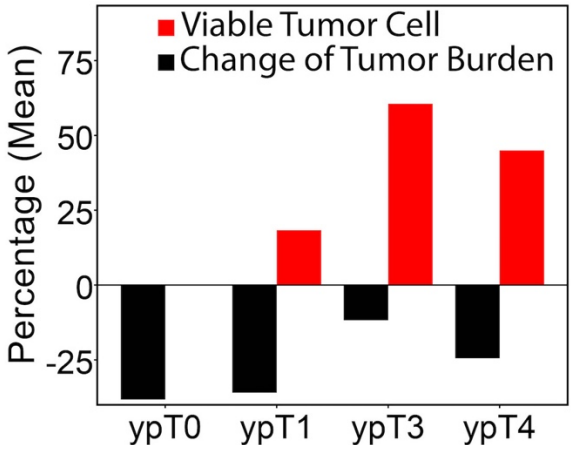

Figure 2 - 866

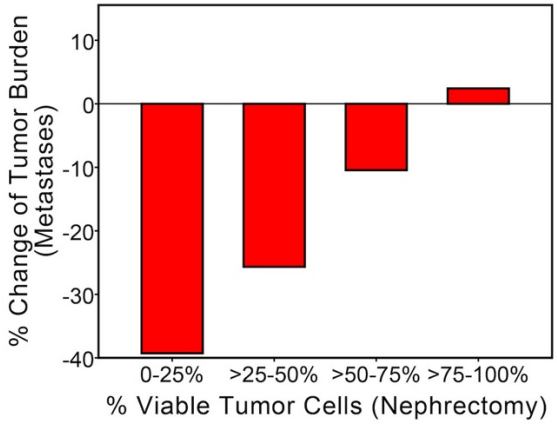

Conclusions: Post neoadjuvant gross T size does not accurately reflect true residual tumor burden. Increased tumor size may occasionally occur due to the presence of pseudoprogression & may be mistaken clinically as disease progression. We propose that the percentage of viable tumor cells, in addition to conventional AJCC staging may be a more accurate measure of tumor response. Standardized guidelines for handling of post immunotherapy specimens are needed. We suggest sampling a complete cross section of the tumor at its greatest dimension & additional sampling of viable appearing tumor, especially with sinus/fat. In discrepancies between the gross & microscopic pT sizes, pT stage should reflect the location & burden of the viable tumor as determined microscopically.

867 Prostatic Ductal Carcinoma Controlled for Cancer Grade, Tumor Volume (TV), And Tumor Nodule (TN) Location Does Not Have A Higher Likelihood of Seminal Vesicle (SV) Invasion Or Positive Margin (M+) But Is An Independent Predictor Of EPE At Prostatectomy (RP)

Oleksii Iakymenko[1], Amin Hayee[2], Isabella Lugo[3], Merce Jorda[4], Oleksandr Kryvenko[4]
[1]Jackson Memorial Hospital, Miami, FL, [2]University of Miami/Jackson Memorial Hospital, Miami, FL, [3]University of Miami, Davie, FL, [4]University of Miami Miller School of Medicine, Miami, FL

Disclosures: Oleksii Iakymenko: None; Amin Hayee: None; Isabella Lugo: None; Merce Jorda: None; Oleksandr Kryvenko: None

Background: Prostatic ductal adenocarcinoma (PDA) is a less frequent variant of prostate cancer. In prior studies PDA was reported to be associated with a higher likelihood of negative outcome at RP. We conducted a study where we controlled the effect of the presence of PDA on adverse RP outcome by Grade Group (GG), TV, and location of TN.

Design: We reviewed all cases with PDA and culled a large control group without PDA. All RP were entirely submitted for histological examination. Each tumor nodule was mapped, staged and its volume was assessed by formula mm2 x 4 (average gross section thickness) x 1.12 (shrinkage factor). First, we conducted a univariate analysis to assess correlation of PDA with age, prostate weight (PW), TV, tumor location, GG, extraprostatic extension (EPE), M+, and SV invasion. We then conducted a multivariate analysis of effect of PDA on EPE, M+, and SV invasion controlled for variables significant in univariate analysis.

Results: PDA was present in 41 of 1288 continuous men who underwent RP. 41 PDA cases and 638 continuous controls were analyzed. PDA was always present in 1 TN per RP. In 1 case PDA was present in a 3 ml GG3 TN with EPE and there was a 0.29 ml GG5 TN without PDA. In another case PDA was present in an organ confined 0.6 ml GG4 TN and separate 0.17 ml GG3 TN had EPE. In the remaining 39 cases PDA was present in the dominant TN determined by grade, stage, and volume. Overall, there were 1848 separate tumor nodules. In 192 TN (1 PDA and 191 not) there was intraprostatic incision and the presence of EPE could not be assessed (pT2+). PDA was not linked to PW (median, 47.5 vs 45 gm, p=0.8). PDA was seen in older men (median, 66 vs 63, p=0.04), higher GG when GG1 was or was not included (both p<0.001), larger tumor nodules (median, 3.13 vs 0.14 ml, p<0.001), and TN with PDA were more likely to be posterior or extend from posterior to anterior than to be anterior (p<0.001). PDA was significantly linked to EPE (29/40 vs 222/1764), SV invasion (11/41 vs 61/1807), and M+ (13/41 vs 142/1807), all p<0.001. In multivariate analysis, PDA lost its effect on SM+ (OR=0.97, p=0.9) and SV invasion (OR=1.69, p=0.27), but remained an independent predictor of EPE (OR=2.3, p=0.04).

Conclusions: We demonstrate that PDA controlled for other variables associated with adverse outcome at RP remains an independent predictor of EPE but loses its association with M+ and SV invasion. These observations may be useful for surgical planning in patients with PDA diagnosed on needle biopsy.

868 Forkhead Box O1 (FOXO1), as a Predictor for Recurrence of Non-Muscle-Invasive Tumor and Progression of Muscle-Invasive Tumor as Well as Chemosensitivity, Is Inactivated in Bladder Cancer

Hiroki Ide[1], Satoshi Inoue[2], Guiyang Jiang[2], Taichi Mizushima[2], Alexander Baras[3], George Netto[4], Hiroshi Miyamoto[2]
[1]Keio University, Tokyo, Japan, [2]University of Rochester, Rochester, NY, [3]Baltimore, MD, [4]University of Alabama at Birmingham, Birmingham, AL

Disclosures: Hiroki Ide: None; Satoshi Inoue: None; Guiyang Jiang: None; Taichi Mizushima: None; Alexander Baras: None; George Netto: None; Hiroshi Miyamoto: None

Background: A transcription factor FOXO1 is known to function as a tumor suppressor in several types of malignancies. However, its roles in the outgrowth of bladder cancer as well as sensitivity to chemotherapy remain poorly understood. The current study aimed to determine the expression status of FOXO1 and an inactivated form, phospho-FOXO1 (pFOXO1), in bladder cancer, and its prognostic significance.

Design: We immunohistochemically stained for FOXO1 and pFOXO1 in bladder tumor and paired non-neoplastic bladder tissue specimens as well as in muscle-invasive bladder cancer specimens from 43 patients who received at least 3 cycles of cisplatin + gemcitabine neoadjuvant chemotherapy prior to radical cystectomy.

Results: FOXO1 and pFOXO1 were positive in 13% and 55% of 129 bladder tumors, which were significantly lower and higher than in benign urothelial tissues [40% (*P*<0.001) and 24% (*P*<0.001)], respectively. Twelve (24%) low grade tumors *vs.* 5 (6%) high grade urothelial carcinomas (*P*=0.005) and 16 (21%) non-muscle-invasive tumors *vs.* 1 (2%) muscle-invasive carcinomas (*P*=0.002) were immunoreactive for FOXO1. There were no statistically significant associations between pFOXO1 positivity and tumor grade or pT stage. However, pFOXO1 expression was significantly higher (*P*=0.020) in lymph node-positive muscle-invasive tumors [11 (85%) of 13] than in lymph node-negative muscle-invasive tumors [17 (47%) of 36]. A negative correlation (*P*=0.005) between FOXO1 *vs.* pFOXO1 was also found. Kaplan-Meier and log-rank tests revealed that patients with FOXO1-negative non-muscle-invasive tumor and pFOXO1-positive muscle-invasive tumor had significantly higher risks of tumor recurrence (*P*=0.016) and progression (*P*=0.041), compared to those with FOXO1-positive non-muscle-invasive tumor and pFOXO1-negative muscle-invasive tumor, respectively. Multivariate Cox model showed

significance in FOXO1 negativity (HR=7.813, 95%CI=1.064-58.824, *P*=0.043) as an independent predictor for tumor recurrence in patients with non-muscle-invasive tumor. Additionally, in a separate set of tissue specimens, 12% *vs.* 8% (FOXO1; *P*>0.1) and 41% *vs.* 69% (pFOXO1; *P*=0.068) were positive in responders *vs.* non-responders to chemotherapy, respectively.

Conclusions: FOXO1 is likely to be inactivated in bladder cancers, especially potentially aggressive tumors. Our results also suggest that FOXO1 negativity and pFOXO1 positivity predict the recurrence of non-muscle-invasive tumor and progression/chemoresistance of muscle-invasive tumor, respectively.

869 Large Cell Calcifying Sertoli Cell Tumor: a Single Institutional Study of 13 Cases

Muhammad Idrees[1], Khaleel Al-Obaidy[1], David Grignon[1], Thomas Ulbright[1]
[1]Indiana University School of Medicine, Indianapolis, IN

Disclosures: Muhammad Idrees: None; Khaleel Al-Obaidy: None; David Grignon: None; Thomas Ulbright: None

Background: Large cell calcifying Sertoli cell tumor (LCCSCT) is a rare testicular tumor that was first described in 1980 and later found to be a component of the Carney complex. We herein present a series of 13 cases.

Design: Thirteen LCCSCTs were found in our institutional records between 2000 and 2017. H&E slides for 11 cases were available. The morphologic features were reviewed. Follow-up information was obtained from physicians' notes.

Results: The mean age and size were 22 years and 2.3 cm (range, 2-40 years and 0.7-5.1 cm, respectively). One was diagnosed following trauma and another during evaluation for precocious puberty. The others presented as masses. The tumors were predominantly right-sided (n=8). None were bilateral. On follow-up, 7 had no evidence of disease; 1 developed widespread metastases and died within 6 months of diagnosis, and 5 were lost to follow-up. Microscopically, 12 cases were limited to testis, while 1 grew within the rete testis. All tumors showed a multinodular-pattern with frequent lymphoid aggregates. Two were multifocal. Within the nodules there were nests and trabeculae of tumor cells interspersed by hypocellular, frequently myxoid stroma with conspicuous neutrophils (n=10). A variable number of lamellated calcifications was noted (n=10). The cells were predominantly polygonal, with pale, eosinophilic cytoplasm, and round, mildly pleomorphic nuclei with prominent nucleoli. Spindle-cell-morphology represented a minority (<5%) of the cellular population in 10 cases but was a conspicuous finding in one. In this case, spindle cells occupied 60-70% of the tumor, with accompanying high-grade nuclei. This case was the one that showed malignant behavior.

Conclusions: LCCSCT is a rare tumor that occurs most frequently in young adults. Although most cases behave in a benign fashion, uncommon tumors behave aggressively. A conspicuous proportion of spindle tumor cells merits further investigation as a potential adverse histologic finding.

870 Fluorescent in Situ Hybridization (FISH) Analysis for 12p Alterations in Sarcomatoid Yolk Sac Tumor.

Muhammad Idrees[1], Thomas Ulbright[1], Jonathan Epstein[2]
[1]Indiana University School of Medicine, Indianapolis, IN, [2]Johns Hopkins Medical Institutions, Baltimore, MD

Disclosures: Muhammad Idrees: None; Thomas Ulbright: None; Jonathan Epstein: None

Background: Sarcomatoid neoplasms in patients with testicular germ cell tumors (TGCTs) are a common form of "somatic-type malignancy." There is support, based on morphology and immunohistochemistry that many such sarcomatous tumors show yolk sac tumor differentiation. A virtually universal chromosomal anomaly in TGCTs is increase in 12p copy number, often in the form of isochromosome 12p [i(12p)]. Since molecular alterations especially overrepresentation of 12p are not well documented in sarcomatoid YST, we sought to investigate the occurrence of overrepresentation of 12p in sarcomatoid YST by fluorescent in situ hybridization (FISH).

Design: Patients with testicular GCTs who developed sarcomatoid YST during the course of their disease were identified from the institutional electronic databases between 1994 and 2018. We performed interphase FISH assay for detection of increased 12p copy number in germ cell tumors using a bacterial artificial chromosome–derived probe localized to 12p12.1 and a commercially available centromeric probe. 16 formalin-fixed, paraffin-embedded specimens from 16 patients, along with normal controls, were studied. Overrepresentation of 12p was expressed as a ratio between the number of signals for 12p and the number of signals for centromere 12. A ratio equal to or higher than 1.3 was considered overrepresentation.

Results: All cases were postchemotherapy recurrences or metastasis. Ages ranged 22-38 years (mean 35.9). Most tumors (12/16) showed myxoid stroma and 10 of 16 were high grade. 13 of 16 specimens showed overrepresentation of 12p by the above criteria. Two cases exhibited loss of 12p and one case indicated gain of a whole chromosome 12 (trisomy 12).

Conclusions: As in other germ cell tumors, sarcomatous differentiation of YST demonstrates 12p alterations that can be identified by interphase FISH. Apart from 12p overrepresentation, these tumors may exhibit loss of 12p or even gain of an entire chromosome 12 (trisomy 12). These alterations may occur as a result of accumulating further mutations and may provide insight into tumor progression. Increase in 12p copy number of a sarcomatous neoplasm provides support for sarcomatoid YST in clinically ambiguous settings, (i.e.- late recurrence, unknown history, etc.).

871 H-TERT Immunohistochemical Staining in Urothelial Cells: A Marker for Malignancy?

Dorian Infantino[1], Rajiv Dhir[2], Juan Xing[3], Gabriela Quiroga[4], Sheldon Bastacky[4]
[1]Ridgewood, NJ, [2]UPMC, Shadyside, Pittsburgh, PA, [3]UPMC Shadyside Hospital, Pittsburgh, PA, [4]University of Pittsburgh Medical Center, Pittsburgh, PA

Disclosures: Dorian Infantino: None; Rajiv Dhir: None; Juan Xing: None; Gabriela Quiroga: None; Sheldon Bastacky: None

Background: Telomerase reverse transcriptase (hTERT) is an enzyme involved in the oncogenesis of urothelial carcinoma. Studies have shown that hTERT expression in mature urothelial cells indicates an increased chance of urothelial carcinoma. We evaluated hTERT expression in 45 specimens using commercially available anti-hTERT antibody in order to assess hTERT staining patterns in different diagnoses of the urogenital tract.

Design: Unstained paraffin-embedded slides were prepared from 45 urothelial specimens with different diagnoses [9 reactive urothelium (RU), 11 high grade urothelial carcinoma (HGUC), 11 carcinoma in situ (CIS), 7 urothelial dysplasia (UD), and low grade urothelial carcinoma (LGUC)] and were stained using anti-hTERT antibody (SCD-A7). The original H&E slides and stained slides were reviewed by 2 genitourinary pathologists independently. The interpretation results were compared between the 2 reviewers and any discrepancies were resolved during consensus conference. A composite staining score was given ranging from 0-300 for each case based upon hTERT staining intensity and percentage positivity (3+%x3 + 2+%x2 + 1+%x1). Patient demographics, staining pattern, staining intensity and diagnoses were recorded in a spreadsheet.

Results: Using staining intensity (0-3+) and percentage positivity for each intensity (0-100%), an average composite staining score and staining range was calculated for each of the 5 diagnostic categories: RU 166 (85-280), HGUC 164 (85-270), CIS 180 (95-295), UD 176 (110-300), LGUC 165 (100-295). All diagnostic groups showed positive staining and each diagnostic group showed similar average composite staining scores (166, 164, 180, 176, 165) and staining ranges (85-280, 85-270, 95-295, 110-300, 100-295).

H-TERT Immunohistochemical Staining Pattern and Composite Staining Score in 45 Urothelial Specimens							
UROTHELIAL SPECIMEN	DIAGNOSIS	UROTHELIUM STAINING 0+ (%)	UROTHELIUM STAINING 1+ (%)	UROTHELIUM STAINING 2+ (%)	UROTHELIUM STAINING 3+ (%)	COMPOSITE STAINING SCORE	AVERAGE COMPOSITE STAINING SCORE
1	Reactive urothelium	5	0	90	5	195	166 RANGE 85-280
2	Reactive urothelium	5	0	5	90	280	
3	Reactive urothelium	10	10	80	0	170	
4	Reactive urothelium	20	75	5	0	85	
5	Reactive urothelium	0	0	100	0	200	
6	Reactive urothelium	5	90	5	0	100	
7	Reactive urothelium	5	5	90	0	185	
8	Reactive urothelium	5	15	80	0	175	
9	Reactive urothelium	10	80	10	0	100	
10	HGUC	5	90	5	0	100	164 RANGE (85-270)
11	HGUC	5	90	0	5	105	
12	HGUC	30	60	0	10	90	
13	HGUC	5	10	80	5	185	
14	HGUC	20	75	5	0	85	
15	HGUC	0	0	50	50	250	
16	HGUC	20	10	60	10	160	
17	HGUC	5	0	15	80	270	
18	HGUC	0	0	90	10	210	
19	HGUC	0	0	95	5	205	
20	HGUC	10	40	50	0	140	
21	CIS	0	0	100	0	200	180 RANGE (95-295)
22	CIS	0	0	100	0	200	
23	CIS	0	0	90	10	210	
24	CIS	5	0	75	20	210	
25	CIS	5	95	0	0	95	
26	CIS	20	10	70	0	150	
27	CIS	5	0	5	90	280	
28	CIS	0	0	5	95	295	
29	CIS	10	15	0	75	240	
30	CIS	90	10	0	0	10	
31	CIS	15	85	0	0	85	
32	DYSPLASIA	5	0	95	0	190	176 RANGE (110-300)
33	DYSPLASIA	0	0	100	0	200	
34	DYSPLASIA	10	10	80	0	170	
35	DYSPLASIA	10	30	60	0	150	
36	DYSPLASIA	0	90	10	0	110	
37	DYSPLASIA	0	90	10	0	110	
38	DYSPLASIA	0	0	0	100	300	
39	LGUC	0	0	5	95	295	165 RANGE (100-295)
40	LGUC	10	75	15	0	105	
41	LGUC	10	60	30	0	120	
42	LGUC	5	90	5	0	100	
43	LGUC	0	15	80	5	190	
44	LGUC	15	15	70	0	155	
45	LGUC	10	0	80	10	190	

HGUC = High grade urothelial carcinoma, CIS = Carcinoma in situ, LGUC = Low grade urothelial carcinoma,
Composite Staining Score = [(3+% X 3) + (2+% X 2) + (1+% X1)]

Conclusions: Interpretation of hTERT staining is challenging due to nuclear staining variability in urothelial cells of the same diagnostic category. Thus, we used a composite staining score to differentiate hTERT staining characteristics of different urothelial diagnoses. Though positive hTERT staining has been shown to have an association with urothelial carcinoma in both cytologic and histologic specimens, our study demonstrates an indistinguishable composite staining score amongst urothelial histologic specimens with different diagnoses owing to non-specific nuclear staining of similar intensity amongst the various diagnostic categories.

872 Expression of ERK/ATF2 Signaling Pathway Proteins in Bladder Cancer as Prognosticators

Satoshi Inoue[1], Guiyang Jiang[1], Taichi Mizushima[1], George Netto[2], Hiroshi Miyamoto[1]
[1]University of Rochester, Rochester, NY, [2]University of Alabama at Birmingham, Birmingham, AL

Disclosures: Satoshi Inoue: None; Guiyang Jiang: None; Taichi Mizushima: None; George Netto: None; Hiroshi Miyamoto: None

Background: ATF2, a transcriptional factor generally activated by its phosphorylation in response to phospho-ERK (pERK) signals, has been shown to function via homo- or hetero-dimerization with oncogenic molecules, such as Jun and Fos, and thereby contribute to the outgrowth of various malignancies. However, the role of ATF2 in urothelial cancer remains poorly understood. The current study aimed to determine the expression status of ATF2, phospho-ATF2 (pATF2), and pERK in bladder cancer and its prognostic significance.

Design: We immunohistochemically stained for ATF2/pATF2/pERK in 129 bladder tumor and paired non-neoplastic bladder tissue specimens. We then evaluated the relationship between the expression of each protein and clinicopathological features of our patient cohort.

Results: ATF2/pATF2/pERK were positive in 84% (26% 1+, 49% 2+, 9% 3+)/32% (32% 1+)/26% (18% 1+, 6% 2+, 2% 3+) of tumors, which were significantly (all $P<0.01$) higher than in non-neoplastic urothelial tissues [64% (32% 1+, 28% 2+, 4% 3+)/2% (2% 1+)/10% (9% 1+, 1% 2+)]. The rate of moderate (2+) to strong (3+) ($P=0.011$) or strong ($P=0.028$) ATF2 expression was significantly higher in high grade tumors (67% or 14%) than in low grade tumors (44% or 2%). Positivity ($P=0.050$) or moderate/strong positivity ($P=0.068$) of ATF2 also tended to be more often seen in muscle-invasive tumors (92% or 69%) than in non-muscle-invasive tumors (78% or 52%). However, there were no significant associations between pATF2/pERK expression and tumor grade or pT stage as well as between ATF2/pATF2/pERK expression and pN status. In tumors, the expression levels of pATF2 versus pERK were correlated (correlation coefficient=0.449, $P<0.001$). Kaplan-Meier analysis revealed significant associations between ATF2(2+/3+) versus the recurrence of low grade tumors ($P=0.034$) as well as pATF2/pERK positivity versus disease progression ($P=0.004$/$P=0.017$) or cancer-specific mortality ($P<0.001$/$P=0.004$) in patients with muscle-invasive tumor. Multivariate analysis further identified ATF2 [hazard ratio (HR)=2.956, $P=0.045$] and pATF2 (HR=2.665, $P=0.025$ for progression; HR=4.271, $P=0.002$ for mortality) as independent prognosticators in patients with low grade and muscle-invasive tumors, respectively.

Conclusions: ATF2 is likely to be activated in bladder cancers, which may result in the promotion of tumor outgrowth. Our findings also suggest that ATF2 and pATF2 precisely predict the recurrence of low grade tumors and the progression of muscle-invasive tumors, respectively.

873 Revisiting Prognostic Significance of Clinicopathological Features in Type 1 Papillary Renal Cell Carcinoma

Liwei Jia[1], Paari Murugan[2], Hikmat Al-Ahmadie[1], Samson Fine[1], Anuradha Gopalan[1], S. Joseph Sirintrapun[1], Satish Tickoo[3], Ying-Bei Chen[1], Victor Reuter[1]
[1]Memorial Sloan Kettering Cancer Center, New York, NY, [2]University of Minnesota, Minneapolis, MN, [3]New York, NY

Disclosures: Liwei Jia: None; Paari Murugan: None; Hikmat Al-Ahmadie: None; Samson Fine: None; Anuradha Gopalan: None; S. Joseph Sirintrapun: None; Satish Tickoo: None; Ying-Bei Chen: None; Victor Reuter: None

Background: Morphological heterogeneity is not uncommonly seen in papillary renal cell carcinoma (PRCC) with a variable proportion of type 1 and type 2 features. We sought to perform a detailed study of a large cohort of PRCC with the WHO-defined type 1 features, emphasizing clinicopathological features, including morphology, progression-free, cancer-specific survival and molecular alterations.

Design: All nephrectomies with a final diagnosis of PRCC with type 1 feature were retrospectively identified (1998-2005). All significant clinicopathological characteristics were thoroughly evaluated. In a selected subset of cases with distinct regions of type 1 and type 2 features, molecular alterations were investigated using a next-generation sequencing (NGS) platform.

Results: A total of 199 cases were retrieved for the study. The median age was 65 years (range 37-84 years), with a male to female ratio of 5:1 and a median size of 3.5 cm (range 1.2-15.2 cm). At presentation, 120 (60%) patients were staged pT1, 61 (31%) pT2 and 18 (9%) pT3. By univariate analysis, age at treatment, tumor size, mitotic rate, lack of circumscription, presence of macrophages, percentage of sarcomatoid architecture or solid architecture, and lymphovascular invasion were significantly associated with cancer-specific survival rates (p=0.048, 0.001, <0.0001, 0.0001, 0.035, <0.0001, 0.046 and <0.0001, respectively). A varying proportion of areas with type 2 features (range 1-98%, median 25%) was present in 95 (48%) tumors. Progression-free survival and cancer-specific survival showed no significant association with the presence of type 2 features (p=0.3 and 0.3, respectively). However, predominant (>50%) high ISUP nucleolar grades (grade 3-4) were significantly associated with adverse clinical outcome (p = 0.024). The mutation analysis of a subset of cases (n=12) demonstrated shared somatic mutations between distinct regions of type 1 and type 2 features in all 12 (100%) cases. The shared mutations accounted for 83% of all detected somatic mutations and included *NFE2L2* in 3 (25%) cases, *MET* in 2 (17%), *TERT* in 2 (17%), and *KRAS* in 1 (8%).

Conclusions: Predominant high nucleolar grades but not type 2 features were associated with adverse prognosis. Type 1 and type 2 areas demonstrated largely shared somatic mutations, consistent with clonal evolution.

874 Expression of Insulinoma-Associated Protein 1 (INSM1) in Small Cell Carcinoma of the Bladder

Liwei Jia[1], Ying-Bei Chen[1], Samson Fine[1], Anuradha Gopalan[1], S. Joseph Sirintrapun[1], Gopa Iyer[2], David Solit[1], Satish Tickoo[2], Victor Reuter[1], Hikmat Al-Ahmadie[1]
[1]Memorial Sloan Kettering Cancer Center, New York, NY, [2]New York, NY

Disclosures: Liwei Jia: None; Ying-Bei Chen: None; Samson Fine: None; Anuradha Gopalan: None; S. Joseph Sirintrapun: None; Gopa Iyer: None; David Solit: *Consultant*, Pfizer Inc.; *Consultant*, Loxo Oncology; *Consultant*, Illumina; Satish Tickoo: None; Victor Reuter: None; Hikmat Al-Ahmadie: None

Background: INSM1 has been recently identified as a sensitive marker of neuroendocrine differentiation, which can be readily investigated by immunohistochemistry (IHC). It has been studied in a number of neuroendocrine tumors from different organs but not in the urinary system. Small cell carcinoma of the bladder (SmCCB) is an aggressive variant of bladder cancer that is critical to differentiate from other high grade urothelial carcinomas (HG-UC) due to different treatment regimens. We aim to investigate the expression of INSM1 in a cohort of SmCCB and HG-UC and compare it to two commonly used neuroendocrine markers, synaptophysin and chromogranin.

Design: We identified 31 SmCCB (19 of which additionally contained conventional UC components) and 18 HG-UC without a small cell/high grade neuroendocrine component. We performed IHC for INSM1, chromogranin and synaptophysin and assessed their staining extent and intensity. The stains were assessed in both small cell/ high grade neuroendocrine and conventional UC areas in mixed cases.

Results: In SmCCB, INSM-1 showed strong nuclear staining in 30/31 (97%) cases, whereas cytoplasmic staining of synaptophysin or chromogranin was detected in 27 (87%) and 21 (68%), respectively. The extent of expression ranged from 1% to 100% for INSM1 (median 93%), 1%-100% for synaptophysin (median 80%) and 3%-100% for chromogranin (median 60%). Notably, INSM1 stained at least 60% of tumor cells in 25/31 (81%) cases, while synaptophysin in 16/27 (59%) and chromogranin in 11/21 (52%). There was focal INSM1 expression (3% and 5%, respectively) in the conventional UC component of 2 of the 19 cases (11%) with mixed components, while expression of both synaptophysin and chromogranin was detected (20%-30% of tumor cells) in 3 such cases (16%). Of the 18 HG-UC, INSM1 expression was identified in 3 cases (17%) with weak and focal staining (5%-20% of tumor cells, median 5%), one of which was positive for both synaptophysin and chromogranin (5% of tumor cells, each).

Conclusions: In this study focused on small cell/neuroendocrine tumors of the bladder, INSM1 proved a more sensitive and specific marker of neuroendocrine differentiation, superior to synaptophysin and chromogranin in this setting. Additionally, it tends to be more diffusely expressed in SmCCB than either synaptophysin or chromogranin. Whether INSM1 can be used as a standalone first-line marker for neuroendocrine tumors of the bladder awaits further study in validation cohorts.

875 Expanding the Morphologic Spectrum of Sporadic Renal Cell Carcinoma (RCC) Harboring Somatic TSC or MTOR Alterations: Analysis of 8 Cases with Clear Cytoplasm and Leiomyomatous Stroma

Liwei Jia[1], Gowtham Jayakumaran[1], Hikmat Al-Ahmadie[1], Samson Fine[1], Anuradha Gopalan[1], S. Joseph Sirintrapun[1], Satish Tickoo[2], Victor Reuter[1], Ying-Bei Chen[1]
[1]Memorial Sloan Kettering Cancer Center, New York, NY, [2]New York, NY

Disclosures: Liwei Jia: None; Gowtham Jayakumaran: None; Hikmat Al-Ahmadie: None; Samson Fine: None; Anuradha Gopalan: None; S. Joseph Sirintrapun: None; Satish Tickoo: None; Victor Reuter: None; Ying-Bei Chen: None

Background: Recent studies have suggested somatic *TSC1*/*TSC2* mutations as the characteristic molecular alterations in eosinophilic solid and cystic (ESC) RCC, a sporadic counterpart of a subset of renal tumors encountered in tuberous sclerosis complex (TSC) patients. We have recently identified a group of sporadic RCC with eosinophilic and vacuolated cytoplasm but distinctive features from ESC that are driven by somatic *TSC2* or *MTOR* alterations (*AJSP* in press). These findings support the presence of sporadic RCCs characterized by somatic alterations in TSC1-TSC2 complex or mTOR pathway, however, the full morphologic spectrum remains undefined.

Design: We retrospectively identified 8 cases of sporadic RCCs with clear cytoplasm and leiomyomatous stroma in which a diagnosis of clear cell papillary, MiTF translocation, or TCEB1-mutated RCC had been excluded by histologic, immunohistochemical or molecular analysis. We examined the clinicopathologic and immunohistochemical features, as well as mutational and copy number alterations using a targeted next-generation sequencing (NGS) platform. Five patients also had independent clinical germline testing.

Results: Mean age was 55 years (22-76y) with a M:F ratio of 1:7. All patients had incidentally detected renal masses, solitary (n=6) or more than one (n=2). Germline testing (*TSC/VHL/FH*) was negative in all 5 patients consented, including one patient with 2 renal masses. At nephrectomy, tumor size ranged from 1.7 to 5 cm (median 2.4 cm), and 6 were pT1 and 2 pT3. At a median follow-up of 35.5 months (range 7-142), 6 (75%) had no evidence of disease and 2 (25%) developed metastasis. A variable proportion of fibromuscular stroma was

readily visible in all cases. The dominant growth pattern included papillary (n=3), solid (n=2), alveolar (n=2), and acinar (n=1). Tumor cells exhibited voluminous, clear cytoplasm with delicate thread-like eosinophilic strands and occasional eosinophilic globules. High nucleolar grade (3-4) was seen in 6 (75%). Immunostain for CK7 was positive in 8/8 (100%), CA-IX patchy or diffusely positive in 6/7 (86%) with variable box or cup-like pattern, and CD10 positive in 6/7 (86%). NGS (n=8) revealed mutually exclusive somatic *TSC1* mutations in 4 (50%) and *MTOR* mutations in 4 (50%). No *VHL* mutation, 3p loss, or trisomy 7/17 was identified.

Conclusions: The morphologic spectrum of sporadic RCC primarily driven by somatic alterations of *TSC* or *MTOR* also includes RCC with clear cytoplasm and leiomyomatous stroma.

876 Bladder Adenocarcinoma Lacks Mismatch Repair Deficiency and Infrequently Expresses PD-L1, with Implications in both Diagnosis and Therapeutics

Derek Jones[1], Carla Calagua[2], Donna Hansel[3], Jonathan Epstein[4], Huihui Ye[2]
[1]Beth Israel Deaconess Medical Center, Allston, MA, [2]Beth Israel Deaconess Medical Center, Boston, MA, [3]University of California, San Diego, La Jolla, CA, [4]Johns Hopkins Medical Institutions, Baltimore, MD

Disclosures: Derek Jones: None; Carla Calagua: None; Donna Hansel: *Advisory Board Member*, Genentech, Inc.; *Grant or Research Support*, Konica Minolta; *Consultant*, Taris; Jonathan Epstein: None; Huihui Ye: None

Background: Bladder adenocarcinoma (BAC) is an uncommon and highly aggressive malignancy. Currently, ?–catenin is the only useful immunostaining marker to distinguish BAC (non-nuclear staining) from secondary involvement by colorectal cancer (CRC), in which nuclear ? –catenin staining indicates WNT pathway activation in 80% of cases. In CRC, DNA mismatch repair (MMR) deficiency marks another molecular subtype that accounts for 15-20% of cases. Standard treatment of BAC includes surgery or radiotherapy, with the role of immunotherapy not defined given the absence of data from randomized clinical trials. Anti-PD-1/PD-L1 agents are effective in a significant proportion of patients with late-stage bladder urothelial carcinoma (BUC), with the response generally correlated with PD-L1 expression levels in tumor cells (TC) and tumor-infiltrating immune cells (IC). We examine MMR status and PD-L1 expression in BAC for the first time, to provide diagnostic tools and predict utility of anti-PD-1/PD-L1 therapeutics in this rare malignancy.

Design: Using tissue microarrays (TMAs) constructed from cases of invasive BAC gathered at the Johns Hopkins Hospital and the Cleveland Clinic from 1984 to 2007, we immunohistochemically examined a total of 43 cases of BAC for the expression of MSH2, MSH6, MLH1, and PMS2 mismatch repair proteins. We also immunohistochemically analyzed a total of 56 cases of BAC for PD-L1 expression in TC and IC. PD-L1 expression on TC and IC was scored on 4 levels: 0 (negative or < 1%), 1 (1-4%), 2 (5-24%), and 3 (?25%).

Results:
Results: Among 43 cases examined for expression of MMR genes, one case was excluded due to suboptimal staining and all the remaining 42 cases (100%) showed retained MMR gene expression. Among 56 cases of BAC examined for PD-L1 expression, only 2 (4%) cases displayed PD-L1 expression in TC, both at the level of TC3. A total of 36% of cases displayed PD-L1 expression in IC at the levels of IC1 (7%), IC2 (18%), and IC3 (11%), respectively.

Conclusions:
Our findings demonstrate uniformly intact MMR protein expression in BAC, indicating that a MMR panel can be combined with ?–catenin to distinguish BAC from secondary involvement by CRC. PD-L1 expression levels in BAC are markedly lower than what have been reported in BUC (13 - 47%), suggesting that PD-1/PD-L1 blockade would likely not be as effective in BAC compared to BUC. An expanded study using whole tissue sections is ongoing to validate these TMA-derived findings.

877 TP53 Missense Mutation is Associated with Increased Tumor-Associated T-cells in Primary Prostate Cancer

Harsimar Kaur[1], Jiayun Lu[2], Laneisha Maldonado[3], Logan Reitz[4], John Barber[2], Angelo De Marzo[1], Scott Tomlins[5], Corinne Joshu[2], Karen Sfanos[6], Edward Schaeffer[7], Tamara Lotan[6]
[1]Johns Hopkins University, Baltimore, MD, [2]Johns Hopkins Bloomberg School of Public Health, Baltimore, MD, [3]Johns Hopkins School of Medicine, Aguada, PR, [4]Johns Hopkins School of Medicine, Alpharetta, GA, [5]University of Michigan, Ann Arbor, MI, [6]Johns Hopkins School of Medicine, Baltimore, MD, [7]Northwestern University Feinberg School of Medicine, Chicago, IL

Disclosures: Harsimar Kaur: None; Jiayun Lu: None; Laneisha Maldonado: None; Logan Reitz: None; John Barber: None; Angelo De Marzo: None; Scott Tomlins: None; Corinne Joshu: None; Karen Sfanos: None; Edward Schaeffer: None; Tamara Lotan: None

Background: TP53 mutation, though rare in primary prostate cancer, is associated with adverse outcomes and lethal disease. The makeup of the tumor immune microenvironment may be associated with specific genomic alterations in the tumor and plays a key role in tumor progression and response to immunotherapy. We examined the association of tumor-associated T-cell density with *TP53* status in surgically treated primary prostate cancer.

Design: The association between T-cell density and p53 protein nuclear accumulation was evaluated in 3 independent tissue microarray cohorts, including one cohort of prostate tumors from grade-matched patients of European-American or African-American ancestry (n=391), a retrospective case-cohort of intermediate and high risk patients enriched for adverse outcomes (n=257), and a cohort of tumors with primary Gleason pattern 5 (n=77). p53 immunohistochemistry was performed using a genetically validated and sensitive and specific assay for detecting *TP53* missense mutations in a CLIA-accredited laboratory. Tumor-associated CD3+, CD8+ and FOXP3+ T-cell densities were assessed using validated automated digital image analysis.

Results: The presence of *TP5*3 missense mutation, indicated by p53 nuclear accumulation, was significantly associated with increased CD3+ T-cell density (median 341 vs. 231 CD3+ T cells/mm^2; p = 0.004) in the combined cohort of matched European-American and African-American ancestry patients. The same association between p53 and CD3+ T-cell density was present in patients of both ancestries when analyzed separately, despite the fact that p53 nuclear accumulation was less frequent among African-American tumors compared to European-American tumors (7% vs 3%, p=0.2). CD8+ and FOXP3 T-cell densities showed a similar trend in the combined cohort and both groups separately, though not all markers reached statistical significance. The validation cohorts of intermediate-high risk patients and primary Gleason pattern 5 patients corroborated the same association of increased CD3+ T-cell density with presence of p53 nuclear accumulation (median 416 vs 308 CD3+ T cells/mm2; p=0.006 and median 662 vs 344 CD3+ T-cells/mm2; p=0.01 respectively).

Conclusions: Our findings highlight that p53 nuclear accumulation and underlying TP53 mutation is associated with a unique tumor immune microenvironment. These findings may be relevant in future clinical trials of immunotherapy in prostate cancer.

878 Germline BRCA2 Mutation is not Associated with Increased Tumor-Infiltrating Lymphocytes in Primary Prostate Cancer

Harsimar Kaur[1], William Isaacs[2], Jessica Hicks[2], Angelo De Marzo[1], Emmanuel Antonarakis[2], Tamara Lotan[3]
[1]Johns Hopkins University, Baltimore, MD, [2]Johns Hopkins University School of Medicine, Baltimore, MD, [3]Johns Hopkins School of Medicine, Baltimore, MD

Disclosures: Harsimar Kaur: None; William Isaacs: None; Jessica Hicks: None; Angelo De Marzo: None; Emmanuel Antonarakis: None; Tamara Lotan: None

Background: *BRCA2* germline mutation in prostate cancer (PCa) is associated with an aggressive tumor phenotype. *BRCA1/2*-deficient ovarian and urothelial cancers are associated with increased tumor infiltrating lymphocytes (TIL) and these tumors, along with *BRCA2*-deficient PCa may be responsive to immune checkpoint inhibitors, similar to findings in mismatch repair (MMR)-deficient PCa. Herein, we explore the tumor microenvironment of primary PCa with *BRCA2* germline mutation.

Design: The association between T-cell density and *BRCA2* mutation status was evaluated in 17 primary PCa cases with pathogenic germline *BRCA2* mutations and 19 grade-matched *BRCA2* germline-proficient tumors. Standard histologic sections of the dominant tumor nodule were immunostained for CD8 and ERG and assessed for tumor-associated CD8+ T-cell densities using validated automated digital image analysis. The association between *BRCA2* status and CD8+ T-cell density was assessed using Mann-Whitney U test.

Results: ERG expression was observed in 29.4% (5/17) *BRCA2*-deficient patients and 38.9% (7/18) *BRCA2*-proficient patients (p=0.72). There was no association between *BRCA2* mutation status and CD8+ T-cell density (median 82 CD8+ cells/mm^2 in *BRCA2*-deficient vs 154 CD8+ cells/mm^2 in *BRCA2*-proficient patients; p=0.327). There was no association observed between CD8+ T-cell density and ERG status in the combined cohort (p=0.477) or when stratified by *BRCA2*germline status (p=0.368 in *BRCA2*-deficient PCa and p=0.787 in BRCA2 proficient PCa).

Conclusions: *BRCA2* mutation has been associated with increased mutational load and increased TILs in various other cancer types, however we find that *BRCA2* mutation is not associated with increased TIL density in primary PCa, a striking contrast with our previous findings in MMR-defiicent PCa. Ongoing clinical trials will determine whether these tumors may still be responsive to checkpoint inhibition.

879 Molecular Characterization of Prostate Carcinoma with Paneth Cell-like Neuroendocrine Differentiation

Harsimar Kaur[1], Iryna Samarska[2], Sanjana Murali[3], Juan Miguel Mosquera[4], Jonathan Epstein[5], Tamara Lotan[6]
[1]Johns Hopkins University, Baltimore, MD, [2]Johns Hopkins University School of Medicine, Maastricht University Medical Center, Maastricht, Netherlands, [3]Johns Hopkins University School of Medicine, Baltimore, MD, [4]Weill Cornell Medicine, New York, NY, [5]Johns Hopkins Medical Institutions, Baltimore, MD, [6]Johns Hopkins School of Medicine, Baltimore, MD

Disclosures: Harsimar Kaur: None; Iryna Samarska: None; Sanjana Murali: None; Juan Miguel Mosquera: None; Jonathan Epstein: None; Tamara Lotan: None

Background: Prostate carcinoma (PCa) with Paneth cell-like neuroendocrine differentiation represents a special variant of PCa with undetermined prognostic significance. Although some studies suggest that these tumors have a favorable prognosis, they have a high frequency of *AURKA* amplification, a finding associated with aggressive neuroendocrine PCa, such as small cell carcinoma (SCC). Since we have previously shown that SCC commonly harbors loss of the tumor suppressor genes *RB1* and *TP53,* as well as loss of androgen receptor (AR) expression, herein, we determined the frequency of these alterations in PCa with Paneth cell-like neuroendocrine differentiation.

Design: The molecular features of Paneth cell-like neuroendocrine differentiation were evaluated in 30 cases (mix of radical prostatectomies and biopsies), including 14 cases from Johns Hopkins Hospital, 8 cases from the Johns Hopkins uropathology consultation service and 8 cases from a previously published Weill Cornell Medicine cohort. Immunostaining for p53, cyclin D1 (shown previously to reflect Rb loss), PTEN and ERG were performed using genetically validated protocols. Ten cases with high Paneth-like cell count were co-labelled for AR and the neuroendocrine marker INSM1 by immunofluorescence.

Results: Overall, 28% (7/25) of PCa with Paneth cell-like neuroendocrine differentiation were Grade Group (GG) 1, 36% (9/25) were GG 2, 28% (7/25) were GG 3 and 8% were GG 4. One case was PIN-like ductal carcinoma and the remaining cases did not have a Gleason grade assigned. We did not see any evidence of Rb1 loss-of-function (intact cyclin D1 in 22/22 evaluable cases). *TP53* missense mutation, as measured by nuclear accumulation of p53 protein, was seen in 17% of evaluable cases (4/24). Interestingly, ERG protein expression was seen in only 13% (3/22) of cases in the tumor nodule containing the Paneth-like cells. INSM1 labeled Paneth-like cells and AR expression was distinctly lower in this population compared to surrounding usual-type PCa cells.

Conclusions: PCa with Paneth cell-like neuroendocrine differentiation molecularly resemble usual-type primary PCa more than SCC in that they are unlikely to show Rb1 loss-of-function and only rarely harbor *TP53* missense mutations. However, there is evidence of decreased androgen signaling based on low AR expression in the Paneth-like cells and tumors containing Paneth-like cells show a low prevalence of ERG expression in this series.

880 Intraductal Carcinoma of the Prostate Occurring in the Absence of High Grade Invasive Carcinoma Shows Unique Molecular Features

Francesca Khani[1], Sara Wobker[2], Jessica Hicks[3], Brian Robinson[1], Christopher Barbieri[4], Angelo De Marzo[5], Jonathan Epstein[6], Colin Pritchard[7], Tamara Lotan[8]
[1]Weill Cornell Medicine, New York, NY, [2]UNC Chapel Hill, Chapel Hill, NC, [3]Johns Hopkins University School of Medicine, Baltimore, MD, [4]Weill Cornell Medical College, New York, NY, [5]Johns Hopkins University, Baltimore, MD, [6]Johns Hopkins Medical Institutions, Baltimore, MD, [7]University of Washington, Seattle, WA, [8]Johns Hopkins School of Medicine, Baltimore, MD

Disclosures: Francesca Khani: None; Sara Wobker: None; Jessica Hicks: None; Brian Robinson: None; Christopher Barbieri: None; Angelo De Marzo: None; Jonathan Epstein: None; Colin Pritchard: None; Tamara Lotan: None

Background: Intraductal carcinoma of the prostate (IDC-P) is typically associated with invasive prostatic carcinoma (PCa) of high grade and stage. Although IDC-P is believed to represent retrograde spread of high grade PCa in most cases, we have collected a unique group of radical prostatectomies (RP) with IDC-P and no invasive cancer or only associated Grade Group 1 disease. In these rare IDC-P cases, we previously reported a low rate of ERG expression and a high rate of PTEN loss; in the current study, we performed a more comprehensive molecular characterization of IDC-P with targeted NGS and copy number alteration (CNA) analysis.

Design: In 7 RP cases with IDC-P and no high grade invasive PCa, DNA from areas of IDC-P was extracted from macrodissected FFPE tissue and analyzed for mutations by targeted NGS (UW-OncoPlex Large Panel) and for CNAs (Oncoscan CNV, Affymetrix). Comparison of the frequency of the types of molecular alterations observed to those in TCGA invasive cancers was performed using Fisher's exact test.

Results: By CNA analysis, 71% (5/7) of cases had copy number gains (*CCND1*), and/or losses of cell cycle genes (*RB1*, *CDKN2A*), 57% (4/7) of cases had *MYC* amplification, and 42% (3/7) had 8p deletions. In 71% (5/7) of cases, activating PI3K pathway alterations (by mutations of *AKT*, *PIK3CA,* or copy number loss involving *PTEN*) were identified. In 42% (3/7) of cases, oncogenic driver mutations in MAPK pathway genes (*MAP2K1*, *BRAF*, *KRAS*) were present, two of which are novel in PCa. Mutations in DNA repair genes (*BRCA2*-somatic, *CHEK2*-germline) were observed in two cases, and other known PCa mutations (*FOXA1*, *SPOP*, *CDK12*) were observed in three

cases. Oncogenic driver mutations occurring in the aforementioned MAPK and PI3K pathway genes were significantly enriched in this cohort, with 5 such mutations present in 57% (4/7) of cases, compared to 4.2% (14/333) in TCGA invasive PCa cases (p=0.0002).

Conclusions: IDC-P in the absence of invasive high grade PCa harbors a unique molecular profile. Alterations such as *MYC* amplification and those seen in PI3K pathway genes are typically seen in invasive high grade/stage PCa, suggesting that IDC-P may be a molecularly distinct precursor lesion to aggressive invasive disease, at least in a subset of cases. However, some of the oncogenic driver mutations we identified in these rare IDC-P cases are relatively unusual in invasive PCa, suggesting this may be a genetically unique non-invasive lesion and potentially therapeutically targetable.

881 Are we under staging clear cell renal cell carcinomas?

Yumi Kojima[1], Miao Zhang[2], Chad Hruska[3], Pheroze Tamboli[1]
[1]The University of Texas MD Anderson Cancer Center, Houston, TX, [2]The University of Texas MD Anderson Cancer Center, Bellaire, TX, [3]Tacoma, WA

Disclosures: Yumi Kojima: None; Miao Zhang: None; Chad Hruska: None; Pheroze Tamboli: None

Background: Renal cell carcinoma (RCC) >7cm, limited to the kidney, are staged as pT2. In our experience clear cell RCC (ccRCC) >7 cm are rarely confined to the kidney. We hypothesize that ccRCCs >7 cm are potentially pT3 tumors, and are under staged. We studied the likelihood of under-staging, and compared overall survival in patients staged as pT2 versus pT3.

Design: We identified 363 pT2 and pT3 ccRCC, received at our center between 1/2012 and 12/2015, from patients referred for further management. Tumor stage was determined after slide review and compared to the stage reported by the referring pathologist.

Results: Of 363 patients, 97 were women and 266 men. Average age 57 yrs (range: 28-84 yrs). The average tumor size: 10.2 cm (range 7.0-22.5 cm). Average nuclear grade 3. We were concordant with the referring pathologist in 245 (67%) pT3 tumors; and, concordant in 68 (19%) pT2. We upstaged 46 (13%) pT2 tumors to pT3 (perinephric fat invasion 17 [38%], renal sinus invasion 14 [31%], segmental branch of renal vein invasion 13 [27%], pelvicalyceal system invasion 1 [2%], and adrenal gland invasion 1 [2%]). 4 (1%) tumors were down-staged. Of 363 patients, 302 (83%) had metastatic disease at referral; 31 (9%) had no evidence of metastatic disease; follow up information was not available in 30 (8%). Average follow up time was 34.8 mo. (range: 1.2-207.6). 195 patients (56%) were alive at last follow up, 156 (44%) were deceased, and, survival status was unknown in 12. Of the upstaged cases (n:46); 40 (87%) patients had metastatic disease; average follow up was 42.7 mo (range: 2.4-154.8 mo); 27 (59%) were alive at the time of last follow up and 19 (41%) were deceased. The 5-year overall survival of upstaged patients was 59%. Potentially understaged tumors (n: 68) had average follow up of 45 mo (range: 1.2-200.4 mo); 39 (57%) patients were alive at the time of last follow up; 28 (41%) were deceased and 1 (2%) was lost to follow up. The 5-year overall survival was 60%.

Conclusions: In our study, ccRCCs staged as pT2 or pT3 had similar 5-year survival rates. This supports our hypothesis that pT2 ccRCC should be evaluated carefully as they may be pT3 tumors rather than pT2.

882 Classifying the Unclassified Renal Cell Carcinomas Using Next-Generation Sequencing Genomic Profiling

Qingnuan Kong[1], Ming Zhou[2]
[1]1.University of Texas Southwestern Medical Center 2.Qingdao Municipal Hospital, Dallas, TX, [2]Clements University Hospital, Dallas, TX

Disclosures: Qingnuan Kong: None; Ming Zhou: None

Background: Accurate classification of renal cell carcinoma (RCC) is critical for prognosis and therapy decision-making. However, approximately 5% of RCC remains unclassifiable after extensive diagnostic work-up. Genomic profiling by next-generation sequencing (NGS) promises high definition elucidation of the genetic pathways in the RCCs and therefore may help classify unclassified RCCs and identify potential therapeutic targets. We report our preliminary results of using NGS in the work-up of unclassified RCCs.

Design: Formalin-fixed and paraffin-embedded (FFPE) tissues from 4 unclassified RCCs were analyzed using a 1385 cancer-related gene panel in the CLIA certified laboratory at authors'institution. FFPE specimens are microdissected to enrich for tumor tissue before DNAseq and RNAseq. Greater than 94% of all exons in the panel have at least 100X coverage with mean coverage of ≥900X and the mutant allele frequency limit of detection for single nucleotide variants is 5%. Point mutations, insertions, deletions, splice site defects, mutation burden, gene fusions and translocations were identified. Alterations of pathways known to be involved in RCCs were used to aid the RCC classification.

Results: The pathological features, NGS findings, final classification based on NGS findings and potential therapeutic targets were summarized in Table.

Case #	Age/gender	Grade/stage	Morphology	IHC	NGS	Final Dx	Therapeutic targets
1	54/F	4/T3a	Nests/sheets with prominent nucleoli	CK/PAX8/ini-1/BAP1/FH+ CAIX/C-kit/GATA3-	PIK3CA c.3140A>G, FANCA c.3584G>A	Unclassified RCC	Copanlisib
2	64/M	3/T1b	Tubulocystic/papillae lined with clear cells	CK7/CAIX/AMACR+ Cathepsin/HMB45-	VHL c.341-2A>G APC c2507C>G	Clear cell RCC	TKIs
3	68/M	3/T3bM1	Compact nests with eosinophilic cytoplasm	CK/PAX8+ CK7/CK20/CAIX/GATA3/MelanA-	MET amplification	Papillary RCC	Crizotinib/cabozantinib
4	36/F	3/T2b	Solid/nests/cysts, epithelioid clear cells with eosinophilic cytoplasm	PAX8/AE1/SDHB+ CAIX-	MALAT1-TFEB fusion	TFEB translocation RCC	None

Conclusions: NGS is a powerful tool in dissecting the molecular pathways in renal carcinogenesis, and may aid tumor classification and therapeutic target identification.

883 KIF3B Expression in Primary and Metastatic Prostate Cancer

Oleksandr Kravtsov[1], Christopher Hartley[2], Kenneth Iczkowski[2]
[1]Medical College of Wisconsin Affiliated Hospitals, Milwaukee, WI, [2]Medical College of Wisconsin, Milwaukee, WI

Disclosures: Oleksandr Kravtsov: None; Christopher Hartley: None; Kenneth Iczkowski: None

Background: Kinesin family member 3B (KIF3B) is a microtubule motor kinesin, involved in regulating mitotic progression and intravasation of cancer cells for metastasis. Its inhibition by shRNA in an avian embryo model most strongly inhibited prostate cancer PC3 and other cancer cell vasculotropism and in mice, head/neck cancer cell metastasis (PMID:29904055, Nature Comm 2018). KIF3B was proposed as a potential therapeutic target to block cancer metastasis.

Design: Tissue microarrays from 71 prostatectomies plus unstained slides from 12 additional cases were stained with rabbit polyclonal KIF3B antibody (Biorbyt, clone orb184776) at 1:400 dilution. Each TMA case contained 3-4 punch cores of prostate cancer (PC) and 3-4 of matched benign prostate. Additional cases included 6 matched primary PC and lymph node (LN) metastases. 6 distant metastases were stained: liver (3 cases), bone (2 cases), and brain (1 case). Lymph node status was obtained from available pathology reports on 50 cases. Two observers scored cytoplasmic immunoreactivity (**Fig. 1**) from 0 (negative) to 3+ (strong and diffuse), including half-steps.

Results: The mean KIF3B stain value of 1.1 in PC was significantly higher than a value of 0.1 in benign prostate (p<0.001, Mann–Whitney U test). KIF3B expression was higher in PC with cribriform morphology (mean 1.6+) compared to non-cribriform PC (mean 1.0+, p=0.07, Mann–Whitney U test). KIF3b had ?1+ staining in 26/38 cases with known negative lymph nodes and 5/12 with positive lymph nodes (p=0.17, Fisher's exact test). Differences were not found by stage, or Grade group.

In additional cases with matched primary PC and LN metastases, KIF3b reactivity was negative in all 6 primary PCs and lymph node metastases, and all 6 distant metastases, except for two primary and two metastatic tissues with weak (0.5+) staining.

	Mean stain value	N (%)	p-value
Total PC	1.1	71 (100)	<0.01
Benign prostate	0.1	71 (100)	
Cribriform PC	1.6	8 (10.3)	0.07
Non-cribriform PC	1.0	70 (89.7)	
PC with LN metastases	<1	7 (14)	0.17
	1 or more	5 (10)	
PC in which LN were	<1	12 (24)	
without metastases	1 or more	26 (52)	

Figure 1 - 883

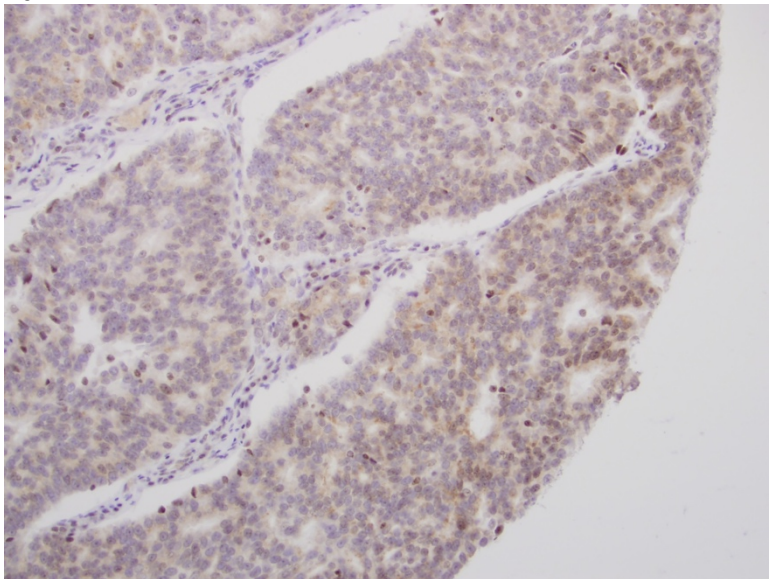

Conclusions: Although RNAi-mediated inhibition of KIF3B blocked metastasis of head/neck HEp3 tumor cells in mice, and in vitro migration of prostate cancer PC3 cells (PMID:29904055), KIF3B reactivity was not significantly altered in either the primary site of metastatic cases, or lymph node or distant metastases in our study. Cribriform morphology is a recognized adverse finding (PMID:28820750), and KIF3B expression had a nearly significant positive correlation with cribriform morphology, suggesting that KIF3B facilitates local aggressiveness.

884 Nephrogenic Adenoma Intermixed with Urothelial Carcinoma (UC) – A Potential Mimicker of Glandular Differentiation and Invasive Carcinoma

Oleksandr Kryvenko[1], Matthew Wasco[2], Sean Williamson[3]
[1]University of Miami Miller School of Medicine, Miami, FL, [2]St Joseph Mercy Hospital, Ann Arbor, MI, [3]Henry Ford Health System, Detroit, MI

Disclosures: Oleksandr Kryvenko: None; Matthew Wasco: None; Sean Williamson: None

Background: Nephrogenic adenoma (NA) is a relatively common urinary tract lesion, and is often present in patients with prior injury and disruption of the urothelial lining, leading to implantation of shed renal tubular cells in the urothelial mucosa. NA may demonstrate a spectrum of architectural and cytological features mimicking UC, adenocarcinoma (including clear cell adenocarcinoma), and invasion. However, admixed UC and NA has been minimally addressed in the current literature. We studied cases from 3 institutions where the NA was intimately intermixed with UC, potentially mimicking variant differentiation or invasion.

Design: Specimens from 21 patients were reviewed which had NA intermixed with UC. Patterns of NA were examined, and clinical implications of misdiagnosing NA as glandular differentiation of UC were estimated.

Results: There were 3 women and 18 men with median age of 72 years (range, 31-89). Fifteen patients underwent TURBT, 2 biopsy, 2 nephroureterectomy, 1 cystectomy, and 1 cystoprostatectomy for UC. All patients had prior manipulations related to their UC. Eight patients had high grade non-invasive papillary urothelial carcinoma, 4 had in situ carcinoma, 8 had invasive high grade urothelial carcinoma, and in one patient NA developed in a prior biopsy site. Nineteen cases had conventional NA, and in 2 cases fibromyxoid nephrogenic adenoma was infiltrated by UC. Classical NA had tubular and papillary architecture (11), tubular (6), and papillary (2). In 12 of 13 cases of non-invasive UC, nests of tubular NA were present in the lamina propria and could be considered invasive carcinoma if were interpreted as glandular differentiation, or other variants, such as small tubular UC. None of the cases demonstrated NA in detrusor muscle. PAX8 (16), racemase (6), and CK7 (3) highlighted NA. NA were negative for GATA3 (11), p53 (6), p40/p63 (7), and CK20 (4).

Conclusions: NA can occur concomitantly with high grade urothelial carcinoma (both non-invasive and invasive), expanding the spectrum of entities that must be considered in the differential diagnosis. The pattern of NA in most non-invasive cancers is such that invasive carcinoma with glandular or tubular differentiation may be considered. The differential diagnosis was indeed considered by the original pathologists performing GATA3, p53, and p40/p63 to rule out the possibility of urothelial carcinoma. Misinterpretation of NA in such setting may incorrectly convey a more aggressive biological potential of cancer to clinicians.

885 Clinicopathological Study of Seven Cases of ALK-positive Renal Tumor Identification of New Fusion Partners including CLIP1 and KIF5B Genes

Naoto Kuroda[1], Yajuan Liu[2], Maria Tretiakova[2], Monika Ulamec[3], Kengo Takeuchi[4], Christopher Przybycin[5], Cristina Magi-Galluzzi[6], Abbas Agaimy[7], Asli Yilmaz[8], Kiril Trpkov[9], Ondrej Hes[10]
[1]Kochi Red Cross Hospital, Kochi City, Japan, [2]University of Washington, Seattle, WA, [3]University Clinical Hospital Center Sestre Milosrdnice, Zagreb, Croatia, [4]Tokyo, Japan, [5]Cleveland Clinic, Cleveland, OH, [6]The University of Alabama at Birmingham, Birmingham, AL, [7]Erlangen, Germany, [8]Calgary Laboratory Services, Calgary, AB, [9]University of Calgary, Calgary, AB, [10]Biopticka laborator s.r.o., Plzen, Czech Republic

Disclosures: Naoto Kuroda: None; Yajuan Liu: None; Maria Tretiakova: None; Monika Ulamec: None; Christopher Przybycin: None; Cristina Magi-Galluzzi: None; Abbas Agaimy: None; Asli Yilmaz: None; Kiril Trpkov: None; Ondrej Hes: None

Background: *ALK-positive renal tumor has been recently identified and incorporated into recent WHO classification as a provisional entity. However, only seventeen cases have been reported to date. In this study, we present the clinicopathological features of seven new cases of ALK-positive renal tumor.*

Design: We selected seven cases from renal tumor files in six institutions and performed the clinical (age, sex, follow-up and outcome), pathologic (gross, macroscopy and immunohistochemistry) and genetic (fluorescence in situ hybridization, FISH and next generation sequencer, NGS) analyses.

Results: The age of patients ranged from 33 to 56 years with a mean age of 44.1 years. Patients consisted of four females and three males. Grossly, all tumors possessed solid part with focal cystic part in two tumors. Necrosis and hemorrhage were observed in two and one. Morphologically, the tumor demonstrated five unclassified RCC including one with peripheral metanephric adenoma-like area, one solid-rhabdoid pattern and sarcomatoid change, one mucinous tubular and spindle cell carcinoma-like features and one metanephric adenoma. Immunohistochemically, all tumors were diffusely positive for ALK protein. The splitting of *ALK* gene in five examined tumors was confirmed using break apart FISH probe. NGS examination of four examined tumors identified fusion partners including *CLIP1* gene in one, *KIF5B* gene in one, *STRN* gene in three and *EML4* gene in one. The pStage in UICC 8th edition consisted of pT1a in four, pT1b in one and pT3a in two. Follow-up data are available in four cases. The duration of follow-up ranged from 4 to 66 months with a mean duration of 65.8 months. Three patients were alive without disease and one patient was alive with metastasis to lymph node.

Conclusions: ALK-positive renal tumor is a genetically distinct entity. We identified new fusion partners to *ALK* gene including *CLIP1* and *KIF5B* genes in renal tumor. Morphologically, the presence of signe-ring cells and solid-rhabdoid pattern may be a diagnostic clue to ALK-positive renal cancer. Immunohistochemistry of ALK protein and break apart FISH of *ALK* gene are useful for definite diagnosis. Some metanephric adenomas may be included into this category. Further examination in a large series will be hopeful to elucidate the clinicopathologic features of ALK-positive renal cancer in the future.

886 Characterization of Adult Unclassified Renal Cell Carcinoma

Regina Kwon[1], Pedram Argani[2], Jonathan Epstein[3], Andres Matoso[3]
[1]Johns Hopkins University School of Medicine, Baltimore, MD, [2]Johns Hopkins Hospital, Ellicott City, MD, [3]Johns Hopkins Medical Institutions, Baltimore, MD

Disclosures: Regina Kwon: None; Pedram Argani: None; Jonathan Epstein: None; Andres Matoso: None

Background: Approximately 3%-5% of renal cell carcinoma (RCC) tumors are reported as unclassified. Several new RCC subtypes have been characterized, including eosinophilic solid and cystic (ESC), fumarate hydratase (FH)-deficient, and succinate dehydrogenase (SDH)-deficient. Previously, we showed that 67% of unclassified eosinophilic RCC in young patients can be put into one of these 3 groups (Histopathology 2018;72:588-600). In this study, we review a series of unclassified RCCs in adults and correlate the morphologic and immunohistochemical findings with prognostic features and clinical outcomes.

Design: We searched for unclassified RCCs diagnosed from 1998-2018. We grouped cases by predominant morphologic pattern and performed immunohistochemistry (IHC) for FH, SDHB, and CK20. Tumor-infiltrating lymphocytes (TILs) in direct contact with tumor cells were assessed (0%, no TILs; ≤ 5%, min-TILs; 6-14%, mod-TILs; ≥ 15%, high-TILs).

Results: We identified 79 cases and grouped them as oncocytoma-/chromophobe-like (n=23); eosinophilic/papillary-like (n=21); clear cell/papillary-like (n=13); clear cell-like (n=9); sarcomatoid/spindled (n=5); mucinous tubular and spindle cell (MTSC)-like (n=3); and lacking a specific pattern (n=5). The mean age was 58 y (range, 29-84); 54% were male and 60% white. RCC-specific mortality in the 56 cases with follow-up data was 8.9%. At diagnosis, 29% of tumors were advanced stage (≥ pT3), 72% had a high nucleolar grade (NG; grade 3-4), and 46% had high-TILs. Using IHC, we identified 7 CK20(+) cases, which we reclassified as ESC, and 1 SDH(-) case, reclassified as SDH-deficient. FH was retained in all tumors. High-TILs was associated with advanced stage (p=0.002), high NG (p=0.013), and papillary morphology (p=0.040). Advanced stage and high-TILs at diagnosis were associated with increased 5-year mortality (p=0.002 and p=0.010,

respectively). Oncocytoma-/chromophobe-like tumors were significantly less likely than others to be advanced stage (OR 0.16) or high-grade (OR 0.20).

Conclusions: Using IHC, 10% of unclassified RCCs in adults can be assigned to one of several recently well-defined entities, most commonly ESC. Our morphologic review also identified a subset of sarcomatoid carcinomas (6%) and a subset that could be reclassified as the recently described high-grade MTSC (4%). Oncocytoma-/chromophobe-like unclassified RCC may confer a better prognosis than other subtypes. Finally, in addition to its association with poor prognosis, high-TILs may have implications for immunotherapy.

887 Tumor micro environment of prostate cancer reveals race associated differences between African American Men and Men of European descent

Priti Lal[1], Kevin Trowell[2], Sahar Farahani[2], Jeremy Adler[3], Kosj Yamoah[4], Timothy Rebbeck[5]
[1]University of Pennsylvania, Philadelphia, PA, [2]Hospital of the University of Pennsylvania, Philadelphia, PA, [3]Philadelphia, PA, [4]H. Lee Moffitt Cancer Center & Research Institute, Tampa, FL, [5]Dana-Farber/Harvard Cancer Center, Boston, MA

Disclosures: Priti Lal: None; Kevin Trowell: None; Sahar Farahani: None; Jeremy Adler: None

Background: African American (AA) men experience a higher incidence of mortality as a result of prostate cancer (PC) than men of other races and ethnicities, including European Americans (EA). While this disparity has been attributed partly to socioeconomic factors and inadequate access to health care, differences in genetic susceptibility plays an important role. Furthermore it is now evident that tumor microenvironment plays an important role in the outcome of cancer. Inactivation of MYC oncogene can elicit immune recognition, which in tumor cells can be associated with immune response and tumor elimination. We sought to study the differences in tumor microenvironment of PC in AA men and EA men and its association with c-MYC expression.

Design: 200 stage matched prostatectomy specimens representing 100 AA and 100 EA men were identified from the archives of the Hospital of the University of Pennsylvania under institutional IRB. Cases were reviewed and one most representative slide was identified from each case. Immunohistochemical stain for c-MYC was performed with adequate controls. Nuclear reactivity in tumor cells was graded semi quantitatively for intensity on a scale of 0-3 and percentage of positive tumor cells recorded. An H score was calculated by multiplying the two values. Average number of TIL clusters (cluster was defined as aggregates of lymphocytes within a tumor nodule) per mm^2 of tumor surface was calculated.

All Patients Irrespective of Ethnicity					
c-MYC status	All patients	Mean of lymphocyte aggregates per mm^2 of tumor area	Std Error	95% CI	P-value
Negative	59	0.021	0.004	0.013-0.0297	**0.021**
Positive	133	0.037	0.004	0.029-0.044	
African American Patients					
Negative	40	0.026	0.006	0.014-0.038	0.383
Positive	52	0.034	0.007	0.0203-0.048	
European American Patients					
Negative	19	0.012	0.004	0.004 - 0.020	**0.008**
Positive	81	0.038	0.005	0.029-0.047	

- There was a statistically significant difference in the average number of lymphocytic aggregates per mm^2 of tumor area between the cases with positive and negative c-Myc. C-Myc positivity was associated with higher average number of lymphocytic aggregates per mm^2 of tumor area
- When considering the patients ethnicity, the significant association between average number of lymphocytic aggregates per mm^2 of tumor area and c-Myc positivity persisted in EAM group

1. Tumor microenvironment of prostate cancer in African American men is distinct from that of European American men.
2. C-Myc positivity is associated with higher average number of TILs per mm^2 of tumor
3. When considering the patient's ethnicity, the significant association between average number of TILs per mm^2 of tumor area and c-Myc positivity persisted in EA men however was not statistically significant in AA men

888 Expression of pRb and PD-L1 as potential predictive biomarkers for oncolytic adenovirus based gene therapy of urothelial carcinoma

Ryan Lau[1], Curtis Chin[2], Weibo Yu[1], Paola Grandi[3], Shihpei Shen[3], Calvin Lai[4], Jianyu Rao[5]
[1]University of California, Los Angeles, Los Angeles, CA, [2]David Geffen School of Medicine at UCLA, Los Angeles, CA, [3]Cold Genesys, Santa Ana, CA, [4]Cold Genesys, Costa Mesa, CA, [5]Los Angeles, CA

Disclosures: Ryan Lau: None; Curtis Chin: None; Weibo Yu: None; Shihpei Shen: None; Calvin Lai: *Employee*, Cold Genesys Inc.; Jianyu Rao: *Primary Investigator*, Coldgenesis

Background: Urothelial carcinoma is the most common tumor of the bladder in the US and Europe. Traditional intravesical Bacillus Calmette-Guerin (BCG) therapy, though effective for non-muscle invasive urothelial/bladder cancer (NMIBC), may be associated with high rate of recurrence. CG0070 is an oncolytic adenovirus, conditionally transcribed in Rb-pathway-defective tumor cells, currently in phase II trials for treatment of NMIBC. The vector also expresses human GM-CSF, which may induce PDL-1 associated immune response. Because the efficacy of this treatment is possibly dependent on Rb and PD-L1, the study aimed to determine if Rb protein (pRb) and PD-L1 protein expression predict response to CG0070 treatment.

Design: Patients ? 18 years of age, with high-risk NMIBC, BCG-unresponsive [unable to achieve disease free state at 6 months after adequate BCG ('BCG-refractory') or developed recurrence after complete response (CR) to BCG ('BCG-relapsed')], and unfit for cystectomy were included in the study. At time of enrollment, immunohistochemical stains against pRb and PD-L1 were performed on patients' tumor samples. pRb expression was scored and categorized: low expression (LE) (0-15%); intermediate expression (IE) (16-90%); high expression (HE) (>90%). PD-L1 expression in the tumor cells was scored and categorized: negative (<1%) or positive (1-100%) (Figure 1). Subjects were treated with intravesical CG0070. Six months after treatment, disease progression was assessed using urine cytology, cystoscopy, and bladder biopsy. The clinical responses were categorized: complete response (CR), stable disease (SD), and disease progression (PD). Intensity of pRb and tumor PD-L1 expression were compared to clinical response.

Results: The study recruited 67 subjects; 27 of these had complete 6 month follow-up and IHC available at time of data analysis. Clinical response compared to pRb expression is shown. CR was seen in 33% of LE, 44% of IE, and 100% of HE (p=0.19, compared HE to IE and LE). Clinical response compared to PD-L1 expression is shown. The rate of CR was 70% in positive cases, and 35% in negative cases (p=0.12). (Figure 2)

Figure 1 - 888

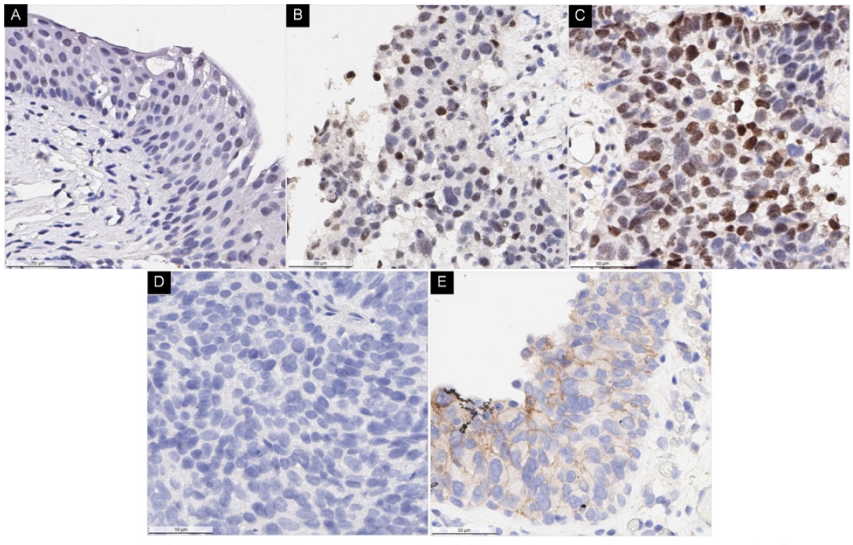

Figure 1. Examples of pRb and PD-L1 expression by IHC **A)** pRb low expression (0-15%) **B)** pRb intermediate expression (16-90%) **C)** pRb high expression (>90%) **D)** Negative PD-L1 expression (0%) **E)** Positive PD-L1 expression (1-100%)

Figure 2 - 888

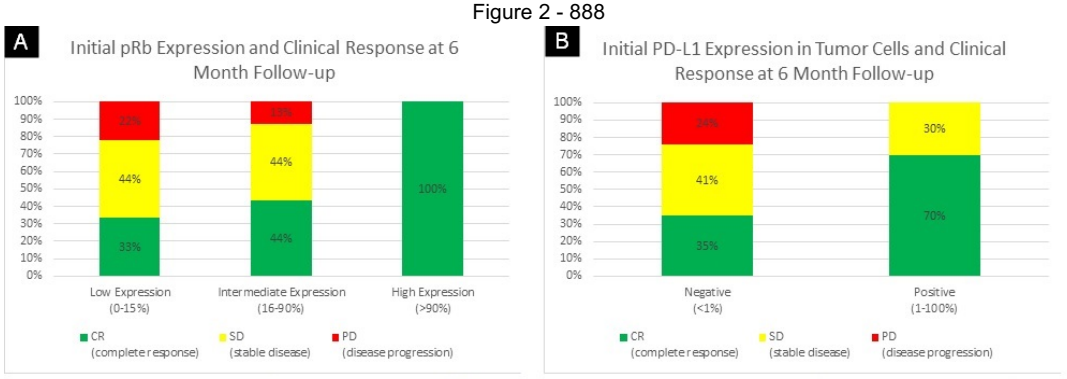

Figure 2. A) Initial pRb expression and clinical response at 6 month followup **B)** Initial PD-L1 expression in tumor cells and clinical response at 6 month followup

Conclusions: The expressions of pRb and PD-L1 in tumor cells appeared to correlate with clinical response following intravesical CG0070 treatment, though such trends did not reach statistical significance owing to the small sample size. Further studies are warranted to determine the predictive value of PD-L1 and pRb for CG0070-based gene therapy for bladder cancer.

889 The Efficacy of MRI-guided Prostate Biopsies – Review of Experience in Four Years from a Single Institution

Whayoung Lee[1], Thomas Lee[2]
[1]University of California Irvine Medical Center, Orange, CA, [2]University of California, Irvine, Irvine, CA

Disclosures: Whayoung Lee: None; Thomas Lee: None

Background: In recent years, a MRI-guided targeted prostate biopsy (MB) has been introduced in addition to the standard 12-core biopsy (SB) to aid localizing and grading the prostate cancer (PC). Limited studies are available to evaluate additional efficacy and accuracy of MB compared to SB.

Design: A retrospective data between January 2015 and August 2018 from a medium-sized academic institution is collected. Total 287 consecutive prostatectomy specimens with corresponding prostate needle biopsies, either MB or SB, in-house or outside cases were identified. Exclusion criteria are i) prostatectomy due to benign prostatic hyperplasia and ii) final grading after prostatectomy was impossible owing to atrophy following androgen deprivation/chemotherapy. Multiple parameters (e.g., age, high-grade, concordance, over-graded and under-graded rate) are analyzed and compared between MB and SB. Correlation between PI-RAD score and high-grade tumor diagnosis was also investigated.

Results: After applying the exclusion criteria, 102 MB and 173 SB cases were identified. Average age was 64.66 (r=42-77) in MB group and 63.13 (r=37-80) in SB group. In the MB group, 82.3% of the cases were performed in our institute, while only 7.5 % of cases were in-house in the SB group. The concordance rates between each biopsy and final diagnosis following radical prostatectomy were 56.8% (MB) and 56.6% (SB). In both groups, under-graded cases were more than over-graded cases, showing 63.6% in MB and 64% in the SB group (Table 1). The percentage of the high-grade tumor (Gleason grade group 4 and 5) was identified at 23.5% and 23%, respectively. Among the high-grade tumors, concordance rate in the MB group was 37.5 % whereas 52 % in the SB group. When limited to the high-grade tumor cases, over-graded cases were more than under-grade cases, 80% vs. 20% in MB group and 57.9% vs. 42.1% in the SB group (Table 1). Among 102 MB cases, 70 cases were PI-RAD score 4 and 5 comprising 68.6 % of all biopsied lesions. 17 cases (24.3%) were called high-grade tumor on the biopsy, and 9 cases (12.8%) were diagnosed high-grade on the final report following radical prostatectomy.

			MRI-guided biopsy (MB)	Standard biopsy (SB)
Number of case			102	173
Age			64.66 ± 7.5	63.13 ± 7.2
In-house biopsy rate			84/102 (82.3%)	13/173 (7.5%)
Concordance			58/102 (56.8%)	98/173 (56.6%)
	Under-graded case		28/44 (63.6%)	48/75 (64%)
	Over-graded case		16/44 (36.4%)	27/75 (36%)
High grade (Grade group 4, 5)			24/102 (23.5%)	40/173 (23%)
	Concordance in high grade group		9/24 (37.5%)	21/40 (52%)
		Under-graded case	3/15 (20%)	8/19 (42.1%)
		Over-graded case	12/15 (80%)	11/19 (57.9%)

Conclusions: Considering the extra cost and time for the procedure, MRI-guided targeted biopsy is not proven more effective nor accurate for diagnosing prostate carcinoma in our limited retrospective study. Furthermore, it appears that the tendency of over-grading is observed with MRI-guided biopsy in relation to high PI-RAD scores.

890 PAX8 Expression in Nested Variant of Urothelial Carcinoma (NVUC): A Potential Diagnostic Pitfall

Teklu Legesse[1], Andres Matoso[2], Jonathan Epstein[2]
[1]JHMI, Columbia, MD, [2]Johns Hopkins Medical Institutions, Baltimore, MD

Disclosures: Teklu Legesse: None; Andres Matoso: None; Jonathan Epstein: None

Background: NVUC is a rare variant of urothelial carcinoma characterized by nests of cytologically bland urothelial cells with different growth patterns including small and large nests, nests with tubules, and nests with microcystic features. It is widely recognized that NVUC can closely mimic von Brunn nests. However, NVUC with tubule formation can also resemble nephrogenic adenoma, where IHC positivity for PAX8 has been used to establish the diagnosis of nephrogenic adenoma. We have seen some examples of PAX8 positive NVUC and this study formally explores this issue.

Design: Tissue blocks from cases diagnosed as NVUC in one of the author's consultation service from 2011 to 2018 were collected. H&E slides were reviewed and the pattern of growth (NVUC with solid nests only versus NVUC with solid nests and tubules) documented. PAX8 IHC was classified as negative if there was faint (+1) or no staining, and positive if there was moderate (+2) or strong (+3) staining. Additionally, extent of immunoreactivity was assessed as focal (positive in <50% of the cells) and diffuse (positive in $\geq$ 50% of the cells).

Results: Out of 29 cases diagnosed as NVUC, tissue blocks were identified in 22 cases. There were 14 (63.6 %) females and 8 (36.3%) males; mean age was 63.4 years (range: 44-77 years). All tumors were located in the bladder. 5/22 (23 %) of the cases had only solid nests with the majority of 17/22 (77.3%) of the NVUCs having solid nests with some tubular differentiation. PAX8 immunoreactivity was strong (3+) diffuse in 4 (18.2%), moderate (2+) in 8 (36.4 %), and negative in 10 (45.4%) cases. Of those cases showing moderate staining, 5/8 (62%) showed focal and 3/8 (38%) showed diffuse immunoreactivity. There was no difference in the staining pattern between the solid nests and tubules in the cases with both patterns.

Conclusions: PAX8 can be positive in a significant proportion of NVUC cases. Recognition of this finding is important to avoid misdiagnosis of NVUC as nephrogenic adenoma based on PAX8 expression, particularly in cases with tubular differentiation.

891 Findings In The Rescue Pelvic Lymphadenectomy Using 68Ga-Prostate-Specific Membrane Antigen (PSMA) Ligand Positron Emission Tomography/Computed Tomography (PET/CT) Imaging In Biochemical Recurrence Of Prostate Cancer Patients Treated Previously With Radical Prostatectomy

Katia Leite[1], Victor Srougi[1], Tiago Zanutto[1], Guilherme Pereira[2], Oswaldo Oliveira Neto[1], Thales Andrade[3], Miguel Srougi[1]
[1]University of Sao Paulo Medical School, São Paulo, SP, Brazil, [2]University of Sao Paulo Medical School, Porto Algre, RS, Brazil, [3]São Paulo, SP, Brazil

Disclosures: Katia Leite: None; Guilherme Pereira: None; Oswaldo Oliveira Neto: None

Background: Radiotherapy and/or androgen-deprivation therapy are options to treat biochemical relapse after radical prostatectomy (RP). Those treatments are not free of morbidity, and a tendency to tailor the best treatment for patients has been proposed recently. ^{68}Ga-

prostate-specific membrane antigen (PSMA) ligand positron emission tomography/computed tomography (PET/CT) imaging is now available to better detect local or distant metastasis, and extended pelvic lymphadenectomy (ePL) is an option to treat local recurrence, delaying the rescue using radio or hormonotherapy. Our aim is to describe the pathological findings of ePL after biochemical recurrence in the follow up of patients previously submitted to RP.

Design: Twenty-three patients were submitted to ePL after biochemical relapse. The mean age was 63.35 years-old (± 6.8yo). Mean PSA before RP was 7.24 ng/mL (± 4.11 ng/mL) and mean PSA at time of recurrence was 1.5 ng/mL(± 1.2 ng/mL). Mean Gleason score from primary tumor was 8.4 (±0.71) and mean ISUP/grade group was 4.4(±0.71). The mean tumor volume was 29.1%(±15.7%). 46.7% were staged pT2, 40.0% pT3a and 13.3% pT3b. Margins were positive in 35.3% of the cases and there were positive lymph nodes (LN) in 14.3%. The mean SUV in PSMA-PT/CT was 20.63 (±13.3). Each LN level dissected was received in separate container, all nodules and all the remaining adipous tissue were included for histological, hematoxylin & eosin staining slides examination.

Results: Obturator, common iliac, internal and external iliac and presacral LN were resected. The mean number of LN dissected was 43.39 (±16.6), median 43(range 18 – 74). The mean number of metastatic LN was 2.83 (± 5.04), median 1 (range 0 – 24). In 30%(7/23) of patients LN were negative for tumor. In 8 (34.7%) patients more than one level had metastatic LN. 31 metastatic LN were found in the internal iliac (12), external iliac (8), common iliac (7), obturator (2) and presacral (2) regions. The mean size of lymph nodes was 7.71 mm(±5.64 mm) ranging from 0.5 to 25 mm.

Conclusions: Using PSMA-PET/CT imaging to detect metastatic pelvic LN the pathological findings will be: In almost one third of patients LN will be negative for metastasis. The mean number of LN dissected is 43.4, variable from 18 to 74. The mean number of metastatic LN will be around 3, being variable in size from 0.5 to 25.0 mm (mean 7.7 mm), most frequently resected from the internal and external iliac region. Unusual sites like presacral region can be affected in less than 10% of the patien

892 Loss of Prostate Specific Membrane Antigen (PSMA) Expression in Prostatic Adenocarcinoma with Lymph Node Metastasis

Guangyuan Li[1], Jenny Ross[2], Ximing Yang[3]
[1]Northwestern University Feinberg School of Medicine, Solon, OH, [2]Feinberg School of Medicine/Northwestern University, Chicago, IL, [3]Northwestern University, Chicago, IL

Disclosures: Guangyuan Li: None; Jenny Ross: None; Ximing Yang: None

Background: PSMA expression in the cell membrane of prostatic adenocarcinoma provides an ideal target for prostate cancer diagnosis and treatment. However, the efficacy of these applications highly depends on the expression patterns of PSMA in tumor cells. Limited studies were done addressing the PSMA expression patterns in metastatic prostate cancer. As the development of PSMA-based in-vivo diagnostic, therapeutic, and prognostic approaches grows, it is of great interest to be aware of potential false negative cases that could influence the management of prostate cancer.

Design: A total of 18 prostatic adenocarcinoma with 22 metastatic lymph nodes were obtained from our institution between January 2017 and August 2018. In addition, 69 cores of 23 cases of primary prostatic adenocarcinoma from tissue microarrays (TMA) were included for comparison. PSMA positivity fraction was classified according to the percentage of all positive tumor cells as negative (0-5%), low (6-20%), moderate (21-50%), and high (>50%). The intensity of the IHC staining was evaluated by using a 4 grade scoring system with intensity from 0-3: 0 (no staining), 1 (weak), 2 (moderate), 3 (strong).

Results: All (23/23) TMA prostatic adenocarcinoma specimen were positive for PSMA with intensity 1.67±0.7 and positive fraction 53.4±28.1%. PSMA positivity was observed in 13/18 cases of prostatic cancer and matched metastatic lymph nodes (intensity = 2.43±0.73 with positive fraction 81.3±24.7%). Negative or weak PSMA staining was observed in 4/18 primary tumors with matched metastatic lymph nodes, which include one case of small cell carcinoma completely negative for PSMA in both the primary tumor and lymph node metastasis. In 1/18 case, which is mixed acinar and ductal adenocarcinoma, PSMA reactivity was present in the primary tumor (intensity 3 and positive fraction 80%), but decreased significantly in the lymph node metastasis (intensity 1 and positive fraction 5%). (Table 1)

Figure 1 - 892

Table 1 Summary of PSMA expression in primary prostate cancer and lymph node metastasis.

	Quantity	Gleason score	PSMA intensity		PSMA positive fraction	
			1° tumor	LN met	1° tumor	LN met
1° tumor +, LN met+	13	8.8±0.7	2.54±0.52	2.44±0.73	76.9±18.0%	81.3±24.7%
1° tumor -, LN met-	4	9±0.7	0.25±0.5	0.5±0.55	1.25±2.5%	1.8±2.5%
1° tumor +, LN met-	1	9	3	1	80%	5%

Abbreviations: 1° tumor, primary tumor; LN met, lymph node metastasis; +, positive; -, negative.

Conclusions: Our study demonstrated the frequent expression and the target potential of PSMA in advanced prostatic adenocarcinoma. However, significantly decreased PSMA expression is present in a subset of both primary tumors and lymph node metastasis. Particularly the decreased or loss of PSMA in metastatic lesions of ductal and small cell carcinomas of the prostate could impact on the PSMA-based imaging staging and therapies. These findings could provide a guidance for better clinical management using PSMA-based diagnostic tests and anticancer therapies.

893 Mismatch Repair (MMR) Deficiency and PD-L1 Expression in the Prostatic Ductal Adenocarcinoma

Guangyuan Li[1], Jenny Ross[2], Ximing Yang[3]
[1]Northwestern University Feinberg School of Medicine, Solon, OH, [2]Feinberg School of Medicine/Northwestern University, Chicago, IL, [3]Northwestern University, Chicago, IL

Disclosures: Guangyuan Li: None; Jenny Ross: None; Ximing Yang: None

Background: Prostatic ductal adenocarcinoma is an aggressive histopathologic variant of prostate cancer and often associated with high grade acinar adenocarcinoma. MMR deficiency was found to be more prevalent in prostatic ductal adenocarcinoma than other prostate cancers of histologic subtype. MMR deficiency is associated with hypermutation phenotype defined as a tumor with an increased mutation burden (a high rate of somatic mutations), which is predictive of response to immune checkpoint blockade in solid tumors. MMR deficient cancers exhibit a markedly high rate of mutations, which can result in the formation of neoantigens, hypothesised to enhance the antitumor immune response. It would be informative to evaluate PD-L1 expression pattern of prostatic ductal adenocarcinoma to direct clinical decisions of PD-L1 targeting therapies.

Design: 28 cases of prostatic ductal adenocarcinoma with >10% ductal differentiation of the tumor volume were obtained from our institution to detect the expression of MMR panel and PD-L1. In addition, 108 cores of 36 cases of primary prostatic adenocarcinoma from tissue microarrays (TMA) consisting of 6 ductal and 30 acinar adenocarcinoma were included for comparison. The primary antibody against PD-L1 was E1L3. Positivity for MMR panel and PD-L1 was classified according to the percentage of all positive tumor cells as negative (positivity of <1%), positive (positivity of >=1%).

Results: 4/28 (14.3%) prostatic ductal adenocarcinoma had lymph node metastases upon presentation. 1/28 (3.6%) case had loss of MLH1 and PMS2 expression. PD-L1 positivity was low in prostatic adenocarcinoma. 2/36 (5.6%) TMA prostate cancer specimens were positive for PD-L1 including 1 ductal adenocarcinoma. In the cohort of 28 prostatic ductal specimens 1/28 (3.6%) showed positive PD-L1 staining.

Conclusions: MMR gene deficiency is a rare finding in prostatic ductal adenocarcinoma. PD-L1 expression is present in a small subset of prostatic adenocarcinoma. These results are important for the future clinical development of MMR deficiency evaluation and PD-L1 targeting therapies in prostatic adenocarcinoma.

894 Evaluation of PD-L1 and Other Immune Markers in Bladder Urothelial Carcinoma Stratified by Histologic Variants and Molecular Subtypes

Huili Li[1], Qingzhao Zhang[2], Lauren Shuman[1], Matthew Kaag[3], Jay Raman[4], Suzanne Merrill[3], David DeGraff[4], Joshua Warrick[5], Guoli Chen[1]
[1]Penn State Health Milton S. Hershey Medical Center, Hershey, PA, [2]Penn State Health, Hershey, PA, [3]Penn State College of Medicine, Hershey, PA, [4]Penn State Health Hershey Medical Center, Hershey, PA, [5]Hershey, PA

Disclosures: Huili Li: None; Qingzhao Zhang: None; Lauren Shuman: None; Matthew Kaag: None; Jay Raman: None; Suzanne Merrill: None; David DeGraff: None; Joshua Warrick: None; Guoli Chen: None

Background: Bladder cancer may be divided into molecular subtypes. Specific subtypes are enriched in specific histologic variants; while histologic variants tend to be aggressive. Advanced bladder cancer has a poor prognosis, though a subset of patients demonstrates durable response to immune checkpoint inhibitors. Response to checkpoint inhibitors may therefore be associated with type and degree of immune infiltrate, as well as molecular subtype. We thus evaluated immune infiltrate and molecular subtype in a set of histologic variants.

Design: We evaluated a series of urothelial carcinomas (UC) by tissue microarray including 77 carcinoma in situ (CIS), 40 non-invasive papillary urothelial carcinoma (NIPUC), and 143 invasive UC, including conventional and six histologic variants. Half of the cases had been assigned a molecular subtype in a prior study, using the Lund University approach. PD1, PD-L1, CD3, CD8 and CD68 were evaluated by immunohistochemistry in tumor cells and tumor infiltrating lymphocytes, and scored semi-quantitatively (score 0-3). Lymphocytic infiltration was quantified by H&E in a similar system. Tumors were clustered by marker scores using agglomerative methods, and associations among markers, histologies, and molecular subtypes were evaluated.

Results: The UC specimens clustered into immune high and immune low groups based on expression of immune markers. Tumors of genetically-unstable molecular subtype were enriched in the immune high cluster (p=0.0255, Fisher's exact test). NIPUC was enriched in

the immune low cluster (p=0.001, Fisher's exact test). Within the invasive UC variants, squamous cell and sarcomatoid UC tended to be immune high, but without statistical significance. Analyzing scores of individual markers demonstrated that CIS had greater lymphocytic infiltration and PD1 expression in lymphocytes than NIPUC and invasive UC (p<0.05). Invasive UC showed higher CD3 (intra-tumoral), CD8, and PD-L1 expression than CIS and NIPUC (p<0.05). Invasive squamous cell UC tended to have more intra-tumoral CD3 expression in lymphocytes, and sarcomatoid UC tended to have more PD-L1, though without statistical significance. As expected, PD-L1 expression in tumor cells clustered with intra-tumoral CD3, indicating PD-L1 is closely related to immune activation.

Conclusions: UC can be classified as immune high and low groups. Immune high group is enriched in higher intra-tumoral CD3, PD-L1, and genomically-unstable UC, suggesting it may respond to checkpoint inhibitors.

895 ERG/SPINK1 Dual Immunohistochemistry Reveals Frequent Prostate Cancer Multiclonality in Low- and Intermediate-Risk Patients with Multiple Involved Prostate Cores

Natalia Liu[1], Javed Siddiqui[2], Scott Tomlins[2], Aaron Udager[3]
[1]Ann Arbor, MI, [2]University of Michigan, Ann Arbor, MI, [3]University of Michigan Medical School, Ann Arbor, MI

Disclosures: Natalia Liu: None; Javed Siddiqui: None; Scott Tomlins: *Primary Investigator*, Ventana Medical Systems; Aaron Udager: *Grant or Research Support*, Ventana Medical Systems, Inc.

Background: Prostate cancer is typically a multifocal disease presenting as one or more clonally-distinct tumors. ETS gene rearrangements, including the dominant *TMPRSS2-ERG* gene fusion, are early clonal events in prostate cancer pathogenesis. Utilizing ERG/SPINK1 dual immunohistochemistry (IHC), our group previously showed that 25% of discontinuous tumor foci within a single prostate core were clonally-distinct. In this study, we sought to extend these initial findings to a cohort of low- and intermediate-risk patients with multiple involved prostate cores to determine the frequency of multiclonality and possible association with adverse pathology on radical prostatectomy (RP).

Design: Cases were identified retrospectively from prostate cancer clinical databases at a single large academic institution using the following criteria: 1) Gleason score (GS) 6 or GS3+4=7 on biopsy; 2) 1-5 cores involved on biopsy; and, 3) at least one core >50% involvement and/or underwent subsequent RP. For each case, ERG/SPINK1 dual IHC was performed on all available formalin-fixed paraffin-embedded (FFPE) tissue blocks corresponding to involved prostate cores. IHC slides were reviewed by a genitourinary pathologist, and ERG and SPINK1 status was recorded for each biopsy. Multiclonality was defined as the presence of ERG-positive and ERG-negative tumor either within a single core or between different cores from a single case. Association between multiclonality and routine biopsy and RP clinicopathologic parameters was evaluated using standard statistical methods.

Results: 146 cases (433 total biopsies) from 142 patients were available for the purposes of this study. 30 cases (20.5%) showed evidence of multiclonality, including 16 cases (11.0%) with multiple clones within a single core. Multiclonality was significantly associated with an increasing number of involved cores (P = 0.001) but was not associated with age at biopsy, family history, serum PSA, highest GS on biopsy, or greatest % involvement of a single core (see Table for details). Similarly, multiclonality on biopsy was not significantly associated with routine RP clinicopathologic parameters, including index tumor nodule GS, size, and pathologic stage, or the presence of GS upgrading from biopsy to RP.

	Multiclonality		
Clinicopathologic Parameter	Yes (*n* = 30)	No (*n* = 116)	*P*-value
Age (years)	Median = 64.4 (range = 47.9-80.5)	Median = 63.3 (range = 45.5-81.3)	0.871
Family History • Yes • No	10 (34.5%) 19 (65.5%)	19 (17.8%) 88 (82.8%)	0.099
Serum PSA (ng/mL)	Median = 5.5 (range = 2.6-26.0)	Median = 4.5 (range = 0.2-18.3)	0.827
Highest GS on Biopsy • GS3+3=6 • GS3+4=7	12 (40.0%) 18 (60.0%)	42 (36.2%) 74 (63.8%)	0.701
Number of Involved Cores • One • Two • Three • Four • Five	0 (0.0%) 3 (10.0%) 11 (36.7%) 6 (20.0%) 10 (33.3%)	12 (10.4%) 36 (31.0%) 25 (21.6%) 31 (26.7%) 12 (10.3%)	**0.001**
Greatest % Involvement of a Single Core	Median = 67.5 (range = 5-100)	Median = 60 (range = 5-100)	0.247

Conclusions: Multiclonality is frequently observed in low- and intermediate-risk prostate cancer patients with multiple involved cores, although preliminary analyses do not detect a significant clinical impact for multiclonality assessment in this setting.

896 DNA Damage Repair Alterations are Frequent in Prostatic Adenocarcinomas with Focal Pleomorphic Giant Cell Features

Tamara Lotan[1], Harsimar Kaur[2], Abdullah Alharbi[3], Colin Pritchard[4], Jonathan Epstein[3]
[1]Johns Hopkins School of Medicine, Baltimore, MD, [2]Johns Hopkins University, Baltimore, MD, [3]Johns Hopkins Medical Institutions, Baltimore, MD, [4]University of Washington, Seattle, WA

Disclosures: Tamara Lotan: None; Harsimar Kaur: None; Abdullah Alharbi: None; Colin Pritchard: None; Jonathan Epstein: None

Background: Prostatic adenocarcinomas with focal pleomorphic giant cell features are a rare tumor subtype with abysmal clinical outcomes. More than one third of cases with this histology die within a year of the initial diagnosis of prostate cancer. Potential targeted therapies are desperately needed, however the molecular features of these tumors remain unknown.

Design: Here, we performed next generation sequencing (UW Oncoscan platform) on somatic tumor DNA extracted from 8 cases of prostatic adenocarcinomas with focal pleomorphic giant cell features, including cases with and without prior treatment for prostate cancer. Six of these cases were from a previously reported case series with clinical follow-up from our group.

Results: We find that DNA damage repair mutations are common in this rare subset of prostate tumors, with 2 of 8 having bi-allelic pathogenic mutations in homologous DNA repair genes (including *BRCA2* and *NBN*) and 2 of 8 having bi-allelic pathogenic mutations in mismatch repair genes (including *MSH2* and *MLH1*).

Table 1: Clinical-Pathologic and Genomic Features of Prostatic Adenocarcinoma with Focal Pleomorphic Giant Cell Features

ID	Age	Grade	Specimen type	Prior treatment	MMR mutation	HRD mutation	Germline suspected?	Limited Study?
18	43	4+5=9	TURP	RP, RT, ADT	none	***BRCA2***(p.L557*) with LOH	yes	no
15	86	5+5=10	TURB	none	none	none	no	yes
20	87	5+5=10	TURP	none	none	none	no	no
17	82	5+5=10	TURP	ADT	none	none	no	yes
16	73	5+5=10	TURP	RT	***MSH2***(p.Q397* + c.1276+2T>A)	none	no	no
29	39	5+5=10	RP	none	none	none	none	no
New#1	66	5+5=10	TURP	unknown	none	***BRCA2***(p.N1666Ifs*4 + LOH), *NBN* (p.P198Kfs*30 + LOH)	no (*BRCA2*), maybe (*NBN*)	no
New#2	90	5+5=10	TURP	unknown	***MLH1***(homozygous copy loss)	***BRCA2*** (exon 9 + part of exon 10 del)	no	no

TURP: transurethral resection of prostate; TURB: transurethral resection of bladder; RP: Radical prostatectomy; ADT: Androgen deprivation therapy; RT: radiation therapy; MMR: mismatch repair; HRD: homologous repair deficiency.

Conclusions: These data are consistent with emerging data that DNA repair alterations are enriched among castration resistant prostate cancer and aggressive subsets of primary tumors. Given that these patients are potential candidates for PARP inhibitor and/or immune checkpoint blockade and have poor prognosis with standard therapy, we recommend tumor and germline DNA sequencing with or without mismatch repair protein immunohistochemistry be considered for all prostatic adenocarcinomas with focal pleomorphic giant cell features.

897 Targeted Molecular Profiling Supports Diagnostic Subclassification of Renal Cell Carcinoma with Clear Cell Features

Zhichun Lu[1], Komal Kunder[2], L. Priya Kunju[3], Rohit Mehra[2], Angela Wu[4], Scott Tomlins[2], Aaron Udager[5]
[1]University of Michigan, Troy, MI, [2]University of Michigan, Ann Arbor, MI, [3]University of Michigan Hospital, Ann Arbor, MI, [4]Ann Arbor, MI, [5]University of Michigan Medical School, Ann Arbor, MI

Disclosures: Zhichun Lu: None; Komal Kunder: None; L. Priya Kunju: None; Rohit Mehra: None; Angela Wu: None; Scott Tomlins: *Employee*, Strata Oncology; *Major Shareholder*, Strata Oncology; *Speaker*, ThermoFisher Scientific; Aaron Udager: None

Background: Renal cell carcinoma (RCC) with clear cell features constitutes a large group of primary kidney tumors, including conventional clear cell renal cell carcinoma (CCRCC), clear cell papillary renal cell carcinoma (CCPRCC), translocation renal cell carcinoma, and renal cell carcinoma, type unclassified with clear cell features (RCCu), for which diagnostic subclassification is not always straightforward due to overlapping morphologic features. In this study, we explored the possibility of integrating morphology and targeted next-generation sequencing data to augment diagnostic subclassification of these tumors.

Design: All available cases of CCPRCC and RCCu at a single large academic institution between 2013 and 2018 were retrospectively identified. [A control group of CCRCC was established in a similar manner.] Blinded to the given diagnosis and available ancillary test results, one representative H&E tumor slide from each case was re-evaluated independently by three subspecialty-trained genitourinary pathologists to establish a consensus morphologic diagnosis. For each case, targeted next-generation DNA sequencing (DNAseq) using the Oncomine Comprehensive Panel was performed on an Ion Torrent Proton sequencer using formalin-fixed paraffin-embedded (FFPE)-extracted DNA from a single representative tumor area. DNAseq data was processed using established in-house bioinformatics pipelines, and variant and copy number calls were manually curated.

Results: A total of 22 RCC with clear cell features were included for analysis: 12 CCRCC, 6 CCPRCC, and 4 RCCu (see Table 1 for details). As expected, *VHL* mutations and chromosome 3p25 deletions were more frequently observed in CCRCC than CCPRCC and RCCu (Fisher's exact test; $P < 0.05$). Morphologic consensus was reached in 80% of CCPRCC and RCCu cases. The two discordant cases by morphologic review (one each of CCPRCC and RCCu) both showed chromosome 3p25 deletion; post-hoc re-review of the H&E slides and available ancillary material revealed areas with CCPRCC-like morphology but only patchy CK7 staining in both cases.

	CCRCC (*n* = 12)	CCPRCC (*n* = 6)	RCCu (*n* = 4)
Age (years)	Average = 52 (range = 30-73)	Average = 65 (range = 57-76)	Average = 46 (range = 36-61)
Gender • Male • Female	10 2	3 3	3 1
Pathologic Stage • T1a • T1b • T2a • T2b	8 2 1 1	6 0 0 0	2 2 0 0
WHO/ISUP Nuclear Grade: • Grade 2 • Grade 3	7 5	6 0	2 2
Morphologic Consensus	N/A	83% (5/6)	75% (3/4)
Molecular Data • *VHL* mutation • 3p25 deletion	6 (50.0%) 11 (91.7%)	0 (0.0%) 1 (16.7%)	0 (0.0%) 1 (25.0%)

Conclusions: While morphologic evaluation alone is sufficient for the majority of RCC with clear cell features, targeted molecular profiling may refine diagnostic subclassification in a small subset of cases – particularly those with areas of CCPRCC-like morphology. Additional targeted next-generation DNA and RNA sequencing is ongoing to further characterize these tumors.

898 Enhanced expression of transcription factor EB (TFEB) predicts prostate cancer recurrence and metastasis after radical prostatectomy

Min Lu[1], Shulin Wu[2], Sharron Lin[2], Zongwei Wang[2], Aria Olumi[3], Chin-Lee Wu[4]
[1]Beijing, China, [2]Massachusetts General Hospital, Boston, MA, [3]Beth Israel Deaconess Medical Center, Boston, MA, [4]Massachusetts General Hospital, Newton Center, MA

Disclosures: Min Lu: None; Shulin Wu: None; Chin-Lee Wu: None

Background: Significantly and constitutively enhanced transcription factor EB (TFEB), a master regulator of lysosomal biogenesis and function, may play a pivotal role in cancer biology. The role of lysosomal biogenesis in the clinical behavior and postoperative outcome of prostate cancer (PCa) remains unclear.

Design: Two hundred and five PCa patients who were treated with radical prostatectomy were included. Using tissue microarray (TMA) and immunohistochemistry (IHC), the expression of TFEB was evaluated. The association between TFEB status and clinicopathological features and oncological outcomes including biochemical recurrence (BCR), metastasis and overall survival (OS) was examined.

Results: High TFEB expression (42.4%) was detected mainly in the cytoplasm as well as perinuclear/nuclear region of cancer cells. TFEB expression status was significantly associated with metastasis (p=0.035), and associated with preoperative PSA (p=0.05). No significant association was detected between TFEB status and Gleason score (GS) (p=0.171) or pathological T stage (p=0.425). Enhanced TFEB expression was related to worse prognosis of BCR (p=0.008) and of metastasis (p=0.029) on univariate analysis. On multivariate analysis, TFEB status sustained the independent prognostic significance of metastasis (p=0.037, HR: 2.38) adjusted by covariate of GS, as well as with a trend of a worse BCR prognosis (p=0.065, hazard ratio (HR):1.57).

Figure 1 - 898

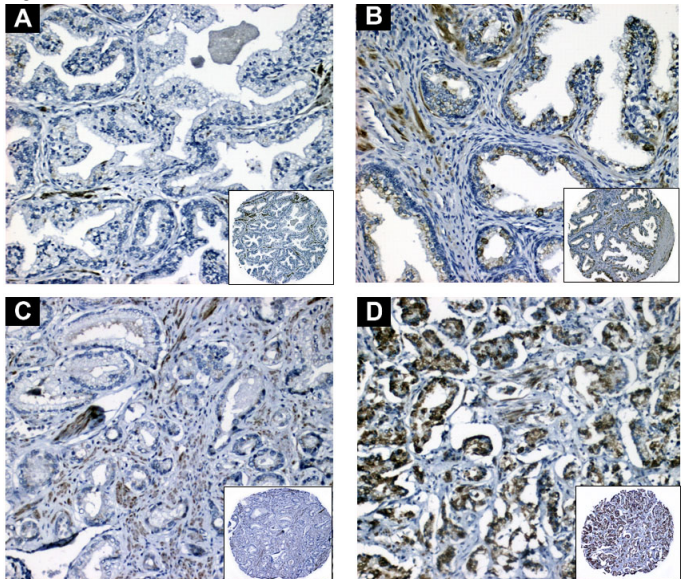

Conclusions: Enhanced TFEB expression correlated with postoperative PCa metastasis and preoperative PSA level, and can predict poor BCR and metastasis prognosis. Our findings provide evidence of TFEB may play a role in the tumorigenesis and progression of PCa.

899 Intraductal carcinoma (IDC) of the prostate in needle biopsy is a significant prognostic factor for distant-metastasis-free-survival (DMFS) in patients treated with external beam radiotherapy (EBRT)

Roberta Lucianò[1], Jane Nguyen[2], Wei Wei[2], Jesse McKenney[2], Cristina Magi-Galluzzi[3]
[1]IRCCS San Raffaele Scientific Institute, Milan, Italy, [2]Cleveland Clinic, Cleveland, OH, [3]The University of Alabama at Birmingham, Birmingham, AL

Disclosures: Roberta Lucianò: None; Jane Nguyen: None; Wei Wei: None; Jesse McKenney: None; Cristina Magi-Galluzzi: None

Background: IDC of the prostate and cribriform Gleason pattern 4 are adverse prognostic factors in localized prostate cancer. We sought to evaluate whether the presence of IDC and/or cribriform Gleason pattern 4 in needle biopsies are an adverse prognostic factor for DMFS in prostate cancer patients treated with EBRT.

Design: We retrospectively reviewed prostate needle biopsy specimens (n=237) in patients treated with EBRT with a Gleason score of 3+4 and 4+3. Their age, race, Gleason score with Grade Group, presence of cribriform Gleason pattern 4 and/or IDC, NCCN risk group, percent positive cores, serum prostate specific antigen (PSA), and androgen deprivation therapy (ADT) status were analyzed. Descriptive statistics were provided. Kaplan-Meier method was used to estimate DMFS by patient group and log-rank test was used to compare DMFS between groups. Cox proportional hazard model was used to estimate hazard ratios.

Results: IDC was present in 30 (13%) patients with cribriform Gleason pattern 4 present in 116 (49%) patients. All IDC patients had cribriform pattern 4. Median follow-up was 116.5 months (range 3-236 months), 85 (36%) patients had died, 10 patients (4%) had died of disease and 75 (32%) had died of other causes. 129 (54%) patients had a PSA < 10, 60 (25%) a PSA between 10-20, and 48 (20%) PSA > 20. 58 (24%) patients were considered with biochemical recurrence, and 21 (9%) patients had distant metastasis. 158 (67%) patients had <50% positive needle core biopsies. 132 (52%) patients received ADT. Univariate Cox proportional hazard model showed that IDC patients had significantly worse DMFS than non-IDC patients (hazard ratio = 3.6, 95% CI: 1.4-9.6, p = 0.01). Patients with Gleason score 4+3 and cribriform Gleason pattern 4 had significantly worse DMFS than those having Gleason score 3+4 without cribriform (HR = 3.5, 95% CI: 1.2-9.7, p = 0.02).

Conclusions: The presence of IDC was a significant prognostic factor for DMFS in patients post EBRT treatment with or without the presence of cribriform Gleason pattern 4.

900 Results and Clinical Utility of Percutaneous Renal Mass Biopsies in a Contemporary Academic Medical Center Cohort

Xilu Ma[1], Kiersten Craig[2], Juan Miguel Mosquera[3], Brian Robinson[3], Timothy McClure[3], Francesca Khani[3]
[1]New York-Presbyterian/Weill Cornell Medical Center, New York, NY, [2]New York-Presbyterian, New York, NY, [3]Weill Cornell Medicine, New York, NY

Disclosures: Xilu Ma: None; Kiersten Craig: None; Juan Miguel Mosquera: None; Brian Robinson: None; Timothy McClure: None; Francesca Khani: None

Background: Historically, renal mass biopsies (RMB) were performed for limited indications, such as unresectable disease. The utility of RMB has been reconsidered recently, especially for patients with small renal masses (SRM) (≤4 cm) who are active surveillance or ablative therapy (AbT) candidates. As such, clinical guidelines now include RMB in management algorithms. We evaluated histopathology results, diagnostic rates, and impact on management of percutaneous RMB in a contemporary cohort.

Design: A total of 152 consecutive RMB were prospectively diagnosed by 3 GU pathologists at our institution from 2015-2018. Patient demographics, radiographic mass size, RMB diagnoses, and subsequent clinical management decisions were retrospectively reviewed. RMBs were considered "diagnostic" if definitive classification was reported (as benign or malignant), "inconclusive" if lesional tissue was present but insufficient for definitive classification, and "non-diagnostic (ND)" when no lesional tissue was present.

Results: The median patient age was 67 years (range: 24-89), and 121 (80%) were SRM biopsies. Among all 152 biopsies, 101 (66%) were diagnostic, 27 (18%) were inconclusive, and 24 (16%) were ND. Of diagnostic cases, 91 (89%) were malignant and 10 (10%) were benign. The diagnoses were 47 (47%) clear cell RCCs, 22 (22%) papillary RCCs, 12 (12%) clear cell papillary RCCs (CCPRCC), 6 (6%) chromophobe RCCs, 4 (4%) unclassifiable RCCs, and the remaining 10 (11%) were benign. Of inconclusive biopsies, 22 (81%) were oncocytic neoplasms, and 5 (19%) were reported as atypical. All ND biopsies occurred in SRM where the mean mass size was smaller vs all other biopsies (1.6 vs 3.2 cm, $p < 0.0003$). Concurrent AbT was performed in 79 (52%) cases (17 (22%) of which were ND), where the mean size of the lesion was 2.7cm (range: 0.6-8.3 cm). Surgical excision was performed in 20 cases; diagnostic concordance with RMB was 95% (19/20). The discordant case was as clear cell RCC on RMB, but diagnosed as a CCPRCC on excision.

Conclusions: In our series, CCPRCC was the third most commonly rendered definitive diagnosis, showing nearly 3 times the incidence as previously reported, likely owing to its higher prevalence among SRMs. Concurrent AbT was frequent, suggesting that RMB informs post-ablative therapy surveillance. Also, in cases where definitive SRM diagnosis is particularly critical, a separate RMB procedure prior to AbT for smaller lesions within this group may be considered to ensure adequate sampling.

901 Histopathologic-Clinical-Radiologic Correlation of Focally Cryoablated Prostate Cancer Biopsies

Xilu Ma[1], Miko Yu[2], Francesca Khani[2], Brian Robinson[2], Daniel Margolis[3], Andrea Sboner[2], Jim Hu[4], Juan Miguel Mosquera[2]
[1]New York-Presbyterian/Weill Cornell Medical Center, New York, NY, [2]Weill Cornell Medicine, New York, NY, [3]Weill Cornell Medical College, New York, NY, [4]Weill Cornell Medicine, New York City, NY

Disclosures: Xilu Ma: None; Miko Yu: None; Francesca Khani: None; Brian Robinson: None; Daniel Margolis: None; Andrea Sboner: None; Juan Miguel Mosquera: None

Background: Focal cryotherapy (FC) for localized prostate cancer (PCa) is primarily patient-driven, owing to its favorable side effects profile. The goal is to treat the index/dominant lesion, while leaving other smaller, insignificant tumor foci untreated. Although studies have shown encouraging outcomes following FC, there are tumors that recur or do not completely respond. The aim of this study was to determine which potential factors may influence treatment response in focally cryoablated PCa.

Design: We reviewed 8 cases (six Grade Group 2, one Grade Group 4, and one Grade Group 5) of patients who underwent FC. Two patients underwent subsequent radical prostatectomy. The histopathology of biopsy (pre and post FC) and radical prostatectomy (RP) specimens was reviewed and correlated with the site of cryoablation. Presence of treatment effect, number of cores, tumor morphology, and tumor volume were assessed. PSA levels and MRI data before and after FC were also reviewed.

Results: Of 8 cases, 3 (two Grade Group 2 and a Grade Group 5) showed no detection of tumor in the post-treatment biopsies. The remaining 5 cases showed apparent reduced tumor volume in the cryoablated areas, as reflected on post-treatment biopsies (e.g. index lesion measured 13mm before to 2.5mm after FC). Evidence of treatment effect included prominent, stromal fibrosis and scattered hemosiderin-pigments. 1 case (Grade Group 2) did not show significant reduction in tumor volume, possibly owing to under-sampling in the pre-treatment biopsy (6 parts were submitted vs 12 parts in the post-treatment biopsy). Both RP specimens showed evidence of treatment effect and revealed that the index tumor spanned a greater area not covered within the cryoablation target areas. All cases showed reduction of PSA levels after treatment – the mean PSA level before treatment was 7.9 ng/mL (range: 4.1-16.9) and after treatment was 3.9 ng/mL (range: 1.1-11.4) ($p<0.003$). 5 of 6 cases which had post-treatment MRI showed positive radiographic-pathologic correlation.

Conclusions: This pilot study shows that possible reasons for failing FC included an initial larger tumor volume that was not sampled on biopsy and undersampling of an index lesion. Although statistically significant, the decrease in PSA levels before and after FC did not predict the extent of tumor response. Moving forward, RNA-seq of targeted index lesions to explore molecular pathways that may contribute to tumor response will be conducted.

902 Prostate Cancer with Comedonecrosis Is Frequently, But Not Exclusively, Intraductal Carcinoma: A Need For Reappraisal Of Grading Criteria

Raghav Madan[1], Mustafa Deebajah[2], Shaheen Alanee[2], Shannon Carskadon[2], Nilesh Gupta[2], Nallasivam Palanisamy[2], Sean Williamson[2]
[1]Wayne State University, Detroit, MI, [2]Henry Ford Health System, Detroit, MI

Disclosures: Raghav Madan: None; Mustafa Deebajah: None; Shaheen Alanee: None; Shannon Carskadon: None; Nilesh Gupta: None; Nallasivam Palanisamy: None; Sean Williamson: None

Background: Since the inception of Gleason grading for prostate cancer, comedonecrosis has essentially always been assigned Gleason pattern 5. However, recent recommendations suggest against the grading of intraductal carcinoma.

Design: We searched our pathology database from 2014-2018 for radical prostatectomy cases with comedonecrosis (specific grade patterns accounting for pattern 4 and 5 have been documented over this period). From an initial cohort of 52 cases, 40 cases were retrieved and had identifiable areas of comedonecrosis on additional whole mount immunohistochemistry slides using a cocktail of anti-p63 and anti-high molecular weight cytokeratin antibodies. Clinical outcome was assessed for biochemical recurrence, metastatic disease, and need for adjuvant therapy.

Results: Comedonecrosis was predominantly located only in intraductal carcinoma (24, 60%); however, 7 (18%) had intraductal and invasive comedonecrosis and 9 (23%) had comedonecrosis exclusively in invasive cancer. Most comedonecrosis was within the prostate, with extraprostatic extension instead containing perineural invasion; however, 5 (13%) had comedonecrosis in the extraprostatic extension. Tumors were overwhelmingly high-stage (15, 38% pT3a and 19, 48% pT3b) with 12 (30%) having positive lymph nodes. Most (25, 63%) had other patterns of Gleason pattern 5 (single cells, solid), although 9 were reclassified as including no invasive pattern 5 when combining morphology and immunohistochemistry. Of these, most were still pT3 (7/9), although this group did not have positive lymph nodes. Metastatic disease (to lymph nodes or distant) was more common in patients with invasive cancer containing comedonecrosis (p=0.02) and need for androgen deprivation was near-significant (p=0.07) in this group, although a difference in biochemical recurrence was not significant (p=0.58).

	Comedonecrosis in IDC only	Comedonecrosis with invasion	No Gleason 5 after reclassification
pT2	3	2	2
pT3a	12	3	5
pT3b	8	11	2
Lymph Nodes Positive	4	8	0
Grade Group 2	4	1	2
Grade Group 3	7	6	4
Grade Group 4	4	1	3
Grade Group 5	9	8	0
Other pattern 5	14	11	0
Total cases	24	16	9

IDC = intraductal carcinoma

Conclusions: Prostate cancer with comedonecrosis is usually, but not exclusively, intraductal; however, tumors are overwhelmingly high-stage regardless of intraductal status, with a modestly higher rate of positive lymph nodes with invasive comedonecrosis. We recommend that immunohistochemistry for basal cell markers be performed only when there is a suspicion that the cancer may be entirely intraductal, as decreasing the grade due to an intraductal carcinoma comedonecrosis component may belie the aggressive nature of these tumors. Future modifications of prostate cancer grading should reconsider how intraductal carcinoma with comedonecrosis is approached.

903 Diagnostic Utility of 5hmC Immunohistochemistry in Differentiating Seminoma from Nonseminomatous Elements: A Study of 83 Testicular Germ Cell Tumors

Elias Makhoul[1], Andrew Siref[2], Brian Cox[1], Daniel Luthringer[3], Mariza De Peralta-Venturina[3]
[1]Cedars-Sinai Medical Center, Los Angeles, CA, [2]Cedars-Sinai, Los Angeles, CA, [3]Cedars-Sinai Medical Center, West Hollywood, CA

Disclosures: Elias Makhoul: None; Andrew Siref: None; Brian Cox: None; Daniel Luthringer: None; Mariza De Peralta-Venturina: None

Background: Loss of 5-hydroxymethlycytosine (5hmC), an epigenetic marker of global methylation, has been reported in testicular tumors, melanoma, and urothelial carcinomas. We aim to study 5hmC immunohistochemical staining in a large cohort of testicular germ cell tumors to better determine its diagnostic utility in differentiating seminoma from nonseminomatous components.

Design: Testicular germ cell tumors found in the Cedars-Sinai Pathology files from 2012-2018 were included for study. Whole tissue section from a representative tumor block was stained with rabbit monoclonal antibody against 5hmC (clone RM 236; RevMD Biosciences, San Francisco, CA). Specific tumor components (seminoma, embryonal carcinoma, yolk sac tumor, teratoma, choriocarcinoma, intratubular germ cell neoplasm (ITGCN)) were identified and individually scored in terms of % and intensity of tumor cell staining (H-score). Lymphocytes and stromal cells served as positive internal control. Median H-scores were calculated and a Kruskal-Wallis Test was performed on H-score mean ranks for pairwise comparisons. Clinical follow up was evaluated on select cases.

Results: The cohort consisted of 83 cases including 29 pure seminomas, 50 mixed germ cell tumors, and 4 pure embryonal carcinomas. The tally of each tumor element analyzed included: 47 seminoma, 64 ITGCN, 41 embryonal carcinoma, 29 yolk sac tumor, 29 teratoma, and 11 choriocarcinoma. The majority of the seminoma cases (94%) showed complete loss or weak nuclear staining; 3 seminoma cases (6%) showed strong nuclear immunoreactivity (all 3 of these cases exhibited aggressive clinical behavior with metastases and recurrence). All ITGCN foci showed loss of 5hmC in contrast to uninvolved tubules. Cases of embryonal carcinoma and choriocarcinoma generally showed strong diffuse nuclear staining while yolk sac tumor showed moderate staining. Teratomas showed variable staining in both epithelial and stromal cell elements. The H-score difference between seminoma and nonseminomatous components was statistically significant (Figure 1 ($p < 0.001$)).

Figure 1 - 903

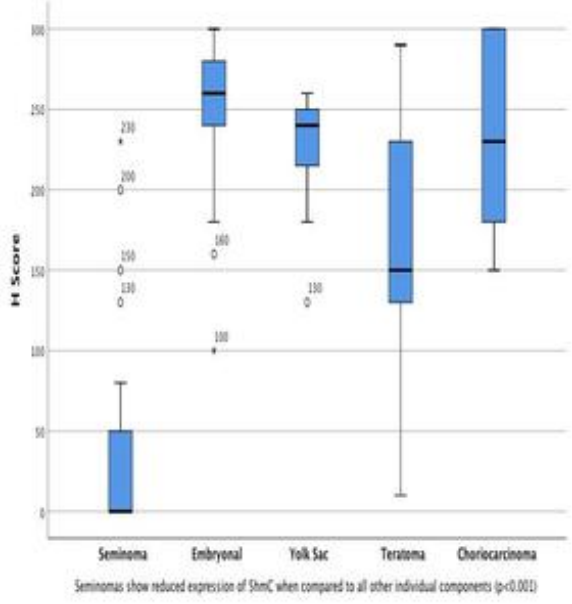

Conclusions: The epigenetic marker 5hmC is lost in seminoma and ITGCN but preserved in nonseminomatous components, indicating potential utility as a diagnostic biomarker in differentiating elements of germ cell tumor of the testis. A positive 5hmC staining in an otherwise typical seminoma may suggest more aggressive behavior.

904 The unrecognized morphology of SDHB Renal Cell Carcinoma and its metastasis. A report of 31 cases treated uniformly in a single Institution

Maria Merino[1], Borja Nevado Polo[2], Xu Naizhen[3], Ramaprasad Srinivasan[3], Marston Linehan[3]
[1]National Cancer Institute, Bethesda, MD, [2]Hospital Universitario 12 de Octubre, Madrid, Spain, [3]National Institutes of Health, Bethesda, MD

Disclosures: Maria Merino: None; Borja Nevado Polo: None; Xu Naizhen: None

Background: Renal cell carcinoma is the most common tumor of the kidney, accounting for approximately 90% of renal cancers. Five to 8% percent of RCCs are associated with hereditary syndromes such as Clear cell RCC seen in Von-Hippel-Lindau disease with mutations in chromosome 3, HLRCC associated with mutations in the Fumarate Hydratase gene, BHD with mutations in the folliculin gene and others such as SDHB with alterations in the genes encoding the proteins comprising the succinate dehydrogenase complex. Less tha 100 cases of this tumor have been reported and their morphology is still under study. We report 31 SDHB tumors their morphologic, genetic and molecular features as well as that of their metastasis. All patients were treated and studied in a single institution.

Design: Renal cell tumors diagnosed as SDHB kidney cancers were obtained from the archives of the Lab of Pathology, NCI, and personal consultation files (MJM). All patients were accepted for evaluation and treatment under an IRB approved protocol. SDHB protein expression was determined by immunohistochemistry (IHC) and genetic testing for SDHB mutation was performed in all patients. Clinical and histological features were studied. PDL-1 IHC staining was also performed in some cases.

Results: The age of the patients ranged from 17 to 69 year. Tumors affected females predominantly. Two patients presented with metastatic disease in bone (1) and liver (1). The size of the tumor varied from 1,5 to 4cm. Morphologically the predominante pattern was that of round clear and eosinophilic cells growing in a solid pattern. Two cases showed marked nuclear pleomorphism and occasional mistosis. Other tumors had a tubular and cystic appearance sometimes surrounded by dense fibrous tissue. A predominant spindle cell component was noted in three cases with the fusiform cells showing nuclear pleomorphism. Focal areas of necrosis were also seen. Two of the cases with the spindle cell areas metastasized to liver and bone and the metastasis were also spindle cell type. A third patient developed peritoneal metastasis similar to the primary tumor. All cases and the metastasis showed negative staining for SDHB. All patients were positive for SDHB mutation. PDL1 performed in some cases showed negative staining.

Conclusions: As new cases of confirmed SDHB are reported, new morphologic features are described that are important to recognize because as in two of our cases, the unrecognized features were present in the initial metastatic tumor.

905 Genital Verruciform Xanthoma: a Clinicopathologic Re-appraisal of 19 Cases

Mark Mochel[1], Jatin Gandhi[2], Aaron Udager[3], May Chan[4], Milton Randall[2], Mahul Amin[5], Rajiv Patel[4], Steven Smith[6]
[1]Virginia Commonwealth University School of Medicine, Richmond, VA, [2]University of Tennessee Health Science Center, Memphis, TN, [3]University of Michigan Medical School, Ann Arbor, MI, [4]University of Michigan, Ann Arbor, MI, [5]Methodist University Hospital, Memphis, TN, [6]Virginia Commonwealth University School of Medicine, Richmond, VA

Disclosures: Mark Mochel: None; Jatin Gandhi: None; Aaron Udager: None; May Chan: None; Milton Randall: None; Rajiv Patel: None; Steven Smith: None

Background: Verruciform xanthoma (VX) may rarely occur on genital sites, raising a differential diagnosis of warty lesions including squamous cell carcinoma. While case reports of unusual VX presentations predominate in the literature, data regarding prevalence of diagnostic histopathologic features in a consecutive series is limited.

Design: Clinicopathologic features of archival VX of genital sites from three academic centers were reviewed retrospectively. Histopathologic features evaluated included architecture, arrangement of parakeratosis, presence of neutrophils, dermal inflammation, and amount of xanthomatous macrophages. Clinical histories were evaluated for the presence of dyslipidemia, associated genital dermatitides, and systemic conditions.

Results: A total of 19 VXs of genital sites from 18 patients (17 M, 1 F) were reviewed. Average age was 67 years (range 45-97), with tumors located on the scrotum (17), penis (1), and perineum (1). Tumors ranged in size from 0.2 to 2.4 cm in greatest dimension. Coexisting genital dermatitis was documented in one patient with mild radiation dermatitis from radiotherapy for penile squamous cell carcinoma. Significant dyslipidemias were not identified. Histopathologic changes seen in all cases included verrucous architecture, wedge-shaped parakeratosis, accompanying neutrophilic infiltrates in the stratum corneum, and xanthomatous macrophages in the dermal papillae. These macrophages were abundant in 12 cases (63%), scattered in 3 cases (16%), and scarce in 4 cases (21%), with some regional variability in cases deemed abundant. Lichenoid inflammation was present in 4 cases (21%). Perivascular lymphocytic inflammation was generally mild (16 cases, 84%), although it was moderate or dense in 3 cases. Significant keratinocyte atypia was absent in all cases.

Conclusions: In addition to the classic histologic changes of VX, we find that the neutrophilic infiltrate in the parakeratotic stratum corneum, noted in prior reports, represents a uniform, characteristic feature. Supporting prior contentions that the diagnostic xanthomatous macrophages may be infrequent or scarce, we observed relative paucity in nearly 37% of VXs, underscoring the importance of recognizing ancillary features to prompt careful inspection. A subset demonstrated lichenoid inflammation. While other studies have noted associations with lichen sclerosus and lichen planus, this association was not seen in this series; in contrast, a single case was associated with radiation dermatitis.

906 Reappraisal of Human Epidermal Growth Factor Receptor 2 (HER2) in High-grade Urothelial Carcinoma (HGUCa) Based on American Society of Clinical Oncology (ASCO)/College of American Pathologists (CAP) Clinical Practice Guidelines, 2018

Sambit Mohanty[1], Ankit Tiwari[2], Manas Baisakh[3], Subhasini Naik[4], Preeti Chawla[5], Subodh Das[6], Manas Pradhan[7], Kali Satapathy[8], Jasreman Dhillon[9]

[1]AMRI Hospital, Bhubaneswar, India, [2]NISER, Jatni, India, [3]Apollo Hospitals, Bhubaneswar, India, [4]Prolife Diagnostics and Apollo Hospitals, Bhubaneswar, India, [5]Prolife Diagnostics, Bhubaneshwar, India, [6]Advanced Medical and Research Institute, Bhubaneswar, India, [7]Kalinga Hospital, Bhubaneswar, India, [8]Apollo Hospital, Bhubaneshwar, India, [9]Moffitt Cancer Center, Tampa, FL

Disclosures: Sambit Mohanty: None; Ankit Tiwari: None; Manas Baisakh: None; Subhasini Naik: None; Preeti Chawla: None; Manas Pradhan: None; Kali Satapathy: None; Jasreman Dhillon: None

Background: Accurate determination of HER2 amplification status in urothelial carcinoma (UCa) is necessary to identify patients that may most likely benefit from HER2-trageted treatment. ASCO and CAP have guidelines for HER2 interpretation via immunohistochemistry (IHC) and in situ hybridization (ISH), particularly dual probe fluorescence in situ hybridization (FISH) for breast cancer. Per 2013 guidelines for breast cancer, cases with mean HER2 signals/cell <4 and HER2/CEP17 ratio ≥2 are reported as HER2 positive, which is frequently observed in the setting of low mean HER2 copy number and loss of chromosome 17 copy number due to monosomy or loss of a portion of chromosome 17. 2018 Guidelines assign HER 2 status for the aforementioned group as positive or negative based on their IHC correlate. We sought to improve and standardize HER2 expression criteria in HGUCa utilizing ASCO/CAP 2018 guidelines, and compared various clinicopathologic parameters with HER2 status.

Design: Demographic data, tumor stage, histopathologic type, and molecular subtypes (based on GATA3, uroplakin 2, CK20, CK5/6 and CK14) of 78 cases of HGUCa were recorded and correlated with HER2 status (IHC, dual-probe FISH assays, 2018 guidelines). HER2 scoring per 2018 and 2013 criteria were compared.

Results: HER2 over expression was observed in 22 (28.2%) of cases (ASCO/CAP 2018) which was more frequent in micropapillary (MP) and squamous (SC) histologies, compared to conventional HGUCa (20 vs 2; p<0.00001). None of the small cell carcinoma cases HER2 amplified. Comparison of classification of tumors per 2013 criteria for HER2 status and re-classification per 2018 criteria is shown in Table 1. HER2 positivity did not show significant association with age, gender and tumor molecular subtypes and stage.

Table 1

2013 Classification	2018 Re-classification
36 positive	21 positive, 15 negative
5 equivocal	1 psitive, 4 negative
37 negative	37 negative

Conclusions: 1. HER2 over expression is observed in 28.2% of UCa and is more frequent with MP and SC histologies

2. Implementing 2018 guidelines, HER2 positive status decreased from 36 to 22 cases

3. The group with HER2/CEP17 ratio ≥2 and average HER2 copy number <4 were predominantly negative by IHC suggest a biologically distinct group of HGUCa, that is different from HER2 amplified tumors, which may not respond to HER2-targeted therapy

4. More studies are needed to generate a standardized HER2 scoring system for UCa

907 Molecular and structural variants in 22 Cases of Clear Cell Papillary Renal Cell Carcinoma

Diana Morlote[1], Jennifer Gordetsky[2], Denise Batista[3], Soroush Rais-Bahrami[2], Shuko Harada[2]
[1]The University of Alabama at Birmingham, Birmingham, AL, [2]University of Alabama at Birmingham, Birmingham, AL, [3]Johns Hopkins Medical Institutions, Baltimore, MD

Disclosures: Diana Morlote: None; Jennifer Gordetsky: None; Denise Batista: None; Soroush Rais-Bahrami: *Consultant*, Philips/InVivo Corp; *Advisory Board Member*, Genomic Health Inc; Shuko Harada: None

Background: Clear cell papillary renal cell carcinoma (CCP-RCC) is a rare entity comprising ~1% of all renal cell neoplasms. It was described in 2009 as being associated with end-stage renal disease, however, most cases have been found to be sporadic. We have previously performed targeted next generation sequencing (NGS) analysis of 16 CCP-RCC cases and identified 15 non-synonymous somatic variants. In this study, we expanded the NGS analysis to include 22 CCP-RCC cases, along with analysis of chromosomal structural variants determined by virtual karyotypes generated from single nucleotide polymorphism (SNP)-array analysis.

Design: Twenty-two morphologically and immunohistochemically typical cases of CCP-RCC were selected and genomic DNA was isolated from the tumor areas of formalin fixed paraffin embedded (FFPE) samples. Targeted NGS of 90 cancer related genes was performed using HaloPlex HS custom probe and Illumina MiSeq. SNP-array analyses were performed on the Illumina Infinium II SNP array with 850K markers after DNA was restored using Infinium HD FFPE DNA Restore Kit.

Results: NGS analysis demonstrated 30 somatic non-synonymous variants (excluding polymorphisms) across 14 of the 22 cases sequenced (64%). These included 14 new variants and one recurrent variant in the ASXL1 gene (p. D905V). Seven variants were previously reported in the COSMIC database (Figure 1). Three cases had VHL variants. One potentially actionable variant was identified in the EGFR gene (p.V765M).
SNP-array analysis found abnormalities in 5 of the 22 cases (23%) (Table 1). These included gain of chromosomes 18 in one case, 3 and 12 in another case, and complex abnormalities in three other cases. An additional case had large regions with absence of heterozygosity with no copy number changes, suggestive of parental consanguinity. Interestingly, cases with no variants detected by NGS failed to show copy number variants.

Table 1. Summary of Next Generation Sequencing and SNP-array Results of 22 Cases of CCP-RCC

NGS Variants															Cases											
Gene	Variant	Cosmic ID	SIFT/Polyphen	1	2	3	4	5	6	7	8	9	10	11	12	13	14	15	16	17	18	19	20	21	22
AKT2	p.D457G		Tolerated/Benign							x															
APC	p.L239F		Deleterious/Probably Probably damaging																x						
ASXL1	p.H633R		Tolerated/Benign		x																				
ASXL1	p.P805T		Tolerated/Benign														x								
ASXL1	p.D905V		NP/Benign													x							x		
ATM	p.E641G		Tolerated/Benign																	x					
ATM	p.T2035I		Deleterious/Probably damaging							x															
ATM	p.C2464R	COSM758329	Tolerated/Possibly damaging																x						
ATM	p.V2915M		Deleterious/Probably damaging													x									
BCOR1	p.S56C		Deleterious/Probably damaging													x									
BRCA2	p.S976I		NP/NP					x																	
BRCA2	p.E3053G		Deleterious/Probably damaging																x						
CALR	p.V349I		Tolerated/Benign							x															
CDH1	p.R545L		Tolerated/Possibly damaging											x											
CDKN2A	p.A108S		NP/Benign		x																				
CDKN2A	p.R165S	COSM4984892	Deleterious/NP																					x	
EGFR	p.V765M	COSM28603	Tolerated/Possibly damaging			x																			
ERBB2	p.S442L		NP/Probably damaging													x									
JAK1	p.Q565*		NP/NP					x																	
KMT2A	p.V1234M		Deleterious/Benign																			x			
NF1	p.S1262Y		Tolerated/Probably damaging																						x
PHF6	p.I33M		Tolerated/Benign																x						
PIK3R2	p.V54M		Deleterious/Benign																		x				
SETBP1	p.A246T		Tolerated/Benign							x															
SMC1A	p.A73D		Deleterious/Probably damaging											x											
VHL	p.V74G	COSM3364888	NP/Benign															x							
VHL	p.N78S	COSM17855	NP/Possibly damaging			x																			
VHL	p.S80N	COSM30216	Deleterious/probably damaging														x								
ZRSR2	p.R448_R449insSR	COSM5762985	NP/NP							x															
			SNP Array Data	N	N	N	N	N	N	N	N	N	N*	N	N	gain 18	N	N	3p-, 3q-, 6q-, 14q-, Xq LOH	CNC or CN-LOH for chromosomes 1, 2, 3, 4, 6, 7, 8, 9, 10, 11, 13, 14,15, 22	N	N	CNC or CN-LOH for chromosomes 2, 3, 4, 5, 8, 10, 11, 12, 16, 18, 19	N	gain 3, gain 12

CNC: Copy-number change
CN: Copy neutral
LOH: Loss of heterozygosity
N: No copy-number changes detected
NP: Not provided
* Absence of heterozygosity with no copy number changes, suggestive of parental consanguinity

Conclusions: Our study reflects the lack of disease-specific variants in CCP-RCC and raises a possibility that CCP-RCC consists of genetically heterogeneous tumors. All cases of CCP-RCC studied proved to be genetically different from papillary renal cell carcinoma in that trisomy 7 and 17 are not characteristic features. A subset of immunohistochemically typical CCP-RCC cases share genetic abnormalities with clear cell renal cell carcinoma. Whether this particular subset of CCP-RCC still behave in an indolent manner remains to be determined.

908 A Clincopathologic Analysis of Patients Undergoing Early Repeat Transurethral Resection of Bladder Tumor Following an Initial Diagnosis of Urothelial Carcinoma with Lamina Propria Invasion

Patrick Mullane[1], Mehrdad Alemozaffar[1], Adeboye O. Osunkoya[2]
[1]Emory University, Atlanta, GA, [2]Emory University School of Medicine, Atlanta, GA

Disclosures: Patrick Mullane: None; Mehrdad Alemozaffar: None; Adeboye O. Osunkoya: None

Background: Patients diagnosed with urothelial carcinoma (UCa) with lamina propria (LP) invasion in bladder biopsies are at significant risk for recurrence and have increased rates of progression to UCa with muscularis propria (MP) invasion. The ability to identify patients at risk of recurrence and progression to UCa with MP invasion based on clinicopathologic characteristics thus holds prognostic significance. Here, we describe the clinical and pathologic characteristics of patients with UCa with LP invasion who underwent early re-resection TURBT at a major academic institution.

Design: We searched our Urologic Pathology files, and expert consult cases of the senior author for patients who subsequently underwent early repeat TURBT within 8 weeks of an initial diagnosis of UCa with lamina propria invasion on biopsy (2014-present). Patients whose re-resections were delayed (>8 weeks), or had a prior diagnosis of UCa with MP invasion were excluded.

Results: Fifty-seven patients were identified. Majority 34/57 (60%) were male, and 23/57 (40%) were female. The mean age was 74 years (range: 52-90 years). MP was identified in 32/57 (56%) of initial resections, and 46/57 (81%) of re-resections. On re-resection, 36/57 (63%) of patients had persistent UCa; 7/57 (12%) were diagnosed with MP invasion, 15/57 (26%) with LP invasion, 5/57 (9%) with non-invasive papillary UCa, and 9/57 (16%) with UCa in situ. In 5/7 (71%) patients who were upstaged to UCa with MP invasion, MP was not identified on the initial biopsy. Newly identified variants of UCa were observed in 5/57 (9%) repeat resections (UCa with squamous differentiation [2 cases, 1 of which had an additional glandular component], UCa with glandular differentiation [1 case], UCa with clear cell component [1 case], and UCa with sarcomatoid differentiation [1 case]).

Conclusions: In our single institutional cohort of patients undergoing early repeat TURBT, the majority of patients (65%) had persistent UCa. Histologic detection of MP increased from 56% to 81% on re-resection with 12% rate of upstaging to UCa with MP invasion. Our findings support early repeat resection for UCa with LP invasion, and highlight the critical role of repeat bladder sampling to improve the diagnosis of UCa with MP invasion. In addition, 5 cases (9%) had potentially aggressive variants of UCa detected (some requiring different therapeutic regimens) in the re-resection specimen, which would otherwise have been missed.

909 Detection of Carcinoma in Situ of the Bladder Using Blue Light Cystoscopy (BLC) and the Role and Reliability of Traditional Histomorphology Over Immunohistochemistry in the Diagnosis of Dubious BLC-Positive Lesions

Belkiss Murati Amador[1], Iryna Samarska[2], Filippo Pederzoli[3], Trinity Bivalacqua[4], Andres Matoso[5]
[1]Johns Hopkins University School of Medicine, Baltimore, MD, [2]Johns Hopkins University School of Medicine, Maastricht University Medical Center, Maastricht, Netherlands, [3]IRCCS San Raffaele Hospital, Milano, Italy, [4]Johns Hopkins University, Baltimore, MD, [5]Johns Hopkins Medical Institutions, Baltimore, MD

Disclosures: Belkiss Murati Amador: None; Iryna Samarska: None; Filippo Pederzoli: None; Andres Matoso: None

Background: Carcinoma in situ (CIS) is difficult to visualize with traditional white light cystoscopy (WLC), whereas blue light cystoscopy (BLC) using a photosensitizing drug improves detection rates.

Design: We retrospectively reviewed our pathology files to identify all the TURBs in which both WLC and BLC evaluations were performed from 2015-2017 (N=255). Only patients with at least one diagnosis of CIS were included in the study (n=135). Biopsies were classified based on the presence/absence of fluorescence under BLC and the final pathological report (CIS/normal/atypical). 11 BLC-positive were diagnosed as dysplasia/atypical, but not definitive for CIS. These 11 atypical cases were anonymized and evaluated by 7 pathologists for concordance of CIS vs. non-CIS. Then, we performed immunohistochemistry for CK20, p53 and Ki67 and the results were interpreted as consistent with CIS if there was full thickness staining of CK20, more than 50% p53-positive cells more than 50% Ki67-positive cells.

Results: Out of 135 biopsies, 41 (30.4%) were diagnosed as CIS; of those, 38 (92.7%) were BLC(+), and 23 of 38 (60%) were BLC(+), but WLC(-). Conversely, 51 (37.8%) lesions were BLC(+), but were classified as non-malignant (benign urothelium, dysplasia or atypia). Review of BLC(+)/pathology-atypical cases showed a mean agreement of 79% by the reviewer pathologists, but none of the cases showed staining pattern consistent with CIS (Table 1). Only one case showed focal full thickness staining for CK20 but was negative for p53 and Ki67 was positive in less than 5% of the cells. Therefore, all 11 cases of BCL(+)/pathology-atypical were considered non-CIS for the final analysis. Using final pathology as the reference standard, sensitivity, specificity and negative predictive value (NPV) of blue light cystoscopy were 92.7% (CI 80.1%-98.5%), 45.7% (CI 35.4%-56.3%) and 93.5% (CI 82.5%-97.8%), respectively.

Pathologists report and IHC staining interpretation of the 11 BLC(+)/pathology-atypical biopsies analyzed.

	Path #1		Path #2		Path #3		Path #4		Path #5		Path #6		Path #7		IHC	
	CIS	Not CIS	CIS	Not CIS	CIS	Not CIS	CIS	Not CIS	CIS	Not CIS	CIS	Not CIS	CIS	Not CIS	p53/Ki67/CK20 pattern	
Lesion 1		X		X		X		X		X		X		X	Not CIS	
Lesion 2		X		X		X		X		X		X		X	Not CIS	
Lesion 3		X		X		X	X			X		X		X	Not CIS	
Lesion 4		X		X		X	X			X		X		X	Not CIS	
Lesion 5		X		X		X		X		X		X		X	Not CIS	
Lesion 6	X			X		X		X		X		X		X	Uninterpretable	
Lesion 7		X		X	X		X			X		X		X	Not CIS	
Lesion 8		X		X		X	X			X		X		X	Not CIS	
Lesion 9	X		X		X		X			X	X		X		Not CIS	
Lesion 10	X			X	X			X		X		X		X	Not CIS	
Lesion 11		X	X			X	X			X		X		X	Not CIS	

Conclusions: BLC is very sensitive in the identification of CIS that may be missed under traditional WLC. Morphological classification of CIS vs. non-CIS lesions is fairly consistent among different pathologists and performing IHC stains for CK20, Ki67, and p53 does not change the classification of atypical cases into CIS. Use of IHC in this setting is only helpful to potentially avoid overcalling CIS.

910 Outcome of Unexpected Prostatic Urethral Involvement at Cystoprostatectomy for Non-Muscle Invasive Bladder Cancer: Implications for Prostate Sparing Cystectomy

Belkiss Murati Amador[1], Iryna Samarska[2], Trinity Bivalacqua[3], Max Kates[4], Andres Matoso[5]
[1]Johns Hopkins University School of Medicine, Baltimore, MD, [2]Johns Hopkins University School of Medicine, Maastricht University Medical Center, Maastricht, Netherlands, [3]Johns Hopkins University, Baltimore, MD, [4]Johns Hopkins Hospital, Baltimore, MD, [5]Johns Hopkins Medical Institutions, Baltimore, MD

Disclosures: Belkiss Murati Amador: None; Iryna Samarska: None; Andres Matoso: None

Background: Prostate sparing cystectomy has been proposed as a less morbid approach to treat high-risk non-muscle invasive urothelial carcinoma in patients with no presurgical clinical/biopsy evidence of prostatic urethral involvement. The effect of PUI in NMIBC who were not upstaged at radical cystoprostatectomy had not been studied before.

Design: From 2000-2016, 183 male patients underwent RCP for high-risk NMIBC and remained pT1, pTis, or pTa, and pN0 on final RCP pathology. The presence of prostatic urethral involvement and the clinical follow-up were recorded.

Results: 65 (35.5%) patients had PUI and 118 (64.5%) did not. Prostatic involvement was non-invasive (pTa or pTis) in 57 (87.7%) patients and superficially invasive (pT1) in 8 (12.3%) patients. No patient had prostatic stromal invasion. Compared to patients without PUI, patients with involvement were more likely to undergo cystectomy >2 years after diagnosis (33.8% vs. 20.2%, p<0.05), more likely to have received intravesical therapy (84.6% vs. 64.4%, p<0.01), and more likely to have positive ureteral margins (18.5% vs. 5.1%, p<0.01). Sensitivity of prostatic urethral biopsy prior to RCP was 68.4% and specificity was 81.6%. Log-rank comparison showed inferior recurrence-free, cancer-specific, and overall survival in patients with prostatic involvement (p<0.03, P<0.05, p<0.01). On Cox regression, prostatic urethral involvement was an independent predictor of recurrence (HR=2.46, P<0.01), cancer-specific mortality (HR=2.25, p<0.04), and overall mortality (HR=2.35, p<0.01). There were no significant differences found for age (p=0.58) race (p=0.66), smoking status (p=0.64), CIS (p=0.07), variant histology (p=0.13), clinical T stage (p=0.17), or pathologic T stage (p=0.27).

Conclusions: PUI is an adverse pathologic finding at RCP independent of its association with upstaging, emphasizing the importance of complete sampling of the urethra. These adverse findings together with the low sensitivity and specificity of presurgical urethral biopsy are important findings that suggest that prostate sparing cystectomy is associated with significant risk of poor oncologic outcome.

911 Morphologic Characterization of High-Grade Bladder Tumors with Negative Urine Cytology: Comparison of Findings with Blue Light versus White Light Cystoscopy

Belkiss Murati Amador[1], Iryna Samarska[2], Christopher VandenBussche[3], Andres Matoso[4]
[1]Johns Hopkins University School of Medicine, Baltimore, MD, [2]Johns Hopkins University School of Medicine, Maastricht University Medical Center, Maastricht, Netherlands, [3]Johns Hopkins Hospital, Baltimore, MD, [4]Johns Hopkins Medical Institutions, Baltimore, MD

Disclosures: Belkiss Murati Amador: None; Iryna Samarska: None; Christopher VandenBussche: *Grant or Research Support*, PapGene; Andres Matoso: None

Background: Urine cytology is used to screen and follow-up patients with history of urothelial carcinoma (UC), but its sensitivity is not 100% leading to a significant number of false negative cases. Blue light cystoscopy (BLC) is a new technology reported to improve detection of lesions when compared to white light cystoscopy (WLC). This higher sensitivity would be of particular importance in patients with negative urine cytology who otherwise would stay undiagnosed. Given its higher sensitivity, we hypothesized that the spectrum of lesions detected with BLC differ from those of WLC.

Design: We searched the pathology database for surgical specimens with diagnosis of UC from 1/1/2009 to 8/31/2018 in patients who had concurrent (within 7 days) urine cytology. Positive biopsies were considered those with carcinoma in situ (CIS), non-invasive high grade (HG) papillary UC, or infiltrating HG UC. Positive biopsies with negative concurrent cytology (false negative cytology) were included in the study and the findings of BLC versus WLC were compared.

Results: A total of 296 concomitant samples from 190 patients were identified. 199/296 (67.2%) samples from 120/190 (63%) patients were concordant. 70/190 (36.8%) patients with 97 discordant pairs were identified. 31 samples from 28/190 (15%) patients had positive biopsies with negative urine cytology (false negative cytology). Of these, 3 were non-invasive papillary UC, borderline between low/high grade (1 detected with BLC, 2 with WLC), 3 were non-invasive HG papillary UC in which the tumor was predominantly (≥90%) low-grade (1 detected with BLC, 2 with WLC). 5 non-invasive HG papillary UC (1 detected with BLC, 4 with WLC), 12 cases were CIS, most cases involving only 1 out of multiple (3-5) samples (6 detected with BLC, 6 with WLC), and 8 infiltrating HG UC including a carcinoma that lacked a papillary component (n=1) and a case with substantial (but <90%) low grade papillary component present (n=1) (3 cases with BLC, 5 with WLC).

Conclusions: The rate of discordant biopsy/cytology is 37% with a false negative rate of 15%. Both BLC and WLC detect similar spectrum of malignant lesions that were missed on concurrent cytology despite the reported higher sensitivity of BLC. A study with a larger number of cases would possibly help to better identify the specific situations in which BLC would result beneficial compared to WLC.

912 Malignant Sex Cord Stromal Tumors of the Testis: A Comprehensive Genomic Profiling Study

Rochelle Nagales Nagamos[1], Gennady Bratslavsky[1], Joseph Jacob[1], Oleg Shapiro[1], Julia Elvin[2], Jo-Anne Vergilio[2], J. Keith Killian[2], Nhu Ngo[2], Shakti Ramkissoon[3], Eric Severson[3], Amanda Hemmerich[3], Siraj Ali[4], Alexa Schrock[2], Jon Chung[2], Venkataprasanth Reddy[2], Vincent Miller[2], Laurie Gay[4], Robert Corona[5], Jeffrey Ross[6]
[1]SUNY Upstate Medical University, Syracuse, NY, [2]Foundation Medicine, Cambridge, MA, [3]Foundation Medicine, Morrisville, NC, [4]Cambridge, MA, [5]Syracuse, NY, [6]Upstate Medical University, Syracuse, NY

Disclosures: Rochelle Nagales Nagamos: None; Oleg Shapiro: None; Julia Elvin: *Employee*, Foundation Medicine, Inc; J. Keith Killian: *Employee*, Foundation Medicine, Inc.; Nhu Ngo: None; Eric Severson: *Employee*, Foundation Medicine, Inc.; Amanda Hemmerich: *Employee*, Foundation Medicine, Inc.; Alexa Schrock: *Employee*, Foundation Medicine Inc.; Vincent Miller: *Employee*, Foundation Medicine Inc.; *Advisory Board Member*, Revolution Medicines; Laurie Gay: *Employee*, Foundation Medicine, Inc.; Jeffrey Ross: *Employee*, Foundation Medicine, Inc.

Background: The molecular features of the uncommon malignant sex cord stromal tumors of the testis (MSCST) have not been widely evaluated. We performed comprehensive genomic profiling (CGP) to compare the genomic alterations (GA) in 3 groups of malignant SCST: Leydig Cell Tumors (LCT), Sertoli Cell Tumors (SCT) and Undifferentiated (USCST).

Design: From a series of 181,782 FFPE tissues from clinically advanced tumors, 10 cases of LCT, 6 cases of SCT and 3 cases of USCST underwent hybrid-capture based CGP to evaluate all classes of genomic alterations. Tumor mutational burden (TMB) was determined on 1.1 Mbp of sequenced DNA and microsatellite instability (MSI) was determined on 114 loci.

Results: All patients had clinically advanced recurrent and/or metastatic disease. The primary testis tumor was used for sequencing in 6 MSCST (32%) and a metastatic site (lymph node, bone, GI tract or lung) in 9 (68%) of the MSCST. Of 11 cases where inhibin IHC staining was performed, 10 (91%) stained positively. The LCT patients were older than the SCT or USCST patients (Table). The total GA was similar in all 3 groups and ranged from 3.0 to 3.5 GA/tumor. The most frequent non-clinically relevant (CR) GA seen in all three tumor types included *CTNNB1* and *CDKN2A/B* both ranging from 20-33% of cases. CRGA were uncommon but included potential for cell cycle inhibitors (*CDK4* in LCT), MTOR inhibitors (*RICTOR*, *NF2* and *PTEN* in all 3 tumor types), hedgehog inhibitors (*PTCH1* in LCT) and PARP

inhibitors (*BAP1* in SCT). All 19 MSCST were MSI stable and TMB was low in all three groups with no (0%) tumors have a TMB of > 10 mutations/MB.

	Leydig (LCT)	Sertoli (SCT)	Undifferentiated (USTST)
Number of Cases	10	6	3
Median age (range) in years	72 (50-85)	44 (12-68)	55 (32-86)
GA/tumor	3.5	3.0	3.0
Top Non-CRGA	*MDM2* 50% *CTNNB1* 20% *CDKN2A* 20% *CDKN2B* 20% *GLI1* 20% *TP53* 10%	*CTNNB1* 33% *PRKAR1A* 33% *CDKN2A* 17% *CDKN2B* 17% *BLM* 17% *TP53* 17%	*RB1* 67% *CDKN2A* 33% *CDKN2B* 33% *CTNNB1* 33% *APC* 33%
Top CRGA	*CDK4* 50% *RICTOR* 20% *PTCH1* 10%	*NF2* 17% *RICTOR* 17% *BAP1* 17%	*ESR1* 33% *PTEN* 33%
MSI-High	0%	0%	0%
Mean TMB (mut/Mb)	2.3	2.0	2.9
Median TMB (mut/Mb)	1.9	1.7	3.5
TMB>10 mut/Mb	0%	0%	0%

Conclusions: MSCST of the testis consist of 3 main tumor types with differing pathologic features but similar genomic signatures on CGP. The MSCST of the testis appear genetically stable, with low levels of aneuploidy, low GA per tumor, absence of MSI high status and low TMB. Although rare cases reveal GA linked to potential targeted therapy benefits in multiple biologic pathways, the low TMB in this patient cohort indicates a likely lack of benefit for immunotherapies for these rare forms of malignancy.

913 Testosterone Replacement Therapy Is Able to Reduce Prostate Inflammation in Men with BPH, Metabolic Syndrome and Hypogonadism: Preliminary Results from a Randomized Placebo-Controlled Clinical Trial

Gabriella Nesi[1], Raffaella Santi[2], Giulia Rastrelli[1], Sarah Cipriani[1], Francesco Lotti[1], Ilaria Cellai[1], Paolo Comeglio[1], Mauro Gacci[1], Sergio Serni[1], Mario Maggi[1], Linda Vignozzi[1]
[1]University of Florence, Florence, Italy, [2]Florence, Italy

Disclosures: Gabriella Nesi: None; Raffaella Santi: None; Giulia Rastrelli: None; Sarah Cipriani: None; Francesco Lotti: None; Ilaria Cellai: None; Paolo Comeglio: None; Mario Maggi: None; Linda Vignozzi: None

Background: BPH results from prostate tissue inflammation, frequent in men with metabolic syndrome (MetS). Recent evidence shows that low T levels are related to BPH/lower urinary tract symptoms (LUTS). The aim of the study was to evaluate if T replacement therapy (TRT) in BPH men with MetS and low T can improve LUTS and prostate inflammation.

Design: A total of 120 men scheduled for BPH surgery and diagnosed with MetS were enrolled. Depending on total T (TT) and calculated free T (cFT), they were categorized as eugonadal (TT≥12 nmol/L and cFT≥225 pmol/L; n=48) and hypogonadal (TT<12 nmol/L and/or cFT<225 pmol/L; n=72). Hypogonadal men were randomly given T gel 2% (5 g/daily; n=38) or placebo (n=34) for 6 months. At baseline and follow-up visit, all men completed the International Prostatic Symptoms Score (IPSS) and NIH-Chronic Prostatitis Symptom Index (NIH-CSPI) questionnaires and underwent a trans-rectal prostate ultrasound. After surgery, prostate tissue was collected for RT-PCR and histologic analysis.

Results: After adjusting for baseline value, age, TT and waist circumference, both groups showed a significant decrease in NIH-CSPI ($p<0.001$ vs. baseline) but not for IPSS total score. IPSS bother score significantly decreased only in T-treated men ($p=0.042$ vs. baseline value). Despite an increase in total prostate and adenoma volume (both $p<0.05$ vs. the baseline value), T arm showed a decrease in ultrasound markers of prostate inflammation, i.e. arterial velocity and acceleration (both $p<0.01$ vs. baseline value). In 67 men (31

eugonadal, 19 placebo and 17 T-treated), inflammatory marker expression was evaluated in prostate tissue. Several genes (i.e. RORγt, PSA, LDLoxR, RAGE) were hyper-expressed in hypogonadal men treated with placebo as compared with eugonaldal men. Conversely, TRT was associated with a significant decrease in mRNA expression of inflammatory markers, including those related to metabolic-induced inflammation (COX2, MCP1, IP10, RORγt, TLR2, LDLoxR, RAGE, IRS1). In 40 men (23 eugonadal, 8 placebo and 9 T-treated), prostate inflammation was histologically assessed. The inflammatory score, comprehensive of anatomic location, grade and extent of inflammation, was similar in eugonadal and placebo-treated men, while a reduction was observed in T-treated men (p= 0.289 and 0.349 vs. eugonadal or placebo-treated men, respectively).

Conclusions: TRT can improve clinical, molecular and histologic proxies of prostate inflammation in hypogonadal men with BPH and MetS.

914 Perivascular Epithelioid Cell Neoplasms (PEComas) of the Urinary Bladder: A Morphological Study Including TFE3 FISH

Neil Neumann[1], Michael Haffner[2], Pedram Argani[3], Jonathan Epstein[4]
[1]Johns Hopkins University, Baltimore, MD, [2]Johns Hopkins Medicine, Baltimore, MD, [3]Johns Hopkins Hospital, Ellicott City, MD, [4]Johns Hopkins Medical Institutions, Baltimore, MD

Disclosures: Neil Neumann: None; Michael Haffner: None; Pedram Argani: None; Jonathan Epstein: None

Background: Perivascular epithelioid cell neoplasms (PEComas) of the urinary bladder are extremely rare, with only 23 case reports in the literature. A subset of PEComas contain TFE3 gene rearrangement and present with distinctive morphological features, with only 3 cases reported in the bladder. Although PEComas are most often benign, malignant PEComas include some of the following features: >5cm; necrosis; infiltrative growth pattern; hypercellularity with atypia; increased mitotic figures; atypical mitotic figures.

Design: 7 cases of bladder PEComas were collected from 01/2008 to 09/2018, including 1 internal and 6 consults.

Results: 5 patients were female and 2 male. The mean age was 44.1 years (range: 24-60 years). In none of the 6 consult cases was PEComa considered in the differential diagnosis by the outside referring pathologists. In 6 of 7 cases, prominent epithelioid features were noted, with the final case having focal epithelioid morphology. In 6 of 7 cases there was typical PEComa cytoplasmic clearing, with the final case having 80% amphophilic cytoplasm. Mitotic rate was increased in 1 of 7 cases, and 2 of 7 cases had cytological atypia. Immunostains and FISH are in Table 1. Regional invasion occurred in 1 case, while another was metastatic to the lungs and brain, ultimately killing the patient. Both of these cases had morphological features of malignancy.

Table 1, Bladder PEComa IHC and FISH

Stain	Positive	Negative	Pending
TFE3 FISH	3	0	4
Cathepsin K	7	0	0
HMB-45	4	2	1
Smooth Muscle Actin	1	6	0
Desmin	2	4	1
Keratin AE1/3	0	7	0
Melan-A	0	6	1

Conclusions: Bladder PEComas are particularly difficult to diagnose, given they are predominantly epithelioid, do not always express melanocytic markers, and due to their rarity at this site are not considered in the differential diagnosis. As in the kidney, there is morphological overlap with TFE3 rearranged renal cell carcinoma (RCC), although the absence of a radiological renal mass rules out metastatic RCC. Other differential diagnoses for this tumor include alveolar soft tissue sarcoma, paraganglioma, melanoma, and prostatic adenocarcinoma. Diagnosis requires a combination of morphological characterization, positive cathepsin K staining, variable melanocytic marker expression, along with a TFE3 gene rearrangement. Also needed are selective negative IHC stains to exclude other differential diagnoses (ie. negative neuroendocrine markers and GATA3 to r/o paraganglioma).

915 Comparison of Immunohistochemical Expression of Biomarkers between Cribriform and Non-Cribriform Gleason 4 Prostate Adenocarcinoma

Elise Nguyen[1], Pamela Unger[2], Guang-Qian Xiao[3]
[1]USC/LAC+USC Medical Center, Los Angeles, CA, [2]New York, NY, [3]Keck School of Medicine of University of Southern California, Los Angeles, CA

Disclosures: Elise Nguyen: None; Pamela Unger: None; Guang-Qian Xiao: None

Background: Gleason 4 cribriform prostate adenocarcinoma (PCa) has been shown in the recent literature to have strong association with adverse pathologic features and clinical outcomes when compared to non-cribriform Gleason 4 PCa. Studies have also demonstrated that particular molecular alterations are more common in patients with cribriform PCa than in those with non-cribriform Gleason 4 PCa. The aim of this study is to compare the immunohistochemical (IHC) profiles of various biomarkers in cribriform and non-cribriform Gleason 4 PCa.

Design: Two tissue microarrays mounted with PCa from radical prostatectomy were subjected to IHC study for various biomarkers, including tumor suppressor, cell cycle regulator, proliferative and survival as well as stem cell-related antibodies (see Table 1). IHC was performed using DAKO automated platform with validated controls. The intensity and extent of the IHC stains were graded semi-quantitatively as follows: 0 (none), 1+ (focal and weak), 2+ (moderate), 3+ (strong and diffuse). At analysis, 0 and 1+ were considered negative, and 2+ and 3+ were considered positive. The IHC expression results were subsequently grouped morphologically into Gleason 4 cribriform and non-cribriform when statistics were performed using two-proportion Z-test.

Results: Cribriform and non-cribriform pattern Gleason 4 PCa differed significantly in IHC staining for EGFR: 65.9% of cases with cribriform Gleason 4 PCa were positive for EGFR, while only 32.7% of cases with non-cribriform Gleason 4 cancer were reactive with EGFR (P = 0.0016). 85.7% cribriform and 71.8% non-cribriform Gleason 4 PCa were negative for stem cell-related marker CD44, with the difference also being statistically significant (P = 0.04). IHC stains did not show statistical significant difference between the two groups for the expression of androgen receptor, NKX3.1, Synaptophysin, EZH2, p53, c-Myc, BCL2, p16, Rb, and Cyclin D1. The results are summarized in Table 1.

	(n)					
	AR	NKX3.1	SYN	EZH2	P53	cMyc
Cribriform PCa						
3+/2+	(34) 91.89%	(43) 84.31%	(4) 22.22%	(26) 49.06%	(9) 12.33%	(3) 5.17%
1+/-	(3) 8.11%	(8) 15.69%	(14) 77.78%	(27) 50.94%	(64) 87.67%	(55) 94.83%
Total	37	51	18	53	73	58
GS4 Non-Cribriform PCa						
3+/2+	(33) 86.84%	(58) 85.29%	(5) 17.24%	(24) 36.36%	(7) 7.07%	(2) 2.67%
1+/ -	(5) 13.16%	(10) 14.71%	(24) 82.76%	(42) 63.64%	(92) 92.93%	(73) 97.33%
Total	38	68	29	66	99	75
P Value	0.4788	0.8826	0.6731	0.1632	0.2406	0.4512
	BLC2	P16	EGFR	Rb	Cyclin D1	CD44
Cribriform PCa						
3+/2+	(9) 12%	(30) 40.54%	(29) 65.91%	(6) 15%	(16) 24.62%	(10) 14.29%
1+/-	(66) 88%	(44) 59.46%	(15) 34.09%	(34) 85%	(49) 75.38%	(60) 85.71%
Total	75	74	44	40	65	70
GS4 Non-Cribriform PCa						
3+/2+	(6) 7.41%	(49) 43.75%	(15) 32.61%	(3) 5.17%	(31) 33.33%	(24) 28.24%
1+/ -	(75) 92.59%	(63) 56.25%	(31) 67.39%	(55) 94.83%	(62) 66.67%	(61) 71.76%
Total	81	112	46	58	93	85
P Value	0.331	0.6647	0.0016	0.0978	0.2382	0.0367

Conclusions: Our results demonstrate that cribriform and non-cribriform Gleason 4 PCa differ significantly in IHC expression of EGFR and CD44. In comparison with non-cribriform Gleason 4 PCa, the significant overexpression of EGFR and downregulation of CD44 in cribriform PCa may partly explain the adverse clinical outcome associated with this growth pattern. The findings may also have potential prognostic and future therapeutic implications.

916 Prostate Cancer with Cribriform and Intraductal Growth at Radical Prostatectomy: Correlation with Biopsy Morphology and NCCN Risk Classification

Sarah Ni Mhaolcatha[1], Susan Prendeville[2]
[1]Cork University Hospital, Cork, Ireland, [2]Cork, Ireland

Disclosures: Sarah Ni Mhaolcatha: None; Susan Prendeville: None

Background: The adverse clinical outcome of prostate cancer (PCa) harbouring intraductal and/or invasive cribriform carcinoma (IDC/CR) is increasingly recognised, making accurate risk classification of IDC/CR+ PCa essential for optimal clinical management. The National Comprehensive Cancer Network (NCCN) risk-stratify PCa based on clinical and pathologic variables at prostate biopsy (PBx) and have recently endorsed active surveillance (AS) as a potential management option in certain Grade Group (GG) 2 PCa. IDC/CR morphology is not included in this risk grouping. This study aimed to 1) determine the NCCN risk classification of IDC/CR+ PCa; 2) determine the sensitivity of PBx for the diagnosis of IDC/CR+ PCa.

Design: 281 consecutive RP cases were reviewed. All IDC/CR+ cases were selected for inclusion in the study. Additional RP variables including GG and stage were recorded.

The corresponding PBx was reviewed and the following parameters recorded: IDC/CR morphology, GG, number of positive cores and maximum % core involvement. IDC/CR was defined using published criteria. Clinical variables including serum PSA level and clinical T-stage were retrieved from the clinical records. Cases were classified into 1 of 6 NCCN defined risk groups based on clinical and pathologic variables at diagnosis (NCCN guidelines 2018).

Results: IDC/CR was identified in 73 cases (26%). RP GG was: GG1 in 0%, GG2 in 48%, GG3 in 43%, GG4 in 4% and GG5 in 5%. The RP T-stage distribution was pT2 in 44%, pT3a in 40% and pT3b in 16%. Lymph node metastases (pN1) were identified in 14% of cases.

Clinical parameters and pathologic variables at PBx are outlined in table 1. Median PSA at diagnosis was 7.35 (range 3-26). IDC/CR was present in the biopsy in 42% (32/73). The majority of cases were classified as NCCN unfavourable intermediate risk (53%) or high risk (18%) at diagnosis. Overall, 29% of cases (n=21) were classified into groups that could be considered eligible for AS, including very low risk (6%), low risk (8%) and favorable intermediate risk (15%). Among these 21 cases, the PBx was IDC/CR+ in 2 of them (10%), both of which were classified as favorable intermediate risk.

Table 1: Clinical and pathologic variables at diagnosis	
	Median (range) or number (%)
PSA at diagnosis (ug/L)	7.35 (3-26)
Clinical T-stage	
T1	38 (52%)
T2	27 (37%)
T3	8 (11%)
GG at PBx	
1	11 (15%)
2	29 (40%)
3	20 (27%)
4	9 (12%)
5	4 (6%)
Number of positive cores	6 (1-13)
Maximum % core volume	60% (5%-95%)
IDC/CR+ in PBx	32 (42%)
NCCN risk group	
1 (very low risk)	4 (6%)
2 (low risk)	6 (8%)
3 (favorable intermediate risk)	11 (15%)
4 (unfavorable intermediate)	39 (53%)
5 (high risk)	13 (18%)
6 (very high risk)	0

Conclusions: A proportion of IDC/CR+ cases were classified into risk groups that could be considered eligible for AS. Incorporation of IDC/CR morphology on PBx may enhance risk stratification of PCa but suffers from low sensitivity. Advances in image-guided targeted biopsy may improve detection of IDC/CR in PBx to aid therapeutic decision-making.

917 Prostate Cancer with Morphologic Features Borderline Between Grade Group 1 and Grade Group 2 at Diagnostic Biopsy: Correlation with Follow-up Biopsy and Radical Prostatectomy in a Prospectively Graded Cohort

Sarah Ni Mhaolcatha[1], Cynthia Heffron[1], Nick Mayer[1], Susan Prendeville[2]
[1]Cork University Hospital, Cork, Ireland, [2]Cork, Ireland

Disclosures: Sarah Ni Mhaolcatha: None; Cynthia Heffron: None; Nick Mayer: None; Susan Prendeville: None

Background: The distinction between Grade Group (GG) 1 and GG2 prostate cancer (PCa) at biopsy (PBx) has important implications for clinical management. The threshold for a minor Gleason pattern (GP) 4 component on PBx is poorly defined and there is considerable interobserver variability in the grade assignment of small foci with ill-formed glands or apparent fusion where tangential sectioning may also be considered. In cases with borderline morphology, the ISUP recommend that the lower grade is favored. This study evaluated follow-up outcome in a cohort of prospectively identified PBx cases with morphologic features borderline for a minor GP4 component.

Design: Cases of PCa with morphologic features borderline between GG1 and GG2 on PBx were prospectively identified (2014-2017). Routine grading of PCa and determination of borderline morphology was based on the consensus opinion of two urologic pathologists. All borderline cases with follow-up PBx and/or subsequent radical prostatectomy (RP) were included in the study. As a control group for the RP cohort, 46 consecutive cases with GG1 PCa on PBx that underwent RP were selected. Pathologic variables on follow-up PBx and RP were recorded.

Results: 96 cases with follow-up sampling were identified during the study period: 60 with follow-up PBx and 36 with subsequent RP. Median PSA was 6.525(1.74-15) u/L.

Follow-up PBx showed benign pathology in 8%(5/60) and PCa in 92%(55/60). GG at follow-up PBx was: GG1 in 64%(35/55), GG2 in 29%(16/55) and GG3 in 7%(4/55). 2 of 4 cases that were upgraded to GG3 had a visible target lesion on MRI.

GG and tumour stage at RP for the cases with borderline PBx and the control group are shown in table 1. Borderline morphology at PBx was associated with a higher rate of upgrading to GG2 at RP compared to the control group (p=0.027). No case in the borderline group was upgraded to >GG2. There was no significant difference in pathological stage distribution at RP between the borderline and control groups (p=0.899).

Table 1: RP variables in Borderline vs Control Groups

Pathologic variables at RP	GG1/GG2 borderline on PBx (n=36)	GG1 on PBx (n=46)	p-value
Grade Group/GG			
GG1	31% (11/36)	54% (25/46)	0.027
GG2	69% (25/36)	44% (20/46)	
GG3	0	2% (1/46)	
GG4	0	0	
GG5	0	0	
T-stage			
pT2	83% (30/36)	87% (40/46)	0.899
pT3a	14% (5/36)	11% (5/46)	
pT3b	3% (1/36)	2% (1/46)	
N-stage			
pNx	67% (24/36)	89% (41/46)	
pN0	33% (12/36)	11% (5/46)	
pN1	0	0	

Conclusions: While PBx with morphologic features borderline between GG1 and GG2 was associated with a higher rate of upgrading to GG2 at final pathology, there was no association with other adverse pathologic features/upstaging at RP in this series. These findings support current ISUP recommendations for conservative grading of small foci with borderline morphology on PBx. Advances in imaging and targeted biopsy may further aid risk-stratification and identification of unsampled higher grade tumour in these cases.

918 Prevalence of Renal Cell Cancer Gene-Related Mutations in Clear Cell Renal Cell Carcinoma with Sarcomatoid Differentiation

Rebecca Obeng[1], Rebecca Arnold[1], John Petros[2], Adeboye O. Osunkoya[3]
[1]Emory University, Atlanta, GA, [2]Emory University and US Department of Veterans Affairs, Atlanta, GA, [3]Emory University School of Medicine, Atlanta, GA

Disclosures: Rebecca Obeng: None; Rebecca Arnold: None; John Petros: None; Adeboye O. Osunkoya: None

Background: Clear cell renal cell carcinoma (CCRCC) with sarcomatoid differentiation has a higher mutational burden than other histologic variants of RCC and is associated with poor prognosis. The aim of this study was to determine the prevalence of a subset of RCC gene-related mutations in CCRCC with sarcomatoid differentiation.

Design: DNA from CCRCC with sarcomatoid differentiation and conventional CCRCC tumor foci and corresponding blood samples was extracted from patients with conventional CCRCC (n=16) and CCRCC with sarcomatoid differentiation (n=6). Sequencing libraries generated from multiplex bar-coded PCR amplification were prepared for the Illumina HiSeq platform. Galaxy workflow was used to identify somatic mutations in genes including VHL, PBRM1, SETD2, BAP1, KDM5C, KIT, NFE2L2, MET, and TP53 by comparing the tumor samples to buffy coat sequencing from the same patients.

Results: Mutations in RCC-related genes were identified in samples from 13/22 (59%) patients. Mutations were identified in samples from 3/6 (50%) patients with CCRCC with sarcomatoid differentiation and 10/16 (63%) patients with conventional CCRCC. The proportion of patients with RCC-related gene mutations increased with the WHO/ISUP Grade of the tumors [Grade 2: 2/5 patients (40%); Grade 3: 6/9 patients (67%); and Grade 4: 5/8 patients: (63%)]. Mutations were identified in samples from 2/2 (100%) patients with Grade 4 conventional CCRCC (with multinucleated tumor cells) whereas mutations were identified in samples from 3/6 (50%) patients with CCRCC with sarcomatoid differentiation. In conventional CCRCC, 0-5 specific mutations were identified in each patient (0-2 specific mutations in WHO/ISUP Grade 2 (5 patients), 0-3 specific mutations in WHO/ISUP Grade 3 (9 patients), and 2-5 specific mutations in WHO/ISUP Grade 4 (2 patients) while only 0-1 mutation was identified in patients with CCRCC with sarcomatoid differentiation (6 patients).

Conclusions: The prevalence of mutations in the RCC-related genes analyzed in this study is low in CCRCC with sarcomatoid differentiation in comparison to conventional CCRCC, and suggests differences in their genetic mutational profile. Studies exploring molecular targeted therapy for patients with CCRCC need to take into consideration the potential differences in the molecular profile between CCRCC with sarcomatoid differentiation and conventional CCRCC.

919 Expression of prostate-specific membrane antigen (PSMA) on biopsies is an independent risk stratifier of prostate cancer patients at time of initial diagnosis

Anne Offermann[1], Marie Christine Hupe[2], Doris Roth[1], Christiane Kuempers[3], Julika Ribbat-Idel[3], Finn Becker[3], Vincent Joerg[1], Axel Merseburger[4], Jutta Kirfel[1], Verena Sailer[5], Sven Perner[3]
[1]Institute of Pathology, University Hospital UKSH, Luebeck, Germany, [2]University Hospital Schleswig-Holstein, Luebeck, Germany, [3]University Medical Center Schleswig-Holstein, Leibniz Center for Medicine and Biosciences, Luebeck, Germany,[4]University Hospital Luebeck, Luebeck, Germany, [5]Pathology of the University Medical Center Schleswig-Holstein, Campus Lübeck and Research Center Borstel, Leibniz Lung Center, Borstel, Germany

Disclosures: Anne Offermann: None; Marie Christine Hupe: None; Doris Roth: None; Christiane Kuempers: None; Julika Ribbat-Idel: None; Finn Becker: None; Vincent Joerg: None; Axel Merseburger: None; Jutta Kirfel: None; Verena Sailer: None; Sven Perner: None

Background: Stratifying PCa patients into risk groups at time of initial diagnosis enabling a risk-adapted disease management is still a major clinical challenge. Existing studies evaluating the prognostic potential of PSMA for PCa were performed on radical prostatectomy specimens (RPE), i.e. decision making for disease management was already completed at time of sample analysis. Aim of our study was to assess the prognostic value of PSMA (prostate-specific membrane antigen) expression for prostate cancer (PCa) patients on biopsies at time of initial diagnosis.

Design: PSMA expression was assessed by immunohistochemistry on 294 prostate biopsies with corresponding RPE, 621 primary tumor foci from 242 RPE, 43 locally advanced or recurrent tumors, 34 lymph node metastases, 78 distant metastases and 52 benign prostatic samples. PSMA expression was correlated with clinico-pathologic features. Primary endpoint was recurrence free survival. Other clinicopathologic features included WHO/ISUP grade groups, PSA serum level, TNM-stage, and R-status. Chi-square test, ANOVA-analyses, Cox-regression and log-rank tests were performed for statistical analyses.

Results: High PSMA expression on both biopsy and RPE significantly associates with a higher risk of disease recurrence following curative surgery. The 5-year-recurrence free survival rates were 88.2%, 74.2%, 67.7% and 26.8% for patients exhibiting no, low, medium or high PSMA expression on biopsy, respectively. High PSMA expression on biopsy was significant in multivariate analysis predicting a 4-fold increased risk of disease recurrence independently from established prognostic markers. PSMA significantly increases during PCa progression.

Conclusions: PSMA is an independent prognostic marker on biopsies at time of initial diagnosis and can predict disease recurrence following curative therapy for PCa. Our study proposes the application of the routinely used IHC marker PSMA for outcome prediction and decision making in risk-adapted PCa management on biopsies at time of initial diagnosis.

920 Characterization of the Mediator complex subunits CDK8 and CDK19 during prostate cancer progression

Anne Offermann[1], Finn Becker[2], Vincent Joerg[1], Marie Christine Hupe[3], Johannes Brägelmann[4], Axel Merseburger[5], Verena Sailer[6], Sven Perner[2]
[1]Institute of Pathology, University Hospital UKSH, Luebeck, Germany, [2]University Medical Center Schleswig-Holstein, Leibniz Center for Medicine and Biosciences, Luebeck, Germany, [3]University Hospital Schleswig-Holstein, Luebeck, Germany,[4]University of Cologne, Cologne, Germany, [5]University Hospital Luebeck, Luebeck, Germany, [6]Pathology of the University Medical Center Schleswig-Holstein, Campus Lübeck and Research Center Borstel, Leibniz Lung Center, Borstel, Germany

Disclosures: Anne Offermann: None; Finn Becker: None; Vincent Joerg: None; Marie Christine Hupe: None; Johannes Brägelmann: None; Axel Merseburger: None; Verena Sailer: None; Sven Perner: None

Background: The Mediator Complex is a variable multiprotein structure playing a crucial role during transcription of protein coding genes. Recently, we identified the subunits CDK8 and its paralogue CDK19 to be overexpressed in advanced prostate cancer (PCa) and to play a functional role during PCa progression. Aim of our study was to access the prognostic value of CDK8 and CDK19 expression on a large PCa cohort in order to proof their potential to distinguish aggressive PCa from indolent disease.

Design: Tissue specimens of 489 patients including 175 diagnostic biopsies, 737 primary tumors, 108 local recurrances, 36 lymphnode metastases, 22 distant metastases and 71 benign prostatic samples were immunohistochemically stained for CDK8, CDK19, androgen receptor (AR) and ERG using the “Ventana Staining System”. CDK8 and CDK19 expression was correlated with clinico-pathologic features. The primary end point was progression free survival (PFS). Chi-square and log-rank tests as well as t-tests were used for statistical analysis.

Results: Level of CDK8 and CDK19 expression increases during disease progression and are highest in recurrent tumors and CRPCs. High CDK19 correlates with reduced PFS independently of WHO groups and PSA. The 5-year PFS was 73,7%, 56,9% and 30,4% in CDK19 negative/low, medium and high expressing tumors, respectively and correlates with CDK19 expression on diagnostic biopsys as well. CDK19 correlates with high expression of androgen receptor and ERG.

Conclusions: Our data highlight the importance of CDK19 in PCa progression to CRPC and suggest CDK19 as prognostic biomarker at time of initial diagnosis. Furthermore, our results emphasize the potential oncogenic role of CDK19 suggesting developing CDK19 as a potential therapeutic target to improve therapy for patients suffering from advanced PCa.

921 Clinicopathologic and transcriptomic predictors of fast urothelial carcinoma relapse post radical cystectomy

Ekaterina Olkhov-Mitsel[1], Anjelica Hodgson[2], Stanley Liu[1], Danny Vesprini[3], Jane Bayani[4], John Bartlett[4], Bin Xu[5], Michelle Downes[1]
[1]Sunnybrook Health Sciences Centre, Toronto, ON, [2]University of Toronto, Toronto, ON, [3]Sunnybrook Health Sciences Centre - University of Toronto, Toronto, ON, [4]Ontario Institute for Cancer Research, Toronto, ON, [5]Memorial Sloan Kettering Cancer Center, New York, NY

Disclosures: Ekaterina Olkhov-Mitsel: None; Anjelica Hodgson: None; Stanley Liu: None; Danny Vesprini: None; Jane Bayani: None; John Bartlett: None; Bin Xu: None; Michelle Downes: None

Background: High-grade muscle invasive urothelial carcinoma of the bladder (HGUC) is a heterogeneous disease with regards to its clinical outcome. Following radical cystectomy, many patients experience rapid disease relapse with a short interval to death (<24 months), while others exhibit sustained disease control. The aim of this study was to investigate the prognostic value of immune markers to identify HGUC patients at a high risk of rapid relapse after surgery.

Design: A retrospective cohort of 40 HGUC cystectomy cases (≥pT2) was identified and reviewed. Clinical and pathologic variables were recorded. A triplicate core tissue microarray was constructed and stained for CD3, CD4, CD8, CD20, CD68, CD163, FOXP3 and PD-1 to evaluate immune protein expression. NanoString nCounter human PanCancer immune panel was used to assess the immune transcriptome. RNA was isolated with the Roche High Pure RNA isolation kit. Data was analyzed by nSolver Analysis Software v4.0, with corrections for multiple testing.

Results: 25/40 HGUC patients experienced fast relapse and/or death < 24 months post-cystectomy. The clinicopathologic factors associated with fast relapse were AJCC stage (p= 0.026), LVI (p= 0.009) and nodal status (p= 0.013). Immunohistochemical analysis

showed that lower CD3 and PD-1 expression was a prognostic indicator of fast-relapse (p=0.006 and p=0.040, respectively). Immune transcriptomic profiling revealed 6 significantly differentially expressed genes; CCL21, CR2 and VEGFC were upregulated while KLRB1, CD36 and HLA-DQA1 were downregulated in fast relapsers. Decreased expression of KLRB1 and HLA-DQA1 was significantly associated with rapid recurrence on univariate log-rank (p=0.007 and 0.006) and cox regression analyses (HR=2.916, p=0.012; and 2.942, p=0.011, respectively). The lymphocyte receptor KLRB1 is a marker of enhanced innate T-cell immunity, known to be suppressed in tumor tissues and a pan-cancer marker of poor outcome. HLA-DQA1 is a member of the MHC class II proteins frequently downregulated during neoplastic transformation. Here we report an additional potential role for this gene in tumor progression.

Conclusions: Our multiplatform strategy allowed the screening of 738 immune markers for HGUC rapid relapse and led to the identification of 4 markers as well as 3 clinicopathologic parameters that could be useful tools for HGUC prognostication. Further validation of these potentially promising immune markers individually and as part of a multiparameter panel is warranted.

922 PD-L1 Expression and Associated Immune Alterations in High Grade Urothelial Carcinoma of the Bladder

Ekaterina Olkhov-Mitsel[1], Anjelica Hodgson[2], Stanley Liu[1], Danny Vesprini[3], Jane Bayani[4], John Bartlett[4], Bin Xu[5], Michelle Downes[1]

[1]Sunnybrook Health Sciences Centre, Toronto, ON, [2]University of Toronto, Toronto, ON, [3]Sunnybrook Health Sciences Centre - University of Toronto, Toronto, ON, [4]Ontario Institute for Cancer Research, Toronto, ON, [5]Memorial Sloan Kettering Cancer Center, New York, NY

Disclosures: Ekaterina Olkhov-Mitsel: None; Anjelica Hodgson: None; Stanley Liu: None; Danny Vesprini: None; Jane Bayani: None; John Bartlett: None; Bin Xu: None; Michelle Downes: None

Background: Programmed death-ligand 1 (PD-L1) plays a critical role in suppressing antitumoral immunity by binding programmed death-1 (PD-1), a negative regulator of T-lymphocyte activation. Blockade of the PD-L1/PD-1 interaction has shown therapeutic benefit in a subset of patients with advanced bladder cancer. In this study we characterized the immune milieu associated with PD-L1 expression to enhance our understanding of the high grade urothelial carcinoma of the bladder (HGUC) immune evasion network and potential implications for immunotherapy.

Design: 40 FFPE HGUC cystectomy specimens were sectioned and stained for PD-L1 (SP263). Immunohistochemistry (IHC) was scored (positive/negative) using recommended cut-offs. Immune transcriptome analysis was performed using NanoString nCounter human PanCancer immune panel and nSolver Analysis Software v4.0, with corrections for multiple testing. RNA was extracted with the Roche High Pure RNA isolation kit. PD-L1 mRNA expression was median dichotomized for comparisons with PD-L1 IHC. Pathway enrichment analyses were performed using g:Profiler.

Results: PD-L1 IHC positivity was identified in 13/40 (33%) HGUC. PD-L1 mRNA strongly correlated with protein expression (r=0.720, P<0.001). The sensitivity, specificity, positive and negative predictive values of PD-L1 mRNA expression for protein detection by IHC were 85%, 96%, 92% and 93%, respectively. There were 3 (8%) discordant cases. Of these, 2 were PDL1 IHC positive based solely on immune cell staining while the mRNA expression in these cases was below the median cut-off value. Immune transcriptome profiling identified a 16 gene signature associated with PD-L1 IHC. Pathway analysis determined enrichment of these genes in interleukin-10 production (e.g. CD46, NOD2), suppression of T cell activation (e.g. FCER1G, PDCD1LG2) and regulation of ERK1/ERK2 cascade (e.g. CTSH, CCL3). The top correlated transcripts with PD-L1 mRNA expression were inducible T-cell co-stimulator (ICOS) and the gamma interferon-stimulated (IFN-γ) genes PSMB9, ISG20 and HLA-DRB3.

Conclusions: We report strong correlation between PD-L1 mRNA expression and IHC positivity. We also demonstrate an association between PD-L1, IL-10, ERK1/ERK2 and IFN-γ signaling in modulation of components of the immunoproteosome and antigen-presenting machinery. This identifies multiple mechanisms that contribute to the immune checkpoint-restrained tumor microenvironment that can be modulated by immunotherapy.

923 Protein and Transcriptomic Characterization of the Immune Milieu of High Grade Bladder Cancer

Ekaterina Olkhov-Mitsel[1], Anjelica Hodgson[2], Stanley Liu[1], Danny Vesprini[3], Jane Bayani[4], John Bartlett[4], Bin Xu[5], Michelle Downes[1]
[1]Sunnybrook Health Sciences Centre, Toronto, ON, [2]University of Toronto, Toronto, ON, [3]Sunnybrook Health Sciences Centre - University of Toronto, Toronto, ON, [4]Ontario Institute for Cancer Research, Toronto, ON, [5]Memorial Sloan Kettering Cancer Center, New York, NY

Disclosures: Ekaterina Olkhov-Mitsel: None; Anjelica Hodgson: None; Stanley Liu: None; Danny Vesprini: None; Jane Bayani: None; John Bartlett: None; Bin Xu: None; Michelle Downes: None

Background: Invasive front inflammation is prognostically significant in high grade urothelial carcinoma of bladder (HGUC). However, the underlying mechanisms remain elusive. In this study, we report a comprehensive multiplatform analysis of the immune milieu associated with invasive front inflammation of HGUC.

Design: A retrospective cohort of 201 muscle invasive HGUC (≥pT2) cystectomy cases was evaluated for invasive front inflammation (high/low) and clinicopathologic variables were recorded. Triplicate core tissue microarrays were constructed and immunohistochemically tested for expression of CD3, CD4, CD8, CD20, CD68, CD163, FOXP3, PD-1 and PD-L1 (SP263). Further, 40 cases (20 high and 20 low) were selected for immune gene expression profiling by NanoString analysis (nCounter human PanCancer immune panel) and analyzed with nSolver Analysis Software v4.0. RNA was extracted with the Roche High Pure RNA isolation kit. Pathway enrichment analyses were performed using g:Profiler.

Results: Low invasive front inflammation was associated with lymphovascular invasion (p=0.006) and positive margins (p=0.014). Immunohistochemical analysis revealed that high invasive front inflammation expressed higher levels of immune cell markers CD3, CD4, CD8, CD20, CD68, CD163 (p<0.001) and immunosuppressive proteins FOXP3, PD-1 and PD-L1 (p=0.002, p=0.008, p=0.002, respectively). Immune transcriptomic profiling followed by unsupervised and supervised clustering identified a distinctive immune-related gene expression profile for high invasive front inflammation, characterized by significant upregulation of 147 genes. These included immune cell signatures (e.g. CD19, CD3, CD45), gamma interferon (IFN-γ) -responsive genes (e.g. IRF4, PRF1, GZMA), immune checkpoints (e.g. CTLA-4, IDO1, LAG3) and chemokines (e.g. CCL5, CXCL10, CXCL11). The top most common overrepresented pathways distinguishing high from low invasive front inflammation included Janus kinase signal transducer and activator of transcription (JAK-STAT), T cell receptor and tumor necrosis factor receptor signaling pathways.

Conclusions: Our findings of both an overall activated immune profile and immunosuppressive microenvironment provide novel insights into the complex immune milieu of HGUC with high invasive front inflammation. Additional research is ongoing to identify the key drivers of the anti-tumor mechanisms associated with invasive front inflammation and may provide opportunities for new immunotherapeutic strategies.

924 Clinicopathological and Hierarchical Cluster Analisis of Immunohistochemical Profiles of 21 Oncocytic Papillary Renal Cell Carcinomas

Angel Panizo[1], Luiz Miguel Nova Camacho[1], Francisco J Queipo[2], Gregorio Aisa[1]
[1]Complejo Hospitalario de Navarra, Pamplona, Spain, [2]Hospital San Jorge, Huesca, Aragón, Spain

Disclosures: Angel Panizo: None; Luiz Miguel Nova Camacho: None; Francisco J Queipo: None; Gregorio Aisa: None

Background: Papillary renal cell carcinoma (PRCC) is the second most common type of RCC. There is increasing recognition of morphologic heterogeneity within PRCC, and its classification remains difficult in a subset of tumors. The classification of oncocytic PRCC remains uncertain, and not yet fully characterized.

Design: We studied retrospectively a series 21 oncocytic PRCC. Clinicopathological and IHC analysis was performed and included CK (7, 19, and 34bE12), vimentin, EMA, CD10, RCC, racemase (AMACR), and E-cadherin. IHC was interpreted as positive when >5% of tumor cells demonstrated strong reactivity. Staining was considered diffuse when >50% of tumor showed reactivity. IHC results were recorded directly into Excel worksheets and reformatted using the freely available TMADeconvoluter software. Unsupervised hierarchical clustering analysis of IHC data was performed using the open source Cluster software and the results were visualized using the TreeView software.

Results: 14 patients were male and 7 female: mean age was 67.4 yrs. (range 49-93 yrs.). Mean size of the tumors was 4.36 cm (range 1.5-17 cm). 12 tumors were treated by partial nephrectomy and 9 by radical nephrectomy. All but five tumors were intrarenal (pT1). The remaining five tumors were pT3a. All tumors demonstrated predominant papillary architecture, lined by a single layer of oncocytic cells. Solid oncocytoma-like areas occurred in 11 cases, tubular structures were identified in 6, and an inverted pattern showing polarization of nuclei toward the surface of the papillae was present in 9 cases. Thirteen tumors were ISUP/WHO grade 2 and 8 were grade 3. In 18 cases, there was available material for IHC study. The IHC and unsupervised hierarchical cluster analysis results are summarized in the table and Figures. Follow-up was available in all cases (median follow-up of 51 months; range 6-121 months): 18 patients were alive and well, 2 died without disease, and 1 died due to progression.

	AMACR	EMA	CK19	Clau-7	CK34bE12	RCC	E-Cadh.	CD10
Positive (%)	100	94.4	83.3	83.3	77.8	66.7	61.1	55.6
focal (n)	*1*	*6*	*2*	*3*	*5*	*3*	*4*	*6*
diffus (n)	*17*	*11*	*13*	*12*	*9*	*9*	*7*	*4*
Negative (%)	0	5.6	16.7	16.7	22.2	33.3	38.9	44.4

Figure 1 - 924

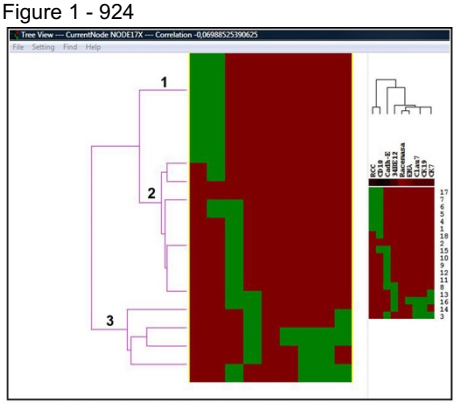

*Results of unsupervised hierarchical cluster analysis of IHC data. For each of the antibodies indicated at the top of the figure, **positive staining** is indicated by a **red square**, and **absence of staining** as **green**. Each row represents a single case and each column a single immunomarker.*
The dendrogram at the top shows the clustering of proteins based on the relatedness of tumors stained by each antibody. The dendrogram on the left side shows the clustering of the tumors based on the degree of similarity of their IHC staining results. In the dendrogram, the length of branch between two elements reflects their degree of relatedness.
Unsupervised hierarchical clustering was able to distinguish three tumor clusters on the basis of this set of antibodies, and two major protein clusters were identified

Figure 2 - 924

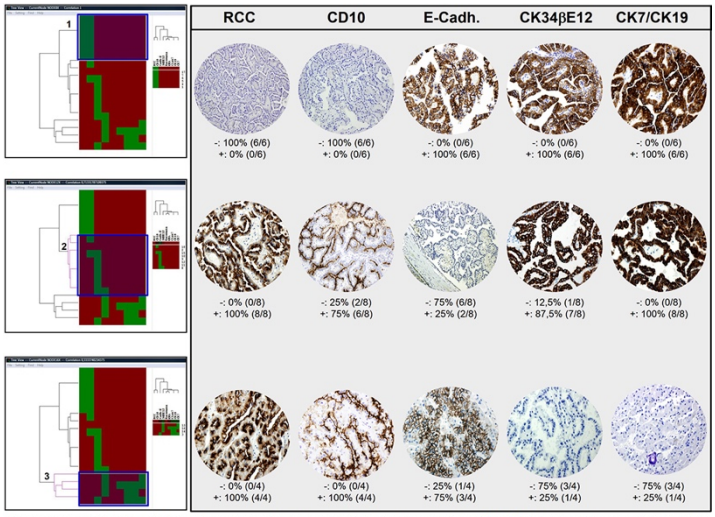

Unsupervised hierarchical clustering of the protein expression data subdivided the oncocytic PRCC into three main clusters. Cluster #1, that was the most homogeneous, consisted a group of 6 tumors. All the tumors in cluster 1 were RCC and CD10 negative (proximal nephron markers), while all cases expressed E-cadherin, CK34bE12, AMACR, EMA, Claudin-7, CK19, and CK7 (distal nephron markers). Cluster #2 and Cluster #3 expressed proximal nephron markers RCC and CD10, but showed absence of E-cadherin in cluster #2, and absence of HMW-CK 34bE12, claudin 7, CK19, and CK7 in cluster #3. These findings may reflect the different histogenesis of oncocytic PRCC, likewise papillary renal cell carcinoma, which has been related to either proximal or distal nephron epithelium.

Conclusions: Oncocytic PRCC could be a distinct variant in the PRCC group. Unsupervised hierarchical cluster analysis of IHC distinguish 3 main clusters: these findings may reflect the different histogenesis of oncocytic PRCC, related to either proximal or distal nephron epithelium. Some cases with solid oncocytoma-like areas pose differential diagnostic problems with renal oncocytoma. In our series, all but one oncocytic PRCC had a good outcome with no recurrence and/or metastasis or death related the disease with a 51-months median follow-up.

925 Integrated Expression (Chromogenic in situ Hybridization) of Long Noncoding RNAs (LncRNAs) Segregate Low Grade from Clinically Significant Prostate Cancer

Vamsi Parimi (Parini)[1], Yuhe Xia[2], Valeria Mezzano[3], Varshini Vasudevaraja[4], Shanmugapriya Selvaraj[5], Cynthia Loomis[6], Andre Moreira[7], Peng Lee[8], David Levy[2], Kyung Park[2], Hongying Huang[2], Qinghu Ren[9], Fangming Deng[1], Jonathan Melamed[1]
[1]New York University Medical Center, New York, NY, [2]NYU Langone Health, New York, NY, [3]NYU Langone Medical Center, New York, NY, [4]New York University, New York, NY, [5]NYU Medical Center, New York, NY, [6]NYU School of Medicine, New York, NY, [7]New York Langone Health, New York, NY, [8]New York Harbor Healthcare System, NYU School of Medicine, New York, NY, [9]New York University Langone Medical Center, New York, NY

Disclosures: Vamsi Parimi (Parini): None; Yuhe Xia: None; Valeria Mezzano: None; Varshini Vasudevaraja: None; Shanmugapriya Selvaraj: None; Cynthia Loomis: None; Andre Moreira: None; Peng Lee: None; David Levy: None; Kyung Park: None; Hongying Huang: None; Qinghu Ren: None; Fangming Deng: None; Jonathan Melamed: None

Background: Long noncoding RNA (LncRNAs) are non-translated transcripts (>200nt) within the introns of protein-coding genes. Currently available criteria for segregating prostate cancer patients into those requiring immediate therapeutic intervention and those who can be carefully followed are inadequate. Our aim was to characterize the differential expression of oncogenic LncRNAs and study their prognostic significance in the prostate cancer (PCa). <

Design: Expression levels of 9 LncRNAs: DANCR, HOTAIR, MALAT1, NEAT1, PCA3, PCAT1, PCAT14, PCGEM1 and SCHLAP1 were assessed by RNA ISH (RNAscope; Advanced Cell Diagnostics) with chromogenic signals evaluated by Visiopharm® (Denmark, Version 2018.4) histopathology software on tissue microarrays (TMA) constructed from 88 matched radical prostatectomy specimens. The quantitative RNA expression was calculated as the average brown area of puncta and clusters for each nuclei. The LncRNA expression was compared with Gleason score, and TNM stage. For external validation, we used the The Cancer Genome Atlas database (https://gdc.cancer.gov/) of 506 patients with primary prostate cancer.

Results: Mean patient age at prostatectomy was 63.2+/-7.9 years, with the following grade group (GG) and pathologic stage distribution (GG1=27%, GG2=32%, GG3=23%, GG4=7%, GG5=8% and pT2=52%, pT3=47%, pT4=1%). By univariate logistic regression model analysis, DANCR, NEAT1, PCA3 and PCAT14, showed significant differential expression between cancer and benign prostate tissue. On

subsequent multivariate backward stepwise selection, the combination of MALAT1, NEAT1, PCA3 and PCAT14 showed significantly higher expression in GG2 or higher as compared to GG1 (P=0.009, AIC = 97.14). The combination of NEAT1, PCA3, PCAT1 and SCHLAP1 showed significantly higher expression in stage pT3 than on pT2 (P=0.004, AIC =103.3). **Figure Legend:** a) Chromogenic RNA In-Situ hybridization showing PCAT14 expression in PCa. b) Automated histopathology algorithm segmentation overlay of RNAScope puncta (green), clusters (red) and counterstained nuclei (outlined blue). c) LncRNA expression in PC3 and LNCap cell lines. d) Differential expression of LncRNAs among GG1 (Group A= '+') and GG2-GG4 (Group B= 'dot').

Figure 1 - 925

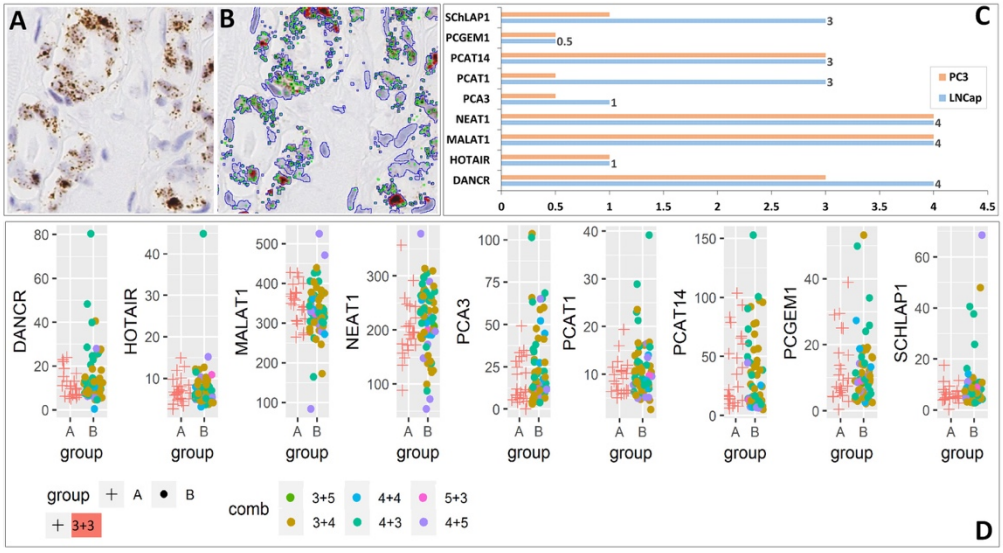

Conclusions: LncRNA signatures may be reliably determined by RNA ISH and provide co-expression patterns in prostate cancer that correlate with higher grade and more advanced stage. Integrated evaluation of LncRNA by RNA ISH may be helpful to distinguish indolent from aggressive prostatic adenocarcinomas.

926 Long Noncoding RNAs (LncRNAs) Signatures in Prostate Cancer: External Validation with The Cancer Genome Atlas (TCGA) database

Vamsi Parimi (Parini)[1], Varshini Vasudevaraja[2], Yuhe Xia[3], Shanmugapriya Selvaraj[4], Valeria Mezzano[5], George Jour[3], Matija Snuderl[2], Aristotelis Tsirigos[6], Fangming Deng[1], Jonathan Melamed[1]

[1]New York University Medical Center, New York, NY, [2]New York University, New York, NY, [3]NYU Langone Health, New York, NY, [4]NYU Medical Center, New York, NY, [5]NYU Langone Medical Center, New York, NY, [6]New York University School of Medicine, New York, NY

Disclosures: Vamsi Parimi (Parini): None; Varshini Vasudevaraja: None; Yuhe Xia: None; Shanmugapriya Selvaraj: None; Valeria Mezzano: None; George Jour: None; Matija Snuderl: None; Aristotelis Tsirigos: None; Fangming Deng: None; Jonathan Melamed: None

Background: Chromogenic in situ hybridization (RNA ISH) is a sensitive technique for quantitative evaluation of RNA and provides cellular context. However, concern on accuracy may be raised in formalin-fixed tissues, embedded in paraffin due to deterioration in RNA content. We evaluated the integrated expression of Long Noncoding RNAs (LncRNAs) in prostate cancer (PCa) by RNA ISH and sought to validate our findings with RNA sequenced data from the frozen tissue derived TCGA Database.

Design: The read count tables for the PRAD RNA-Seq samples (n=506) in TCGA were downloaded from the National Cancer Institute's (NCI) Genomic Data Commons (GDC) (https://gdc.cancer.gov/). Of these samples, primary prostate tumor samples (n=455) were used and normal tissue samples (n=51) are ignored. Among the 455 patients, 10% are Gleason 6, and 411 represent Grade Group (GG) GG2 to GG5 [51% are Gleason 7 (GG2&3) [30% Gleason 3+4 and 21% Gleason 4+3], 13% are Gleason 8 (GG4), 26% are Gleason 9 and are 0.6% Gleason 10 (GG5)]. Our institutional cohort (n=88) represented GG1=27%, GG2=32%, GG3=23%, GG4=7%, GG5=8%. Using the DESeq2 package (v3.0), we analyzed 9 LncRNA (DANCR, HOTAIR, MALAT1, NEAT1, PCA3, PCAT1, PCAT14, PCGEM1 and SCHLAP1) expression. Thereafter the samples are separated into two groups GG1 vs GG2-5 (higher grade PCa). Logistic regression model was used to test for the association between these two groups.

Results: By univariate logistic regression model analysis, among 9 LncRNAs, we found the only SCHLAP1 to be significantly differentially expressed between the low grade (GG1) and higher grade groups (GG2-5) (P=0.0083). On subsequent multivariate backward stepwise selection, the combination of HOTAIR + NEAT1 + PCA3 + SCHLAP1 showed significantly different expression in GG2 or higher as

compared to GG1 (model selection P=0.007). In comparison, our institutional cohort showed the combination of DANCR + MALAT1 + NEAT1 + PCA3 + PCAT14 + SCHLAP1 showed significantly different expression in GG2 or higher as compared to GG1 (model selection P=0.013)

Conclusions: Even though the institutional PCa cohorts have a different grade distribution (with lower GG1 subgroup in TCGA cohort), we were able to show that common and unique LncRNAs playing a prominent role in the separation of low grade prostate cancers from high grade types. The LncRNA signatures may be reliably determined by RNA ISH and is helpful to distinguish low grade from high grade prostatic adenocarcinomas.

927 Beta-hCG Expression in Urothelial Carcinoma of the Urinary Bladder as a Predictor of Lymph Node Metastasis

Sang Hui Park[1], Divya Sahu[2], Donna Hansel[2]
[1]Ewha Womans University, Seoul, Korea, Republic of South Korea, [2]University of California, San Diego, La Jolla, CA

Disclosures: Sang Hui Park: None; Divya Sahu: None; Donna Hansel: *Advisory Board Member*, Genentech; *Grant or Research Support*, Konica Minolta; *Consultant*, Taris

Background: Beta-hCG-producing tumors tend to be correlated with stage and grade. Beta-hCG is expressed preferencially at the forefront of invasion, deep invasive and highly proliferative area. Beta-hCG may act as a local immunosuppressor favoring the proliferation and invasion of the tumor cells and the presence of beta-hCG in the tumor cells may indicate the presence of proliferative undifferentated cells. Beta-hCG expression was more intense in the recurrent or metastatic tumors. The expression of beta-hCG occur in 11.5-46.2% of high-grade urothelial carcinomas but usually not expressed in urothelial carcinoma in situ or low-grade urothelial carcinomas. Urothelial carcinomas with beta-hCG expression combined with squmous differentation often showed relatively good reponse to radiotherapy.The expression of beta-hCG in urothelial carcinomas of the urinary bladder has been reported to be correlated with poor clinical outcome in some studies. However, the significance of beta-hCG expression in urothelial carcinomas as a prognostic predictor has not been clarified yet.

Design: This study included patients for whom retrospective data had been collected in pathology archives at University of California of San Diego. A retrospective histologic review of bladder cancers was performed on 121 cases and clinical data were retrieved from electronic medical records. A quadruplicate core tissue microarray was constructed from 121 cases of high-grade urothelial carcinoma treated by cystectomy, and was stained with beta-hCG. The percentage cytoplasmic staining was recorded for each core. Cases were classified as negative (0), weak (1+), moderate (2+), and strong (3+).

Results: Patients' average age was 70.7 years (median, 73.5 years) and the average lenght of follow-up was 16.8 months (median, 16.9 months). The ratio of male and female was 76:39 (1.95:1). Correlation with age and stage was not significant, but beta-hCG expression was associated with increased risk of metastasis (P<0.01). High level beta-hCG expression (3+) was associated with higher rate of death from recurrence and death of disease.

Beta-hCG level	*Patient number*	*Age average (years)*	*T stage (average)*	*Metastasis present at surgery*	*Length of follow up (months)*	*Dead of disease*	*Recurrence*
0	53	71.1	2.8	17/53 (32%)	26.6	5/53 (9.4%)	6/53 (11%)
1+	44	69.3	2.9	27/44 (61%)	31.4	2/44 (4.5%)	5/44 (11%)
2+	15	70.5	3.0	10/15 (67%)	30	0 (0%)	0/15 (0%)
3+	9	71.9	2.9	3/9 (33%)	21.6	2/9 (22%)	3/9 (33%)

Conclusions: The immunohistological expression of beta-hCG in urothelial carcinomas of the urinary bladder would likely predict recurrence or metastasis with poor clinical outcome.

928 Comparison of Two Commonly Used Methods in Estimation of Cancer Volume in the Prostate

Vihar Patel[1], Wei Huang[2], Samuel Hubbard[2]
[1]Madison, WI, [2]University of Wisconsin, Madison, WI

Disclosures: Vihar Patel: *Grant or Research Support*, PathomIQ, INC; Wei Huang: None

Background: Currently there is no consensus among pathologists on how to measure the cancer volume in prostate core biopsies. In this study, we compared the cancer volume measured with two commonly used methods by practicing pathologists and analyzed their correlation with the cancer volume in the corresponding prostatectomy specimens.

Design: Forty-nine patients with at least two separate foci of prostate cancer in a signal core were selected from Pathology Archive at University of Wisconsin-Madison. Biopsy slides were scanned with Aperio CS2 (Leica Biosystem). Prostate cancer volume (%) was measured with two methods using digital slides and Aperio ImageScope software: the scattered method (S) and the exact method (E). The scattered method calculates the ratio of the core length (mm) encompassing all the tumor foci including the intervening uninvolved benign tissue to the total core length (mm). The exact method calculates the ratio of the sum of each discrete cancer foci in length (mm) to the total core length (mm). The means of cancer volume by each method were compared and correlation of cancer volume in biopsy samples to that in corresponding prostatectomy specimens was analyzed. IBM SPSS Statistics 22 was used for the analysis.

Results: The cancer volume distribution by the two methods is shown in Figure 1. The means and standard deviations of cancer volume for each method are shown in Table 1. There is significant difference (p=0) in cancer volume between the two methods. Spearman correlation coefficeincy (R_s) of biopsy vs. prostatectomy cancer volume is 0.426 and 0.412 for the E and S methods, respectively.

Prostate Cancer Tumor Volume (%)			
	Exact	Scattered	Prostatectomy
N	49	49	49
Mean	*26.7%	*40.0%	12.6%
Std. Deviation	21.0%	26.3%	12.3%
*p = 0.000			

Figure 1 - 928

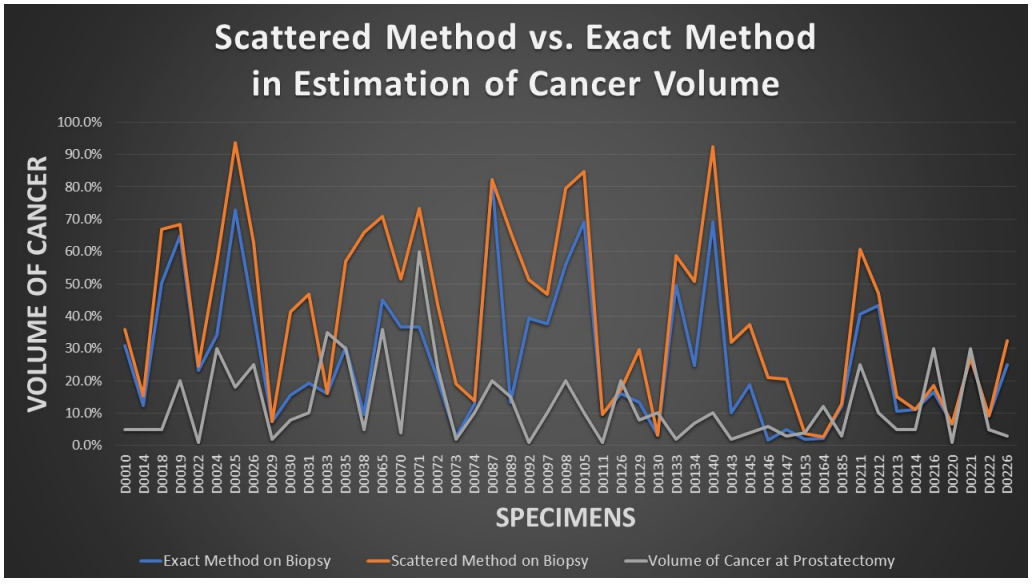

Conclusions: When evaluating the prostatic cancer volume in core biopsies, due to sampling limitations, both E and S methods tended to overestimate cancer volume in the prostate. However, the E method is more accurate than the S method in predicting cancer volume in the prostate.

929 Detecting ETV4 Fusion by Immunohistochemistry (IHC) stain in Prostatic adenocarcinoma

Rugved Pattarkine[1], Alexandra Budhai[2], Kemin Xu[1], Ximing Yang[3], Fei Ye[1], John Fallon[4], Minghao Zhong[1]
[1]Westchester Medical Center, Valhalla, NY, [2]New York Medical College at Westchester Medical Center, Valhalla, NY, [3]Northwestern University, Chicago, IL, [4]New York Medical College and Westchester Medical Center, Valhalla, NY

Disclosures: Rugved Pattarkine: None; Alexandra Budhai: None; Kemin Xu: None; Ximing Yang: None; Fei Ye: None; John Fallon: None; Minghao Zhong: None

Background: Background: The most common genetic alterations in prostate cancer are fusions of *ERG* and other members of the E26 transformation-specific (ETS) family of transcription factors, including: *ETV1*, *ETV4* and *FLI1*. Analyzing TCGA data, we found that similar to *ERG* fusion (Figure1A), *ETV4* fusion associated *ETV4* mRNA level increase (Figure1B). ERG IHC stain has been a surrogate test for *ERG* fusion. Therefore, we hypothesize that ETV4 IHC stain could be used to detect *ETV4* fusion in prostate cancer.

Design: Methodology: 111 Primary prostate adenocarcinoma (>10 % by volume) cases from our institute were selected for tissue microarray (TMA) construction. The regular full section slides and TMA slides were subject for IHC stain of ERG and ETV4 (Santa Cruz, SC-113). One Ewing-like sarcoma with *CIC* translocation is included as positive control for ETV4 IHC stain. The criteria for positive ETV4 are: 1. nuclear staining; 2. only in tumor cells, not in non-tumor cells; 3. ETV4 positive cells should be negative for ERG IHC staining.

Results: Results: The cells of *CIC* translocation sarcoma are diffusely and strongly positive for ETV4. For prostate TMA slides, ~50% of cases were positive for ERG; ~10% of cases were weakly positive for ETV4. For those ETV4 positive TMA cases, we did ETV4 IHC stain on regular full section. Finally, 6 (~5%) of cases were confirmed with positive ETV4 IHC staining. We are in the process of validating *ETV4* fusion by next generation sequencing (NGS) and FISH.

Figure 1 - 929

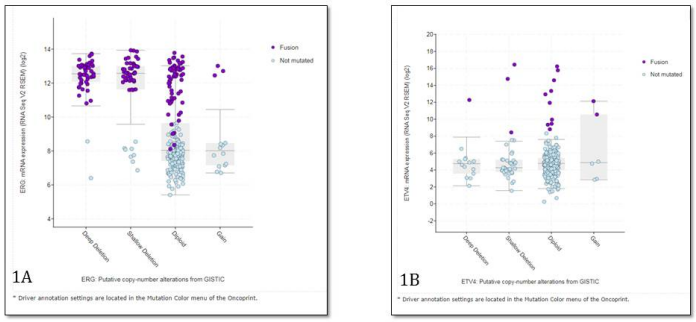

Figure 1. The correlation of mRNA level with fusion status for 333 TCGA prostate cancer data (from CbioPortal website). The X axis is gene copy number alteration. The Y axis is mRNA level. Each dote represent individual sample. Purple dotes are samples with fusion. Light blue dotes are samples without fusion. A. ERG fusion and ERG mRNA level. B. ETV4 fusion and ETV4 mRNA level. Both ERG and ETV4 show the similar pattern: mRNA level is higher in those cases with gene fusion than those cases without gene fusion.

Figure 2 - 929

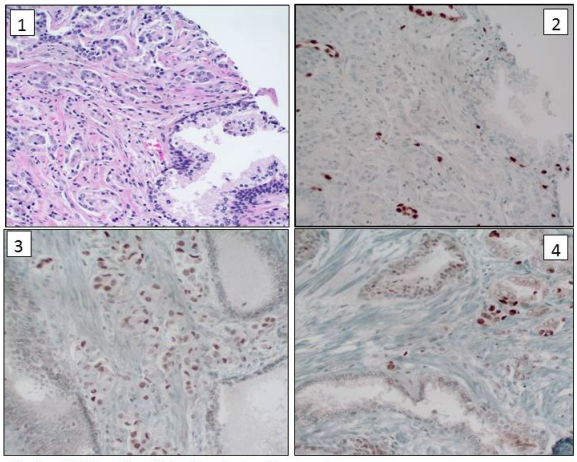

Fig. 1 – 1) H&E section with benign gland and tumor cells.
2) Tumor cells staining negative for ERG and positive for endothelial cells for same case.
3) & 4) ETV4 staining positive for tumor cells and negative for benign glands (same case).

Conclusions: Conclusion: Overall we conclude that the ETV4 IHC stain can be useful to detect *ETV4* fusion. The IHC method will be cheaper and faster than other methods (such as: NGS, FISH). In addition, IHC also can provide morphological correlation.

930 Recutting Blocks of Prostate Core Biopsies: How Much Diagnostic Yield is Gained?

Adina Paulk[1], Isabell Sesterhenn[1], Allen Burke[2]
[1]Joint Pathology Center, Silver Spring, MD, [2]UMMS, Baltimore, MD

Disclosures: Adina Paulk: None; Isabell Sesterhenn: None; Allen Burke: None

Background: The use of multiple levels at initial cutting with retention of unstained slides is currently standard practice in urologic pathology. In a second opinion center serving VA and military prostate biopsy samples, approximately 2/3 of cases are submitted with blocks. It has been the practice to cut all blocks for diagnostic rendering including those without diagnostic concern.

Although it is known that a reasonable number of cores with atypical glands fail to show diagnostic material on recuts of the block, there is little information reported about the finding of more extensive, additional, or higher grade tumors on recuts of the block. Despite the data reported on the limitations of recutting blocks to establish a diagnosis in questionable cores, there are no data that demonstrate the finding of unexpected cancers on blocks where initial standard sections fail to show atypical glands or carcinoma.

Design: A retrospective search from 2011-2016 of all prostate biopsies with submitted blocks was performed to determine what diagnoses were changed based on findings on recut tissue. Diagnoses changed due to immunohistochemistry results were not included.

Results: Of 1321 prostate cases sent in for consultation with blocks, there were 64 cases (4.7%) where either a grade group (GG) was increased, an additional focus of cancer was found, or there was a diagnosis of carcinoma based solely on the recut slide. 40 of these showed additional foci of GG1 in cases where there was definitive carcinoma elsewhere in the original slides. In 23 cases (1.7%) the diagnosis on recut increased the overall highest GG or showed the only carcinoma in the case (Table 1). In 3 of these cases (0.22%) the diagnosis on recut changed the highest GG by >1 (Table 2) to GG3 or GG4. 1 case with GG2 on original slides showed an additional focus of GG2 on the recut. Of the 1321 cases, in 47(3.6%) cases the diagnosis was not changed but the carcinoma was found to be more extensive on recut. Of the 1321 cases, in 111 cases (8.4%) there was more limited diagnostic sampling, with at least one focus of atypical glands or carcinoma was not present on recut slides.

Table 1: Cases of first time diagnosis of carcinoma or increase in GG based on recut

Original diagnosis/ Original highest GG	Highest GG on Recut	Number (%)
Benign prostate tissue	Prostatic carcinoma, GG1	5 (0.4%)
High grade PIN	Prostatic carcinoma, GG1	1 (0.1%)
Focus of atypical glands/ suspicious for carcinoma	Prostatic carcinoma, GG1	10 (0.8%)
Prostatic carcinoma, GG1	Prostatic carcinoma, GG2	3 (0.2%)
Prostatic carcinoma, GG4	Prostatic carcinoma, GG5	1 (0.1%)
Prostatic carcinoma, any GG	Prostatic carcinoma, with increase of GG >1 (see Table 2)	3 (0.2%)

Table 2: Cases where GG seen on recut increased by >1 GG than original slide

Original diagnosis (highest GG)	Diagnosis on recut	Number
GG1	GG3	1
GG1	GG4	1
GG2	GG5	1

Conclusions: In a small percentage of cases the diagnosis was changed in a clinically meaningful way, most frequently showing more extensive carcinoma or confirming carcinoma in areas of atypical glands. The majority of additional tumor foci found on recuts were GG1.

931 Extent of High-Grade Prostate Cancer in Multiparametric MRI-Targeted Biopsy Enhances Prediction of Pathologic Stage

Nathan Paulson[1], Robin Vollmer[2], Peter Humphrey[3], Preston Sprenkle[1], Steffen Huber[3], Kamyar Ghabili Amirkhiz[1], Angelique Levi[4]

[1]Yale University School of Medicine, New Haven, CT, [2]VA Healthcare System, Durham, NC, [3]Yale University, New Haven, CT, [4]Yale University, Fairfield, CT

Disclosures: Nathan Paulson: None; Peter Humphrey: None; Preston Sprenkle: None; Steffen Huber: None; Kamyar Ghabili Amirkhiz: None; Angelique Levi: None

Background: There is a growing trend towards active surveillance for select low risk prostate cancers. Which patients fall into this category, therefore, is of increasing importance. Data have shown correlation of amount of high-grade (Gleason pattern 4/5) disease (HG) on biopsy with negative prognostic factors. Multiparametric magnetic resonance imaging (mMRI) is increasingly being used to enhance risk stratification through identification of nodules with features associated with clinically significant cancer. Adding mMRI-targeted biopsies to the standard 12 cores has been shown to increase diagnostic yield of HG. To our knowledge, there are no data on the utility of amount of HG in mMRI-targeted biopsies versus standard 12 core biopsies in predicting negative outcomes on radical prostatectomy (RP).

Design: We performed retrospective review of all prostate biopsies collected at our institution from June 2015 to April 2018 which had corresponding RP, at least one set of mMRI-targeted biopsies, and Grade Group 2 disease or higher in at least one core. For the 169 cases identified, total mm of carcinoma, total mm HG and longest length HG in a single core were recorded for the standard 12 core biopsies and each set of mMRI-targeted biopsies. Lengths of HG for Gleason pattern 4 was calculated in each core using the percentage in the report. For RP specimens, overall Gleason grade, extraprostatic extension (EPE), seminal vesicle (SV) involvement and lymph node metastasis were recorded. PSA levels at time of biopsy were recorded when available. The main outcome studied was the presence of tumor beyond the prostate, a binary outcome. Thus, the logistic regression model was used to test which pre-RP variables related to this outcome.

Results: Total mm of carcinoma in all cores (standard 12 + mMRI-targets) was the factor most significantly associated (p = ~0) with adverse RP outcomes in the logistic regression model. With total mm of carcinoma in all cores included in the logistic regression model, the longest length of HG in a single mMRI-targeted core provided added value (p=0.03) in prediction of pathologic stage, while all other variables did not.

Conclusions: mMRI-targeted biopsies provide additional value over standard 12 core biopsies alone in prediction of non-organ confined prostate cancer at radical prostatectomy. Linear mm of high-grade prostate cancer in mMRI-targeted biopsies is a significant parameter associated with higher pathologic stage and should be considered for standardized reporting.

932 Dynamic Duos and Treacherous Trios of the Kidney: 15 Collision Tumors

Garrison Pease[1], Maria Tretiakova[2], Ryan Morse[2]
[1]*University of Washington - Harborview, Seattle, WA,* [2]*University of Washington, Seattle, WA*

Disclosures: Garrison Pease: None; Maria Tretiakova: None

Background: Collision tumors are defined as one mass with two or more concurrent tumors of different lineages that have grown into each other. Tumor components, or partners, may have any combination of malignant, borderline, or benign neoplasms. They are considered extremely rare in the kidney, with most reported as single cases or small series. Herein, we report 15 cases from files of a senior author collected within the last 12 years.

Design: Archives were searched for nephrectomies with focus on collision tumors. The more common multifocal, synchronous (distinct tumors without interaction) or composite/hybrid tumors (divergent histologies of one) and renal tumor syndrome cases were excluded. Characteristics (age, gender, diagnosis, size, benign vs. malignant, grade stage, immunohistochemistry) were tracked.

Results: From 15 recovered cases 12 had 2 tumor partners (80%) and 3 had 3 partners (20%), totaling 33 partners. Size of tumor partners ranged broadly from 0.2 to 17 cm (mean 4.2). Mean patient age was 63 years (range 51-73) with male predominance (2:1). Twelve cases included immunohistochemical workup, 3 of which underwent FISH or cytogenetic studies.

Summary of partners is in table 1. Thirteen (87%) of cases featured a malignant entity: 11 cases with malignant renal epithelial tumor and 2 cases with liposarcoma or lymphoma. Seven cases included a single malignancy and 6 cases included 2 or 3 malignant partners, most commonly clear cell RCC (5) and papillary RCC (4). Five cases featured a borderline entity (33%) including 2 cases with carcinoid and 3 with multilocular cystic neoplasm of low malignant potential (MCN-LMP). Six cases featured a benign partner (40%), 1 of them being a collision of 2 benign partners. Papillary adenoma was most common, occurring 4 times, followed by oncocytoma (3) and medullary fibroma (1). Epithelial renal tumors (benign or malignant) were present in all 15 cases, non-epithelial were seen in 5 cases (33%).

Figure 1 - 932

Table 1 – 33 Partner tumors of 15 kidney collision tumors

Epithelial	Type	Freq.	Mesenchymal	Type	Freq.
Clear cell RCC*	M*	5 (16%)	Liposarcoma†	M	1 (3%)
Papillary RCC	M	4 (12%)	Medullary fibroma†	B	1 (3%)
Chromophobe RCC	M	3 (9%)	**Lymphoid**		
Clear cell papillary RCC	M	2 (6%)	CLL/SLL	M	1 (3%)
ACD-RCC†	M	1 (3%)	**Neuroendocrine**		
Translocation RCC†	M	1 (3%)	Carcinoid	Bd	2 (6%)
SDH-deficient RCC†	M	1 (3%)			
Urothelial carcinoma	M	1 (3%)	**Type (of 15)**		**Freq.**
MCN-LMP†	Bd	3 (9%)	M/M/M, M/M, or M/M/Bd		6 (40%)
Papillary adenoma†	B	4 (12%)	M/Bd/B, M/Bd, or M/B		7 (47%)
Oncocytoma	B	3 (9%)	B/Bb or B/B		2 (13%)

*RCC – renal cell carcinoma; ACD – acquired cystic disease; SDH – succinate dehydrogenase; MCN-LMP - mucinous cystic neoplasm of low malignant potential.
*M – malignant; Bd – borderline; B – benign. †First report of partner in a kidney collision tumor.

Conclusions: Our cohort suggests that collision tumors of the kidney are more common than previously considered. This largest to date series of 15 collision kidney tumors encompasses 33 tumor partners. We report for the first time 12 new dual combinations, 3 triple collision tumors and 7 new collision partners including rare entities of SDH-deficient RCC, translocation RCC, acquired cystic disease-associated RCC and carcinoid occurring within an urothelial carcinoma.

933 Can INSM1 as a Sole Immunohistochemical Marker Replace Synaptophysin and Chromogranin in Detecting Neuroendocrine Differentiation in Advanced Prostate Cancer?

Garrison Pease[1], Colm Morrissey[2], Lawrence True[3], Maria Tretiakova[2]
[1]University of Washington - Harborview, Seattle, WA, [2]University of Washington, Seattle, WA, [3]University of Washington Medical Center, Seattle, WA

Disclosures: Garrison Pease: None; Colm Morrissey: None; Lawrence True: None; Maria Tretiakova: None

Background: Neuroendocrine (NE) differentiation in prostatic carcinoma is an increasingly common resistance mechanism to androgen deprivation therapy. In the setting of small biopsies and multiple immunohistochemical markers, detection of NE differentiation can be difficult. Insulinoma-associated protein 1 (INSM1) is a novel nuclear IHC marker with reported equivalent or superior sensitivity and specificity in identifying a NE phenotype in various tumors compared with the traditionally used markers synaptophysin (SYP) and chromogranin (CHGA). We assessed the performance of INSM1 immunohistochemical (IHC) stains in detecting NE differentiation in a large series of metastatic castration resistant prostate cancer (mCRPC) compared to well-established NE markers.

Design: We used IHC for INSM1, SYN and CHGA on tissue microarrays of mCRPC from 56 patients (245 tumors, 735 cores) and LuCaP patient-derived xenografts (PDX) enriched for a NE phenotype (42 patients; 125 tumors, 375 cores). Each tumor was represented by at least 3 cores (N=1110 cores total). We scored stains using the modified H-score including % positivity (0-100) and staining intensity (0-2). Diffuse and strong reactivity was defined as H-score of 50 or more.

Results: mCRPCs expressed INSM1, SYP, and CHGA in 15%, 25% and 11%, respectively; diffuse and strong reactivity was detected in 11%, 12.5%, and 3% cases, respectively. All cases staining for CHGA were captured by SYN. Pair-wise concordance correlation between INSM1 and SYP had coefficient of 0.80.

PDXs expressed INSM1, SYP, and CHGA in 26%, 34%, and 9% cores, respectively; diffuse and strong reactivity was detected in 12%, 16%, and 2% cases, respectively. All cases staining for CHGA were captured by SYP. Pair-wise concordance correlation between INSM1 and SYP had a coefficient of 0.89.

For each group, marker sensitivity based on H-score ranked from highest to lowest as follows: SYP, INSM1, CHGA. Compared to other NE markers, INSM1 staining was easier to interpret due to crisp nuclear and minimal background staining.

Conclusions: In our study of mCRPC and PDX biopsies, INSM1 has sensitivity close to that of SYP and is an easy-to-interpret IHC marker of NE differentiation in advanced prostate cancer. While INSM1 has shown promise as a stand-alone assay in other organ systems, potentially replacing dual staining with SYP and CHGA, further studies may be warranted in order to make the same conclusion for advanced prostate cancer.

934 Should We Report the Percentage of Components of Primary Mixed Germ Cell Tumors of the Testis?

Marie Perrone[1], Maria Tretiakova[2], Funda Vakar-Lopez[2], Lawrence True[3]
[1]Seattle, WA, [2]University of Washington, Seattle, WA, [3]University of Washington Medical Center, Seattle, WA

Disclosures: Marie Perrone: None; Maria Tretiakova: None; Funda Vakar-Lopez: None; Lawrence True: None

Background: Primary mixed germ cell tumors (GCTs) of the testis vary in morphology. There is histologic overlap in the morphology of GCTs. Although, according to the NCCN guidelines, the treatment of GCTs is not based on the percent of each component, cancer templates of the College of American Pathologists and clinicians request that pathologists report the percent of each component. Studies report that a large embryonal carcinoma component (more than 50%) provides a rationale for more aggressive adjuvant therapy. (PMID 26453693). Estimating the percent of each component is a quantitative assay. The accuracy of any quantitative assay is important for test interpretation. To our knowledge, the accuracy of pathologists' estimates of percent of components in GCTs has not been assessed. The purpose of this study is to evaluate interobserver variability in estimating component percentages of GCTs.

Design: In this study, 3 genitourinary pathologists retrospectively reviewed selected slides from 34 cases of GCTs. They independently recorded the percent of each component of GCTs (embryonal carcinoma, choriocarcinoma, yolk sac tumor, teratoma, seminoma) on the slides, without the use of immunohistochemical (IHC) stains. Reported percentages of each component were compared.

Results: In 8 cases, all 3 pathologists agreed perfectly on the percentages of each component. In 5 cases, pathologists agreed within 10 percentage points. However, there was significant disagreement in the reported percentage of each component in 21 cases. The interrater reliability (IRR), to within 10%, was 38%. IRR was best for choriocarcinoma (CC). IRR was the worst (at 56%) for both embryonal carcinoma and teratoma. Notably, in 8 cases (24%), there was a difference in reported percentages of at least one component by 50 percentage points or more.

Conclusions: Our study raises the question: Do our estimates of the composition of GCTs provide a reliable metric for clinical care? Pathologists have poor interobserver agreement on the percentage of each component of GCTs. It is possible that the use of IHC may improve agreement. Published literature that discusses the relationship of component percent and clinical outcome have not been based on a proven reliable assay. We suggest that clinicians be aware of the poor reliability of this assay for influencing their treatment decisions, and that future versions of NCCN guidelines acknowledge the limitations of this metric.

935 Handling and Reporting of Pelvic Lymphadenectomy Specimens in Prostate and Bladder Cancer: A Web-based Survey by the European Network of Uropathologists (ENUP)

Susan Prendeville[1], Daniel Berney[2], Lukas Bubendorf[3], Eva Compérat[4], Lars Egevad[5], Ondrej Hes[6], Glen Kristiansen[7], Jon Oxley[8], Geert van Leenders[9], Murali Varma[10], Theodorus Van Der Kwast[11]
[1]Cork, Ireland, [2]Queen Mary University of London, London, United Kingdom, [3]University Hospital Basel, Basel, Switzerland, [4]Tenon Hospital, Paris, France, [5]Karolinska University Hospital, Stockholm, Sweden, [6]Biopticka laborator s.r.o., Plzen, Czech Republic, [7]University of Bonn, Bonn, Germany, [8]North Bristol NHS Trust, Bristol, United Kingdom, [9]Erasmus Medical Centre, Rotterdam, Netherlands, [10]University Hospital of Wales, Cardiff, United Kingdom, [11]University Health Network, Toronto, ON

Disclosures: Susan Prendeville: None; Daniel Berney: None; Lukas Bubendorf: None; Eva Compérat: None; Lars Egevad: None; Ondrej Hes: None; Glen Kristiansen: None; Jon Oxley: None; Geert van Leenders: None; Murali Varma: None; Theodorus Van Der Kwast: None

Background: Pathologic evaluation of lymphadenectomy specimens plays a pivotal role in accurate lymph node (LN) staging. Guidelines standardizing the gross handling and reporting of pelvic lymph node dissection (PLND) in prostate (PCa) and bladder (BCa) cancer are currently lacking. This study aimed to establish current practice patterns of PLND evaluation among pathologists with an interest in urologic pathology.

Design: A web-based survey was circulated to all members of the European Network of Uropathology (ENUP). This included 29 questions focusing on the macroscopic handling, LN enumeration and microscopic reporting of PLND specimens in PCa and BCa. Two questions related to images where the survey participants were asked to determine the number of LNs present (figure 1).

Results: 280 responses were received from pathologists across 23 countries. PLND tissue was received in multiple containers indicating anatomic sites by 62% and in two containers merely indicating right/left by 30%. Intra-operative frozen section on LN was frequently done by 7%.

Only LNs palpable at grossing were submitted by 58%, while 42% routinely embedded the entire specimen. A minority used fat-clearing agents routinely (4%) or occasionally (7%).

According to 64% of respondents at least some of their urologic colleagues regarded LN count as a quality indicator for their surgery. Average LN yield from PLND was ?10LNs in 56% and <10LNs in 44%. For LN enumeration, 93% correlated gross information with the microscopic LN count. Serial section(s) and immunohistochemistry were routinely performed on LN blocks by 48% and <1% of respondents respectively.

To designate a LN microscopically, the majority (91%) required the presence of a LN capsule/subcapsular sinus. In pN+ cases, 72% reported the size of the largest metastatic deposit and 94% reported extracapsular extension. 77% interpreted isolated tumour cells as pN1. Deposits identified in fat without associated lymphoid tissue were considered to represent tumour deposits (pN0) by 36% and replaced LNs (pN+) by 27%. In PCa, LNs identified in periprostatic fat were included in the PLND LN count by 69%.

In *Case 1* two LNs were counted by 67% and in *Case 2* one LN was counted by 91% of respondents (figure 1).

Figure 1 - 935

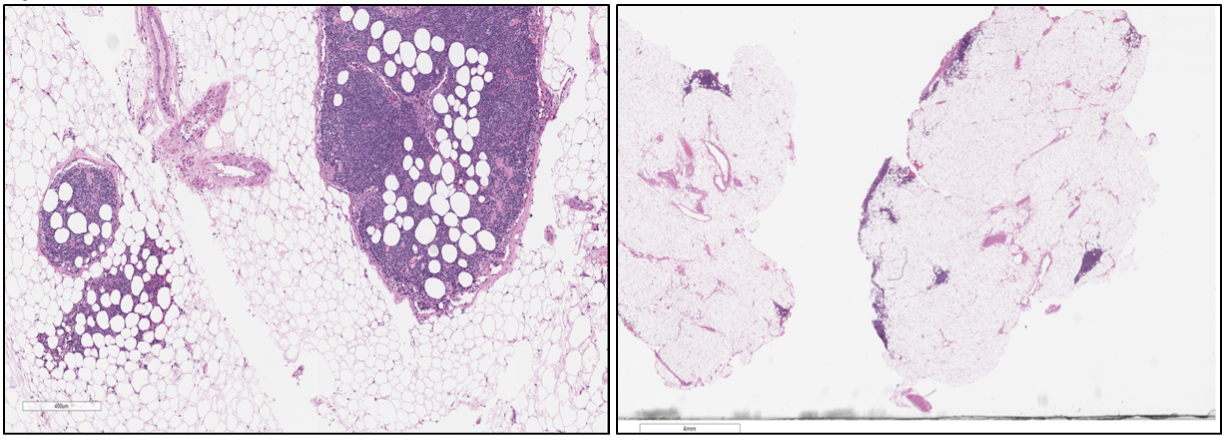

Case 1: Grossing information = 1 nodule palpated, embedded in toto with surrounding adipose tissue in one cassette.

Case 2: Grossing information = 1 nodular area was palpated, bisected and embedded in one cassette.

Conclusions: This study highlights variations in practice with respect to the gross sampling and microscopic evaluation of PLND in urologic malignancies. A consensus protocol may provide a framework for more consistent and standardized reporting of PLND specimens.

936 Is hTERT(SCD-A7) IHC Staining on Urine Cytology Useful?

Dana Razzano[1], Samuel Barasch[2], Minghao Zhong[3]
[1]New York Medical College, Valhalla, NY, [2]Poughkeepsie, NY, [3]Westchester Medical Center, Valhalla, NY

Disclosures: Dana Razzano: None; Samuel Barasch: None; Minghao Zhong: None

Background: Increased telomerase activity is one of the hallmarks for most cancers, including urothelial carcinoma. Previous studies have demonstrated that up to 90% of urothelial carcinoma has increased hTERT at the mRNA level. Recently, a commercially available hTERT antibody (SCD-A7) has been indicated to have some clinical utility on urine cytology specimens. Therefore, we sought to evaluate the reliability of this antibody for immunohistochemistry (IHC) stain.

Design: The IHC staining was performed on the BenchMark ULTRA IHC/ISH System Ventana platform using protocols that were provided by the vendor for both cytology and surgical urothelial carcinoma (UC) specimens. The evaluation material included: one cytology control slide (provided by vendor); 5 cases of bladder resection specimens containing both non-neoplastic urothelium and urothelial carcinoma; tissue microarray (TMA) slides containing 121 urothelial carcinoma samples.

Results: Evaluation of the cytology control slide showed lymphocytes demonstrating strong nuclear staining, while the benign urothelium was negative for hTERT. In the resection specimens, lymphocytes stained weak positive (weaker than in the cytology specimen) with normal urothelium staining positive in 1 of 5 cases and urothelial carcinoma in 2 of 5 cases were positive. In the TMA tissue, only 10 of 121 UC cases showed positive staining. Highlighted results are included in Figure 1. A-F: hTERT (SCA-A7) stained tissues. A. Urine cytology demonstrating strong nuclear positive staining in the lymphocytes and complete negative staining of benign urothelial cells. B. High-grade UC showing patchy weak staining intensity. C. In-situ UC showing moderate staining intensity. D. Benign urothelium showing moderate to strong nuclear staining with accompanying submucosal lymphocytes showing similar staining pattern (inset: high-power focus of mucosa). E-F. TMA of UC showing (E) complete negative staining and (F) demonstrating a peripheral rim of moderate staining intensity. Blue arrow, benign urothelial cells. Black arrow, lymphocytes. Thin blue arrow, urothelial mucosa. Thin black arrow, peripheral rim of staining.

Figure 1 - 936

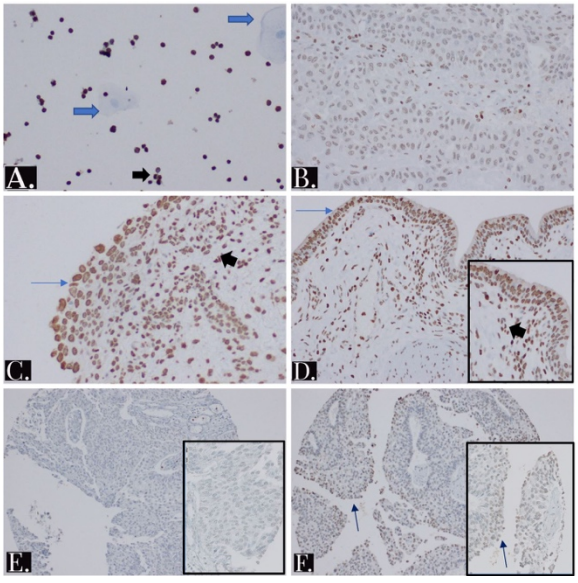

Conclusions: TERT activation and expression upregulation has been demonstrated in urothelial carcinoma. However, using hTERT (SCA-A7) antibody cannot reliably distinguish UC vs benign urothelium. Therefore, the clinical value of this test should be questioned.

937 Combined extraprostatic extension (EPE) and seminal vesicle invasion (SVI) of prostate cancers associated with worse biochemical failure (BCF) than SVI alone: proposal for further pT3 subclassification

Aseeb Rehman[1], Jae Ro[2], Alberto Ayala[3], Brian Miles[1], Mukul Divatia[2], Steven Shen[1], Megan Ketcham[4], Sang Han[1], Betty Chung[1]
[1]Houston Methodist Hospital, Houston, TX, [2]Houston, TX, [3]The Methodist Hospital, Houston, TX, [4]University of Washington, Seattle, WA

Disclosures: Aseeb Rehman: None; Jae Ro: None; Mukul Divatia: None; Megan Ketcham: None; Betty Chung: None

Background: The 8th edition of the AJCC TNM staging system subdivides prostatic pT3 tumors into pT3a(determined by the presence of EPE) and pT3b(determined by presence of SVI with or without EPE). According to Baylor group, involvement of seminal vesicle can take place along the ejaculatory duct plane(Type 1) or through breach of prostatic capsule(Type 2). Further stratification of pT3b cases into SVI only (Type I) or combined EPE and SVI; EPE+SVI(Type II) and correlation with BCF may be significant in determining pathogenesis, treatment options, and prognosis in these patient.

Design: Patient database query identified 116 radical prostatectomy(RP) patients with pT3B disease seen at our institution from 2000-2013. Patient demographics, prostate-specific antigen (PSA) level, and biochemical failure(BCF) data were obtained from medical records. Biochemical failure was defined as PSA rise ? 0.2 ng/mL. Exclusion criteria included prostatectomy post hormonal treatment(2) and unavailability of PSA level(47, included 2 post-treatment prostatectomies). RP slides(n = 69) were retrospectively reviewed for Gleason score(GS), EPE, and SVI by two pathologists and correlated with BCF status.

Results: Average patient age was 66.6 years (range: 53-81). Gleason scores of 7, and 8-10 were found in 21, and 48 cases, respectively. The majority of cases showed EPE+SVI(76.8%) versus SVI alone(23.2%). A higher rate of BCF was seen in EPE+SVI(33.9%) versus SVI alone(12.5%)($P < 0.05$). Cases with type II involvement were associated with higher GS(75.5% cases with GS of 8-10 versus 24.5% cases with a GS of 7)

pT3 substaging		BCF			Total
		Absent	Present	No data available	
	only SVI	14	2	10	26
	Both EPE and SVI	35	18	37	90
Total		49	20	47	116

Conclusions: Our data showed that prostate cancer with combined EPE and SVI are associated with higher rates of BCF than SVI alone. Based on our date, we propose further subdividing pT3 prostate cancers into 3 groups: 1)EPE alone(pT3a), 2)SVI alone(pT3b), and 3)combined EPE+SVI(pT3c). This classification system would more accurately identify those patients who are most likely to experience BCF and provide clinicians with additional information to aid in follow-up and treatment decisions

938 Biomarkers of Cisplatin Resistance in Urothelial Bladder Cancer: HMGA2 and Survivin

Henning Reis[1], Ulrich Krafft[1], Stephan Tschirdewahn[1], Jochen Hess[1], Nina Harke[1], Boris Hadaschik[2], Susanne Krege[3], Peter Nyirády[4], Attila Szendroi[4], Miklós Szücs[4], Orsolya Módos[5], Eszter Székely[6], Tibor Szarvas[1], Tibor Szarvas[4]
[1]West German Cancer Center, University of Duisburg-Essen, Essen, Germany, [2]University of Duisburg-Essen, University Hospital Essen, Essen, Germany, [3]Kliniken Essen-Mitte, Essen, Germany, [4]Semmelweis University, Budapest, Hungary,[5]Clinic of Urology, Semmelweis University, BP, Hungary, [6]University Hospital Budapest, Semmelweis University, Budapest, Hungary

Disclosures: Henning Reis: None; Boris Hadaschik: *Consultant*, Janssen Research and Development Inc.; *Consultant*, BMS; Attila Szendroi: None; Orsolya Módos: None; Tibor Szarvas: None

Background: Both in the adjuvant and neoadjuvant setting, cisplatin-based chemotherapy represents the primary standard in the treatment of advanced bladder cancer (BC). Due to the emergence of novel immunooncologic agents for cisplatin-resistant or ineligible patients, prediction of cisplatin resistance by biomarkers becomes more important in treatment decisions. Therefore, we evaluated the predictive value of 8 promising tissue biomarkers for cisplatin therapy success in BC.

Design: FFPE tumor samples of 106 patients who underwent adjuvant cisplatin-based chemotherapy for BC were analyzed for expression of Emmprin, Survivin, HMGA2, MTA1, RhoGDI, PEG10, TGM2 and TLN1 by immunohistochemistry. Clinicopathological and follow-up data were collected and correlated including univariable and multivariable survival analyses.

Results: Presence of survivin nuclear staining and stronger HMGA2 nuclear staining intensity were associated with worse overall survival (OS) (p=0.002, p=0.045 respectively). In addition, shorter progression free survival (PFS, p=0.024) was detected in cases with nuclear survivin staining, while HMGA2 nuclear positivity tended to correlate with shorter PFS (p=0.069) after at least 2 cycles of chemotherapy. Survivin also proved to be an independent predictor of both OS and PFS (p=0.008, p=0.025 respectively) in multivariable analyses. None of the other markers demonstrated to be significant predictors of adjuvant cisplatin-based chemotherapy.

- Survivin is a promising marker for the prediction of cisplatin resistance in BC.
- The predictive role of HMGA2 should be further investigated to this regard.
- Immunohistochemical marker-analysis provides an easy and time/cost-effective tool which might be used for optimizing treatment decisions in advanced BC for the prediction of cisplatin-resistance.

939 PDL1 Expression in Urothelial Bladder Carcinoma and Multiple Lymph Node Metastases

Jose Antonio Rodriguez Calero[1], Vera Genitsch[2], Achim Fleischmann[3]
[1]Institute of Pathology, University of Bern, Liebefeld, Switzerland, [2]University of Bern, Bern, Switzerland, [3]Institut fur Pathologie Kantonsspital, Munsterlingen, Switzerland

Disclosures: Jose Antonio Rodriguez Calero: None; Vera Genitsch: None; Achim Fleischmann: None

Background: Anti-PD1/PDL1 therapies represent new treatment options for advanced urothelial bladder carcinoma (UBC). However, information about PDL1 expression pattern and levels in UBC is still limited.

Design: Out of 126 patients with UBC treated by cystectomy and extended pelvic lymphadenectomy 36 had one and 90 had ? two lymph node metastases. Tissue microarrays (TMA) were constructed with four samples from all primary tumors and two from each metastasis. PDL1 expression level was assessed by immunohistochemistry (SP263 Ventana) separately for tumor (TC) (membranous staining) and immune cells (IC) and mean percentages of positive cells in the primary tumors and the metastasizing components were determined.

Results: PDL1 expression was variable in the primary tumors and their metastasizing component: TC showed partial or complete membranous staining with weak to strong intensity, cytoplasmic staining with in general lower intensity, and both cell compartments could be stained. IC presented rather with an, often granular, cytoplasmic staining. Within a given primary tumor expression in different areas was similar, and this was also true for many metastasizing components. However, a number of patients showed substantial PDL1 expression differences between their metastases. Comparing the mean PDL1 expression in primary tumors and their corresponding lymph node metastases revealed a moderate correlation for TC (r=0.592, figure 1) and no relevant correlation for IC (r=0.241, figure 2).

Figure 1 - 939

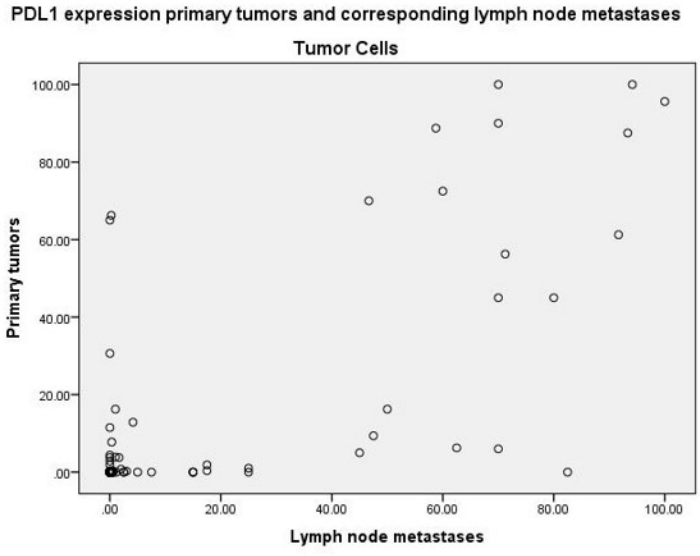

Figure 2 - 939

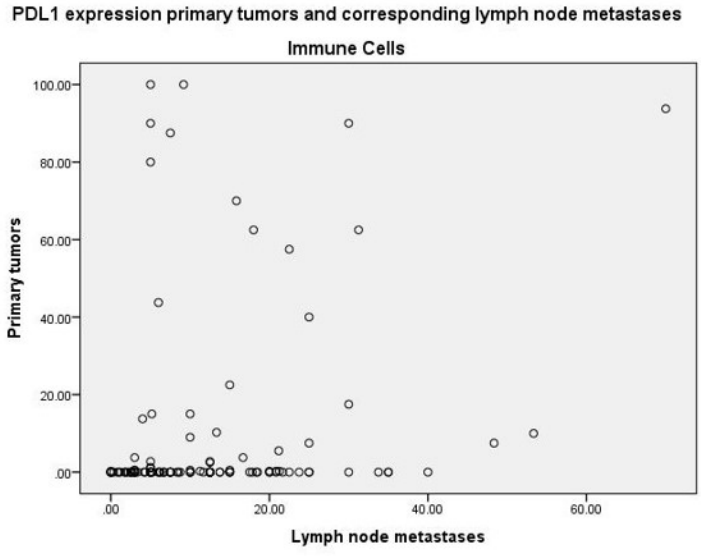

Conclusions: PDL1 expression pattern and intensity levels were similar to the more extensively described ones in lung cancer. There was a weak positive correlation between the neoplastic cells and to a lesser degree between the lymphocytes of the primary tumor and its metastasizing component. Interestingly, we noted large expression differences between different corresponding metastases of a given primary tumor in a subset of patients, indicating that the primary tumor is not necessarily a surrogate for all its metastases. Our data provide information, which might help to select patients for anti-PDL1 therapies in the future.

940 Is MRI/US Fusion Targeted Biopsy Alone Adequate for Detecting Prostate Cancer in Patients with a Prior Negative Prostate Biopsy?

Maria Del Carmen Rodriguez Pena[1], Marie-Lisa Eich[2], Kristin Porter[1], Zachary Glaser[2], Jeffrey Nix[1], Soroush Rais-Bahrami[1], Jennifer Gordetsky[1]
[1]University of Alabama at Birmingham, Birmingham, AL, [2]The University of Alabama at Birmingham, Birmingham, AL

Disclosures: Maria Del Carmen Rodriguez Pena: None; Marie-Lisa Eich: None; Kristin Porter: None; Zachary Glaser: None; Jeffrey Nix: *Speaker*, Intuitive Surgical; *Consultant*, Phillips InVivo Corp; Soroush Rais-Bahrami: *Consultant*, Philips/InVivo Corp; *Advisory Board Member*, Genomic Health Inc; Jennifer Gordetsky: None

Background: Magnetic resonance imaging (MR)/ultrasound (US) fusion targeted biopsy can more accurately identify clinically significant prostate cancer compared to the standard sextant prostate biopsy. This new technique could potentially replace the traditional standard prostate biopsy for the detection of cancer. We compared the clinical, imaging, and pathologic findings in patients with a prior negative prostate biopsy who underwent targeted biopsy and concurrent standard biopsy versus those who underwent targeted biopsy alone.

Design: A retrospective review was performed of our database of patients who underwent MR/US targeted prostate biopsy. Patients were selected who had a previous biopsy negative for prostate cancer. Patients were then categorized by those who underwent targeted biopsy only (TBO) versus those underwent targeted biopsy with concurrent standard biopsy (T+S). Clinical, pathologic, and imaging characteristics were compared between the two groups.

Results: A total of 138 patients met inclusion criteria. Of these, 101 patients were in the T+S group and 37 patients were in the TBO group. There was no significant difference between the two groups in terms of race, body mass index and prostate specific antigen level. Patients in the TBO group were older, 68.29 ± 6.05 vs 64.81 ± 6.35 years, respectively (p=0.004). Patients in the TBO group also had a higher average PIRADS score, 4.54 ± 0.56 vs 3.63 ± 0.88, respectively (p<0.0001). The T+S group detected more Grade Group (GG) 1 tumors (36.8%) compared to the TBO group (14.3%), p=0.04. There was no significant difference between the groups for the average number of targeted lesions (p=0.53) or number of targeted cores sampled (p=0.16). However, the T+S group took more total cores on average (16.1±1.7) compared to the TBO group (4.6±1.8), p<0.0001. In addition, the TBO group had a higher percentage of positive cores (55.0%) compared to the T+S group (9.5%), p<0.0001. The cancer detection rate also favored the TBO group, 94.6% vs 37.6% (p<0.0001).

Conclusions: In patients with a prior negative biopsy for prostate cancer, the use of MR/US targeted biopsy alone is an acceptable method for cancer detection compared to targeted biopsy with concurrent standard biopsy, while requiring less cores sampled.

941 Adenocarcinoma of the Urinary Bladder: A Comprehensive Genomic Profiling Study

Jeffrey Ross[1], Gennady Bratslavsky[2], Oleg Shapiro[2], Joseph Jacob[2], Laurie Gay[3], Julia Elvin[4], Jo-Anne Vergilio[4], J. Keith Killian[4], Nhu Ngo[4], Shakti Ramkissoon[5], Eric Severson[5], Amanda Hemmerich[5], Siraj Ali[3], Alexa Schrock[4], Jon Chung[4], Venkataprasanth Reddy[4], Vincent Miller[4]

[1]Upstate Medical University, Syracuse, NY, [2]SUNY Upstate Medical University, Syracuse, NY, [3]Cambridge, MA, [4]Foundation Medicine, Cambridge, MA, [5]Foundation Medicine, Morrisville, NC

Disclosures: Jeffrey Ross: *Employee*, Foundation Medicine, Inc.; Oleg Shapiro: None; Laurie Gay: *Employee*, Foundation Medicine, Inc.; Julia Elvin: *Employee*, Foundation Medicine, Inc; Nhu Ngo: *Employee*, Foundation Medicine, Inc.; Eric Severson: *Employee*, Foundation Medicine, Inc.; Amanda Hemmerich: *Employee*, Foundation Medicine, Inc.; Alexa Schrock: *Employee*, Foundation Medicine, Inc.; Vincent Miller: *Employee*, Foundation Medicine Inc.; *Advisory Board Member*, Revolution Medicines

Background: The molecular features of the uncommon adenocarcinoma of the bladder (ABC) has not been widely evaluated. We performed comprehensive genomic profiling (CGP) to compare the genomic alterations (GA) in ABC with those found in the common urothelial carcinoma (UBC).

Design: From a series of 181,782 FFPE tissues from clinically advanced tumors, 143 cases of ACB and 2,142 cases of UCB underwent hybrid-capture based CGP to evaluate all classes of genomic alterations. Tumor mutational burden (TMB) was determined on 1.1 Mbp of sequenced DNA and microsatellite instability (MSI) was determined on 114 loci.

Results: the ABC patients were significantly younger and less often female than the UBC patients (P<0.0001) (Table). UBC featured significantly more GA/tumor than ABC possibly reflecting the higher tobacco exposure in these patients. The most frequently altered non-clinically relevant (CR) GA varied with *TP53*, *KRAS* and *APC* GA more frequent in ABC and *TERT*, *CDKN2A/B* and DNA-repair genes (*ARID1A* and *KDM6A*) more frequently altered in UBC. MTOR pathway GA (*PIK3CA*, *TSC1*, *PTEN*) were more frequent in UBC as were targetable kinase alterations (*FGFR3* and *ERBB2*). Kinase GA in *ERBB2*, *MET* and *EGFR* were noteworthy in ABC. UBC featured a significantly higher predictive profile for potential immunotherapy benefit with significantly higher TMB parameters than ABC including mean TMB and TMB>20 mut/Mb (P<0.0001). MSI high status was very uncommon in both tumor types.

	Adenocarcinoma (ACB)	Urothelial Carcinoma (UCB)
Number of Cases	143	2,142
Males/Females	57/86	1597/545
Median age (range) in years	58 (24-83)	67 (19-88)
GA/tumor	5.4	7.7
Top Non-CRGA	*TP53* 79% *KRAS* 30% *SMAD4* 14% *MYC* 13% *CDKN2A* 13% *TERT* 12% *ARID1A* 10% *APC* 8%	*TERT* 68% *TP53* 56% *CDKN2A* 35% *CDKN2B* 38% *ARID1A* 23% *KDM6A* 23% *KMT2D* 22% *APC* 3%
Top CRGA	*PIK3CA* 10% *ERBB2* 8% *PTEN* 4% *MET* 4% *EGFR* 4%	*PIK3CA* 21% *FGFR3* 19% *ERBB2* 16% *TSC1* 9% *PTEN* 5%
MSI-High	2/106 (2%)	11/1661 (1%)
Mean TMB (mut/Mb)	2.4	9.9
Median TMB (mut/Mb)	3.6	7.0
TMB>10 mut/Mb	14 (10%)	697 (32%)
TMB>20 mut/Mb	4 (3%)	243 (11%)
PD-L1 IHC Positive	2/11 (18%)	75/243 (31%)

Conclusions: CGP reveals that ABC differs widely from UBC in a wide range of genomic features including less frequent opportunities for both targeted and immunotherapies than UBC. Nonetheless, ABC does feature potential kinase targets and, although significantly less often than UBC, biomarkers predictive of immunotherapy benefit in a subset of cases.

942 Comparison of Comprehensive Genomic Profiling Results in Ductal Carcinoma and Acinar Carcinoma of the Prostate

Jeffrey Ross[1], Laurie Gay[2], Elizabeth Ferry[3], Joseph Jacob[3], Oleg Shapiro[3], Sherri Millis[4], Julia Elvin[5], Jo-Anne Vergilio[5], J. Keith Killian[5], Nhu Ngo[5], Shakti Ramkissoon[6], Eric Severson[6], Amanda Hemmerich[6], Siraj Ali[2], Alexa Schrock[5], Jon Chung[5], Venkataprasanth Reddy[5], Vincent Miller[5], Gennady Bratslavsky[3]
[1]Upstate Medical University, Syracuse, NY, [2]Cambridge, MA, [3]SUNY Upstate Medical University, Syracuse, NY, [4]Phoenix, AZ, [5]Foundation Medicine, Cambridge, MA, [6]Foundation Medicine, Morrisville, NC

Disclosures: Jeffrey Ross: *Employee*, Foundation Medicine, Inc.; Laurie Gay: *Employee*, Foundation Medicine, Inc.; Sherri Millis: *Employee*, Foundation Medicine Inc.; Julia Elvin: *Employee*, Foundation Medicine, Inc; Nhu Ngo: *Employee*, Foundation Medicine, Inc.; Eric Severson: *Employee*, Foundation Medicine, Inc.; Amanda Hemmerich: *Employee*, Foundation Medicine, Inc.; Alexa Schrock: *Employee*, Foundation Medicine, Inc.; Vincent Miller: *Employee*, Foundation Medicine Inc.; *Advisory Board Member*, Revolution Medicines

Background: In contrast to the common acinar carcinoma of the prostate (PAC), the prostatic ductal carcinoma (PDC) is uncommon. With unique central location and tubulopapillary configuration, PDC shares some bi0omarker features with PAC including PSA expression. This study compares the genomic signatures of the two tumor types.

Design: Comprehensive genomic profiling (CGP) was performed on FFPE samples from 61 cases of clinically advanced PDC and 4,132 similar cases of PAC. Tumor mutational burden (TMB) was determined on 1.1 Mbp of sequenced DNA and microsatellite instability (MSI) was determined on 114 loci.

Results: The PAC and PDA had a similar age, frequency of genomic alterations (GA) per tumor and *TP53* GA (Table). In the frequent GA group, *TMPRSS2:ERG* fusions and *AR* GA were more often identified in PAC than PDC whereas *PTEN* GA were more common in PDC than PAC. The frequencies of potential therapy targeting GA were similar in both groups involving *BRCA2* (PARP inhibitors), *BRAF* (BRAF/MEK inhibitors) and *PIK3CA* (MTOR inhibitors). *ATM* GA (PARP inhibitors) were more common in PAC than PDC. *CDK12* GA associated with immunotherapy (IO) benefit were similar in both groups as were the frequencies of MSI-High status, median TMB and high TMB levels.

	Prostatic Ductal Adenocarcinoma		Prostatic Acinar Adenocarcinoma	
Cases	61		4,132	
Median Age/Range (years)	66 (51-86)		66 (34-88)	
GA/tumor	4.1		4.4	
Most Frequently Altered Genes	*PTEN* *TP53* *TMPRSS2* *AR* *PIK3CA* *FAS* *RB1*	48% 46% 21% 11% 11% 11% 10%	*TP53* *TMPRSS2* *PTEN* *AR* *MYC* *BRCA2* *PIK3CA*	43% 32% 32% 21% 12% 10% 7%
Potential Targeted Therapy Impacting Alterations	*PTEN* *AR* *PIK3CA* *BRCA2* *BRAF* *RET*	48% 11% 11% 9% 7% 4%	*PTEN* *AR* *BRCA2* *PIK3CA* *ATM* *BRAF*	32% 21% 10% 7% 6% 4%
CDK12 GA	8.2%		6.0%	
MSI High Status	1.9%		2.6%	
TMB Median (mut/Mb)	2.6		2.6	
TMB > 10 mut/Mb	3.3%		3.8%	
TMB > 20 mut/Mb	1.6%		0.7%	

Conclusions: Although PDC and PAC are maintained as different tumor types with potentially contrasting histogenesis, this CGP based study did not identify significant differences in genomic signatures. In both tumor types, individual PDC and PAC samples may harbor biomarkers that could direct patients to targeted (PARP, MTOR and BRAF/MEK inhibitors) or immunotherapies (*CDK12* GA, MSI-High or high TMB status). Continued enrollment of both PDC and PAC patients into mechanism driven clinical trials appears warranted.

943 Should Treated Prostatic Adenocarcinoma Be Graded?

Jenny Ross[1], Guangyuan Li[2], Xiaoqi Lin[3], Ximing Yang[3]
[1]Feinberg School of Medicine/Northwestern University, Chicago, IL, [2]Northwestern University Feinberg School of Medicine, Solon, OH, [3]Northwestern University, Chicago, IL

Disclosures: Jenny Ross: None; Guangyuan Li: None; Xiaoqi Lin: None; Ximing Yang: None

Background: Many treatment modalities are available for patients with prostatic adenocarcinoma aside from surgery. When some patients recur after treatment, they need sufficient pathologic information to allow for best clinical treatment options; however, treated prostatic adenocarcinoma is traditionally not graded. We are studying whether the histologic features including grade are correlated to biologic behavior of such cases.

Design: Over 2014-2018, 42 cases of prostatic adenocarcinoma with relevant treatment history were evaluated for clinical and pathologic parameters. Tumors were graded using Grade Groups (GG): GG1, Gleason score (GS) ?6, GG2 (GS=3+4), GG3 (GS=4+3), GG4 (GS=8), and GG5 (GS?9). Selected cases were subjected to Ki-67 immunohistochemical analysis. The histologic features of treatment effect were defined as atrophic prostatic glands, vacuolated cytoplasm, and bland small nuclei with reduced nucleoli.

Of the 42 cases, 25 had hormone therapy, 19 had radiotherapy, and 6 included both; 9 cases had other treatments with 5 of them also including hormone therapy, radiotherapy, or both. Other treatments included neoadjuvant chemotherapy, high intensity focused ultrasound (HIFU), cryotherapy, herbal medicine, and an undisclosed clinical trial.

Results: Of 42 cases 38 contained residual adenocarcinoma and 4 had no carcinoma detected within prostate, although 2 of these negative cases had positive lymph nodes. Biopsies and transurethral resections (22) were examined separately from prostatectomies (20). Biopsy cases with higher Grade Group tumors had higher tumor volume and were more likely to have extraprostatic extension detected. Prostatectomy cases with higher Grade Group tumors had higher tumor volume, higher pathologic T and N stages, and were more likely to have a positive margin (Table 1).

Treatment effect was absent in most cases (10/20 prostatectomies and 13/22 biopsy cases), was mild in most of the rest, and prominent in only 7/40 cases. Prominent treatment effect correlated with lower Grade Group tumors. Of 7 cases with Ki-67, 6 had higher values corresponding to higher Grade Group except 1 case which appeared high grade but had strong treatment effect and low Ki-67 index.

	P:	Average volume	T0	T2	T3	T4	N0	N1	Positive Margin	B:	Average volume	EPE
GG 0, 1		0.05%	1	1	0	0	1	1	0		1.25%	0
GG 2, 3		15.5%	0	2	4	0	6	0	1		51.4%	1
GG 4, 5		38.3%	0	1	10	1	7	5	9		69.4%	5

Key: P: Prostatectomy specimens, B: biopsies and transurethral resection specimens, GG: Grade Group, EPE: Extraprostatic extension identified on biopsy

Conclusions: When tumor shows no obvious treatment effect, prostatic adenocarcinoma should be graded to provide useful clinical information. When significant treatment effect is present, immunohistochemistry for Ki-67 may be useful to stratify biologic behavior of these tumors.

944 Fluciclovine (18F) PET Detection of Lymph Node Metastasis in High-risk Primary Prostatic Adenocarcinoma Patients

Faisal Saeed[1], Olayinka Abiodun-Ojo[1], Akinyemi Akintayo[2], Mehrdad Alemozaffar[1], David Schuster[1], Adeboye O. Osunkoya[2]
[1]Emory University, Atlanta, GA, [2]Emory University School of Medicine, Atlanta, GA

Disclosures: Faisal Saeed: None; Olayinka Abiodun-Ojo: None; Akinyemi Akintayo: None; Mehrdad Alemozaffar: None; David Schuster: *Grant or Research Support*, Blue Earth Diagnostics, Ltd; *Grant or Research Support*, Nihon Medi-Physics Co. Ltd.; *Consultant*, Syncona; Adeboye O. Osunkoya: None

Background: The FDA recently approved a new positron emission tomography (PET) radiotracer, fluciclovine (^{18}F), for the detection of prostate cancer (PCa) recurrence in patients with elevated prostate specific antigen (PSA) levels following treatment. Fluciclovine detects the upregulation of amino acid transport that occurs in PCa, and can potentially identify recurrent PCa more reliably than conventional imaging techniques. In this study, we investigated the efficacy and limitations of fluciclovine in detecting PCa lymph node metastasis in high-risk primary prostate cancer patients.

Design: We analyzed 210 lymph node packets from 14 patients with metastatic PCa following robot-assisted radical prostatectomy and super-extended pelvic lymph node dissection. We retrospectively correlated the fluciclovine PET results with histologic findings on a per region basis. The size of all lymph nodes, number of positive lymph nodes, size of metastatic foci, and status of extranodal extension were documented. For every lymph node packet, the median size of metastatic foci was utilized for analysis.

Results: Metastatic lesions were identified in 54/210 (25.7%) template lymph node packets. Of the 54 malignant lymph node packets, 22 (40.7%) with median sizes of metastatic foci ranging between 2.0-21.0 mm were identified (true positives) on fluciclovine PET, while 32 (59.3%) were not identified (false negatives). There was no significant difference in the median long axis diameters in the packets of true positive and false negative lymph nodes which contain the metastatic foci (9.6 vs. 9.1 mm, respectively; $p>0.69$). However, the median long axis diameters of metastatic foci within the true positive lymph nodes, 8.5 mm (range 2.0-21.0 mm) was significantly higher than false negative metastatic foci, 3.2 mm (range 0.35-13.0 mm; $p<0.01$). Metastatic foci ≤1 mm were reported in 13/54 (24.1%) lymph node packets, none of these were visualized on fluciclovine PET.

Conclusions: This study demonstrates that the ability of fluciclovine PET to detect lymph node metastasis in patients with intermediate to high-risk PCa is dependent on the size of the metastatic foci. Lymph nodes with micrometastatic foci (≤1 mm) are unlikely to be detected by fluciclovine PET.

945 Validation of the Proposed Biological Classification System of Papillary Renal Cell Carcinoma in a New Cohort of 80 Patients

Rola Saleeb[1], Kiril Trpkov[2], Carl Boulos[3], Sung Sun Kim[4], Fabio Rotondo[4], George Yousef[5]
[1]Toronto, ON, [2]University of Calgary, Calgary, AB, [3]St Michael's Hospital, Markham, ON, [4]St Michael's Hospital, Toronto, ON, [5]Hospital for Sick Children, Toronto, ON

Disclosures: Rola Saleeb: None; Kiril Trpkov: None; Carl Boulos: None; Sung Sun Kim: None; Fabio Rotondo: None; George Yousef: None

Background: Papillary renal cell carcinoma (PRCC) has two subtypes. Recently a combined morphological and molecular classification system has been proposed. This classification includes new type 3 and oncocytic low grade (OLG) PRCC. PRCC3 is molecularly and clinically similar to PRCC2, however morphologically it is frequently classified as PRCC1. OLG is a rare subtype with a favourable prognosis. In this study we aim to assess the validity of the new classification system in another cohort of PRCC, correlating the different subtypes with their corresponding clinical parameters.

Design: A cohort of 80 PRCCs was selected from resection specimens. Tissue microarray (TMA) was constructed using 3 cores per tumor. The TMA was stained with ABCC2, CA9, GATA3, CK7 and racemase. The cohort was subtyped by two pathologists using combined morphologic and IHC criteria. ABCC2 scoring was further quantified by image analysis software. Clinicopathologic information was gathered on tumor size, necrosis, pathologic stage, disease recurrence and specific survival, and overall survival. Graphpad Prism 7 was used for statistical analysis.

Results: The PRCC cohort analysis revealed 25% PRCC1, 37.5% PRCC2, 36.3% PRCC3 and 1.3% OLG. Racemase strongly stained all PRCC subtypes except OLG. The mean tumor sizes for PRCC1 and OLG (4.5 cm and 1.4 cm) were smaller than the PRCC2 and PRCC3 groups (5.8 cm and 5.1 cm). PRCC1 and OLG had significantly less necrosis ($p=0.0018$) and lower disease stage ($p=0.05$) than the PRCC2 and 3. Log rank test showed near significant ($p=0.07$) differences in the overall survival between the PRCC1 group and the PRCC2 + PRCC3 groups together (HR 3.6, 95% CI 0.9-15.11).

Table 1: Scoring criteria for subtyping PRCC cohort

IHC	PRCC1	PRCC2	PRCC3	PRCC OLG
ABCC2 manual	Negative	Strong=renal tubules	Weak patchy	Strong
CA9	Negative	Perinuclear dot like staining	Negative	Negative
GATA3	Negative	Negative	Negative	Positive
ABCC2 digital score	<10 $x10^3$	>15 $x10^3$	5 $x10^3$ – 30 $x10^3$ Overlap cases judged on morphology	>15 $x10^3$

Figure 1 - 945

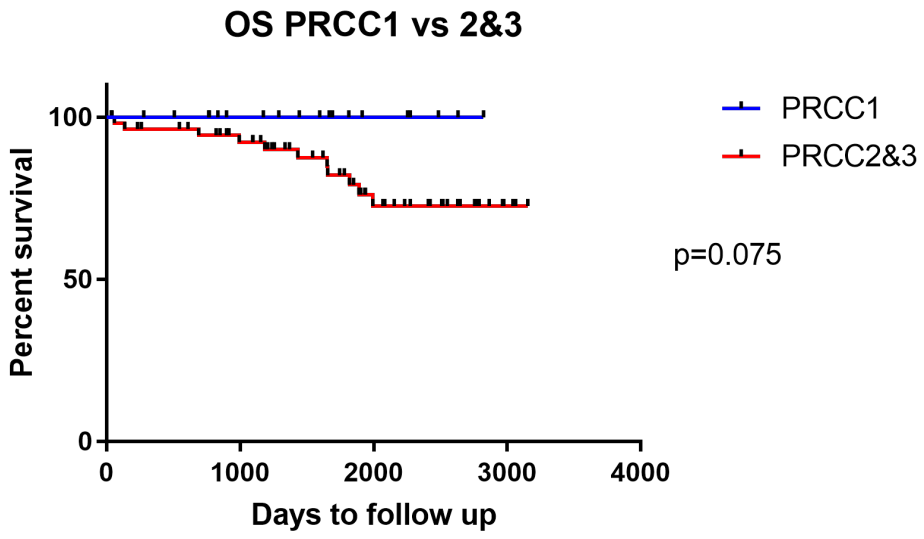

Conclusions: The reported classification system of PRCC had shown PRCC1 and OLG to be more indolent tumors than the PRCC2 and PRCC3. Our results also show significant differences in a number of clinical and pathologic parameters between the two groups. Tumor associated necrosis and disease stage were significantly higher in PRCC2 and PRCC3 tumors, while the overall survival was lower in these two subtypes. The tumor subtype frequencies were similar to the ones previously reported. OLG are small sized, lower stage tumors. The proposed classification shows better separation of the PRCC both prognostically and biologically, and in particular, in delineating PRCC3 subtype.

946 Histologic Evaluation of False Positive PIRADS 4 and 5 Lesions of the Prostate: Single Institute Experience

Akash Sali[1], Andre Abreu[1], Suzanne Palmer[1], Inderbir Gill[1], Manju Aron[1]
[1]Keck School of Medicine of University of Southern California, Los Angeles, CA

Disclosures: Akash Sali: None; Andre Abreu: None; Suzanne Palmer: None; Inderbir Gill: None; Manju Aron: None

Background: Multiparametric prostate MR imaging (mpMRI) is currently the most accurate imaging modality to detect, localize and stage prostate cancer. PIRADS categories 4 and 5 (4/5) of the 5-point reporting system of mpMRI has high accuracy in detecting prostate cancers (PCa). However, benign mimickers have been reported to masquerade as PIRADS 4/5 lesions on mpMRI, contributing to a false positive result. In this study, we reviewed the histological findings associated with a benign diagnosis of PIRADS 4/5 lesions on mpMRI.

Design: A retrospective review of the institutional prostate database from 2012 to 2018 was performed to select patients with PIRADS 4/5 lesions on mpMRI with MRI-ultrasound fusion targeted biopsies (MRF-TB). The histopathology slides were reviewed and the cohort was further divided into two subsets, one showing benign prostatic tissue with no significant pathological findings (NSPF) and the other with significant benign pathological findings (SPF), including inflammation, atrophy, granulomas, calcification, and adenosis. Follow up MRI and targeted biopsies when present were evaluated.

Results: We identified 270 patients with PIRADS 4/5 lesions on mpMRI (191 PIRADS 4 and 79 PIRADS 5). Benign histology was present in 45 cases (17%) with SPF in 30 cases (67%) and NSPF in the remaining 15 (33%). The distribution of the cases in the various benign

categories according to the PIRADS status is highlighted in Table1. The commonest SPF was atrophy (15/30; 50%). Most of the cases with atrophy showed accompanying focal chronic inflammation with increased prostatic stroma. Of the 30 cases with SPF, data regarding follow up MRI and biopsies were available in only 8 cases. Of these only 2 were diagnosed with PCa. Of the 15 cases with NSPF follow up data was available in 3 cases of which 2 were diagnosed with PCa.

	PIRADS 5	PIRADS 4	Total
Atrophy	3	12	15
Inflammation	3	6	9
Granulomas	1	2	3
Calcification	1	1	2
Adenosis	0	1	1
No Significant Pathologic Findings	2	13	15

Conclusions: MRF-TB from PIRADS 4/5 lesions detects PCa in a majority of cases. False positivity can, however, occur in 17% of the cases, less often in PIRADS 5 than in PIRADS 4 (13% vs 18%) lesions. Atrophy is the most common SPF associated with a false positive MRI finding, present in 50% of the cases in this cohort. Although not conclusive NSPF is more likely to be associated with PCa on follow up.

947 Histopathologic Findings in Testes Post-Immunotherapy for Metastatic Melanoma

Iryna Samarska[1], Belkiss Murati Amador[2], Karl Benz[3], Mahir Maruf[3], Eleonora Duregon[4], Jody Hooper[5], Amin Herati[3], Adeboye O. Osunkoya[6], Shamlal Mangray[7], Andres Matoso[8]
[1]Johns Hopkins University School of Medicine, Maastricht University Medical Center, Maastricht, Netherlands, [2]Johns Hopkins University School of Medicine, Baltimore, MD, [3]James Buchanan Brady Urological Institutions, Johns Hopkins Hospital, Johns Hopkins Medical Institutions, Baltimore, MD, [4]Baltimore, MD, [5]Johns Hopkins University, Baltimore, MD, [6]Emory University School of Medicine, Atlanta, GA, [7]Nationwide Children's Hospital, Providence, RI, [8]Johns Hopkins Medical Institutions, Baltimore, MD

Disclosures: Iryna Samarska: None; Belkiss Murati Amador: None; Karl Benz: None; Mahir Maruf: None; Eleonora Duregon: None; Jody Hooper: None; Amin Herati: None; Adeboye O. Osunkoya: None; Shamlal Mangray: None; Andres Matoso: None

Background: Ipilimumab, Pembrolizumab and Nivolumab are immune checkpoint inhibitors (ICI) used in the setting of metastatic melanoma. While outcomes for ICI treatment of melanoma is encouraging, there is paucity of data regarding treatment related side effects, specifically the effect on male fertility is largely unknown. Based on the findings of an index patient who developed azoospermia following ICI therapy, we sought to characterize the histologic changes in testes from men treated for metastatic melanoma with ICI.

Design: Autopsy testicular tissue was obtained from adult males with advanced melanoma who had undergone ICI therapy without chemotherapy for more than 1 month (n=6). The control group consisted of adult males with terminal melanoma (n=10). H&E stained slides were scanned and the digital images used for morphometric analysis. The morphometric findings were correlated with patient demographics, melanoma treatment history, type of immunotherapy, and duration of therapy.

Results: The median age was 54 years (range 30-67) for the study group and 57.3 (range: 23-83) for the control group. Four patients (4/6: 66.7%) received Ipilimumab and Nivolumab and two patients (2/6: 33.3%) received Ipilimumab and Pembrolizumab. Two patients in study group received BRAF inhibitors, accompanied by MEK-inhibitor in one case. No patients received genital radiotherapy. Mean tubular diameter was significantly smaller in patients treated with ICI compared to controls (138.55±15.4 vs. 169.86±23.4; p=0.006). The seminiferous epithelium height was also significantly reduced in study cases compared to controls (36.96±4.3 vs. 47.58±8; p=0.013). The number of tubules, the thickness of the tubular wall, number of Leydig cells were not significantly different between these two groups. Impaired spermatogenesis was seen in 5/6 (83.3% Johnsen score 9-2) ICI patients compared to 5/10 (50%; Johnsen score 9-2) in the control group. There was no correlation between hypospermatogenesis and age, and the only study patient with normal spermatogenesis was 58 years old at the time of autopsy.

Conclusions: Impaired spermatogenesis observed in patients treated with ICI invites consideration of this as a potentially significant adverse event that has been previously unreported. Further studies are needed to better establish a causal relationship and understand the potential mechanism for the changes.

948 Relation of Squamous Cell Carcinoma (SCC) to Condyloma Acuminatum of Urinary Bladder

Iryna Samarska[1], Jonathan Epstein[2]
[1]Johns Hopkins University School of Medicine, Maastricht University Medical Center, Maastricht, Netherlands, [2]Johns Hopkins Medical Institutions, Baltimore, MD

Disclosures: Iryna Samarska: None; Jonathan Epstein: None

Background: Condyloma acuminatum rarely occurs in the urinary bladder with the 2 largest series each reporting only 3 cases each. Furthermore, these lesions have not been systematically studies with more sensitive RNA in-situ hybridization (ISH).

Design: We studied 51 cases of condyloma acuminatum of the urinary bladder from TURBs of 38 patients from the consult files of one of the authors. We were able to obtain clinical follow-up information on all 38 patients. RNA ISH was performed in all 38 patients.

Results: TURBs were obtained from 25 males with a median age of 73 yrs. [range 41-87] and 13 females with a median age of 68 yrs. [range 30-86]. Follow-up period ranged from 15 months to 20 years [median 6 years]. Bladder lesions were accompanied by urethral lesions in four men. 7 patients had a history of multiple recurrent episodes of condylomas in urinary bladder [range 2-10] (18%; 7/38 patients) and a history of immunosuppression. Only one patient had a history of multiple condylomas of penis/anorectal region and anal intraepithelial neoplasia Grade 3. 13/38 (36.1%) patients had condylomas with moderate to severe dysplasia in their condylomas.13/38 (34.2%) patients were diagnosed with SCC in situ, 8/38 (21.0%) had invasive SCC, and in 3/38 (7.9%) invasive SCC could not be excluded with certainty (some patients with >1 lesion). In total 16/38 (42.1%) patients squamous cell carcinoma (either in situ or invasive) diagnosed at the time of presentation with condyloma or within 1 year of follow up. 20/38 (52.6%) patients had a history of urothelial carcinoma: 5/38 (13.1%) invasive; 7/38 (18.4%) non-invasive high grade; 8/38 (21.0%) non-invasive low grade. ISH for low-risk HPV (6/11 HPV) was positive in 15/38 (39.5%) cases. ISH for high risk HPV was positive 8/38 (21.1%) cases. Lesions from 19 patients were negative for both low risk and high risk HPV (19/38; 50%).

Conclusions: Our study showed a strong association of condyloma acuminatum of the urinary bladder with SCC of the bladder. Immunosuppression is a risk factor for developing of condyloma acuminatum of the bladder. It is important to distinguish bladder condylomas from papillary urothelial carcinoma, given their different risks for panurothelial disease and risk of SCC. Recognition of bladder condylomas histologically is often challenging given their rarity; they can be negative for both low-risk and high-risk HPV, and most patients do not have a history of condylomas of their external genitalia.

949 Clinicopathologic Findings of Recurrent and Non-recurrent urethral stricture disease

Iryna Samarska[1], Belkiss Murati Amador[2], Andres Matoso[3]
[1]Johns Hopkins University School of Medicine, Maastricht University Medical Center, Maastricht, Netherlands, [2]Johns Hopkins University School of Medicine, Baltimore, MD, [3]Johns Hopkins Medical Institutions, Baltimore, MD

Disclosures: Iryna Samarska: None; Belkiss Murati Amador: None; Andres Matoso: None

Background: Urethral stricture disease is a relative often problem in urological practice. The present study is aimed to describe the clinicopathologic features of the initial urethral stricture from patients who later recurred compared to those who did not recur on follow-up.

Design: We identified 37 consecutive cases of primary urethral stricture excision. A retrospective review was performed to collect patient demographics and history of infection, trauma, and previous urological procedures. Histopathological analysis included evaluation of the inflammatory infiltrate based on the predominant (>50%) cell type: lymphocyte rich, neutrophil rich, plasma cell rich, mixed infiltrate; and of the degree of fibrosis: loose fibrosis (>40 stroma nuclei/HPF) or dense fibrotic plaque (<40 stroma nuclei/HPF).

Results: The average follow-up time was 48.7months. 20 patients recurred and 17 did not. The clinical findings are summarized in table 1. Cases with non-recurrent stricture showed predominantly loose fibrosis (11/17, 65%) with lymphocyte rich infiltrate (11/17; 65%), plasma cell rich infiltrate (3/17; 18%) and dense fibrotic plaques (3/17; 18%). Patients with recurrent urethral strictures showed dense fibrotic plaques in 14 cases (14/20; 70.0%); loose fibrosis with lymphocyte rich infiltrate (3/20; 15.0%), loose fibrosis with plasma cell rich infiltrate (3/20; 15.0%) [p=0.0007, χ^2/df=11.51].

Table 1. Data on demographics, etiological factor, localization and size of strictures in both groups.

Parameters	Non-recurrent	Recurrent	P value
Age , yrs (range)	43 (25-74)	47 (26-81)	NS
Number	17	20	
Race			
White	10 (58.82%)	13 (65%)	NS
African American	4 (23.53%)	6 (30%)	NS
Other	3 (17.65%)	1 (5%)	NS
Etiology of disease			
Post-procedural	7 (41.18%)	10 (50%)	NS
Trauma	6 (35.29%)	2 (10%)	NS
Infectious	1 (5.88%)	1 (5%)	NS
Congenital	1 (5.88%)	2 (10%)	NS
Unknown	2 (11.76%)	5 (25%)	NS
Location of stricture			
Bulbar	14 (82.35%)	15 (75%)	NS
Bulbomembranous	1 (5.88%)	1 (5%)	NS
Membranous	1 (5.88%)	1 (5%)	NS
Penile	0	2 (10%)	NS
Prostatic	1 (5.88%)	0	NS
Size of excised stricture, cm (mean+/-SD)	2.84+/-1.15	2.59+/-1.26	NS

NS: Not significant. SD: standard deviation.

Conclusions: Our study showed that the clinical features of strictures that recur are not different than those that do not recur. Dense fibrotic plaques are more often seen in patients who later recur. Our results suggest that the histologic description of the resected plaque as done in this study could help identify those patients at higher risk of recurrence.

950 Detection of Human Papilloma Virus (HPV) in Invasive Penile Carcinoma According to Histological Subtypes. An International Study of 935 cases

Diego F Sanchez[1], Laia Alemany[2], Belen Lloveras[3], Sofía Cañete-Portillo[1], María José Fernandez-Nestosa[4], Omar Clavero[5], Ingrid Rodríguez[4], Nubia Munoz[6], Wim Quint[7], Silvia de Sanjosé[2], Francesc Xavier Bosch[8], Antonio Cubilla[9]
[1]Instituto de Patologia e Investigacion, Asuncion, Paraguay, [2]Institut Catala d'Oncologia, Barcelona, Spain, [3]Hospital del Mar, Barcelona, Spain, [4]Universidad Nacional de Asunción, Asunción, Paraguay, [5]1. Centro de Investigación Biomédica en Red de Cáncer 2.Institut Català d'Oncologia, L'Hospitalet de Llobregat, Madrid, Spain, [6]National Cancer Institute of Colombia, Bogota, Colombia, [7]DDL Diagnostic Laboratory, Rijswijk, Netherlands, [8]Catalan Institute of Oncology (ICO), L'Hospitalet de Llobregat, Spain, [9]Instituto de Patologia e Investigacion, Asunción, Paraguay

Disclosures: Diego F Sanchez: None; Laia Alemany: None; Belen Lloveras: None; Sofía Cañete-Portillo: None; María José Fernandez-Nestosa: None; Ingrid Rodríguez: None; Antonio Cubilla: None

Background: About a third to half of penile carcinomas are related to HPV. Since the pioneering studies of Kurman (in vulvar cancer) and Gregoire (in penile cancer) a distinct correlation of morphology and presence of the virus have been determined. We are presenting the largest series of HPV detection according to histological subtypes of penile carcinomas.

Design: From an initial group of 1095 cases (Alemany et al, Eur Urol 2016) and exclusion of non-invasive lesions, rare tumors and inconclusive HPV, 935 cases of invasive carcinomas from 5 continents were studied. HPV DNA detection and genotyping were performed using SPF-10/DEIA/LiPA$_{25}$ system **(version 1).** P-values were determined by Fisher's exact test using R version 3.4.3.

Results: HPV positivity was higher in carcinomas with a Basaloid component (Table 1). Three distinctive groups were noted according to the prevalence of HPV, as follows: High prevalence group included Warty-basaloid, Basaloid and Papillary-basaloid subtypes; Intermediate prevalence was comprised by Warty and Mixed tumor with Warty and or Basaloid component and the third group, with low HPV prevalence was entirely conformed by usual, papillary NOS, verrucous and sarcomatoid carcinomas.

Table 1. Histological subtypes and HPV detection.

Carcinoma subtype	HPV Positive	HPV Negative	Total
Warty Basaloid	26 (87)	4 (13)	30 (100)
Basaloid	103 (85)	18 (15)	121 (100)
Papillary Basaloid	11 (85)	2 (15)	13 (100)
Warty (condylomatous)	33 (52)	30 (48)	63 (100)
Mixed with W/B	31 (43)	41 (57)	72 (100)
Usual SCC	75 (16)	395 (84)	470 (100)
Papillary	9 (15)	51 (85)	60 (100)
Sarcomatoid	2 (11)	17 (89)	19 (100)
Mixed Non-HPV-related	2 (7)	26 (93)	28 (100)
Verrucous	3 (5)	56 (95)	59 (100)
Total	295 (32)	640 (68)	935 (100)

Fisher's test P-value = 0.0005.

Conclusions: High rates of HPV were detected in Warty-basaloid, Basaloid and Papillary-basaloid carcinomas (87, 85 and 85%). Lower rates were present in Verrucous, Sarcomatoid, Papillary NOS, Usual SCC and Mixed Non-Warty/Basaloid tumors. This is the largest series of HPV detection evaluating subtypes of penile carcinomas which validates current hypothesis of a bimodal carcinogenesis pathway of penile cancer.

951 Penile Carcinoma: Prevalence of HPV and Genotypes Distribution in Tropical vs Non-Tropical Countries. A Study of 863 cases

Diego F Sanchez[1], Laia Alemany[2], Sofía Cañete-Portillo[1], María José Fernandez-Nestosa[3], Belen Lloveras[4], Omar Clavero[5], Nubia Munoz[6], Wim Quint[7], Silvia de Sanjosé[2], Francesc Xavier Bosch[8], Antonio Cubilla[9]
[1]Instituto de Patologia e Investigacion, Asuncion, Paraguay, [2]Institut Catala d'Oncologia, Barcelona, Spain, [3]Universidad Nacional de Asunción, Asunción, Paraguay, [4]Hospital del Mar, Barcelona, Spain, [5]1. Centro de Investigación Biomédica en Red de Cáncer 2.Institut Català d'Oncologia, L'Hospitalet de Llobregat, Madrid, Spain, [6]National Cancer Institute of Colombia, Bogota, Colombia, [7]DDL Diagnostic Laboratory, Rijswijk, Netherlands, [8]Catalan Institute of Oncology (ICO), L'Hospitalet de Llobregat, Spain, [9]Instituto de Patologia e Investigacion, Asunción, Paraguay

Disclosures: Diego F Sanchez: None; Laia Alemany: None; Sofía Cañete-Portillo: None; María José Fernandez-Nestosa: None; Belen Lloveras: None; Antonio Cubilla: None

Background: There is a geographic variation in the incidence of penile carcinoma with figures of 0.5-1 and 2-4 per 100.000 habitants in regions of low and high risk, respectively. Countries of high incidence are usually in tropical regions and the warm climate is considered a risk factor. A possible explanation for the difference may be the unequal distribution of HPV, which is causative of about 30 to 50% of all penile cancers. The aim of this study was to evaluate the prevalence of HPV in tropical and non-tropical regions.

Design: Cases from 25 countries of 5 continents were grouped as tropical or non-tropical based on the geographical location or climate classification. If more than one-third of the country was located between the tropic and the Equator line it was classified as tropical, otherwise was non-tropical. HPV was determined by whole tissue section PCR.

Results: HPV status (and prevalence of HPV16) of penile squamous cell carcinoma according to tropical vs non-tropical regions are shown in Table 1.

Table 1. Presence of HPV tropical vs non-tropical regions and HPV16 prevalence.

HPV	Non-Tropical	Tropical	Total
*Negative	294 (70)	305 (69)	599
*Positive	124 (30)	140 (31)	264
**HPV 16	90 (73)	96 (69)	186
**Non-HPV 16	34 (27)	44 (31)	78

P-value= *0.605014696298071, **0.501540627120436

Conclusions: Overall, HPV was found in 31% of the cases. There were no differences in the prevalence of HPV in tropical and non-tropical regions of the world. In the same manner, the distribution of HPV genotypes was similar in both regions. Explanation other than variable frequency of HPV and their genotypes should be considered for the worldwide geographic variation of penile cancer.

952 Gleason Score 3 + 4 = 7 Cancers with High Proportion of Gleason Pattern 4 in Small Cancer Foci at Biopsy Show Similar Frequency of Postoperative Adverse Pathological Findings and Risk of Biochemical Recurrence to Gleason Score 6 Cancers

Shun Sato[1], Takahiro Kimura[2], Takashi Yorozu[3], Masahiro Ikegami[1], Hiroyuki Takahashi[3]
[1]The Jikei University School of Medicine, Minato-ku, Japan, [2]Jikei University School of Medicine, Tokyo, Japan, [3]Tokyo, Japan

Disclosures: Shun Sato: None; Takahiro Kimura: None; Takashi Yorozu: None; Masahiro Ikegami: None; Hiroyuki Takahashi: None

Background: Active surveillance (AS) has been broadly accepted as an option for management of low risk prostate cancer. Recently, certain Gleason score (GS) 3 + 4 = 7 cases have been included in AS candidate in several criteria, although definite pathological inclusion criteria have not yet been established well. At the previous USCAP 2018 annual meeting, we have shown that GS 3 + 4 = 7 cases with < 5% of highest proportion of Gleason pattern 4 (%GP4) at biopsy indicating similar risk of adverse pathological findings (AP) at radical prostatectomy (RP) specimen and biochemical recurrence (BCR) to GS 6 cases. Though, clinical significance of small amount of GS 3 + 4 = 7 cancer with high %GP4 (%GP4 >= 5%) is still unknown. This study was performed to examine clinicopathological features of those cases.

Design: A total of 315 RP cases with GS 6 or 3 + 4 = 7 cancer at biopsy were utilized. For all biopsy cores, length of cancer, GS, and %GP4 had already been analyzed in the prior study. We adopted total length of Gleason pattern 4 (GP4-L) as a new parameter. The GP4-L was calculated by "sum of (cancer length x %GP4) of each core" (mm). Cases with highest %GP4 >= 5% were divided as < 0.5mm or >= 0.5mm; < 1mm or >= 1mm of GP4-L, respectively. Simultaneously, the cases were subdivided by number of cores of GS 3 + 4 = 7. The cases were ultimately divided into the subgroups shown in Table 1. The AP at RP specimen and BCR were adopted as outcome measures. The AP was defined as either GS upgrade to 4 + 3 = 7 or higher, pT3b cancer or lymph node metastasis. Statistical difference of each outcome measure was analyzed between GS 6 cases and each subgroup.

Results: The cohort consisted of 115 cases of GS 6 and 200 cases of GS 3 + 4 = 7 cancer, including 155 cases of %GP4 >= 5%. Case number of each subgroup was shown in Table 1. The cases with GP4-L < 0.5mm showed no significant difference in the frequency of AP, although showed significantly higher hazard ratio (HR) for BCR (Table 1). On the other hand, they showed no significant difference both in the frequency of AP and HR for BCR, only when the cases were limited to those with only 1 core of GS 3 + 4 = 7.

Table 1. Case number with AP and hazard ratio for BCR in each subgroup

Subgroup	Case number	Case number with AP (%)	P-Value	Hazard ratio for BCR (95% CI)	P-Value
GS 6	115	12 (10.4)	N/A	1	N/A
%GP4 >= 5% & GP4-L < 0.5mm	45	8 (17.8)	NS*	2.591 (1.052-6.380)	< 0.05
%GP4 >= 5% & GP4-L >= 0.5mm	110	36 (32.7)	< 0.0001	3.105 (1.483-6.502)	< 0.005
%GP4 >= 5% & GP4-L < 1mm	86	18 (20.9)	< 0.05	3.179 (1.496-6.756)	< 0.005
%GP4 >= 5% & GP4-L >= 1mm	69	26 (37.7)	< 0.0001	2.607 (1.124-6.045)	< 0.05
%GP4 >= 5%, GP4-L < 0.5mm & 1 core of GS 7	31	4 (12.9)	NS*	2.000 (0.684-5.853)	NS*
%GP4 >= 5%, GP4-L < 0.5mm & >= 2 cores of GS 7	14	4 (28.6)	NS*	4.116 (1.288-13.150)	< 0.05

P-Value shows result of comparison between GS 6 cases and each subgroup.

*NS: Not Significant

Conclusions: Our results suggest that the cases with highest %GP4 >= 5% show similar clinical significance to GS 6 cases under the condition of GP4-L < 0.5mm and only 1 core of GS 3 + 4 = 7, concluding they may also be eligible in AS category in addition to the cases with highest %GP4 < 5%.

953 AJCC TNM 8th edition is superior to the UICC/AJCC 7th editions in predicting Clinical Stage in Non-Seminomatous Germ Cell Tumors

Glenda Scandura[1], Luis Beltran[2], Constantine Alifrangis[3], Jonathan Shamash[3], Daniel Berney[2]
[1]Barts Cancer Institute, London, United Kingdom, [2]Queen Mary University of London, London, United Kingdom, [3]Barts Health NHS Trust, London, United Kingdom

Disclosures: Glenda Scandura: None; Luis Beltran: None; Constantine Alifrangis: None; Jonathan Shamash: None; Daniel Berney: None

Background: 70% of germ cell tumors (GCTs) are clinical stage (CS) I at presentation, with 20-30% relapsing because of occult disease. Cure rates are high for clinically localised GCTs and surveillance is generally recommended. There is controversy on the risk factors that predict relapse and indications for adjuvant therapy. The AJCC 8th edition has updated the TNM staging of GCTs with epididymal and soft tissue invasion both considered pT2. We wished to identify significant pathological predictors of clinical stage in non-seminomatous germ cell tumors (NSGCT) in a specialist GCT treatment center with reference to both AJCC and UICC TNM 7th and 8th editions.

Design: Two expert testicular pathologists diagnosed or reviewed 221 NSGCT cases referred to a supra-regional center from 2007 to 2017. Tumor size, invasion of vessels, hilar fat, rete testis, epididymis, spermatic cord, tunica vaginalis, tumor at the spermatic cord margins and percentage of embryonal carcinoma were assessed in all cases. Demographic, clinical records and imaging were accessed and correlated with clinical stage and possible pathological risk factors

Results: Of the 221 NSGCTs, 152 (69%) were CS I and 69 (31%) CS II/III. Mean age of CS I was 30 years (11 months - 67), mean age of CS II/III was 32.4 years (16 - 62). Mean tumor size of CS I was 37 mm (5 - 110); mean tumor size of CS II/III was 46 mm (8 -190). On univariate analysis, the parameters significantly associated with higher CS were: vascular invasion (P<0.0001), hilar fat invasion (P=0.009), rete testis invasion (P<0.0001), epididymal invasion (P=0.02), direct spermatic cord invasion (P=0.001), tumor at spermatic cord margin (P=0.002), tumor size (P=0.008) and % of embryonal carcinoma (P=0.011). However, on multivariate analysis only vascular invasion (P=0.002), rete testis invasion (P=0.010), tumor size (P=0.007) and % of embryonal carcinoma (P=0.019) and were found to be significant.

Table 1. Multivariate logistic regression model of risk factors for higher clinical stage		
	p-value	Odds Ratio (95% Confidence Interval)
% Embryonal Carcinoma	0.019	1.012 (1.002-1.022)
Vascular Invasion	0.002	2.890 (1.479 -5.649)
Rete Testis Invasion	0.010	2.288 (1.216 - 14.113)
Tumor Size (mm)	0.007	1.023 (1.006 - 1.041)

Conclusions: These results validate the AJCC 8th edition of TNM rather than the UICC 8th edition or TNM 7th editions, as soft tissue and epididymal invasion were univariately highly predictive of high stage. However multivariate analysis showed that a limited number of factors (tumor size, vascular and rete testis invasion, and percentage of embryonal carcinoma) could be utilised in risk prediction models. Rete testis invasion and tumor size should also be considered in any future TNM classification as they were highly predictive in multivariate analysis.

954 Validation of the AJCC TNM 8th edition to predict Clinical Stage in Testicular Seminomas

Glenda Scandura[1], Luis Beltran[2], Constantine Alifrangis[3], Jonathan Shamash[3], Daniel Berney[2]
[1]Barts Cancer Institute, London, United Kingdom, [2]Queen Mary University of London, London, United Kingdom, [3]Barts Health NHS Trust, London, United Kingdom

Disclosures: Glenda Scandura: None; Luis Beltran: None; Constantine Alifrangis: None; Jonathan Shamash: None; Daniel Berney: None

Background: 60% of germ cell tumors (GCTs) are diagnosed as seminoma and approximately 80% of them are clinical stage (CS) I. The cure rates for clinically localised GCTs are close to 99% and surveillance is generally recommended. However, there is a 15-20% relapse rate for patients treated by orchidectomy and surveillance only. There is a controversy on the risk factors that predict metastatic disease and indications for adjuvant therapy. The AJCC TNM 8th edition has proposed a size of 3cm to separate pT1a and 1b tumors. We wished examine this and identify the significant pathological predictors of clinical stage at presentation in seminoma in a specialist GCT treatment center with reference to the differences between the UICC and AJCC TNM classifications.

Design: Two expert testicular pathologists diagnosed or reviewed the pathological reports of patients referred to a supra-regional center from 2007 to 2017. Tumor size, invasion of vessels, hilar fat, rete testis, epididymis, spermatic cord, tunica vaginalis, and tumor at spermatic cord margins as well as demographic and clinical records were accessed and correlated. Frequencies of number of cases < and ?2 cm, 2.5 cm, 3 cm and 4 cm were calculated in both clinical stage I and clinical stage II/III.

Results: We identified 279 cases diagnosed with seminoma. Of them, 242 (87%) were CS I and 37 (13%) were CS II/III. Mean age of CS I was 38 years (20-81) and mean age of CS II/III was 39 years (26-63). Mean tumor size of CS I was 38 mm (5-112 mm) and mean tumor size of CS II/III was 54 mm (12-99 mm). On univariate analysis, the following parameters were associated with a higher clinical stage: vascular invasion (P=0.035) and tumor size (P<0.0001). All other factors including rete invasion, soft tissue invasion were not significant. On multivariate analysis, only tumor size remained significant (P<0.0001). In our cohort a cut off of 2.5 cm was found to be the most significant in discriminating CS1 and CSII/III patients.

Conclusions: In our cohort, most of the information on likelihood of high tumor stage at presentation was contained within tumor size measurements, and all other factors appear secondary to this. This validates the use of tumor size in AJCC TNM 8th edition. 3cm was chosen as a cut off in the new AJCC staging, and our optimal cut off is close to this value. We suggest that tumor size is therefore the most important predictor of high stage disease in seminoma.

955 Proposal of a Prostatectomy Grossing Protocol Exploring Different Anatomic Planes

Luciana Schultz[1], Rogerio da Silva[2], Cesar Loiacono[3], Marcus Sadi[4], Gustavo Lemos[5], Marcelo Wroclawski[5], Roberto E Ibrahim[6]
[1]Instituto de Anatomia Patológica, Anatomia Patologica Rede D'Or, Santa Barbara dOeste, SP, Brazil, [2]School of Medical Sciences, State University of Campinas (Unicamp), Campinas, SP, Brazil, [3]Diagnóstika, Anatomia Patológica Rede D'Or, São Paulo, SP, Brazil, [4]UNIFESP, São Paulo, SP, Brazil, [5]Hospital Israelita Albert Einstein, São Paulo, SP, Brazil, [6]Diagnóstika, Hospital Israelita Albert Einstein, São Paulo, SP, Brazil

Disclosures: Luciana Schultz: None; Rogerio da Silva: None; Cesar Loiacono: None; Marcus Sadi: None; Gustavo Lemos: None; Marcelo Wroclawski: None; Roberto E Ibrahim: None

Background: Excellent results of prostate targeted biopsy have brought pathologists' attention to prostate imaging, which explores different anatomic planes. Current radical prostatectomy (RP) grossing protocols are based on axial sectioning, so we sought to evaluate a partial embedding protocol based on sagittal and coronal sectioning.

Design: Following fixation and complete inking, apical and bladder neck margins were taken by the cone method and a sagittal cut through the urethra divided left and right lobes. From each lobe, coronal sections separated a lateral, an anterior and a posterior segment that included the seminal vesicle base. The peripheral zone from the posterior and lateral segments was cut perpendicular and fully submitted to histology. The anterior segment was sampled as one fragment of each lobe. Twenty RP processed according to the new proposal were compared to 38 RP processed according to ISUP partial embedding recommendations.

Results: The proposed method rendered a mean of 12.2 cassets (range 8-22). In this group, mean age, pre-operative PSA and prostate weigh were 62 yo, 5.9 ng/mL and 44.3 g (23 – 90g). Suspicious/grossly identifiable tumors were reported in 17/20 RP, with multiple areas in 10/20 specimens. Thirty-two/34 nodules were in the postero-lateral segments and 2/34 were exclusively mid-anterior. Mean tumor volume was 1.43 ml (0,02 – 10,0). The two cohorts did not differ as to age, pre-operative PSA, number of positive cores in the biopsy or prostate weight (p>0.7), although 62% of the study group fulfilled criteria for minimal volume disease compared to 37% in the control cohort (p=0.05). Gleason 6 was scored on 47% of study group RP vs. 32% (p=0.15). Positive margin and extraprostatic extension detection rates were both 5%, compared to 21% and 15%, respectively, in the control cohort (p>0.08). Mean follow-up time in both cohorts was 8.9y and biochemical recurrence occurred in 1 patient from the study group.

Figure 1 - 955

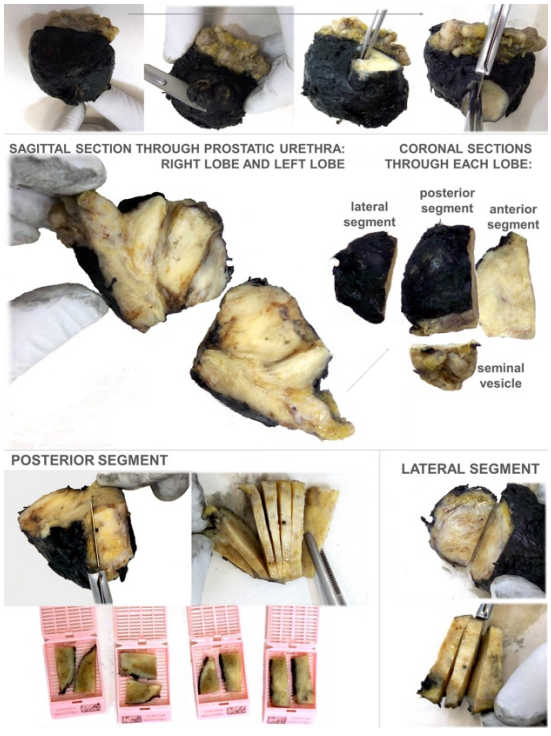

Conclusions: The proposed protocol performed similar to current recommended partial embedding protocol. Next, we aim to evaluate its correlation to contemporary prostate imaging, in a larger study set.

956 Extramammary Paget Disease of the Scrotum: A Contemporary Clinicopathologic Analysis of 20 Cases

Maryam Shabihkhani[1], Pallavi Patil[2], Adeboye O. Osunkoya[3], Jonathan Epstein[4], Andres Matoso[4]
[1]Johns Hopkins University School of Medicine, Baltimore, MD, [2]Brown University Lifespan Academic Medical Center, Providence, RI, [3]Emory University School of Medicine, Atlanta, GA, [4]Johns Hopkins Medical Institutions, Baltimore, MD

Disclosures: Maryam Shabihkhani: None; Pallavi Patil: None; Adeboye O. Osunkoya: None; Jonathan Epstein: None; Andres Matoso: None

Background: Primary Extramammary Paget disease (EMPD) is a rare intraepithelial adenocarcinoma that typically presents as an eczematous plaque with symptoms including burning and pruritus. EMPD most often involves apocrine gland-bearing locations such as the vulva and perianal area. EMPD of the scrotum or penis is less common. Scrotal EMPD mostly involves Asian male and our knowledge of its clinical and histopathological characteristics remains very limited in western countries.

Design: Pathology databases from four institutions in the US were searched for patients with scrotal EMPD between 2000 to 2018. Clinicopathological and immunohistochemical features were reviewed.

Results: 20 patients (15 Caucasian, 1 Black, 1 Asian, 3 unknown race) with scrotal EMPD were identified. Mean age at presentation was 73 years (range: 63-87). Erythema or/and itching were the most common clinical presentations. Time from symptom onset to definite diagnosis was from 4 months to 10 years. Two patients had a history of prostate cancer and one patient was diagnosed with prostate cancer 4 years later. Perianal skin involvement was noted in six cases and the penis was involved in two cases. No patient had inguinal lymphadenopathy. Histologically, three cases showed dermal invasion. The epidermis showed marked verrucous hyperplasia in three cases. Chronic inflammation was present in eleven cases. Reexcision was required in eight patients, due to positive margins. Immunohistochemically, GATA3 and GCDFP15 were expressed in 6/6 cases. CK7 was expressed in 8/8 cases. Focal strong expression of CK20 (17%) was noted in one case. 13/13 cases were positive for androgen receptor (AR). HER2 was positive in 5/12 cases. PSA was positive in one patient with history of prostate cancer, however, other prostate markers (NKX3.1 and prostein) were negative. This case was positive for CK7, GCDFP15 and HER2; therefore a diagnosis of EMPD was rendered. Twelve other cases were negative for PSA and NKX3.1. Follow up data was available in eleven patients for a median period of 54 months (range: 12-132) and none died of the disease.

Conclusions: EMPD has an insidious onset and its nonspecific clinical manifestations can be misdiagnosed often as dermatitis or fungal infection. While localized and in situ EMPD has a favorable prognosis, margins are frequently positive requiring re-excision. Occasionally, cases can be positive for PSA.

957 NapsinA is a sensitive marker for nephrogenic adenoma of the urinary tract

Nima Sharifai[1], Brooj Abro[2], Dengfeng Cao[3]
[1]Brentwood, MO, [2]Washington University, St. Louis, MO, [3]Barnes Jewish Hospital/Washington University, St. Louis, MO

Disclosures: Nima Sharifai: None; Brooj Abro: None; Dengfeng Cao: None

Background: Nephrogenic adenoma (NA) is an uncommon lesion in the urinary tract and can show several histologic patterns including flat, papillary, tubular, microcystic and signet-ring like cells. These patterns may pose diagnostic difficulty. Recently, napsinA has been identified as a sensitive marker for pulmonary adenocarcinoma and gynecologic clear cell carcinoma. In this study, we investigated the expression of napsinA in a large series of NAs in the urinary tract and compared its sensitivity to PAX8, GATA3, p63 and cytokeratin 34BE12 (CK903) in these tumors.

Design: The surgical pathology file of Washington University between 2011 and 2018 was searched for nephrogenic adenoma and 43 such cases were included for this study (42 bladder, 1 prostatic urethra). Unstained slides were generated for immunohistochemical staining with antibodies to napsinA, PAX8, GATA3, p63 and 34BE12. For napsinA, cytoplasmic granular staining is considered positive, whereas 34BE12 shows cytoplasmic/membranous staining. Nuclear staining is considered positive for PAX8, GATA3 and p63. The staining was semi-quantitatively scored as 0 (no cells stained), 1+ (1-25%), 2+ (26-50%), 3+(51-75%) and 4+ (76-100%). The percentage of tumor cells was visually estimated with 5% increments.

Results: PAX8 was the most sensitive marker for NA, with all cases (43/43) showing 4+ staining. P63 had the highest negative predictive value for NA, with no cases (0/43) showing positive staining. For GATA3, 26% of cases (11/43) had ?2+ staining. 34betaE12 and napsinA showed high sensitivity for NA, with ?2+ staining in 39/42 and 42/43 cases, respectively. Most cases were 4+ with moderate staining intensity for both markers. While 34betaE12 was also expressed in adjacent areas of benign urothelial cells, napsinA and PAX8 were restricted to NA tumor cells. Finally, we found that the papillary/flat architectures of NA showed more extensive napsinA staining compared to the microcystic/tubular patterns.

	0	1+	2+	3+	4+		Mean (% positive tumor cells)	Median (% positive tumor cells)	Range (% positive tumor cells)	p-value for Mean (compared to napsinA)
napsinA	0	1	11	8	23		72%	80%	15-100%	n/a
PAX8	0	0	0	0	43		99%	100%	90-100%	<0.00001
p63	43	0	0	0	0		0%	0%	0-0%	<0.00001
GATA3	18	14	5	4	2		18%	5%	0-100%	<0.00001
34BE12	0	4	1	4	34		82%	90%	10-100%	0.05912

Conclusions: NapsinA is highly expressed in nephrogenic adenomas (100%), with greater expression in surface (papillary, flat) versus stromal (microcystic, tubular) architectures. While 34betaE12 is also sensitive for NA, its specificity is inferior to that of napsinA and PAX8. Confirming previous reports, GATA3 is suboptimal for distinguishing NAs from urothelial lesions. Another nuclear stain, p63, is much more helpful in excluding NA. Further studies are in progress to assess the specificity of napsinA in bladder and prostatic carcinomas.

958 Immunohistochemistry of Immune Checkpoint Markers PD-1 and PD-L1 in Prostate Cancer

Meenal Sharma[1], Qi Yang[2], Loralee Mcmahon[3], Hiroshi Miyamoto[4]
[1]Unity Hospital, Rochester Regional, Rochester, NY, [2]Pittsford, NY, [3]University of Rochester Medical Center, Rochester, NY, [4]University of Rochester, Rochester, NY

Disclosures: Meenal Sharma: None; Qi Yang: None; Loralee Mcmahon: None; Hiroshi Miyamoto: None

Background: Programmed cell death protein 1 (PD-1) and its ligand programmed death-ligand 1 (PD-L1) have gained much attention mainly due to recent availability of targeted therapy and immune checkpoint inhibitors. However, the incidence and clinical implication of PD-1 and PD-L1 expression in prostate cancer remain far from being fully understood. The current study aimed to determine the status of PD-1/PD-L1 expression in prostate cancer tissue specimens and its prognostic significance.

Design: We immunohistochemically stained for PD-1 and PD-L1 in our tissue microarray consisting of 220 radical prostatectomy specimens. The expression of PD-1/PD-L1 was designated as positive when moderate to strong staining was seen in at least 1% of tumor cells or weak staining was seen in at least 10% of tumor cells. We then evaluated the relationship between the expression of each protein and clinicopathological features available for our patient cohort.

Results: PD-1 and PD-L1 were positive in 17 (7.7%) and 29 (13.2%) of prostate cancers, respectively. PD-1 and PD-L1 were also expressed in tumor-infiltrating lymphocytes in 172 (78.2%) and 33 (15.0%) cases, respectively. PD-L1 expression in tumor cells was more often seen in high pT stage cases (pT2: 10.7% *vs.* pT3/4: 20.4%, $P = 0.072$; pT2/3a: 11.4% *vs.* pT3b/4: 31.6%, $P = 0.013$), whereas PD-1 expression was not significantly associated with pT stage. In addition, there were no statistically significant associations between PD-1/PD-L1 expression in tumor cells or tumor-infiltrating lymphocytes versus preoperative prostate-specific antigen (PSA) level, Gleason score, or lymph node involvement. Kaplan-Meier analysis coupled with log-rank test further revealed no significant associations between PD-1/PD-L1 expression in tumor cells ($P = 0.619$/$P = 0.315$) or tumor-infiltrating lymphocytes ($P = 0.964$/$P = 0.767$) versus biochemical recurrence (defined as a PSA value of 0.2 ng/mL or greater) following radical prostatectomy.

Conclusions: PD-1/PD-L1 expression was detected in a subset of prostate cancers. In particular, PD-L1 expression was considerably up-regulated in non-organ-confined tumors. However, PD-1/PD-L1 expression in our tissue microarray was found to be not very helpful in predicting tumor recurrence in prostate cancer patients who underwent radical prostatectomy.

959 Tumor PD-L1 Expression is Detected in a Significant Subset of High-Risk Localized and Metastatic Prostate Cancer but is Rare in Ductal Subtype

Kristin Shaw[1], Carla Calagua[1], Joshua Russo[1], David Einstein[1], Steven Balk[1], Huihui Ye[1]
[1]Beth Israel Deaconess Medical Center, Boston, MA

Disclosures: Carla Calagua: None; Joshua Russo: None; Huihui Ye: None

Background: Tumor PD-L1 expression generally correlates with response to anti-PD-1/PD-L1 therapy. Although prostate cancer (PCa) has been considered non-immunogenic, PD-L1 positivity was seen in 14% of primary PCa and was enriched in aggressive PCa in our recent study. A prior study reported an enrichment of DNA mismatch repair (MMR) gene alterations in ductal adenocarcinoma of the

prostate (D-PCa). Due to rarity of metastatic PCa (mPCa) samples, PD-L1 expression level in mPCa remains unknown. In this study, we use immunohistochemistry (IHC) to assess tumor PD-L1 expression, MMR deficiency (MMRD), and the density of tumor-infiltrating lymphocytes (TILs) in high-risk localized prostate cancer (HLPCa), mPCa, and D-PCa.

Design: 50 cases of HLPCa, 41 cases of mPCa, and 27 cases of D-PCa (pure or mixed) were retrospectively collected. Representative 1-2 tumor blocks were selected to examine the expression of PD-L1, MMR proteins, ERG, PTEN, and CD8. PD-L1 positivity was defined by membranous staining in >=1% of tumor cells. PTEN loss was defined as negative staining in >=5% tumor cells. CD8+ TIL to tumor cell ratio was recorded in in 1-4 hot spots on CD8 IHC.

Results: PD-L1 was positive in 26% of HLPCa, 17% of mPCa, and 4% of D-PCa. Overall, PD-L1 positivity was significantly higher in resection specimens compared to biopsies (p=0.045). In the 69 cases in which TILs assessed, TIL density was significantly increased in PD-L1(+) PCa (p=0.045). PD-L1(+) tumors were significantly enriched in African Americans (AA) (p=0.039), while no significant association was seen with ERG and PTEN status. Further, AA ethnicity was independently associated with PD-L1 positivity in multivariate analysis. MMRD was identified in only 4 (3%) of 118 cases, including 2 mPCa, 1 HLPCa, and 1 D-PCa. Of the 4 MMRD cases, 3 showed loss of MSH2 (& MSH6), and one showed loss of PMS2. Only 1 of the 4 MMRD cases was PD-L1(+).

Figure 1 - 959

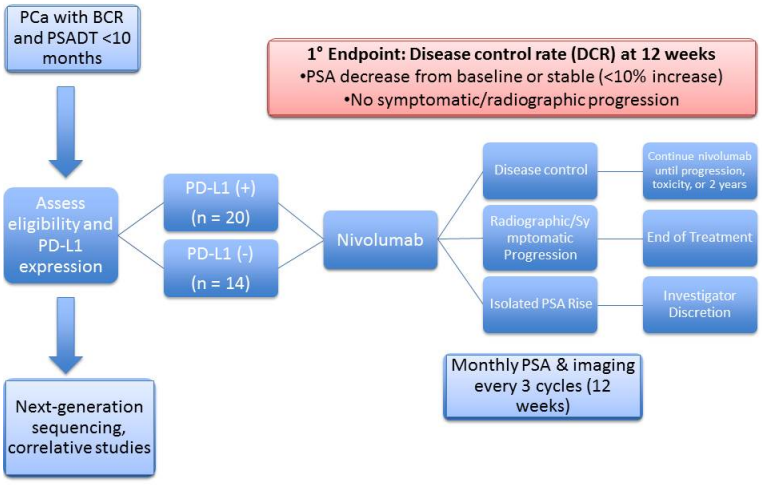

Conclusions: A significant subset of high-risk (26%) and metastatic PCa (17%) show PD-L1 positivity. PD-L1 positivity is uncommon (4%) in D-PCa. MMRD is markedly rare (3%). Our findings provide the rationale for a forthcoming clinical trial of Nivolumab in patients with high-risk biochemically recurrent PCa, using PD-L1 IHC as a classifier. Proposed correlative studies will include correlation of clinical responses with PD-L1 expression, subtypes of TILs, tumor genomic alterations, soluble biomarkers in peripheral blood, and T-cell recognition of tumor neoantigens.

960 The Expression of EZH2 and Polycomb Genes in Neuroendocrine Prostate Cancer

Mingxia Shi[1], Shu Yang[2], Imtiaz Khalil[2], Fenghua Chen, Xiuping Yu[2]
[1]LSU Health Sciences Center, Shreveport, LA, [2]LSU Health Shreveport, Shreveport, LA

Disclosures: Mingxia Shi: None; Shu Yang: None; Imtiaz Khalil: None; Fenghua Chen: None; Xiuping Yu: None

Background: After prostate cancer (PCa) fails androgen deprivation therapy, there is an increase of neuroendocrine (NE) phenotype. More knowledge concerning NE differentiation process and its association with castration-resistant prostate cancer is needed. In this study, we evaluated the involvement of EZH2 and Polycomb genes in neuroendocrine prostate cancer (NEPCa). EZH2 is the catalytic subunit of Polycomb repressive complex 2 (PRC2) that functions to regulate histone H3 methylation and repress the transcription of target genes.

Design: Using microarray data extracted from GEO database, we examined the expression of EZH2 and other Polycomb genes during PCa progression. Additionally, using immunohistochemistry staining, we assessed the expression of EZH2 in benign and various prostatic specimens, including sections derived from benign prostate hyperplasia (BPH, n=6), low- and high- grade prostate adenocarcinoma (n=6), patient-derived NEPCa xenograft tumors (n=1), and mouse models of NEPCa (12T10 LADY and TRAMP). Also, we cultured prostate adenocarcinoma, LNCaP cells in androgen-depleted media and assessed the expression of major Polycomb genes and NEPCa markers by qPCR.

Results: We found that the expressions of Polycomb genes (EZH2, EED, SUZ2, CBX1) were up-regulated in metastatic castrate resistant prostate cancer, and the increased EZH2 expression was associated with elevated expressions of NEPCa marker (CHGA, FOXA2, SOX2) and decreased expression of FOXA1, a prostate differentiation marker. IHC staining results indicated that EZH2 and FOXA2, a NEPCa marker, were overexpressed in all NEPCa tumors while FOXA1 expression was abundant in prostate adenocarcinoma but diminished in NEPCa. Also, we found when PCa cells were induced to undergo NE differentiation, the expression of multiple Polycomb genes (BMI1, RING1a, CBX1) was induced, concurrent with the induction of NEPCa marker, CD56.

Conclusions: Our findings indicate that EZH2 and Polycomb genes are highly expressed in both human and mouse NEPCa, and the expression of these genes are induced during androgen-deprivation induced NE differentiation of PCa. Elevated EZH2 could provide a mechanism to silence the expression of prostate differentiation-related genes, induce anaplastic state of PCa cells, and promote the acquisition of "stemness" and trans-differentiation to NEPCa.

961 p62 Protein Expression Correlates with Aggressive Disease in Prostatic Adenocarcinomas (PACs)

Mohammed Shiekhmohammed[1], Zhiyan Fu[1], Saleh Najjar[1], Tipu Nazeer[2]
[1]Albany Medical Center, Albany, NY, [2]Albany Medical College, Albany, NY

Disclosures: Mohammed Shiekhmohammed: None; Zhiyan Fu: None; Saleh Najjar: None; Tipu Nazeer: None

Background: P62 involves the pathway of autophagy, which is a programmed cell survival mechanism with a key role in physiologic and pathologic conditions. It is located throughout the cell from nucleus to cytosol and functions as a receptor for ubiquitinated targets in selective autophagy and serves as a scaffold in various signaling cascades. p62 has been reported to be up regulated in several human malignancies. However, its expression in prostatic adenocarcinoma has not been thoroughly studied. In this study, we assessed the p62 protein expression and potential correlation between p62 and PAC grade, stage and biochemical disease recurrence.

Design: Formalin-fixed paraffin-embedded tissue sections from 107 PACs were immunostained by an automated method (Ventana/Roche, Tucson, AZ) using monoclonal SQSTM1/p62 antibody (clone D5L7G, Cell Signaling). Cytoplasmic (Cp62) and nuclear (Np62) p62 immunoreactivity was semiquantitatively assessed in the tumor and adjacent benign component (when present) in all cases. Scoring was based on staining intensity (weak, moderate, intense) and percentage of positive cells (focal <= 10%, regional 11-50%, diffuse >50%). Presence of Cp62 and Np62 immunoreactivity was also assessed within the tumor microenvironment (Cp62tm and Np62tm, respectively). Results were correlated with clinicopathologic variables.

Results: Cp62 was overexpressed in 56/107 (52%) tumors and correlated with high (HG≥Gleason 7) vs low (LG≤Gleason 6) tumor grade [33/45 (73%) HG vs 23/62 (37%) LG; p<0.0001], advanced (stage III, IV) vs early (stage I, II) tumor stage [39/54 (72%) adv vs 17/53 (32%) early; p<0.0001] and disease recurrence [33/53 (62%) recurrent vs 23/54 (43%) non-recurrent; p=0.042]. Np62 was overexpressed in 17/107 (16%) tumors and showed a trend toward disease recurrence [12/53 (23%) recurrent vs 5/54 (9%) non-recurrent; p=0.058]. There was no correlation between Cp62 and Np62 immunoreactivity in the same case. Cp62tm and Np62tm immunoreactivity were observed in 39/107 (37%) and 103/107 (96%) tumors, respectively; there were no correlations. On multivariate analysis, advanced tumor stage independently predicted biochemical disease recurrence (p=0.013).

Conclusions: Cytoplasmic p62 protein overexpression correlates with high tumor grade, advanced tumor stage and post-surgical biochemical disease recurrence in PACs, while nuclear overexpression shows an association with disease recurrence. Further study of p62 protein expression and its potential role in prostate cancer prognosis appears warranted.

962 5-hmC as a Potential Biomarker in Urothelial Neoplasia

Andrew Siref[1], Brian Cox[2], Mariza De Peralta-Venturina[3], Daniel Luthringer[3]
[1]Cedars-Sinai, Los Angeles, CA, [2]Cedars-Sinai Medical Center, Los Angeles, CA, [3]Cedars-Sinai Medical Center, West Hollywood, CA

Disclosures: Andrew Siref: None; Brian Cox: None; Mariza De Peralta-Venturina: None; Daniel Luthringer: None

Background: Loss of 5-hydroxymethylcytosine (5-hmC), an epigenetic marker of global methylation, has been reported in urothelial carcinoma, melanoma, and various other malignancies. We sought to expand these observations in a range of neoplastic and non-neoplastic urothelial lesions and ascertain whether 5-hmC expression could be useful in separating difficult-to-classify lesions. The distinction between carcinoma in-situ (CIS) and reactive urothelial atypia can be challenging and often comes in the context of intra-vesicle therapies for an established carcinoma. Additionally, papillary lesions may show variation in histomorphologic features, sometimes making the distinction between low grade and high grade lesions problematic.

Design: 85 cases were selected from our surgical pathology archives to represent a range of urothelial lesions. Cases included normal (n = 10) and reactive urothelium (n = 10), low grade (n = 14) and high grade (n = 16) papillary urothelial carcinoma, CIS (n=20), and invasive urothelial carcinoma (n = 15). H&E stained sections were reviewed and diagnoses confirmed. Cases were then examined by

immunohistochemistry for nuclear 5-hmC (RevMAb Biosciences, clone RM236 at 1:10,000 dilution) expression and scored by 2 genitourinary pathologists and 2 residents to generate semi-quantitative H-scores. Median H-scores were calculated and a Kruskal-Wallis Test was performed on H-score mean ranks for pairwise comparisons.

Results: Reduced 5-hmC expression is seen in urothelial neoplasms, as compared to normal and reactive urothelium. Reactive urothelium showed a modest reduction in 5-hmC expression as compared to normal urothelium, and there is a general trend towards greater loss of 5-hmC with increasing 'grade' of lesion. 5-hmC loss is significantly greater in CIS than in normal or reactive urothelium ($p < 0.001$, each). A trend toward further diminished expression was observed in the high grade papillary carcinomas as compared to low grade papillary carcinomas, although this difference did not reach statistical significance.

Figure 1 - 962

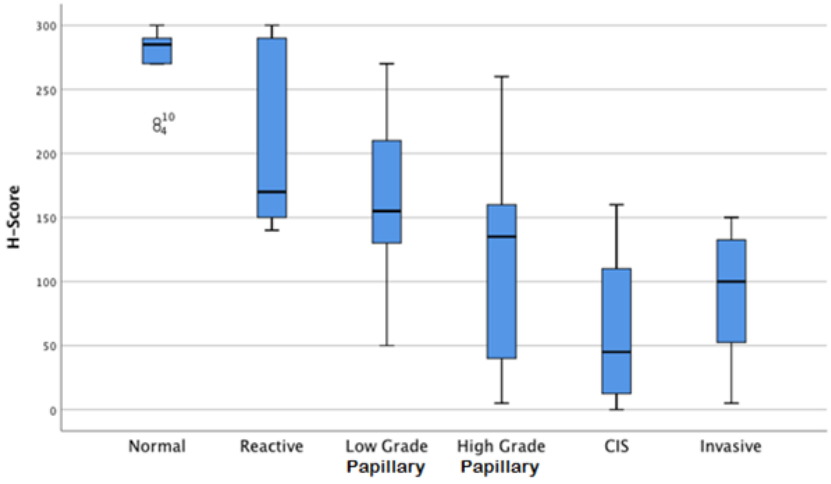

Urothelial neoplasia shows reduced nuclear 5-hmC and trending with increasing 'grade' of lesion (black lines show group mean; whiskers show 95% confidence intervals). Cases 4 and 10 from the 'Normal' group are outliers.

Conclusions: Loss of 5-hmC in urothelial neoplasia is a real phenomenon. Our scoring indicates a trend in 5-hmC loss based on lesion 'grade', which is consistent with published results from various other neoplasms. Moreover, the difference in staining observed between normal and reactive urothelium and CIS suggests 5-hmC has potential utility in distinguishing between them.

963 SDH-deficient versus FH-deficient Renal Cell Carcinoma: A Comparison of Genome-Wide Alterations in Oncometabolic Neighbors with Divergent Prognoses

Steven Smith[1], Mahul Amin[2], Anthony Gill[3], Sean Williamson[4], Kiril Trpkov[5], Maria Picken[6], Santosh Menon[7], Isabela da Cunha[8], Anthony Faber[9], Mikhail Dozmorov[10], Colleen Jackson-Cook[11], Sosipatros Boikos[12]
[1]Virginia Commonwealth University School of Medicine, Richmond, VA, [2]Methodist University Hospital, Memphis, TN, [3]University of Sydney, Greenwich, NSW, Australia, [4]Henry Ford Health System, Detroit, MI, [5]University of Calgary, Calgary, AB,[6]Loyola University Medical Center, Maywood, IL, [7]Tata Memorial Hospital, Mumbai, India, [8]Rede D'OR - São Luiz, São Paulo, SP, Brazil, [9]VCU Massey Cancer Center, Richmond, VA, [10]VCU School of Medicine, Richmond, VA, [11]Virginia Commonwealth University, Richmond, VA, [12]Glen Allen, VA

Disclosures: Steven Smith: *Consultant*, Elsevier/Amirsys Publishing; Anthony Gill: None; Sean Williamson: None; Kiril Trpkov: None; Maria Picken: None; Santosh Menon: None; Isabela da Cunha: None; Anthony Faber: *Advisory Board Member*, Abbvie; Mikhail Dozmorov: None; Colleen Jackson-Cook: None; Sosipatros Boikos: None

Background: Despite experimental data confirming overlapping oncometabolic consequences of loss of function of key Krebs cycle enzymes, fumarate hydratase (FH), and succinate dehydrogenase (SDH), recent series documented that the renal cell carcinomas (RCCs) harboring loss of function of these enzymes show markedly divergent morphologies and prognoses. SDH-deficient RCC is usually a lower (nucleolar) grade carcinoma with relatively homogeneous oncocytic histology, evincing progression in a subset of cases (~20%). In contrast, FH-deficient RCC is usually a high grade carcinoma, showing striking inter- and intratumoral morphologic variation, and represents one of the most aggressive known RCCs. The reasons for these biologic and clinical differences are presently unknown, as are the characteristic genomic changes in these tumors *vis a vis* the more common subtypes of RCC.

Design: We report an interim genome-wide copy number and LOH analysis of 8 SDH-deficient and 6 FH-deficient RCCs studied by high density SNP microarray analysis (planned N=10 each).

Results: Preliminary analyses identified frequent 1p losses and/or 1q gains (or LOH) in 8/8 SDH-deficient RCC; less frequent but recurrent gains involved 21q (5/8), 15q and 17q (each 4/8), and 8q (3/8). In contrast, FH-deficient RCC showed greater heterogeneity, but frequent whole chromosome level gains and losses, with at least one aneuploid event present in 5/6 cases and frequently including full or partial monosomy of chr. 18 (5/6), trisomy or tetrasomy of chr. 2 and chr. 8 (each 3/6) and monosomy of 22 (3/6).

Conclusions: SDH- and FH-deficient RCC show complex patterns of copy number variations and chromosomal changes that underlie their divergent morphology and clinical behavior. However, their patterns appear distinct from each other and from the more common subtypes of RCC, further supporting their classification as distinct entities. Although these changes may provide clues for prospective diagnosis in unclassified RCC, immunohistochemical staining and molecular evaluation of SDH and FH expression and gene mutation represent the key diagnostic tools in identifying these rare cases. Importantly, with the analysis of additional cases, the overlapping regions involved may yield additional diagnostic or therapeutic targets.

964 PD-L1 Expression in Chromophobe Renal Cell Carcinomas

Robert Ta[1], Zaid Mahdi[2], Carla Calagua[1], Huihui Ye[1], Douglas Lin[3]
[1]Beth Israel Deaconess Medical Center, Boston, MA, [2]Beth Israel Deaconess Medical Center, Newton, MA, [3]Beth Israel Deaconess Medical Center, Needham, MA

Disclosures: Robert Ta: None; Zaid Mahdi: None; Carla Calagua: None; Huihui Ye: None; Douglas Lin: None

Background: Programmed death-ligand 1 (PD-L1) acts as an immune checkpoint molecule in various cancers. Anti-PD-1/PD-L1 treatment has been proven effective in clear cell renal cell carcinoma, but its utility in chromophobe renal cell carcinoma remains unknown. Data regarding PD-L1 expression in chromophobe renal cell carcinoma is limited. The aim of this study was to evaluate PD-L1 expression in chromophobe renal cell carcinoma and associated inflammatory cells.

Design: Forty-four cases of chromophobe renal cell carcinomas were retrospectively identified at a large tertiary academic hospital. Tissue microarrays were prepared containing 3 mm tumor cores for each case. PD-L1 immunostaining was performed and scored in tumor cells and inflammatory cells. PD-L1 expression in tumor cells were calculated via a tumor proportion score (TPS) as the number of tumor cells staining positive divided by the total number of tumor cells and quantified as <1%, 1-5%, 6-25%, 25-50%, and >50%. Similarly, percentage of tumor-associated mononuclear inflammatory cells expressing PD-L1 was also calculated.

Results: PD-L1 tumor proportion score was <1% in 13 of 44 chromophobe renal cell carcinoma cases (29.5%), 1-5% in 3 of 44 cases (6.8%), 6-25% in 5 of 44 cases (11.4%), 25-50% in 8 of 44 cases (18.2%) and >50% in 15 of 44 cases (34.1%). In contrast, 13 of 44 cases did not have associated inflammatory cells, and PD-L1 expression in tumor-associated mononuclear inflammatory cells was assessed in 31 of 44 cases. PD-L1 expression in tumor- associated inflammatory cells was <1% in 11 of 31 cases (35%), 1-5% in 14 of 31 cases (45%), 6-25% in 6 of 31 cases (20%), and 25-50% in 0 of 31 cases (0%) and >50% in 0 of 31 cases (0%).

Conclusions: PD-L1 is frequently expressed in chromophobe renal cell carcinoma in tumor cells and associated inflammatory cells, suggesting that anti-PD-1/PD-L1 treatment may be effective in patients with recurrent/metastatic chromophobe renal cell carcinoma. Future studies are needed to determine PD-L1 TPS cut off criteria for potential response to immunotherapy as a predictive marker in patients with chromophobe renal cell carcinoma.

965 Clear Cell Renal Cell Carcinoma With a Poorly-Differentiated Component: A Novel Variant Causing Potential Diagnostic Difficulty

Kanika Taneja[1], Liang Cheng[2], Khaleel Al-Obaidy[2], Chia-Sui (Sunny) Kao[3], Justine Barletta[4], Brooke Howitt[3], Matthew Wasco[5], Nallasivam Palanisamy[1], Nilesh Gupta[1], Craig Rogers[1], Shannon Carskadon[1], Ying-Bei Chen[6], Tatjana Antic[7], Maria Tretiakova[8], Sean Williamson[1]
[1]Henry Ford Health System, Detroit, MI, [2]Indiana University School of Medicine, Indianapolis, IN, [3]Stanford University School of Medicine, Stanford, CA, [4]Brigham and Women's Hospital, Harvard Medical School, Boston, MA, [5]St Joseph Mercy Hospital, Ann Arbor, MI, [6]Memorial Sloan Kettering Cancer Center, New York, NY, [7]University of Chicago, Chicago, IL, [8]University of Washington, Seattle, WA

Disclosures: Kanika Taneja: None; Liang Cheng: None; Khaleel Al-Obaidy: None; Chia-Sui (Sunny) Kao: None; Justine Barletta: None; Brooke Howitt: None; Matthew Wasco: None; Nallasivam Palanisamy: None; Nilesh Gupta: None; Craig Rogers: None; Shannon Carskadon: None; Ying-Bei Chen: None; Tatjana Antic: None; Maria Tretiakova: None; Sean Williamson: None

Background: Several variant histologic patterns of clear cell renal cell carcinoma (RCC) are well known, especially those with sarcomatoid and rhabdoid features. However, we have encountered rare cases in which a high-grade adenocarcinoma or urothelial carcinoma-like component would be difficult to appreciate as clear cell RCC.

Design: We retrieved 21 tumors with histologically typical clear cell RCC juxtaposed to a high-grade non-clear cell component, defined as non-sarcomatoid, non-rhabdoid areas that would be difficult to assign as renal cell in origin if viewed in isolation. Tumors were studied with immunohistochemistry and fluorescence in situ hybridization (FISH) or sequencing.

Results: Median percentage of poorly differentiated component was 40% (IQR25-70). All tumors showed abrupt transition from clear cell carcinoma to poorly differentiated (non-sarcomatoid or non-rhabdoid) areas, which showed micropapillary (6/21;29%), urothelial-like (6/21;29%), and adenocarcinoma not otherwise classifiable features (9/21;42%). Necrosis was present in 14 tumors. Whereas carbonic anhydrase IX (CA-IX) was uniformly positive in the well-differentiated component (18/18), the poorly differentiated component showed a median positivity of 82.5% (IQR 65-100). Additionally, the poorly differentiated component was positive for cytokeratin 7 (5/17;29%), cytokeratin 20 (3/12;25%), alpha-methylacyl-CoA racemase (AMACR) (6/11;55%), and PAX8 (12/15;80%) and showed intact FH (6/6;100%). CDX2 was uniformly negative (0/9;0%). Chromosome 3p loss or *VHL* mutation was present in 7/12 (58%) cases tested with either FISH (n=9) or sequencing (n=3). All tested cases were negative for *TFE3* (0/11) and *TFEB* (0/9) rearrangements using FISH. Upon follow-up, 3/18 (17%) patients were alive with metastatic disease and 5/18 (28%) had died of disease. One metastasis was composed only of the poorly-differentiated component and was near-negative for CA-IX.

Figure 1 - 965

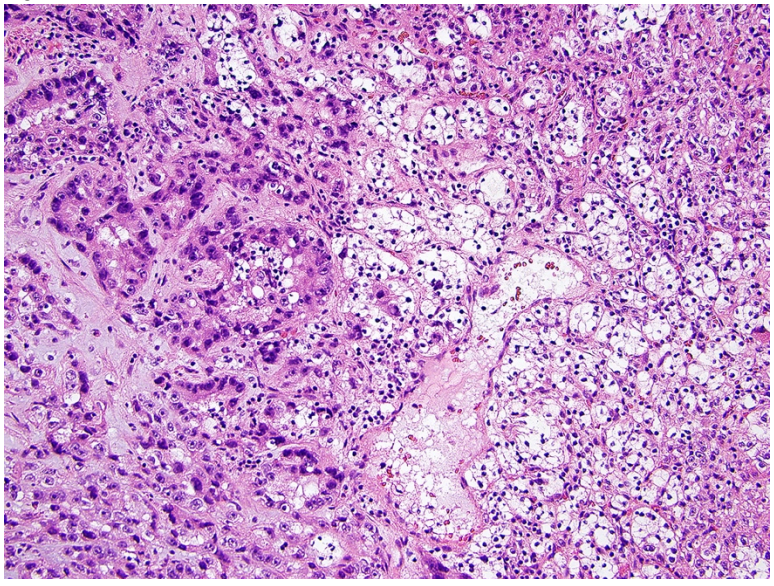

Conclusions: Clear cell RCC with a poorly differentiated component resembling adenocarcinoma or urothelial carcinoma is a novel source of morphologic heterogeneity that has not been previously well characterized. Potential pitfalls include decreased or absent CA-IX staining the high-grade component and aberrant positivity for cytokeratin 7 or 20. With the increasing use of renal mass biopsy and biopsies of metastatic sites for targeted therapy, pathologists should be aware of this entity and consider the possibility of clear cell RCC even for morphologically unusual tumors.

966 Cribriform Prostatic Adenocarcinoma is Associated with Higher Risk of Clinical Metastasis and Mortality via the Decipher Genomic Classifier

Alexander Taylor[1], Todd Morgan[1], Arul Chinnaiyan[2], Daniel Spratt[1], Rohit Mehra[1]
[1]University of Michigan, Ann Arbor, MI, [2]Plymouth, MI

Disclosures: Alexander Taylor: None; Todd Morgan: *Grant or Research Support*, GenomeDx; Arul Chinnaiyan: None; Daniel Spratt: None; Rohit Mehra: None

Background: The Decipher test (GenomeDX) measures the expression of 22 RNA biomarkers associated with aggressive prostate cancer and issues a score to better predict 5-year metastatic risk and 10-year prostate cancer specific mortality. Practically, Decipher use has led to improved risk stratification of patients and may improve patient selection for adjuvant radiation therapy. To date, Decipher's genomic classification has not been faithfully correlated with histologic features of prostatic adenocarcinoma. With a better understanding of the clinical aggressiveness associated with cribriform prostatic adenocarcinoma, we sought to determine if cribriform growth pattern is associated with an increased genomic risk (Decipher score) across a spectrum of Gleason scores (GS) of prostatic adenocarcinoma.

Design: The Decipher assay was performed on the highest GS tumor nodule of prostatectomy specimens from a prospective cohort of 48 patients with GS varying from 7 through 9 to help guide clinical risk stratification into observation/surveillance or adjuvant radiation therapy categories. The tumors were assessed for cribriform growth pattern on a 0-2 scale (0 or non-cribriform = not present, 1 or cribriform-minor

= present in less than 50% of the Gleason 4 component, 2 or cribriform-predominant= present in more than 50% of the Gleason 4 component), which was then compared to the risk category (low, intermediate, or high) as assigned by the Decipher assay as well the Decipher scores. Statistical significance for risk category and scores were determined by Chi squared contingency analysis and Mann-Whitney test, respectively.

Results: The presence of any cribriform growth pattern was significantly associated with Decipher risk categorization (p=0.035) with 2 of 10 (20%) non-cribriform and 22 of 38 (58%) cribriform adenocarcinomas assessed as high genomic risk by Decipher, respectively (Fig 1). In addition, within the 3+4 GS adenocarcinoma category, the presence of cribriform growth pattern was significantly associated with Decipher score (p=0.031) (Fig 2).

Figure 1 - 966

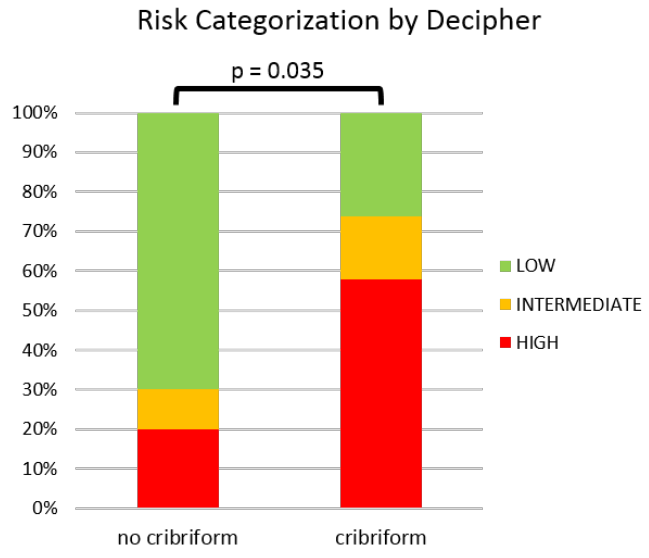

Figure 2 - 966

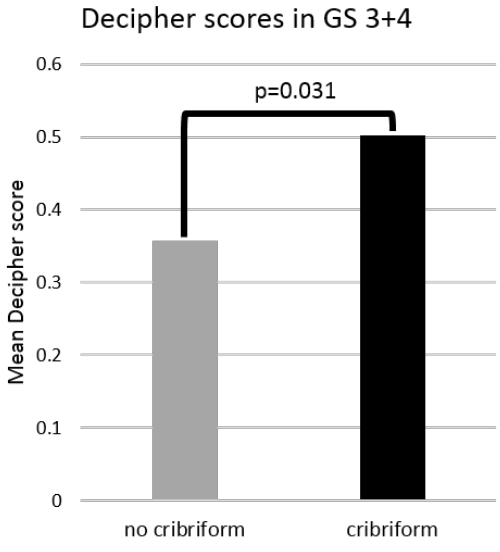

Conclusions: Our findings add to an expanding knowledge base that supports cribriform growth pattern as a unique and clinically relevant pattern in prostatic adenocarcinoma; based on Decipher assessment, cribriform growth pattern should be considered an independent risk factor for metastasis and mortality, especially in the GS 3+4 category.

967 The Practice Utilization Pattern of Prolaris® Test and its Correlation with AUA Risk Groups for Over 500 Patients Diagnosed with Prostate Cancer in a Community Practice

Wei Tian[1], Karen Shore[2], Ji Yoon Yoon[3], Rajal Shah[4]
[1]Inform Diagnostics, Irving, TX, [2]Rice University, Houston, TX, [3]Irving, TX, [4]Cleveland Clinic, Cleveland, OH

Disclosures: Wei Tian: None; Karen Shore: None; Ji Yoon Yoon: None; Rajal Shah: *Employee*, Inform Diagnostics

Background: The Prolaris® test developed by Myriad® Genetics is a commercially available multi-gene assay that measures the expression of 31 cell cycle progression genes to generate a Prolaris® score (PS) to predict the aggressiveness of prostate cancer (Pca). The 2018 National Comprehensive Cancer Network (NCCN) guidelines recommend the utilization of the Prolaris® test for patients diagnosed with NCCN low-risk and favorable-intermediate-risk PCa categories.

Design: The study cohort comprised a total of 530 cases of PCa with PS. The tumor with the highest volume and/or Gleason score (GS) was selected for the test. Clinicopathological information gathered included the patient's age, PSA level, highest GS and Grade Group (GG), % of positive cores, tumor length, tumor % in the core, and American Urological Association (AUA) risk group (RG) (low, intermediate and high-risk).

Results: Of 530 patients evaluated, the GG distribution was as follows: 229 (43.2%) GG1, 193 (36.4%) GG2, 71 (13.3%) GG3, and 37 (6.9%) GG 4/5. 210 (40%) were in low, 261 (49%) intermediate and 59 (11%) high risk AUA RG (Table 1). The median PS was 3.3 (range: 1.2-7). In this study, the PS positively correlated with GG, tumor length, % of positive cores and AUA RG (Pearson and Spearman correlation). In 47.5% patients, the PS aggressiveness interval was consistent with respective AUA RG, 29.8% were less/considerably less aggressive, and 22.6% more/considerably more aggressive.

AUA Risk Group	Prostate Cancer Grade Group	Prolaris® Score aggressiveness in relation to average AUA Risk Group					
		Considerably less aggressive	Less aggressive	Consistent	More aggressive	Considerably more aggressive	Total
Low	1 (n=210)	5 (2.4%)	67 (31.9%)	102 (48.6%)	30 (14.2%)	6 (2.8%)	210
Interm	1 (n=16) 2 (n=183) 3 (n=62)	4 (1.5%)	66 (25.3%)	123 (47.1%)	61 (23.4%)	7 (2.7%)	261
High	1 (n=3) 2 (n=10) 3 (n=9) 4 (n=18) 5 (n=19)	3 (5%)	13 (22%)	27 (45.8%)	13 (22%)	3 (5%)	59
Total	530	12 (2.3%)	146 (27.5%)	252 (47.5%)	104 (19.6)	16 (3%)	530

Conclusions: In this community practice cohort, 89% of the patients were in AUA low and intermediate RG, while 11% were in AUA high RG. There was significant discordance between AUA RG and Prolaris® aggressiveness; over 50% of cases showed that the PS was either more or less aggressive than average AUA RG, which may provide value in a more personalized approach for treatment decision-making. We are currently examining the influence of other pathological factors such as inflammation, presence of intraductal carcinoma, and desmoplastic stromal reaction, etc., to ascertain if these parameters may also be instructive in determining PS aggressiveness.

968 Molecular Pathology Approach to Improve Diagnostic Certainty for Genomic Studies of Prostate Cancer Development

Levent Trabzonlu[1], Qizhi Zheng[1], Jessica Hicks[2], Tracy Jones[2], William Nelson[2], Christopher Heaphy[2], Alan Meeker[2], Michael Haffner[3], Srinivasan Yegnasubramanian[2], Angelo De Marzo[1]
[1]Johns Hopkins University, Baltimore, MD, [2]Johns Hopkins University School of Medicine, Baltimore, MD, [3]Johns Hopkins Medicine, Baltimore, MD

Disclosures: Levent Trabzonlu: *Grant or Research Support*, Janssen Research and Development Inc.; Jessica Hicks: None; Tracy Jones: None; Christopher Heaphy: None; Michael Haffner: None; Srinivasan Yegnasubramanian: None; Angelo De Marzo: *Grant or Research Support*, Janssen Research and Development Inc.

Background: There has been a great interest in developing prevention strategies for prostate adenocarcinoma (CaP) by using the successful model from other cancer types in which patients with identified precursor lesions are enrolled in clinical trials to prevent the progression to invasive disease. Prostate cancer trials using this approach to date have been hampered by random sampling using needle biopsies and poor molecular characterization of potential precursor lesions. For example, at times what appears to be a precursor may represent already invasive carcinoma mimicking high grade PIN (HGPIN). Therefore, better genomic characterizations of putative prostate cancer precursors in relation to nearby invasive cancers are needed. While FFPE tissues can be used for genomic studies, fresh frozen tissue still has advantages. We used H&E staining and a panel of IHC and in situ markers to delineate HGPIN, CaP and benign epithelium for laser capture microdissection and genomic approaches.

Design: Radical prostatectomy specimens were sectioned fresh and 8 mm punch biopsies were taken (n = 49 patients). The remainder of the prostate was submitted for FFPE. Frozen sections (H&E) of the punch biopsies were evaluated for benign, HGPIN away from adenocarcinoma (CaP) (>2 mm), HGPIN near to CaP (<2 mm), and CaP. Adjacent frozen sections were used for IHC (PIN4, ERG, and MYC) and chromogenic staining for telomere lengths, which all aided in diagnoses for benign, HGPIN, and CaP that guided laser capture microdissection. DNA and RNA extractions were performed on microdissected samples. RNA quality was measured by an Agilent Bioanalyzer.

Results: 298 areas were laser captured from 49 patients from 187 frozen tissue blocks (Table 1). The mean and median RIN values for all lesions were over 8, indicating very high quality RNA. Preliminary data from RNAseq on a subset of specimens shows clear over and underexpression of a number of expected genes in CaP vs. normal with HGPIN generally falling in between. Clonality analysis among lesions is ongoing.

	Benign (n=49)	PIN-Away (n=51)	PIN-Near (n=77)	Cancer (n=107)
RIN	8.29±0.97	8.24±0.89	8.28±0.94	8.19±0.87
Total RNA (ng)	58±34.53	51.12±33.29	59.11±40.83	59.9±28.11
Total DNA (ng)	39.85±44.99	24.41±22.86	30.87±30.88	27.75±25.59

Figure 1 - 968

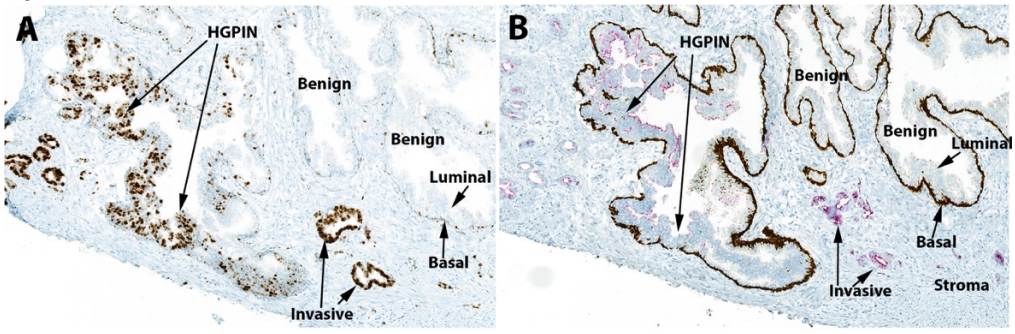

Figure 2 - 968

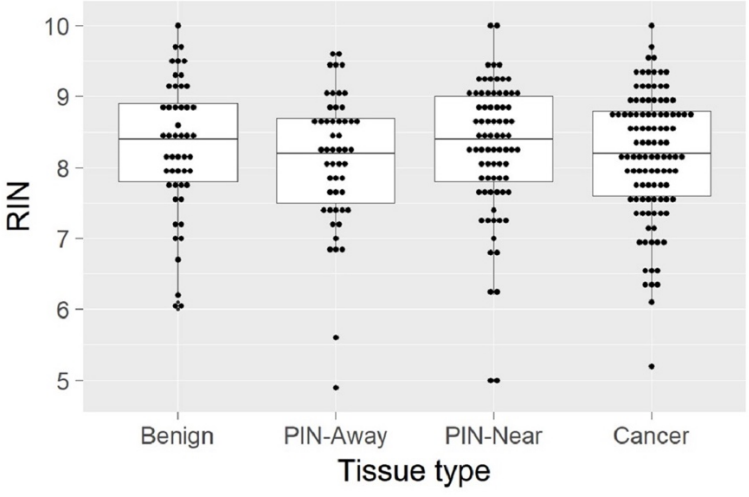

Conclusions: The use of our selected panel of IHC and CISH was useful to guide diagnoses on frozen sections, in which rendering an accurate diagnosis of benign vs PIN is often challenging. This molecular pathology approach facilitates genomic studies which can be used to improve our understanding of precursor-progeny relations during multistep prostate carcinogenesis and will help develop a better understanding of precursor PIN vs. intraductal spread of carcinoma.

969 Analysis of Translocation Renal Cell Carcinomas with the FusionPlex RNA-seq Platform

Maria Tretiakova[1], Scott Tykodi[1], Yajuan Liu[1]
[1]*University of Washington, Seattle, WA*

Disclosures: Maria Tretiakova: None; Scott Tykodi: None; Yajuan Liu: None

Background: Translocation renal cell carcinomas (tRCC) encompass a diverse group of renal tumors affecting younger patients, and often developing advanced disease. Accurate diagnosis is required to guide clinical management. Morphologic and IHC findings can prompt

reflex FISH studies, but with significant limitations of fixation and cutting artifacts, borderline results due to low-frequency split signals - especially for inversions, and inability to detect cryptic fusions or partner genes in re-arrangements.

Design: From our institutional files, we retrieved 16 cases with morphologic and IHC features highly suggestive of either *TFE3* tRCCs (N=15) or recently described *ALK* translocation RCC (N=1). We performed RNA-sequencing using FusionPlex assay with 108-gene panel covering a wide spectrum of partnering genes for *TFE3, TFEB, ALK* and *CCND1* in comparison to well-established IHC and FISH assays.

Results: The 16 patients ranged in age from 17 to 55 (mean 41), male to female ratio was 1.7:1. Primary tumor size ranged from 1.9 to 7.6 cm (mean 5 cm). Pathologic stage was pT1NX (7), pT2N0 (2), pT3N0 (5), and pT3M1 (2). ISUP tumor grade was 2 (2), 3 (11) or 4 (3). Morphology included clear to oncocytic cells with predominantly papillary architecture (8), alveolar architecture (3), solid (2), or mixed papillary and solid (3). Diffuse strong labeling for TFE3 was present in 14/16 cases, 2 cases with weak TFE3 expression were HMB45/Melan-A or Cathepsin positive. ALK1 was positive in 1/1 case. FusionPlex was performed on all 16 tumors and detected 9 gene re-arrangements: *PRCC-TFE3* (3), *ASPSCR1-TFE3* (2), *SETD1B-TFE3* (1), *LUC7C3-TFE3* (1), *SFPQ-TFE3* (1) and novel *ALK-CLIP1*. FISH was performed on 12 tumors verifying 7 positive and 5 negative cases with 100% concordance vs FusionPlex. Two cases positive for gene re-arrangement without previous FISH analysis were confirmed by RT-PCR. No gene fusions of *TFE3, TFEB*, or *ALK* were evident in all 10 negative control cases. IHC showed 100% sensitivity and negative predictive value, but 59% specificity and 56% positive predictive value.

Conclusions: FusionPlex was superior to FISH by providing precise breakpoints for tRCC related genes in a single assay and allowing the identification of both known and novel fusion partners facilitating further clinicopathological correlations. FusionPlex allowed discovery of a novel *CLIP1-ALK* fusion broadening our knowledge of this unique tumor entity. This assay can also reduce turn-around time by eliminating the need for reflex testing.

970 The Prognostic Impact of Large Cribriform Carcinoma, of Other Subpatterns 4 and of Intraductal Carcinoma of the Prostate

Dominique Trudel[1], Nazim Benzerdjeb[2], Hélène Hovington[3], Alain Bergeron[4], Yves Fradet[4], Kip Brown[5], Theodorus Van Der Kwast[6]

[1]Centre Hospitalier de l'University de Montreal, Montréal, QC, [2]Centre de recherche du CHUM/Institut du cancer de Montreal, Montreal, QC, [3]Centre hospitalier universitaire de Québec-Université Laval, Quebec, QC, [4]Centre hospitalier universitaire de Quebec-University Laval, Quebec, QC, [5]Centre de recherche du CHUM, Montréal, QC, [6]University Health Network, Toronto, ON

Disclosures: Dominique Trudel: None; Nazim Benzerdjeb: None; Hélène Hovington: None; Alain Bergeron: None; Yves Fradet: None; Kip Brown: None; Theodorus Van Der Kwast: None

Background: The controversy about the effect of each subpattern of the Gleason 4, especially large cribriform carcinoma (LC) and of IDCP is still ongoing. Our objective was to evaluate the association between IDCP, LC and other subpatterns of Gleason 4 prostate cancer with biochemical recurrence.

Design: Slides from first line radical prostatectomy (RP) at the Centre hospitalier universitaire de Québec-Université Laval (1993-2003) were reviewed to update grade, stage and IDCP status. The presence/absence of each subpattern of Gleason 4 was recorded. Ill-defined/small-fused glands (ID/SF) were combined to avoid low reproducibility, whereas glomeruloid (G), mucinous cribriform (MC), complex vascular (CV) and LC were evaluated individually. Descriptive statistics and Cox regression analysis were performed to evaluate the association between each pattern and biochemical recurrence. Multiple correspondence analysis (MCA) was performed to identify the structure of the association between the subpatterns.

Results: Two pathologists reviewed 277 RPs, in which IDCP has been found in 22.4%, ID/SF in 74%, LC in 49.1%, CV in 19.1%, G in 47.3%, and MC in 14.1%. In almost all RPs with pattern 4, ID/SF subpattern was identified (93%). Pattern 5 was identified in 9.4% of the RPs. Univariate analysis showed that all Gleason 4 subpatterns but for MC were significantly associated with biochemical recurrence, while multivariate analysis pointed the effects of ID/SF pattern (hazard ratio (HR)=2.96, 95% confidence interval (CI) 1.11-7.92; p=0.03) and of IDCP (HR=2.30, 95%CI 1.41-3.76, p<0.001) (Table 1). Of the 62 RPs with IDCP and the 136 with LC, 40 presented both patterns. There was no interaction between IDCP and LC. Lastly, a scatterplot of individual observations (Fig 1) reveals that IDCP and non-IDCP patients are clearly distinguished along the two dimensions. Indeed, the presence of IDCP contributes very strongly to one principal component, while presence of other subpatterns (excepting MC) contributed together to the second principal component (Fig 2).

		Gleason 4 subpatterns	Gleason 4 subpatterns + IDCP	Grade, IDCP, stage, margin status
Characteristics	Univariate Hazard ratios (95% confidence interval); p-value	Multivariate hazard ratios (95% confidence interval); p-value	Multivariate hazard ratios (95% confidence interval); p-value	Multivariate hazard ratios (95% confidence interval); p-value
Small-fused/ill-defined	6.07 (2.45-15.02); <0.001	4.35 (1.65-11.42); 0.003	3.16 (1.19-8.40); 0.02	2.96 (1.11-7.92); 0.03
Cribriform	2.43 (1.51-3.91); < 0.001	1.59 (0.97-2.62); 0.07	1.49 (0.90-2.46); 0.12	1.42 (0.84-2.39); 0.19
Complex vascular	2.01 (1.23-3.26); 0.005	1.42 (0.86-2.35); 0.17	1.39 (0.85-2.29); 0.19	1.30 (0.79-2.15); 0.30
Glomeruloid	1.98 (1.26-3.12); 0.003	1.09 (0.67-1.78); 0.73	1.34 (0.81-2.21); 0.25	1.20 (0.73-2.00); 0.47
Mucinous cribriform	1.27 (0.70-2.31); 0.43	0.92 (0.50-1.69); 0.8	0.94 (0.51-1.74); 0.85	0.79 (0.41-1.51); 0.47
IDCP	3.37 (2.15-5.29); <0.001		2.76 (1.73; 4.40); <0.001	2.30 (1.41-3.72), <0.001
Gleason pattern 5	S/O			1.31 (0.68-2.52); 0.43
Grade Groups GG 2-3 GG 4-5	3.34 (1.95-5.69); <0.001 5.53 (2.40-12.73); <0.001			S/O*
pT stage pT3a pT3b	2.62 (1.61-4.26); <0.001 3.99 (2.08-7.62); <0.001			1.51 (0.88-2.59); 0.13 1.42 (0.64-3.15); 0.39
Positive margins	2.56 (1.62-4.05); < 0.001			1.86 (1.13-3.05); 0.015

* Gleason pattern 5 was used in the multivariate analysis to avoid overadjustment for grade groups which included pattern 4.

Figure 1 - 970

Figure 2 - 970

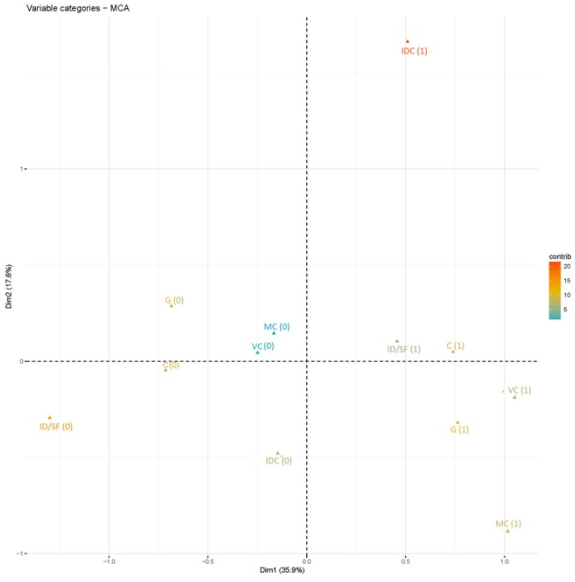

In our cohort, within the Gleason 4 subpatterns, ID/SF was the factor the most associated with biochemical recurrence. While other subpatterns showed similar prognostic impact in univariate analyses, MC was not associated with recurrence. IDCP was a strong independent predictor of recurrence, including in multivariate analysis, and was completely distinct from the other subpatterns, including LC.

971 Aberrant expression of lineage biomarkers in advanced prostate cancer

Dominique Trudel[1], Nazim Benzerdjeb[2], Roula Albadine[3], Mathieu Latour[4], Anne-Marie Mes-Masson[5], Véronique Ouellet[6], Fred Saad[7]
[1]Centre Hospitalier de l'University de Montreal, Montréal, QC, [2]Centre de recherche du CHUM/Institut du cancer de Montreal, Montreal, QC, [3]Montreal, QC, [4]CHUM, St-Eustache, QC, [5]Centre de recherche du CHUM, Montreal, QC, [6]Centre de recherche du CHUM/Institut du cancer de Montreal, Montréal, QC, [7]Centre Hospitalier de l'University de Montreal, Montreal, QC

Disclosures: Dominique Trudel: None; Nazim Benzerdjeb: None; Roula Albadine: None; Mathieu Latour: None; Anne-Marie Mes-Masson: None; Véronique Ouellet: None; Fred Saad: None

Background: Bladder and colorectal carcinoma are the most common source of direct extension to the prostate. Distant metastases to the prostate from carcinomas arising in other organs are unusual, but lung adenocarcinoma is the major cause of metastasis of prostate. In the study of undifferentiated carcinoma identified in a prostate resection, markers such as CK7, CK20, CDX-2, GATA-3 are usually performed, and occasionally TTF-1 can be added to the panel. The objective of this study was evaluate the proportion of aberrant expression of these five lineage biomarkers in a cohort of clinically proven advanced primary prostatic adenocarcinomas.

Design: Transurethral resection of the prostate specimens (TURPs) (N=91) performed between 1989 and 2006 were identified from the Centre hospitalier Universitaire de Montréal (CHUM) prostate biobank. Control radical prostatectomies (RPs) (N=23) were also included in the cohort. One to three tissues cores from each specimen were embedded in tissue microarrays. Slides were then submitted to immunohistochemistry (CK7, CK20, GATA-3, CDX-2, TTF-1) following clinical protocols. Descriptive statistics were performed.

Results: Tissues from TURPs showed higher grade than tissues from RPs (44% of grade group 1 in RPS, 14% of grade group 1 in TURPs). There were from 1 to 3 TURP for each patient – 75 specimens were from an initial TURP procedure. For men who had multiple TURPs (17.5%), the average time between procedures was 2 years (1-7 years). Approximately 35% of RPs and initial TURPs expressed non-prostatic biomarkers (Table 1). The two most frequent aberrant expressions in RPs were CDX-2, which was positive in 13% of the RPs, and CK7, which was positive in 13% of RPs. Initial TURPs showed a more variable profile, with CDX-2 being the most frequent aberrant marker (12.5%). Marker expression in subsequent TURPs was similar to marker expression in initial TURPs, however with an increase of proportion of aberrant markers with an observed statistical difference among first, second and third TURP (p=0.001, Friedman rank sum test). TTF-1 was not expressed in any of the specimens.

Marker	Radical prostatectomies (N=23) n (%)	Initial Transurethral resection of the prostate (N=75) n (%)	Subsequent Transurethral resection of the prostate (N=16) n (%)
CDX-2	3 (13.0%)	8 (12.5%)	5 (31.3%)
CK20	0 (0%)	4 (5.5%)	1 (6.3%)
CK20/CDX2	0 (0%)	2 (2.7%)	1 (6.3%)
GATA3	0 (0%)	4 (5.3%)	0 (0%)
CK7	3 (13.0%)	1 (1.3%)	1 (6.3%)
CK7/GATA3	1 (4.3%)	1 (1.3%)	1 (6.3%)
CK7/CK20	1 (4.3%)	1 (1.3%)	0 (0%)
CDX-2/GATA3	0 (0%)	3 (4.0%)	0 (0%)
Other combinations excluding TTF-1	0 (0%)	2 (2.7%)	0 (0%)
TTF-1	0 (0%)	0 (0%)	0 (0%)

Conclusions: Aberrant expression of lineage biomarker is frequent in prosatic adenocarcinoma, including in RPs and TURPs. As this aberrant expression tends to be higher in subsquent specimens, clinical history and caution should be used when selecting an immunohistochemistry panel to confirm tumour origin.

972 Comparison of the prognosis between pT3 urothelial carcinoma of the renal pelvis and pT3 urothelial carcinoma of the ureter

Toyonori Tsuzuki[1], Tomoyasu Sano[2], Mashashi Kato[3], Naoto Sassa[3], Toshinori Nishikimi[4], Ryohei Hattori[5], Momokazu Gotoh[3]
[1]Toyonori Tsuzuki, Nagoya, Japan, [2]Komaki City Hospital, Komaki, Japan, [3]Nagoya University Hospital, Nagoya, Japan, [4]Japanese Red Croos Nagoya Daini Hospital, Nagoya, Japan, [5]Japanese Red Cross Nagoya Daiichi Hospital, Nagoya, Japan

Disclosures: Toyonori Tsuzuki: None; Tomoyasu Sano: None; Mashashi Kato: None; Naoto Sassa: None; Ryohei Hattori: None

Background: Whether pT3 urothelial carcinoma of the renal pelvis (UCRP) and urothelial carcinoma of the ureter (UCU) show the same prognosis or not remains controversial. This study aims to reveal whether the prognosis of pT3 UCRP shows similar to those of pT3 UCU.

Design: We retrospectively evaluated 954 patients who underwent nephroureterectomy between 1984 and 2017 at our institutions. None of the patients received neoadjuvant therapy. All HE slides for each patient were reviewed by a single genitourinary pathologist (TT). pT3 UCRP was subdivided pT3a (urothelial carcinomas that extend only to the renal medulla) and pT3b (urothelial carcinomas that extend to the renal cortex and/or peripelvic adipose tissue) according to the criteria previously we proposed (Histopathology. 2012; 61:620-8). Fine and Gray model was developed to predict the disease-free survival (DFS) and cancer-specific survival (CSS).

Results: The clinical characteristics of this study are shown in Table 1. The CSS according to each pT stage is shown in Table 2.

Table 1: Clinical characteristics

	UCRP	UCU
Cases	493	461
Male to female ratio	2.76 (362:131)	2.27 (320:141)
Age (years)	22–94 (Median: 69)	36–92 (Median: 69)
Follow up period (months)	1–323 (Median: 50)	1–343 (Median: 39)

Table 2: Cancer specific survival

Category	n	Hazard ratio (CI: 95%)	p-value
PRUC			
pTa+pT1	247	Reference	1
pT2	30	2.60 (0.67-10.03)	0.166
pT3a	79	3.78 (1.45–9.86)	0.008
pT3b	123	11.71 (4.97–27.61)	<.001
pT4	14	57.99 (18.09–185.82)	<.001
UCU			
pTa+pT1	202	1.74 (0.68–4.45)	0.216
pT2	106	2.48 (0.94–6.55)	0.037
pT3	146	8.65 (3.61–20.74)	<.001
pT4	7	42.78 (11.31–161.76)	<.001

pT3a UCRP demonstrated similar prognosis to those of pT2 UCRP and UCU, and pT3b demonstrated similar prognosis to those of pT3 UCU. The DFS according to each pT stage stastistically showed same tendecy compared to those of CCS.

pT3 renal pelvis urothelial carcinoma was heterogeneous. Moreover, subclassifying pT3 UCRP into pT3a and pT3b was useful in determining the prognosis of different patients. Only pT3 UCRP showed similar outcome compared to those of UCU. The anatomic difference and degree of invasion could affect the prognosis of patients with UCRP and UCU.

Conclusions: pT3 renal pelvis urothelial carcinoma was heterogeneous. Moreover, subclassifying pT3 UCRP into pT3a and pT3b was useful in determining the prognosis of different patients. Only pT3 UCRP showed similar outcome compared to those of UCU. The anatomic difference and degree of invasion could affect the prognosis of patients with UCRP and UCU.

973 Proposal of the recurrence risk grouping in non-muscle invasive bladder cancer

Katsunori Uchida[1], Kunimasa Morio[2], Takehisa Ohishi[3], Watanabe Masatoshi[2]
[1]Tsu, Japan, [2]Mie University, Tsu, Japan, [3]Ise Red Cross Hospital, Ise, Japan

Disclosures: Katsunori Uchida: None; Watanabe Masatoshi: None

Background: The American Urological Association (AUA) and the European Association of Urology (EAU) have proposed their own recurrence risk classification for non-muscle invasive bladder cancer, which evaluate the risk of recurrence with more than 8 factors including clinical findings and pathological findings. We have attempted to simplify the complicated risk classification.

Design: Of the 250 patients with primary non-muscle invasive bladder cancer who underwent TUR at Ise Red Cross Hospital, 189 cases were enrolled for the study. The Patients who underwent post-TUR BCG intravesical instillations or second TUR were excluded. As a recurrence risk classification, cases of solitary tumor were classified into a low risk group and cases of multiple tumor were hierarchized into an intermediate risk group and a high risk group by one of following factors: pT(pTa or pT1), WHO 1973 grade(G1, 2 or 3), WHO 2004 grade(low or high), and the presence or absence of variant histology. The utility as a prognostic predictor was examined in 6 classifications including four types of risk classification (IRC risk classification - pT / WHO 1973 / WHO 2004 / variants) in addition to AUA and EAU risk classification.

Results: Significant differences were found in any classification in the log rank test. The c-indices of IRC risk classification - pT / WHO 1973 / WHO 2004 / variants, AUA risk classification, EAU risk classification were 0.63, 0.609, 0.617, 0.632, 0.607 and 0.612 respectively, and the p-value were 0.005, 0.019, 0.012, 0.004, 0.043 and 0.043 respectively. When cases with concomitant cis were excluded, significant differences were observed in IRC risk classification-pT / WHO2004/variants. The c-indices of IRC risk classification - pT / WHO 1973 / WHO 2004 / variant, AUA risk classification and EAU risk classification was 0.637, 0.626, 0.627, 0.642, 0.601 and 0.610 respectively, and the *p*-value were 0.015, 0.026, 0.026, 0.013, 0.076 and 0.053 respectively.

Conclusions: Compared with conventional AUA and EAU risk classification, improvement of c-indices was observed in all types of IRC risk classification. Even when cases with concomitant cis were excluded, IRC risk classification-pT/WHO2004/variants showed an advantage over conventional AUA and EAU risk classification with regard to prognosis.

974 Bladder cancer rapid tissue acquisition (BCRTA) program at the University of Washington: Genetic profiling and histologic characterization of metastatic urothelial carcinoma and establishing xenograft models of metastatic disease

Funda Vakar-Lopez[1], Hung-Ming Lam[1], Brian Winters[1], Navonil De Sarkar[2], Sonali Arora[2], Hamid Bolouri[2], Heather Cheng[1], Michael Schweizer[3], Evan Y Yu[1], Bruce Montgomery[1], Eva Corey[1], Petros Grivas[1], Jonathan L Wright[1], Andrew C Hsieh[2]
[1]University of Washington, Seattle, WA, [2]Fred Hutchinson Cancer Research Center, Seattle, WA, [3]University of Washington School of Medicine, Seattle, WA

Disclosures: Funda Vakar-Lopez: None; Hung-Ming Lam: None; Brian Winters: None; Navonil De Sarkar: None; Petros Grivas: *Consultant*, Merck; *Consultant*, Bristol-Myers Squibb; Foundation Medicine; Seattle Genetics; Driver Inc., QED Therapeutics; *Consultant*, Astra Zeneca; *Consultant*, Pfizer and EMD Serono; *Consultant*, Clovis Oncology

Background: Advanced urothelial carcinoma (aUC) has poor prognosis with median survival of 9-15 months. In order to understand the biology of aUC, we established a BCRTA program to systematically acquire tissue from patients with aUC to establish patient-derived xenograft (PDX) and organoid models and characterize the genomic landscape of these tumors by whole exome sequencing (WES).

Design: Patients (n=12) with aUC, treated with surgery and/or systemic therapy, had necropsy within 2-6 hours of death. Tissue samples from the primary, when available, and metastatic sites were obtained under sterile conditions. Tumors were implanted subcutaneously into SCID mice to establish PDX. Subsequently organoid cultures were initiated from the established PDX. In parallel, tumors were deposited in frozen and formalin-fixed paraffin embedded tissue blocks and reviewed by the designated GU pathologist for histologic evaluation and selection of tumor-enriched samples for sequencing. WES was performed on matched primary and metastatic tumors (n=37) from 7 patients: 4 from lower tract (LTUC), 3 upper tract (UTUC). Somatic single nucleotide variants (sSNV) were identified using Mutect and Strelka. Genome scale somatic copy number aberrations (sCNA) were estimated using Sequenza and normalized for ploidy to derive gene definition restricted copy number estimation outcomes. Multi-dimensional scaling (MDS) was used to visualize how copy number and high impact, mutation-derived genomic distances differed between and within LTUC and UTUC.

Results: The most common metastatic site was liver, followed by lung and lymph nodes in 5 men 2 women. Two of the tumors had squamous differentiation in addition to UC, one had plasmacytoid and another had both glandular differentiation and a micropapillary component. 2 PDX models were established successfully and had concordant histology with the original tumor. In our preliminary analysis, when the tumors were stratified as UTUC (3 primary ,13 metastases) or LTUC (4 primary, 17 metastases) based on primary tumor origin, sSNV burden (mean mutation per mega base) was significantly lower in the UTUC than LTUC (3.8 vs. 6.6, $p<0.001$), even when stratified by primary (2.9 vs. 6.1, $p=0.03$) or metastatic sites (4.1 vs. 6.7, $p=0.001$).

Conclusions: Our BCRTA program is successful in characterization of the genomic profile and establishment of PDX models of aUC which reflect tumor histological features in patients. Further WES and transcriptomic analysis in all available casses is pending.

975 Three-Dimensional Analysis of Prostate Cancer Reveals Two Fundamentally Different Subgroups of Gleason Growth Patterns

Geert van Leenders[1], Esther Verhoef[1], Gert Cappellen[1], Johan Slotman[1], Gert-Jan Kremers[1], Adriaan Houtsmuller[1], Martin van Royen[1]
[1]Erasmus Medical Centre, Rotterdam, Netherlands

Disclosures: Geert van Leenders: None; Esther Verhoef: None; Gert Cappellen: None; Gert-Jan Kremers: None; Martin van Royen: None

Background: The Gleason score is one of the most important parameters for therapeutic decision-making in prostate cancer. Gleason growth patterns are defined by their histological features on 4-5 µm cross-sections, while little is known about their three-dimensional architecture. The objective of this study was to characterize the three-dimensional architecture of prostate cancer growth patterns.

Design: Intact tissue punches (n=46) of representative Gleason growth patterns derived from formalin-fixed, paraffin-embedded radical prostatectomy specimens were fluorescently stained with antibodies targeting Keratin 8-18 and Keratin 5 for detection of luminal and basal epithelial cells, respectively. Punches were optically cleared in benzyl alcohol: benzyl benzoate and imaged using a long-distance confocal laser scanning microscope up to a depth of 500-1000 µm.

Results: Gleason pattern 3, poorly formed pattern 4 and cords pattern 5 formed a continuum of interconnecting tubules with gradually decreasing diameter and lumen size. Fused Gleason pattern 4 consisted of tubules with closely spaced interconnections. In these patterns, all tumor cells were in direct contact with the surrounding stroma. In contrast, cribriform Gleason pattern 4 and solid pattern 5 demonstrated

a three-dimensional continuum of malignant epithelial cells, where the vast majority of tumor cells had no contact with the stroma. There was a gradual decrease in number and size of inter-cellular lumens form cribriform to solid pattern. Glomeruloid pattern 4 showed an intermediate pattern consisting of a tubular network with intra-luminal epithelial protrusions close to tubule splitting points.

Conclusions: Three-dimensional microscopy revealed both continuity between Gleason growth patterns in prostate cancer as well as discriminating features. Two essentially different groups of growth patterns were distinguished by either presence of direct contact to the surrounding stroma or not. Three-dimensional architecture provides a morphological rationale for both inter-observer variability and the added prognostic value of individual growth patterns in prostate cancer.

976 Histopathologic Findings in Orchiectomy Specimens for Gender Confirmation Surgery

Alejandro Vargas[1], Margaret Black[2], Qinghu Ren[3], Hongying Huang[4], Jonathan Melamed[5], Fangming Deng[5]
[1]NYU School of Medicine, New York, NY, [2]NYU, Long Island City, NY, [3]New York University Langone Medical Center, New York, NY, [4]NYU Langone Health, New York, NY, [5]New York University Medical Center, New York, NY

Disclosures: Alejandro Vargas: None; Margaret Black: None; Qinghu Ren: None; Hongying Huang: None; Jonathan Melamed: None; Fangming Deng: None

Background: An estimated 1.4 million adults in the United States identify as transgender, and this number is rapidly increasing. Many persons undergoing the male-to-female transition pursue hormonal therapy and subsequent gender confirmation surgeries, resulting in increased numbers of orchiectomy specimens in pathology labs. While the histologic changes associated with hormonal therapy have been described, the incidence of other significant pathologic findings that may impact routine specimen evaluation remains largely unknown. Guidelines for appropriate specimen submission and histologic evaluation have not yet been established.

Design: The database at a large medical institution was retrospectively searched to identify orchiectomy performed for gender dysphoria. Typical hormone-related changes were noted, including an expanded interstitium, germ cell hypoplasia, Leydig cell hypoplasia, and thickened seminiferous tubule basement membranes. The incidence of malignant, pre-malignant, and unusual non-malignant pathologic findings were recorded. Grossing and evaluation procedures were also reviewed.

Results: A total of 84 patients with 167 orchiectomy specimens were identified from January 1, 2013 to August 1, 2018. The number of testicular parenchyma sections obtained varied widely from 1 to 6 (mean: 1.84), and 96 specimens (57.5%) were submitted without orientation in the same container. Of these, 164 specimens (98.2%) exhibited only hormone-related changes, while 3 specimens (1.8%) exhibited significant pathologic abnormalities, including lymphocytic vasculitis (0.6%), peri-testicular adrenal rests (0.6%), and mixed germ cell tumor (0.6%). Immunohistochemical (IHC) staining of OCT3/4 was performed on 12 orchiectomies (7.2%) with atypical cellular features, and no cases of germ cell neoplasia in situ were identified.

Conclusions: As more orchiectomy specimens are received for gender confirmation surgery, standard procedures must be established to allow appropriate clinical follow up and judicious resource allocation. Specimen laterality should be clearly designated, as it may affect clinical management. In our cohort, clinically significant pathologic findings were rare. The only case of germ cell tumor was grossly evident, and no cases of germ cell neoplasia in situ were identified. Therefore, one cassette of representative testicular parenchyma is sufficient for orchiectomy specimens received for gender confirmation surgery, and no routine IHC stains for germ cell neoplasia in situ are warranted.

977 Next Generation Sequencing Analysis of Acquired Cystic Disease Associated Renal Cell Carcinoma

Erica Vormittag-Nocito[1], John Groth[2], Julia Rewerska[1], Manmeet Singh[3], Gayatry Mohapatra[1], Frederick Behm[1], Magdalena Rogozinska[1], Ravindra Kumar[1]
[1]University of Illinois at Chicago, Chicago, IL, [2]University of Illinois Hospital & Health Sciences, Libertyville, IL, [3]Burr Ridge, IL

Disclosures: Erica Vormittag-Nocito: None; John Groth: None; Julia Rewerska: None; Manmeet Singh: None; Gayatry Mohapatra: None; Frederick Behm: None; Magdalena Rogozinska: None; Ravindra Kumar: None

Background: Acquired cystic disease associated renal cell carcinoma (ACD-RCC) is a relatively new category of renal cell carcinoma exclusively arising in end stage renal disease (ESRD) patients with acquired cystic kidney disease (ACKD). Cytogenetic and FISH studies have reported copy number alterations frequently involving chromosomes 3, 9, and 16. Molecular studies are yet to be published on this new entity.

Design: At the University of Illinois Hospital and Health Sciences System, a case search from July 2016 through July 2018 for ACD-RCC was performed. Five cases were identified with ACD-RCC. Histologic retrospective review of the five cases was performed and areas of ACD-RCC, atypical cyst formation, and classic ESRD areas were identified when present in archived tissue. Microdissection of these specific areas was performed for nucleic acid extraction. Next generation sequencing (NGS) of each designated area was performed using

a gene panel, and whole exome sequencing using Ion AmpliSeq Exome RDY assay. In addition, clinical history data were collected from a retrospective chart review.

Results: Patient age ranged from 38 to 70 y/o, and all patients were male. All had a history of dialysis and renal transplant, or were scheduled for transplant at the time of nephrectomy (Table 1). NGS of solid tumor gene panel identified frameshift mutation in ATM gene in 2/5 (ATM p.Thr2921fs; ATM p.Lys3018fs) and ARID1A p.Gln1327del mutation in 2/5 cases respectively. Whole exome sequencing was performed in all 5 cases to identify additional genetic alterations.

Clinical Characteristic of patients diagnosed with ACD-RCC.

Case #	Age (y/o)	Gender	Race	Months on Dialysis	Reason for ESRD	Tumor Size (in cm)	Tumor Stage	Furhman Nuclear Grade	Recurrence	Metastasis	Months of Follow-Up
1	38	male	Hispanic	168	Polycystic Kidney Disease and hypertension	9.6	pT3a	3	None	None	23
2	58	male	African-American	37	hypertension	3.2	pT1a	3	None	None	23
3	52	male	African-American	24	Diabetes Mellitus and hypertension	1.3	pT1a	3	N/A	None	0
4	70	male	African-American	>120	hypertension	3.0	pT3a	3	None	None	10
5	63	male	African-American	29	Diabetes Mellitus and hypertension	1.9	pT1a	3	None	None	3

Conclusions: Preliminary analysis suggests defect in DNA damage response and chromatin remodeling pathways. Exome sequencing data are being analyzed to identify additional mutations and to gain deeper understanding of these rare tumors.

978 A Novel Lineage and Cancer Specific Long Non-Coding RNA for Detection of Metastatic and Primary Chromophobe Renal Cell Carcinoma

Xiaoming (Mindy) Wang[1], Stephanie Skala[1], Lisha Wang[1], Yuping Zhang[2], Xuhong Cao[1], Fengyun Su[1], Rui Wang[1], Javed Siddiqui[1], Arul Chinnaiyan[3], Saravana Dhanasekaran[1], Rohit Mehra[1]
[1]University of Michigan, Ann Arbor, MI, [2]Michigan Center for Translational Pathology, Ann Arbor, MI, [3]Plymouth, MI

Disclosures: Xiaoming (Mindy) Wang: None; Stephanie Skala: None; Lisha Wang: None; Yuping Zhang: None; Xuhong Cao: None; Fengyun Su: None; Rui Wang: None; Javed Siddiqui: None; Arul Chinnaiyan: None; Saravana Dhanasekaran: None; Rohit Mehra: None

Background: Chromophobe renal cell carcinoma (ChRCC) is one of the three main subtypes of renal cell carcinoma (RCC). The genetic basis of ChRCC is known to a limited extent and there is a lack of specific biomarkers to support the morphologic diagnosis of ChRCC (when needed). We analyzed next generation RNA sequencing (RNAseq) data from RCCs and normal kidney tissues to identify novel lineage/cancer specific biomarkers.

Design: We performed integrative analysis of RNAseq data on 1,049 RCC specimens combined from The Cancer Genome Atlas (TCGA), in-house studies, and the Knepper dataset of micro-dissected rat nephrons to identify cancer/lineage specific biomarkers, including a novel long non-coding RNA (lncRNA), LINC01187, located on chr5q35, 100kb downstream of the gene FOXI1, which is another important ChRCC marker that we previously characterized. Next, we validated the lncRNA marker utilizing a RNA *in situ* hybridization (RNA-ISH) platform on a cohort of 163 whole tissue sections, including 34 classic ChRCC, 10 eosinophilic ChRCC, 18 metastatic ChRCC sites, 6 unclassified RCC with oncocytic features, 17 oncocytomas, 2 hybrid oncocytic tumors (HOT), 10 clear cell RCC (CCRCC), 4 clear cell papillary RCC (CCPRCC), 11 papillary RCC (PRCC), 4 translocation RCC (TRCC), 3 collecting duct carcinoma (CDC), 1 mucinous tubular and spindle cell RCC (MTSCC), and 29 RCC metastases at various sites.

Results: We characterized the transcription and localization of LINC01187 in this RCC cohort by RNA-ISH. All metastatic ChRCC sites (18/18), all primary (34/34) classic ChRCCs and almost all eosinophilic ChRCCs (9/10) demonstrated high level of LINC01187 nuclear expression; expression in all positive cases was homogeneous. No LINC01187 was detected in primary CCRCC, CCPRCC, papillary RCC, TRCC, CDC, or MTSCC. All the evaluated metastatic non-ChRCC cases (29/29) showed completely negative LINC01187 expression. In normal kidney, LINC01187 is detected in the distal nephron segment. Other oncocytic tumors including unclassified RCC with oncocytic features, oncocytomas, and HOTs, also showed high level of nuclear LINC01187 expression, suggesting a common segment of nephron origin for such tumors.

Conclusions: We identified and validated LINC01187 as a highly sensitive and lineage/cancer specific marker for ChRCC, which can aid the clinical diagnosis in a metastatic setting, as well as challenging primary RCC cases.

979 Comparison of the Genetic Signatures of Primary and Metastatic Prostate Carcinoma

Dandan Wang[1], Huy Pham[2], Kyle Hurth[2], Guang-Qian Xiao[2]
[1]University of Southern California, Los Angeles, CA, [2]Keck School of Medicine of University of Southern California, Los Angeles, CA

Disclosures: Dandan Wang: None; Huy Pham: None; Kyle Hurth: None; Guang-Qian Xiao: None

Background: Prostate cancer (PCa) is a histologically and biologically heterogeneous disease that may behave unpredictably. PCa most commonly metastasizes to lymph nodes and bone. Although visceral metastasis is uncommon, when it occurs, liver and lung are the most commonly involved organs. The genetic features underlying PCa metastasis and its specific organ tropism are not well understood. This study aims to investigate this question at the molecular level by analyzing comprehensive genomic profiling data.

Design: Next generation gene sequencing (NGS) was performed on specimens of 34 patients with PCa during a 12-month period at Keck Medical Center of University of Southern California (USC). The NGS panel assesses over 300 genes for genetic abnormalities including deletion, copy number change, gene amplification, microsatellite stability and tumor mutation burden (TMB). All patients have PCa with Gleason scores of 8 or above and they were divided into 4 groups: 5 patients with liver metastases, 4 with bone metastases, 17 with lymph node metastases and 8 with non-metastatic primary PCa.

Results: The average TMB (mutations per Mb) for liver, lymph node and bone metastases and primary PCa groups were 5.6 (28/5), 4.8 (76/16), 3.7 (11/3) and 3.4 (27/8), respectively. The genes altered in each of the study groups are listed in Table1.

Genes	Liver metastasis (N=5)		Bone metastasis (N=4)		Lymph node metastasis (N=17)		Primary PCa (N=8)	
	n	Percentage	n	Percentage	n	Percentage	n	percentage
AR	2	40%	2	50%	4	24 %	0	0%
PTEN	2	40%	2	50%	7	41%	4	50%
TMPRSS2	2	40%	2	50%	9	53%	3	38%
PIK3	2	40%	1	25%	5	29%	2	25%
RUNX	2	40%	0	0%	4	24%	1	13%
MLL	2	40%	0	0%	6	35%	4	50%
SPEN	1	20%	0	0%	2	12%	0	0%
TP53	1	20%	1	25%	10	59%	1	13%
EPHA	1	20%	1	25%	2	12%	3	38%
BRCA2	1	20%	1	25%	3	18%	0	0%
APC	1	20%	1	25%	2	12%	0	0%
MDM4,RICTOR	1	20%	1	25%	0	0%	0	0%
ATM,CCND1,CDH1,PRKDC,RANBP,SPTA,STK11	1	20%	0	0%	1	6%	0	0%
BRCA1	1	20%	0	0%	3	18%	0	0%
CDC73,EGFR,EMSY,ERCC1,FGF19,GNAS,IGF2IKBKE,SPOP	1	20%	0	0%	0	0%	0	0%
CREBBP	1	20%	0	0%	1	6%	1	13%
CTNNB1,LYN,SDHA	1	20%	0	0%	0	0%	1	13%
ERBB, FAS	1	20%	0	0%	3	18%	0	0%
KMT2, PREX2	1	20%	0	0%	2	12%	0	0%
MYST3	1	20%	0	0%	2	12%	1	13%
PDGFR	1	20%	0	0%	1	6%	2	25%
MYC	0	0	1	25%	3	18%	2	25%
NOTCH	0	0	0	0%	3	18%	0	0%
ETV1	0	0	1	25%	1	6%	0	0%
MAP3K1	0	0	2	50%	0	0%	2	25%
FOX	0	0	0	0	0	0	1	13%
IDH	0	0	0	0	2	12%	0	0
CDKN	0	0	2	50%	1	6%	0	0
BRAF	0	0	2	50%	0	0	1	13%
FGFR	0	0	1	25%	2	12%	2	25%

Conclusions: An increased TMB in metastatic versus non-metastatic PCa was observed. In addition, TMB was found to be highest in liver metastases, suggesting an increased genetic instability may play an important role in cases with visceral metastases. Alterations of AR, APC, BRAC1 and BRAC2 genes tend to have a higher frequency in metastatic cases. Alterations in PTEN, p53, PI3K, and TMP-RSS2 genes tend to have a similar frequency in primary and metastatic groups, suggesting these changes could be relatively early events or these are non-specific genes. Analysis of expanded data sets may allow for better delineation of the genetic influences underlying the organ tropism of PCa metastasis. However, based on our preliminary data, it does not appear that a single or limited number of genetic events can fully account for the differences in the tropism of PCa metastasis. The great variability of genetic alterations observed among cases in different metastatic site group and even among cases within the same group suggests the complexity of metastasis and the heterogeneity of primary PCa. It indicates that the biologic behavior of PCa involves diverse and a constellation of genetic an

980 Clinicopathological Findings in End Stage Kidneys Resected for Mass Lesions: A Single Institution experience

Lin Wang[1], Daniel Schwartz[2], Satish Tickoo[3], Judy Sarungbam[4]
[1]Montefiore Medical Center, Bronx, NY, [2]Bronx, NY, [3]New York, NY, [4]Montefiore Medical Center, New York, NY

Disclosures: Lin Wang: None; Daniel Schwartz: None; Satish Tickoo: None; Judy Sarungbam: None

Background: Patients with end-stage renal disease (ESRD) are at approximately 100-times higher risk of developing renal cell carcinoma (RCC). This risk correlates with duration of dialysis. We analyzed the clinicopathological findings in ESRD removed for mass lesions at a single tertiary care institution.

Design: After institutional board review approval, pathology database was searched for all nephrectomies to identify patients with ESRD with any mass from 2014 to 2018. Clinical details were obtained from medical charts. The nephrectomies were assessed for gross and microscopic features. Tumors when present were classified according to WHO 2016 and staged according to AJCC 2018. In kidneys with multiple tumors, only the dominant tumor was considered for this analysis.

Results: A total of 486 nephrectomies performed for mass lesions were identified. Of them, 52 were from 42 patients with ESRD, all of whom had been on dialysis. The distribution of tumors in ESRD patients compared to non-ESRD kidneys and clinical features of the patients with ESRD are tabulated.

Among ESRD cases,

- 90.4 % (47/52) showed acquired cystic disease.
- Only 42 kidneys (80.8 %) had tumors, 22/42 unifocal and 20/42 multifocal. Tumors ranged in size from 0.2 to 7.5 cm (mean: 2.5); none of the tumors showed sarcomatoid features.
- 85.7 % (36/42), 9.5 % (4/42) and 4.8 (2/42) were staged as pT1a, pT1b and pT3a, respectively.
- Both the stage pT3a tumors were clear cell renal cell carcinoma.
- 10 kidneys (19.2%) did not contain any tumor. They showed acquired cystic disease with multiple cysts clustered together, lined by simple epithelium to complex epithelial proliferation with the lining cells showing abundant clear to eosinophilic cytoplasm without forming solid nodules. Most had associated oxalate crystals.
- 30.8 % (16/52) showed papillary adenomas, single or multiple.
- Only one developed metastatic tumor/recurrence, at the site of prior surgery, and patient had clear cell RCC.

Types of tumors		
Type of tumor	Tumors in ESRD (n=52)	Tumors in non-ESRD (n = 434)
Clear cell RCC	3(5.8%)	199 (45.9 %)
Papillary RCC	8 (15.4%)	107 (24.7 %)
Clear cell papillary RCC	8 (15.4%)	25 (5.8 %)
Acquired cystic disease associated RCC	22 (42.3%)	0
Multilocular cystic renal neoplasm of low malignant potential	1 (1.9%)	0
Chromophobe RCC	0	37 (8.5 %)
Oncocytoma	0	45 (10.4%)
RCC, unclassified	0	21 (4.8%)
Clinical features		
Age (range/mean)	38 - 78 (58) years	
Male :Female (31:11)	3:01	
Race (n = 42)		
Black/African American	26 (61.9 %)	
White /Caucasian	2 (4.8 %)	
All others/unknown	14 (33.3 %)	
Type of dialysis (n = 42)		
Hemodialysis	37 (88 %)	
Peritoneal and hemodialysis	5 (12 %)	
Causes of ESRD (n = 42)		
Hypertension	18 (42.9 %)	
Diabetes Mellitus	5 (11.9 %)	
Hypertension/diabetes	6 (14.3 %)	
Focal Segmental glomerulosclerosis	5 (9.5 %)	
Systemic Lupus erythematosus	3 (7.1 %)	
Others	6 (14.3 %)	

Conclusions: 1. Acquired cystic disease associated renal cell carcinoma is the most common tumor in kidneys with end stage renal disease.

2. Approximately 1/5th of nephrectomy specimens in end-stage kidney with suspected mass do not reveal any tumor, but show clustered cysts.

3. In this series, none of the acquired cystic disease-associated carcinomas showed aggressive clinical behavior; all tumors with adverse outcome were clear cell renal cell carcinoma.

981 Recurrence of Non-Invasive Papillary Urothelial Carcinoma is Associated with Signatures of Cell Cycle Activation and Immune Response

Joshua Warrick[1], Michael Zaleski[2], Augustyna Gogoj[3], Guoli Chen[2], Jay Raman[4], Matthew Kaag[5], Suzanne Merrill[5], Lauren Shuman[2], Vonn Walter[4], Fumaki Kawasawa[5], David DeGraff[4]
[1]Hershey, PA, [2]Penn State Health Milton S. Hershey Medical Center, Hershey, PA, [3]Penn State College of Medicine, Hummelstown, PA, [4]Penn State Health Hershey Medical Center, Hershey, PA, [5]Penn State College of Medicine, Hershey, PA

Disclosures: Joshua Warrick: None; Michael Zaleski: None; Augustyna Gogoj: None; Guoli Chen: None; Jay Raman: None; Matthew Kaag: None; Suzanne Merrill: None; Lauren Shuman: None; Vonn Walter: None; Fumaki Kawasawa: None; David DeGraff: None

Background: Non-invasive papillary urothelial carcinoma accounts for the majority of new bladder cancer diagnoses. While this tumor type does not metastasize, it frequently recurs, and may progress to invasive carcinoma. Molecular signatures that predict recurrence are desirable. In this study, we investigated RNA sequencing signatures as markers of recurrence risk.

Design: We assembled a retrospective cohort of 60 non-invasive papillary urothelial carcinomas. Tumor grade and mitotic index were assigned. RNA sequencing was performed on tumors from transurethral resection material, using the Illumina HiSeq platform and macrodissected formalin fixed paraffin embedded tissue. Analysis focused on expression signatures operative in bladder cancer. Specifically, 57 relevant gene lists were interrogated via agglomerative clustering, with three-cluster solutions. For each gene list, Cox linear models were constructed, with the dependent variable of recurrence free survival and independent variables of cluster assignment and BCG treatment status. Gene lists were considered significant if clusters associated with recurrence at $p<0.02$.

Results: Signatures of cell cycle activity were strongly associated with recurrence free survival, including the Hallmark lists "E2F targets," "G2M checkpoint," and "mitotic spindle assembly." Each gene list demonstrated a cluster with prominently high hazard of recurrence (E2F targets, hazard ratio (HR)=3.2, p=0.006; G2M checkpoint, HR=2.9, p=0.02; Mitotic spindle list, HR=3.1, p=0.009). Two other gene lists associated with recurrence free survival: interferon response (HR=3.2, p=0.016) and mitochondria (HR=3.3, p=0.01). In all five gene lists, the high-risk cluster remained significantly associated with recurrence free survival in multivariate Cox regression models including tumor grade and mitotic index ($p<0.05$), with the exception of "mitotic spindle assembly," which lost significance in models including mitotic index.

Conclusions: Cell cycle, interferon response, and mitochondrial gene signatures associate with recurrence of non-invasive papillary urothelial carcinoma, independent of tumor grade and mitotic index.

982 CK7, Inhibin, and p63 in Testicular Germ Cell Tumor: Superior Markers of Choriocarcinoma Compared to b-hCG

Sonya Wegman[1], Anil Parwani[2], Debra Zynger[3]
[1]The Ohio State University Medical Center, Galloway, OH, [2]The Ohio State University, Columbus, OH, [3]The Ohio State University Medical Center, Columbus, OH

Disclosures: Sonya Wegman: None; Anil Parwani: None; Debra Zynger: None

Background: Choriocarcinoma can be difficult to differentiate from other subtypes of testicular germ cell tumor (GCT) and can occur unexpectedly in distant, late metastases. Current immunohistochemical markers, such as b-hCG, lack specificity. We sought to compare the expression of several widely available yet poorly studied markers in testicular GCT, including CK7, inhibin, and p63, to b-hCG in order to distinguish a superior marker for the identification of choriocarcinoma.

Design: 60 mixed or pure testicular GCT were analyzed (27 choriocarcinomas, 19 yolk sac tumors, 29 embryonal carcinomas, 28 seminomas, 22 teratomas). Of the 60 cases, 50 were primary and 10 were metastases. Immunohistochemistry specific for CK7, inhibin, p63, and b-hCG was performed on paraffin embedded tissue. Statistical analysis was completed using a two-tailed Fisher's exact test.

Results: All cases of choriocarcinoma were strongly and diffusely positive for CK7, while seminomas were negative and half of embryonal carcinomas (52%) had weak reactivity. Most yolk sac tumors (84%) and teratomas (59%) had at least focal CK7 reactivity. The majority of choriocarcinomas (89%) were positive for inhibin, with reactivity predominantly highlighting syncytiotrophoblasts. Inhibin was negative in seminomas, embryonal carcinomas, yolk sac tumors, and teratomas. The majority of choriocarcinomas (85%) were strongly positive for p63, with staining mostly in mononucleated trophoblasts. p63 was negative in seminomas, embryonal carcinomas, and yolk sac tumors, while teratomas had variable expression (32%). b-hCG reactivity was diffuse with high background and was found in 96% of choriocarcinomas, 46% of seminomas, 54% of embryonal carcinomas, 47% of yolk sac tumors, and 32% of teratomas. b-hCG staining within other subtypes was more likely if choriocarcinoma or syncytiotrophoblasts were present elsewhere in the tumor (p=0.0002).

Conclusions: CK7 is a highly sensitive marker for testicular choriocarcinoma and differentiates choriocarcinoma from seminoma and embryonal carcinoma. Inhibin and p63 are sensitive and specific for choriocarcinoma versus seminoma, embryonal carcinoma, and yolk sac tumor. Due to the secretory nature of b-hCG yielding frequent background staining and nonspecific reactivity for other GCT subtypes, CK7, inhibin, and p63 are superior to b-hCG for the identification of choriocarcinoma.

983 Renal Cell Carcinomas with Borderline Features of Eosinophilic Solid and Cystic Renal Cell Carcinoma are Most Likely Papillary Renal Cell Carcinomas

Sean Williamson[1], Khaleel Al-Obaidy[2], Chia-Sui (Sunny) Kao[3], Craig Rogers[1], David Grignon[2], Lauren Schwartz[4], Maria Tretiakova[5], Tatjana Antic[6], Liang Cheng[2], Nilesh Gupta[1]
[1]Henry Ford Health System, Detroit, MI, [2]Indiana University School of Medicine, Indianapolis, IN, [3]Stanford University School of Medicine, Stanford, CA, [4]Perelman School of Medicine at the University of Pennsylvania, Bala Cynwyd, PA,[5]University of Washington, Seattle, WA, [6]University of Chicago, Chicago, IL

Disclosures: Sean Williamson: None; Khaleel Al-Obaidy: None; Chia-Sui (Sunny) Kao: None; Craig Rogers: None; David Grignon: None; Lauren Schwartz: None; Maria Tretiakova: None; Tatjana Antic: None; Liang Cheng: None; Nilesh Gupta: None

Background: Eosinophilic solid and cystic renal cell carcinoma (ESC RCC) has been recently recognized sporadically and in tuberous sclerosis as a potential new entity; however, precise diagnostic criteria remain to be fully defined. We have encountered cases in which distinction between ESC RCC and other RCC types, especially papillary RCC, is challenging.

Design: We retrieved tumors from our institutional files that had some features suggesting the diagnosis of ESC RCC (cytoplasmic stippling, cytokeratin 20 immunohistochemical labeling, hobnail-shaped eosinophilic cells lining cysts, or a combination of these), with other features suggesting papillary or other RCC types.

Results: We identified 15 tumors from 12 patients, ranging from 0.3-10.9 cm. Pathologic pT was pT1a (6), pT1b (3), pT2b (1), pT3a (1), and pT3b (1). Five patients had multiple tumors, (4 with papillary RCCs and papillary adenomas and 1 clear cell RCC). Three patients had end-stage renal disease or acquired cystic kidney disease. Morphologic features included cytoplasmic stippling (9/12 patients), papillary architecture (9/12), hobnail-shaped cyst lining cells (8/12), foamy macrophages (5/12), and psammoma bodies (1/12). Almost all (11/12 patients) had diffuse labeling for alpha-methyl-acyl-CoA-racemase (AMACR), usually strong intensity, and 10/12 had at least rare cells labeling for cytokeratin 20 (<5% to 90%). Cytokeratin 7 staining ranged from 0-50% of cells (median 0%, mean 7%). Five tumors were studied with molecular techniques: 2 with copy number analyses or FISH, 1 showing gain of chromosomes 7/17 and cnLOH for 3p. One had low level abnormal *TFE3* FISH, but no rearrangement was confirmed with a next generation sequencing fusion assay. Two had sequencing studies, neither revealing *TSC1* or *TSC2* alterations, but showing 1 with *KRAS* and *BCORL1* mutations and 1 with *PRBM1* mutation. Four patients developed metastases and 3 died of disease.

Conclusions: Although ESC RCC has been recently established as a novel tumor entity, RCC with equivocal features occurs and seems to be best classified as papillary RCC, as evidenced by multifocality with concurrent papillary RCCs, areas of papillary architecture and foamy macrophages, and diffuse, strong labeling for AMACR. Cytokeratin 20 labeling and cytoplasmic stippling may not be entirely specific for this diagnosis. We propose that the diagnosis of ESC RCC be reserved for cases with prototypical features and/or molecular confirmation of the recently discovered TSC gene alterations.

984 Urothelial Carcinoma in Situ Versus Early High-Grade Papillary Urothelial Carcinoma: A Survey of Pathologist and Urologist Interpretations

Sean Williamson[1], Ankur Sangoi[2], Chia-Sui (Sunny) Kao[3], Mustafa Deebajah[1], Justine Barletta[4], Gladell Paner[5], Steven Smith[6], David Grignon[7], Eva Compérat[8], Mahul Amin[9], Fiona Maclean[10], Rajal Shah[11], Kenneth Iczkowski[12], Warick Delprado[13], Liang Cheng[7], Chin-Chen Pan[14], Jesse McKenney[11], Jae Ro[15], Francesca Khani[16], Rodolfo Montironi[17], Brian Robinson[16], Hikmat Al-Ahmadie[18], Jonathan Epstein[19], Kiril Trpkov[20], Maria Tretiakova[21], Steven Shen[22], Shaheen Alanee[1], Michelle Hirsch[23]
[1]Henry Ford Health System, Detroit, MI, [2]El Camino Hospital, Mountain View, CA, [3]Stanford University School of Medicine, Stanford, CA, [4]Brigham and Women's Hospital, Harvard Medical School, Boston, MA, [5]University of Chicago, Chicago, IL,[6]Virginia Commonwealth University School of Medicine, Richmond, VA, [7]Indiana University School of Medicine, Indianapolis, IN, [8]Tenon Hospital, Paris, France, [9]Methodist University Hospital, Memphis, TN, [10]Douglass Hanly Moir Pathology, Macquaire Park, NSW, Australia, [11]Cleveland Clinic, Cleveland, OH, [12]Medical College of Wisconsin, Milwaukee, WI, [13]Douglass Hanly Moir Pathology, McMahons Point, AUS, Australia, [14]Veterans General Hospital Taipei, Taipei, Taiwan,[15]Houston, TX, [16]Weill Cornell Medicine, New York, NY, [17]University Politecnica delle Marche/Medicine, Ancona, Italy, [18]Memorial Sloan Kettering Cancer Center, New York, NY, [19]Johns Hopkins Medical Institutions, Baltimore, MD, [20]University of Calgary, Calgary, AB, [21]University of Washington, Seattle, WA, [22]Houston Methodist Hospital, Houston, TX, [23]Brigham and Women's Hospital, Boston, MA

Disclosures: Sean Williamson: None; Ankur Sangoi: None; Chia-Sui (Sunny) Kao: None; Mustafa Deebajah: None; Justine Barletta: None; Gladell Paner: None; Steven Smith: *Consultant*, Elsevier/Amirsys Publishing; David Grignon: None; Eva Compérat: None; Mahul Amin: *Advisory Board Member*, Precipio Diagnostics; *Advisory Board Member*, Cell Max; *Advisory Board Member*, Core Diagnostics; *Consultant*, Urogen; *Consultant*, Advanced Clinical; Fiona Maclean: *Speaker*, Mundipharma; Rajal Shah: None; Kenneth Iczkowski: None; Warick Delprado: None; Liang Cheng: None; Chin-Chen Pan: None; Jesse McKenney: None; Jae Ro: None; Francesca Khani: None; Rodolfo Montironi: None; Brian Robinson: None; Hikmat Al-Ahmadie: None; Jonathan Epstein: None; Kiril Trpkov: None; Maria Tretiakova: None; Steven Shen: None; Shaheen Alanee: None; Michelle Hirsch: None

Background: Urothelial carcinoma in situ (CIS) "with early papillary formations" has been proposed as a term for incipient high-grade papillary urothelial carcinoma (PUC). However, confusion may arise between true CIS and lateral flat spread of PUC. It remains unclear how pathologists and urologists interpret this scenario.

Design: Web surveys were circulated to pathologists and urologists. Pathologists were divided into 3 groups: P1 = 28 invited academic genitourinary (GU) pathologists, P2 = 17 pathologists recruited online with self-reported GU focus, and P3 = 23 pathologists self-reported as non-GU specialists. Urologists yielded 32 responses (25 self-reported cancer specialists).

Results: P1 noted reporting CIS in the same specimen (but different tissue fragment) as PUC (57%) "regularly," compared to P2 (41%) or P3 (17%), and "regularly" diagnosed CIS in a specimen clinically labeled as "tumor" (61% vs 47% vs 22%). Pagetoid spread was considered to favor CIS predominantly by P1 (61% vs 35% vs 22%). All groups (65-76%) tended to consider previous PUC history before making a diagnosis. Cytokeratin 20 was the most used immunostain (83-95%), followed by p53 (63-100%). MIB-1 was least preferred by P1 (29% vs 67% vs 56%). Only 24-36% interpret negative p53 staining as null mutant, highest in P1. Case image interpretation as pure CIS was higher in P3 compared to P1 and P2 for 4/5 cases, who gave more descriptive or mixed diagnoses. Urologists felt that the term "lateral spread/shoulder" was unclear (75%) and preferred either "early" PUC (44%) or PUC with "early growth" (44%) mentioned in a note. Some urologists (47%) felt pagetoid spread could affect treatment, and 63% would like it documented. Over half (59%) of urologists considered CIS in the "base of tumor" to be part of the tumor; however, 71% of the non-cancer specialists (n=7), interpreted this as a second diagnosis. Half (53%) of urologists felt that reporting CIS instead of lateral spread of PUC would change management.

Conclusions: Interpretation and documentation of flat lesions (CIS and early PUC) lack consensus among pathologists, and may benefit from distinctive terminology, such as "CIS" and "non-invasive high-grade urothelial carcinoma". Moreover, the distinction between CIS and early PUC is not always clear to urologists and can influence management.

985 Integrated Somatic and Transcriptional Profiling of Acquired Cystic Kidney Disease Associated and Clear Cell Papillary Renal Cell Carcinomas Arising in Patients with End-Stage Kidney Disease

Parker Wilson[1], Peter Humphrey[2], Adebowale Adeniran[3]
[1]Washington University, St. Louis, MO, [2]Yale University, New Haven, CT, [3]Yale University School of Medicine, Seymour, CT

Disclosures: Parker Wilson: None; Peter Humphrey: None; Adebowale Adeniran: None

Background: End-stage kidney disease is a well-established risk factor for the development of renal cell carcinoma. It's unclear whether somatic variants arising in a background of end-stage kidney disease are similar to those in tumors arising in this setting. We report somatic and transcriptional profiles of acquired cystic kidney disease associated renal cell carcinomas (ACD) and clear cell papillary carcinomas (CCP) arising in a series of 4 patients with end-stage kidney disease.

Design: FFPE tissue cores were obtained from 4 radical nephrectomy specimens with multifocal tumors arising in a background of end-stage kidney disease. Exome and RNA-seq was performed on background end-stage kidney selected for areas of atypical tubular epithelium, multifocal tumors, and extra-renal controls in each patient. Somatic SNV-Indels (Mutect2) and copy number variants (CNVkit) were called in a tumor-normal configuration following sample preprocessing. Differential gene expression and gene clustering was performed with DESeq2.

Results: Rare somatic SNV-indels (n=15/1706, 0.8%) were shared between one or more sample types (Figure 1) and represented 2.7% (4/148) of coding variants present in the catalogue of somatic mutations in cancer. The overlapping variants (Table 1) included a frameshift insertion in *HNF1A* (patient 4) previously implicated in hepatocellular adenomas, and nonsynonymous variants in *CR1* (patient 2) and *ZNF695* (patient 3). The CCP sample from patient 3 showed copy number gains in chromosomes 2,3,5,6,7,10,12,16,17 and 21 and the ACD sample from patient 2 showed copy number loss in chromosomes 1,6,9,10,11,14,15,18,19, and 21 that were not present in the matched background end stage kidney sample. Rare copy number variable regions were present in multiple samples and included a 5Mbp region of copy number gain on chromosome 6p21-22 that was shared between the background end stage kidney, ACD, and CCP in the same patient. Differential gene expression analysis and gene clustering revealed that samples grouped primarily based on patient (Figure 2) with loss of kidney cell type specific markers (*SLC12A3, SLC12A1*) and increased expression of mediators of glycolysis and gluconeogensis (*G6PC*, *PCK1*, *ALDOB*) seen in tumor samples.

CHR	POS	GENE	REF	ALT	SAMPLES	FUNCTION
1	207614451	CR1	T	C	2acd-2ccp	exonic nonsynonymous
1	246987366	ZNF695	C	T	3acd-3atyp	exonic nonsynonymous
3	31620009	STT3B	A	T	2acd-4ccp2	intronic
4	122235544	KIAA1109	A	G	4atyp-4ccp1	intronic
5	143103349	ARHGAP26	G	C	3acd-3atyp	intronic
5	177603161	B4GALT7	G	A	2acd-2ccp	intronic
8	22691754	EGR3	G	A	4atyp-4ccp1-4ccp2	intronic
11	48132598	PTPRJ	T	C	4atyp-4ccp1	UTR3
12	120994313	HNF1A	G	GC	4atyp-4ccp1-4ccp2	exonic frameshift insertion
14	104946865	AHNAK2	G	A	1atyp-1ccp	exonic synonymous
15	48136743	SLC24A5	C	A	2atyp-2ccp	exonic synonymous
16	67680792	GFOD2	C	T	2atyp-4ccp1	UTR3
17	3398025	OR1E1	G	A	2acd-2ccp	exonic nonsynonymous
17	3675830	P2RX5-TAX1BP3	T	C	2atyp-2ccp	ncRNA_intronic
19	44387676	ZNF285	CA	TG	4atyp-4ccp1	exonic nonframeshift substitution

Figure 1 - 985

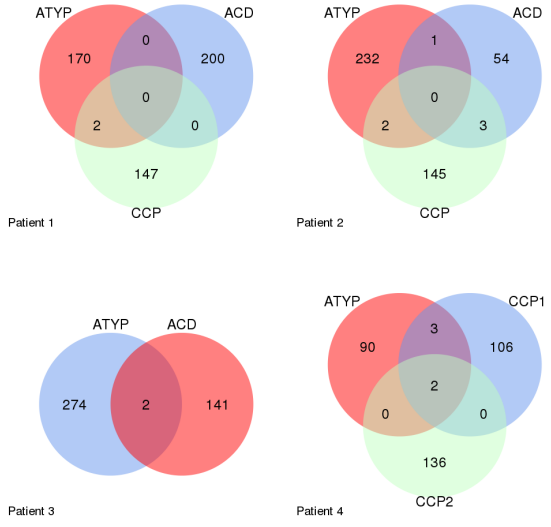

Figure 2 - 985

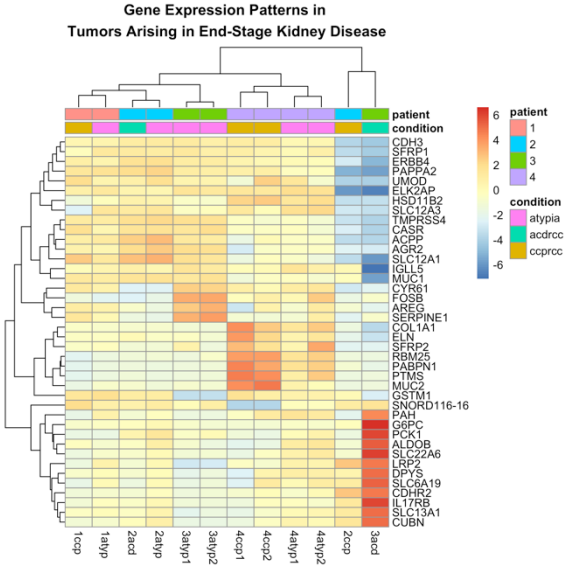

Conclusions: Somatic SNV-indels and CNVs arise in end-stage kidney disease that may predispose patients to renal cell carcinoma.

986 Comparative Analysis of p16 Expression Among African American and European American Prostate Cancer Patients

Myra Wong[1], Yaeli Bierman[1], Michael Ittmann[1]
[1]*Baylor College of Medicine, Houston, TX*

Disclosures: Myra Wong: None; Michael Ittmann: None

Background: Expression of p16 is increased in a number of malignancies, including prostate cancer. Recent studies in a European cohort showed that expression of p16 is correlated with expression of the TMPRSS2/ERG fusion protein. The TMPRSS2/ERG fusion is significantly less common in prostate cancers in African American (AA) men. Thus, it would be predicted that p16 expression should be less common in prostate cancers in AA men. The objective of our study is to compare expression of p16 in benign prostate and prostate cancers from AA and Europe American (EA) men.

Design: Immunohistochemistry for p16 was performed on tissue microarrays constructed from radical prostatectomies performed on AA and EA veterans. Staining was scored and the scores compared to demographic, clinical and pathological parameters. Percent West African ancestry in the AA cohort was assessed using ancestry informative markers.

Results: Contrary to our predictions, p16 expression was similar in the AA and EA cohorts. Consistent with prior reports, expression of p16 was quite low in benign prostate tissues from EA patients but surprisingly was significantly higher in benign tissues from AA patients. In addition, expression of p16 was associated with a family history of prostate cancer in AA men.

Correlation between cytoplasmic and nuclear staining in benign prostate and prostate cancer cells in samples from African American and European American patients.

African American		**Benign**		**Cancer**	
		Cytoplasmic	**Nuclear**	**Cytoplasmic**	**Nuclear**
Benign	**Cytoplasmic**	1	**.85; p<.0001**	.15; p=.09	**.38; p<.001**
	Nuclear	X	1	.11; p=.19	**.49; p<.001**
Cancer	**Cytoplasmic**	X	X	1	**.64; p<.0001**
	Nuclear	X	X	X	1
European American		**Benign**		**Cancer**	
		Cytoplasmic	**Nuclear**	**Cytoplasmic**	**Nuclear**
Benign	**Cytoplasmic**	1	**.85; p<.0001**	.03; p=.69	.02; p=.73
	Nuclear	X	1	.07; p=.38	.03; p=.73
Cancer	**Cytoplasmic**	X	X	1	**.81; <.0001**
	Nuclear	X	X	X	1

Correlation coefficients and p-values for Pearson Product Moment test for various comparisons are shown

Figure 1 - 986

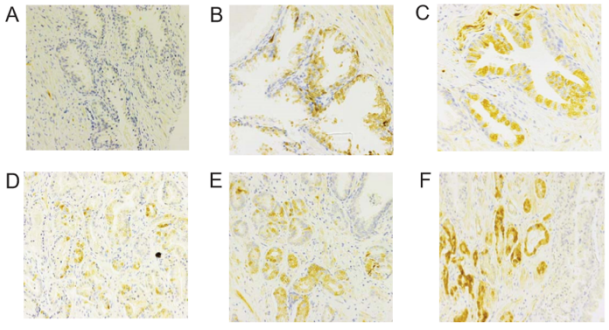

Figure 1. p16 immunohistochemistry in African American prostate cancer,

A. Benign prostate, no staining. B. Benign prostate, moderate staining. C. Benign prostate, strong staining. D. Prostate cancer, weak staining. E. Prostate cancer, moderate staining. Normal prostate to upper right. F. Prostate cancer, strong staining. Normal prostate gland is on the right. Original magnification 200X.

Figure 2 - 986

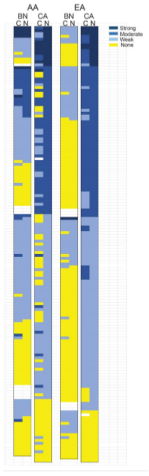

Figure 2. Heat map of p16 staining in African American and European American prostate cancer.

Heat map with cases as individual rows. AA African American; EA: European American; BN: benign tissue; CA: cancer tissue; C: cytoplasmic staining; N: nuclear staining. Staining intensity is indicated by the shade of blue as shown, with dark blue indicating strong staining (7-9), medium blue moderate staining (4-6); light blue weak staining (1-3) and yellow, no staining. Cases within each racial group arranged by intensity of cancer nuclear staining.

Conclusions: Expression of p16 is similar in prostate cancers from the two racial groups despite the lower incidence of the TMPRSS2/ERG fusion in in AA prostate cancer. The expression of p16 in benign tissues from a subset of AA men implies that there may be different mechanisms for p16 overexpression in prostate cancers from the two racial groups.

987 Programmed Death-Ligand 1 (PD-L1) Expression in Pheochromocytoma: Clinicopathologic Correlation

Meng-Jun Xiong[1], Haydn Kissick[2], Viraj Master[1], Adeboye O. Osunkoya[2]
[1]Emory University, Atlanta, GA, [2]Emory University School of Medicine, Atlanta, GA

Disclosures: Meng-Jun Xiong: None; Haydn Kissick: None; Viraj Master: None; Adeboye O. Osunkoya: None

Background: Programmed death-ligand 1 (PD-L1) IHC has been widely explored, but its expression and prognostic significance in Pheochromocytoma (PCT) has not been well characterized. PD-L1 is theorized to promote PCT tumorigenesis through dysregulated hypoxia pathways. Herein, we evaluated the correlation between PD-L1 expression and clinicopathologic features including potential for malignant behavior and metastasis.

Design: All PCT cases came from our Urologic Pathology database and expert consult files from 2015-2018. Clinicopathological data was documented. PD-L1 (DAKO PDL1 IHC 28-8 pharmDx) was performed and scored as negative or positive. Positive was pre-defined as any membranous or cytoplasmic staining of viable tumor cells >1% of total tumor volume. Positive staining was further characterized by pattern (focal/diffuse) and intensity (weak/strong).

Results: Thirty-eight PCT cases were included (26 female; 12 male). Mean age was 52 years (range: 16-75). Over 50% of PCTs resected <40 years of age had a heritable mutation. Mean size was 4.7 cm (range: 1.5-14.5). Vascular invasion, positive margin, MIB-1 (?5%), and mitoses (>3/10 hpf) were each reported in 7-11% of all cases. Capsular invasion was present in 24% of the cases. Seven cases (18%) had mutations: RET (n=3), VHL (2), SDHB (1), and ATM and PDGFRA (1). Two cases (5%) were malignant. Nearly 50% of patients had >1 year of follow-up, ranging up to 16 years. No patients died of disease. PD-L1 was positive in 6/38 (16%) of cases, and most had weak staining. Positive PD-L1 included: focal pattern-weak intensity staining (n=3), diffuse pattern-weak intensity staining (2), and diffuse pattern-strong intensity staining (1). Mean size of PD-L1 positive cases was 5.6 cm, greater than that of the cohort. PD-L1 positive cases with a PASS score ?4 comprised 20% of the subset with scores ?4. A single case with diffuse pattern-strong intensity PD-L1 positivity had the largest tumor size of the study cohort (14.5 cm), was >3 times the mean tumor size, had vascular and capsular invasion, and a PASS >4. All genetically mutated cases were negative for PD-L1.

Conclusions: This study is one of the largest to date on PD-L1 in PCT resections. In view of the positive PD-L1 expression in larger PCTs with relatively high PASS, it suggests PD-L1 may play a distinctive clinicopathologic and immuno-biologic role in PCT. In addition, these findings support a potential therapeutic role for PD-L1 targeted checkpoint inhibitors in a subset of patients with PCT.

988 The Study of Urothelial Carcinoma with Prostate Involvement: by Clinicalmorphology and Immunohistochemistry (IHC) Stains

Qiqi Ye[1], John Phillips[1], Minghao Zhong[1]
[1]Westchester Medical Center, Valhalla, NY

Disclosures: Qiqi Ye: None; John Phillips: None; Minghao Zhong: None

Background: Urothelial carcinoma (UC) with prostate involvement is not uncommon due to the proximity of two organs. Some cases of UC with prostate involvement will create a dilemma regarding diagnosis (UC vs prostate carcinoma) or staging (invasive vs non-invasive). On the other hand, there is a paucity of literature on this entity. Therefore, our aim is to assess the clinicopathologic features and IHC pattern of UC with prostatic involvement.

Design: Retrospective review of all urothelial carcinoma cases (2000 cases) at our institution from 2005 to 2018 identified 177 cases with prostate tissue. Among them, UC with prostate involvement was identified in 31 patients. Demographic, clinical and pathologic variables were shown in Table 1. The H&E slides were reviewed by 2 pathologists. Cases also subjected for IHC stains of Triple stain and GATA3.

Results: Among 31 patients with prostate involvement UC, 7 (22.6%) had carcinoma in situ and 20 (64.5%) were invasive UC. 4 cases of primary prostatic urethral urothelial carcinoma were identified. The rest of cases were bladder UC. Of the 20 invasive UC cases, 17 (85.0%) cases resulted from direct transmural invasion from the primary tumor in the bladder, and 3 (15.0%) cases from transurethral invasion. Morphologically, UC invading prostate can mimic prostate neoplasm. For example, high grade UC with glandular differentiation and extensive prostatic glandular involvement could mimic prostatic adenocarcinoma or intraductal carcinoma (Fig. 1A and B). Moreover, IHC stain may be insufficient to aid in diagnosis under these circumstances. As shown in Fig. 1C, UC was negative for urothelial marker P63 and HMWCK while positive for prostatic marker AMACR. Furthermore, we found that UC with transmural invasion to prostate were

usually basal type (HMWCK+, GATA3-) and with extensive stromal invasion. While UC with transurethral invasion were usually luminal type (HMWCK-, GATA3+) with extensive glandular involvement without or with minimal stromal invasion (Fig. 1D).

Variables	
Median age at surgery (yr)	75 (54 to 92)
Pathological Stage, n (%)	
pT1	2 (6.4)
pT2	2 (6.4)
pT3	2 (6.4)
pT4	11(35.5)
Median number of removed lymph nodes	9 (29.0)
Lymph nodes metastasis, n (%)	6 (19.4)
Lymphovascular invasion, n (%)	10 (32.3)
High grading, n (%)	15 (48.4)
Positive soft tissue surgical margin, n (%)	6 (19.4)
Concomitant carcinoma *in situ*, n (%)	4 (12.9)
Median tumor size (cm)	4.5 (0.1-9.5)

Figure 1 - 988

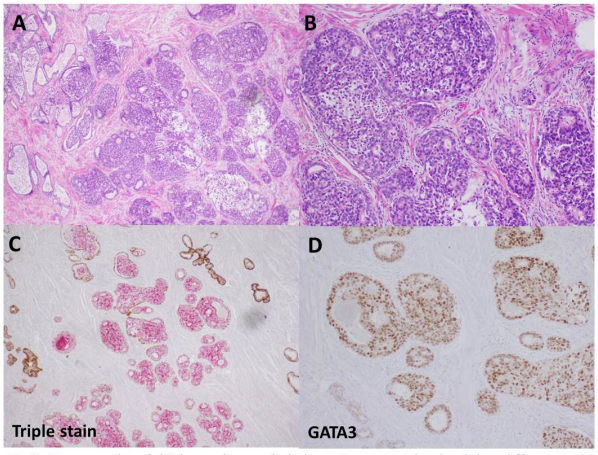

Fig.1 An example of high grade urothelial carcinoma with glandular differentiation extensively involving prostate glands. Both morphology and IHC pattern mimicking prostate neoplasm. A, low power, neoplasm with glandular differentiation extensively involving prostate gland. B, high power showing clearly glandular differentiation neoplasm confined in basal cell lining space. C, prostate triple stain (p63, HMWCK and AMACR). IHC pattern mimicking intraductal carcinoma of prostate. Neoplasm are negative for HMWCK and P63 while positive for AMACR. D, GATA3 highlights neoplasm confirming urothelial origin.

Conclusions: Our study revisited this well-known phenomenon: urothelial carcinoma involving prostate. Our data demonstrated a novel finding: the basal type UC associated with transmural invasion, extensive stromal invasion and higher stage disease; while luminal type UC associated with transurethral invasion, extensive glandular involvement with minimal stromal invasion and lower stage disease.

989 Molecular Characterization of Prostatic Adenocarcinoma: A Next-Generation Sequencing Study

Yunshin Yeh[1], Michael Constantinescu[1], Catherine Chaudoir[1], Anthony Tanner[1], Xiuping Yu[2], Aubrey Lurie[1]
[1]Overton Brooks VA Medical Center, Shreveport, LA, [2]LSU Health Shreveport, Shreveport, LA

Disclosures: Yunshin Yeh: None; Michael Constantinescu: None; Catherine Chaudoir: None; Anthony Tanner: None; Xiuping Yu: None; Aubrey Lurie: None

Background: Molecular characterization of prostate cancer has revealed recurrent genomic alterations. Next-generation gene sequencing may guide cancer chemotherapy.

Design: Thirty-four prostatic adenocarcinomas from 34 patients were retrospectively retrieved from case archives. Clinical data including patients' ages, PSA levels, and tumor stages were obtained from the medical records. These cases included 20 radical prostatectomies, 2 transurethral prostate resections, and 12 needle biopsies. Thirty-four samples of formalin-fixed paraffin embedded tissues were submitted for a panel of 181 genes of next-generation gene sequencing studies.

Results: Thirty-four male patients have an age ranging from 50 to 85 years old and PSA levels from 0.17 to 188. There is one neuroendocrine small cell carcinoma and 33 acinar adenocarcinomas with Gleason score ranging from 7 (3+4) to 9 (5+4) and grade group 2 to 5. Thirty-three of 34 samples had at least one gene mutation. There are 54 genes with alterations including 71 missense mutations, 6 frameshift alterations, 4 deletions, 1 nonsense mutation, 1 duplication, and 9 gene fusions, in the 34 prostatic adenocarcinoma samples.

These genes are involved in DNA repair system, cell cycle regulations, cell signaling pathways, and chromosomal translocations. The results are shown in the following table.

Table 1. Gene Mutations in 34 Prostatic Adenocarcinomas

Pathway	Gene Mutation (number of cases; percentage)
DNA damage repair	ATM (5;15%), BRCA2 (3;9%)
DNA mismatch repair	MSH2 (2;6%), MSH (2;6%)
Cell cycle regulation	CDKN1A (1;3%), CDKN1B (1;3%), CDKN2A (1;3%)
Oncogenes, tumor suppressor genes, signal transduction	APC (6;18%), TP53 (5;15%), CTTNB1 (2;6%), PIK3CA (2;6%), EGFR (2;6%), ERBB2 (3;9%), FGFR4 (2;6%), HRAS (1;3%), KRAS (2;6%), NF1 (2;6%)
Chromosomal translocation	TMPRSS-ERG (5;15%), ERG-TMPRSS (1;3%), ERG-PDILT (1;3%), SLC45A-ERG (1;3%), PRPSAP1-NTRK3 (1;3%)
Undetermined significance	NUP214 (3;9%), MECOM (3;9%), MYH11 (3;9%), ALK (2;6%), BCOR (2;6%); CSF1R (2;6%), KIF5B (2;6%), KMT2A (2;6%), RET (2;6%), ROS1 (2;6%)
	ASXL1, AKT1, BRAF, CREBBP, FGFR3, JAK3, KDR, KIF5B, KIT, MED12, MAP2K1, MKL1, MET, NTRK1, PDGFRA, RAB35, SRC, SYK, STK11, TET2, TERT, TGFBR1, TSC2 (each gene: 1;3%)

Conclusions: In our study consistent with previous reports, APC, ATM, and TP53 alterations commonly ocuur in prostatic adenocarcinoma. The NUP214 and MECOM alterations, previously reported in acute leukemia, may play a role in the pathogenesis of prostate cancer. DNA mismatch repair gene mutations are involved in 12% of the cases. The most common translocation involved in prostatic carcinogenesis is TMPRSS-ERG. We report a novel PRPSAP1-NTRK3 translocation in prostate cancer. The gene mutations in DNA mismatch repair and receptor tyrosine kinase signaling pathways may serve as therapeutic targets for precision medicine guided chemotherapy.

990 Morphological and Molecular Characterization of Prospectively and Sequentially Analyzed Prostate Tumors from Men with Castration Sensitive, de novo Metastatic Prostate Cancer (M1PCa)

Miao Zhang[1], Ana Aparicio[2], Brian F Chapin[2], Patricia Troncoso[2]
[1]The University of Texas MD Anderson Cancer Center, Bellaire, TX, [2]The University of Texas MD Anderson Cancer Center, Houston, TX

Disclosures: Miao Zhang: None; Ana Aparicio: None; Brian F Chapin: None; Patricia Troncoso: None

Background: Prostate cancer (PCa) is clinically and biologically heterogeneous. While the vast majority of cases present as localized non-lethal disease, PCa is the cause of death in approximately 15% of affected men, up to one third of whom present with M1PCa at diagnosis. However, most molecular studies in PCa are performed in samples obtained from the primary tumors of men with localized disease or from biopsies of those with metastatic castration-resistant PCa (mCRPCa). In these settings, the expression of the androgen receptor (AR), the ARv7 splice variant, and the tumor suppressors Tp53, RB1 and PTEN have been associated with outcome. The frequency at which these markers are expressed in the primary tumors of men with M1 castration-sensitive PCa and whether this frequency changes as a result of exposure to systemic therapies are unknown.

Design: In the context of a prospective clinical trial (NCT01751438) we evaluated PCa core biopsies obtained at initial diagnosis, as well as core biopsies and radical prostatectomy and pelvic lymph node specimens obtained from men with M1PCa after 6 months of systemic therapy. We reviewed their morphological features and used immunohistochemistry (IHC) to evaluate the frequency at which AR N-terminus (AR441, cat#M3562, Dako), AR C-terminus (SP242, cat#LS-C210456), ARv7 (RM7, 31-1109-00), Tp53 (D0-7, cat#M7001, Dako), RB1 (Ab-5, cat#OP66, Millipore Sigma) and PTEN (clone 6H2.1, cat#CM278, BioCare) are expressed. ARv7 and Tp53 were categorized as ‘positive’ (abnormal) if expressed in ? 10% of tumor cell nuclei. The remaining markers were categorized as ‘negative’ (abnormal) if expressed in ? 10% of tumor cell nuclei.

Results: To date the specimens from 38 men have been evaluated. The Gleason score was 8-10 in 92% of men. All baseline (BL) biopsies and all radical prostatectomy specimens showed cribriform and/ or intraductal features. IHC results are shown below.

Figure 1 - 990

	BL Prostate Core Biopsies (n=38)	6mo Prostate Core Biopsies (n=38)	6mo Pelvic Lymph Node Metastases (n=15)
AR N-terminus, n	37	34	15
Negative	1 (2.7%)	7 (20.6%)	0
AR C-terminus, n	37	33	15
Negative	6 (16.2%)	17 (51.5%)	0
ARv7, n	38	37	15
Positive	2 (5.3%)	4 (10.8%)	4 (27%)
Tp53, n	34	35	15
Positive	13 (38.2%)	7 (20.0%)	5 (33%)
RB1, n	38	36	15
Negative	5 (13.2%)	3 (8.3%)	2 (13%)
PTEN, n	32	27	15
Loss, homogeneous	11 (34.4%)	17 (63.0%)	9 (60%)
Loss, heterogeneous	7 (21.9%)	3 (11.1%)	3 (20%)

Conclusions: We present the first molecular characterization of prospectively and sequentially analyzed prostate tumors in men with M1PCa, an understudied subset of lethal PCa. Data to date suggest that AR expression decreases with exposure to androgen ablative therapies, ARv7 can be detected (rarely) at diagnosis and the rate of tumor suppressor defects in M1PCa is similar to that observed in mCRPCa.

991 Prostate Cancer with Expansile Cribriform Gleason Pattern 4 Has Distinct Genetic Profile and Prognostic Significance

Xiaotun Zhang[1], Laureano Rangel Latuche[1], William Sukov[2], R. Jeffrey Karnes[1], John Cheville[1]
[1]Mayo Clinic, Rochester, MN, [2]Rochester, MN

Disclosures: Xiaotun Zhang: None; Laureano Rangel Latuche: None; William Sukov: None; R. Jeffrey Karnes: None; John Cheville: None

Background: Expansile cribriform prostate cancer (PCa) glands can be observed in Grade Groups 2 to 5. These glands are characterized by large cribriform gland with less opened lumens, distinct irregular edge and expansile growth. In the most recent consensus, expansile cribriform is classified as Gleason pattern 4. To date, the clinical-pathological correlations and genetic profiles of expansile cribriform glands are poorly understood.

Design: Pathology files were searched for patients with diagnoses of Gleason score 7 or higher PCa. Clinicopathologic factors were collected through reviewing medical records. All cases were re-reviewed and disagreements were solved by consensus. Tissue microarrays (TMAs) were constructed with quadruplicate 0.6 mm cores containing the Gleason pattern 4 from each case. Fluorescence in situ hybridization (FISH) using probes detecting *PTEN* and *CHD1* was performed on TMAs. Cox proportional hazard regression analysis and logistic regression analysis were used for statistical study.

Results: A total of 409 cases with a median follow-up time of 15.1 years were included in this study. In univariate Cox regression analyses, the expansile cribriform pattern had a significantly higher risk of SP (p<0.0001), and PCa related death (p<0.001) than other Gleason pattern 4 morphologies. FISH data showed 18.3% cases with *CHD1* gene loss and 24.7% cases with *PTEN* gene loss. A total of 6.4% of cases harbored both gene losses. There was a statistically significant association between expansile cribriform glands with CHD1 loss (p=0.004) but there was not a significant association with PTEN loss.

Conclusions: In combination with previous data, our results suggest that the expansile cribriform pattern of PCa is morphologically, genetically and clinically different from other Gleason Grade 4 patterns. Morphologically, these glands are large with less open/ill formed lumens and irregular sprawling edges. Genetically, *CHD1* gene losses are frequently identified with these glands. Most importantly, expansile cribriform glands exhibit strong association with aggressive tumor behavior and significantly worse outcomes suggesting that an expansile cribriform architecture is more appropriately included in Gleason pattern 5.

992 PD-L1 and Stem Cell Markers (CD44, OCT4) in Micropapillary Variant of Urothelial Carcinoma (MPUC): Its Correlation with Clinical Progression

Adriana Zucchiatti Ll.[1], Maria Eugenia Semidey-Raven[1], Nikaoly Ciriaco[1], Armando Reques[1], Jordi Temprana-Salvador[2], Douglas Sanchez[3], Carles Raventos Busquets[1], Santiago Ramon Y Cajal[4], Ines de Torres[5]
[1]Vall d'Hebron University Hospital, Barcelona, Spain, [2]Barcelona, Spain, [3]Arnau de Vilanova University Hospital, Lleida, Spain, [4]Vall d'Hebron University Hospital, Barcelona, Catalonia, Spain, [5]Vall d'Hebron Campus and Autonomous University of Barcelona (UAB), Barcelona, Spain

Disclosures: Adriana Zucchiatti Ll.: None; Maria Eugenia Semidey-Raven: None; Nikaoly Ciriaco: None; Armando Reques: None; Jordi Temprana-Salvador: None; Douglas Sanchez: None; Carles Raventos Busquets: None; Santiago Ramon Y Cajal: None; Ines de Torres: None

Background: MPUC represents 0.6-2.2% of all urothelial carcinomas. It has an aggressive clinicopathological behavior with frequent lymphovascular invasion without therapeutic targets. So far there are limited data on the immunohistochemical PD-L1 and stem cell markers expression in MPUC. Our objective was to study PD-L1, CD44 and OCT4 immunoexpression in a large cohort of patients of a single institution and correlate it with clinical findings and prognosis of this entity.

Design: A cohort of 64 MPUC patients diagnosed at Vall d'Hebron University Hospital between 1999-2017 were selected with complete histological data and clinical follow-up. Tissue-microarrays blocks (Advanced Tissue Arrayer, Chemicon Int.) were constructed. For each case, two selected cylinders of 2 mm from different and representative tumor areas were included. Immunohistochemical staining was performed for PD-L1 (22C3 Dako pharmDx), CD44 and OCT4. PD-L1 expression was evalued in percentage of tumoral cells stained (as negative if <1%, positive: 1-4%, 5-10% and >10%). Stem cell markers (CD44, OCT4) expression were evaluated using a semiquantitative method scored on a scale from 0 to 300 (HScore). The results were analyzed with SPSS Data Analysis Program 20.0.

Results: The mean age at diagnosis was 69.14, with male predominance in 58 cases (90.6%). There was 74.54% frequency of tobacco consumption and 5.45% alcoholic habit. All the cases were histologically high grade. PD-L1 expression was positive in 25% of cases (<5% in 25% of the cases, 5-10% in 75%. None of the cases showed PDL-1 expression >10%). No statistically significant association of PDL-1 expression with overall survival rate was demonstrated (p=0.168). OCT4 expression was observed only in 1 case, whereas CD44 expression was demonstrated in 21.8% of the cases. 78.2% did not show any CD44 expression. Although there was no statistically significant association with the overall survival rate (p = 0.092), interestingly all CD44 negative cases showed metastasis at the time of diagnosis or in the following two years (p = 0.057).

Conclusions: 1. PD-L1 (22C3) expression in MPUC did not correlate with overall survival rate. 2. Stem cells do not seem to play a relevant role in the progression of this tumor subtype. 3. The loss of CD44 expression as an adhesion molecule may contribute to the lymphovascular permeation and early metastasis.